European Commission Grant Agreement Number: 869300

Call identifier: H2020-LC-CLA-2018-2019-2020 Topic: LC-CLA-06-2019

Type of action: RIA, Research and Innovation action

Starting date: 01.09.2020 Duration: 48 months

Project website: futuremares.eu

Project Deliverable Report 3.1

Report on Assessment of key species and community performance and functions in the face of global change

Dissemination level: Public

Type of deliverable: Report

Due date: Project month [M28, June 2023]

Project Milestone(s) achieved: Milestone #20

FutureMARES Project

FutureMARES - Climate Change and Future Marine Ecosystem Services and Biodiversity is an EU-funded research project examining the relations between climate change, marine biodiversity and ecosystem services. Our activities are designed around two Nature-based Solutions (NBS) and Nature-inclusive Harvesting (NIH):

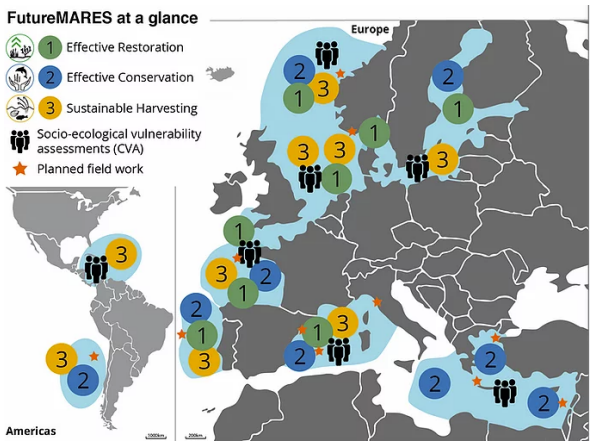

Effective Restoration (NBS1)

Effective Conservation (NBS2)

Nature-inclusive (sustainable) Harvesting (NIH)

We are conducting our research and cooperating with marine organisations and the public in Case Study Regions across Europe and Central and South America. Our goal is to provide science-based policy advice on how best to use NBS and NIH to protect future biodiversity and ecosystem services in a future climate.

FutureMARES provides socially and economically viable actions and strategies in support of NBS for climate change adaptation and mitigation. We develop these solutions to safeguard future biodiversity and ecosystem functions to maximise natural capital and its delivery of services from marine and transitional ecosystems. To achieve this, the objectives of *FutureMARES* defined following goals:

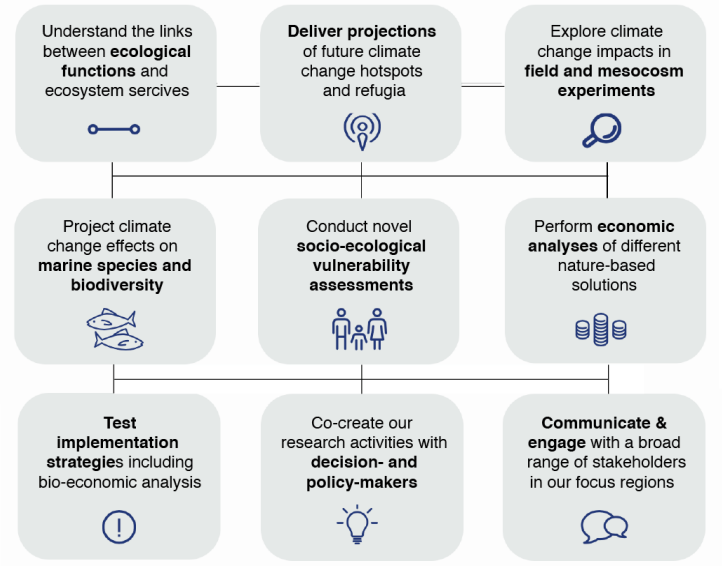

Deliverable data	
Work Package(s) / Task(s):	WP3 / Tasks 3.1
Lead beneficiary:	Israel Oceanographic and Limnological Research (IOLR)
Responsible author:	Gil Rilov
Contact:	rilovg@ocean.org.il
Co-authors:	**IOLR**: Gil Rilov, Martina Mulas, Tamar-Guy Haim, Erez Yeruham, Jacob Silverman; **UNIPI**: Fabio Bulleri, Chiara Ravaglioli, Ludovica Pedicini; **HCMR**: Eva Chatzinikolaou, Panos Grigoriou, Giorgos Chatzigeorgiou, Manolis Mandalakis, Ioannis Rallis, **WUR**: Brenda Walles, Lara Jansen, Pauline Kamermans; **NIVA**: Camilla With Fagerli, Eli Rinde; **CIIMAR**: Axel Chabrerie, Francisco Arenas; João Franco, Bianca Reis CSIC**-CEAB**: Emma Cebrian, Celia Sitija, Cristina Galobart, **PML**: Ana Queiros, Daniela Almeida; **NIOZ**: Katharina Alter, Myron Peck
Date of delivery:	1.9.2023
Deliverable type:	Report
Date of internal approval (for the submission to EC)	1.9.2023

Involved partners

Partners involved in workshops, discussions and/or performing work reported in this deliverable: IOLR, CIIMAR, CSIC-CEAB, HCMR, ICETA-CIBIO, IOLR, NIOZ, NIVA, UNIPI, WUR, PML

Document history

Version	Date	Description
01	15.6.2023	V1.0 – Initial version, by Gil Rilov
02	22.6.2023	V2.0 – by Gil Rilov
03	27.6. 2023	V3.0 – by Gil Rilov
04	30.6.2023	V4.0 – review by Scientific Coordinator
05	30.8.2023	V5.0 – Final version, including implemented review comments, ready for submission

Suggested citation for this report:

Rilov, G., Almeida, D., Alter, K., Arenas, F., Bulleri, F., Cebrian, E., Chabrerie, A., Chatzigeorgiou, G., Chatzinikolaou, E., Fagerli, C.W., Franco, J., Galobart, C., Grigoriou, P., Haim, T.-G., Jansen, L., Kamermans, P., Mandalakis, M., Mulas, Peck, M.A., M., Pedicini, L., Queiros, A., Rallis, I., Ravaglioli, C., Reis, B., Rinde E., Silverman J., Sitija, C., Walles, B., Yeruham, E., 2022. Assessment of key species and community performance and functions in the face of global change. FutureMARES Deliverable Report

Contents

List of symbols, abbreviations and a glossary

please include explanations in an alphabetical order for symbols (if used), abbreviations and a glossary if needed

AIC	Akaike's Information Criterion
ALAN	Artificial Light at Night
CC	Climate change
CT_{MAX}	Critical Thermal Maximum
DO	Dissolved oxygen
DoA	Description of Action, a part of the project Grant Agreement describing the project work plan
EC	European Commission
EC GA	European Commission Grant Agreement – a contract between the European Commission and FutureMARES consortium
GA	Grant Agreement
MO_2	Oxygen consumption rate
MPAs	Marine Protected Areas
NBS	Nature-based Solutions
TA	Total alkalinity

Tn.x Task – a sub-component of a work package where "n" is a number of the work package and "x" is a number of the task within this work package

TPC	Thermal Performance Curve
WP	Work Package

Executive Summary

The overall objective of Task 3.1 was to fill important ecological knowledge gaps on how human-driven biodiversity change may affect ecosystem functions, and the sensitivity of key species to climate change (CC) impacts together with local stressors. Activities included field, laboratory and mesocosm experiments. The work was designed to support downstream Workpackages (WPs) regarding, for example, the assessment of climate risks and ecological projection modelling. We specifically focused on **1)** comparing the ecosystem functioning of relatively healthy vs. degraded, changed (for example by alien species domination) or restored coastal benthic communities in the context of several key Storylines using similar protocols and approaches, and **2)** improving our understanding of how CC and other local stressors act independently or together to impact on species performance, biodiversity and ecosystem functions (and their inter-relations), again, in the context of some of our Storylines.

Field experiments using metabolic (incubation) chambers across ecoregions and Storylines in the Mediterranean Sea demonstrated that in the fast-warming and highly invaded southeast Levant region, some alien macroalgal species may support similar functions as habitat providers and alternative “Blue Carbon potential” to thermally-sensitive forest-forming native species that are in serious decline. Similarly, in the Tyrrhenian Sea to the north, non-canopy forming macroalgal meadows on urbanized coastlines were shown to have similar functions as those provided by canopy forests on pristine islands in the Tuscany Archipelago. Finally, in the Balearic Islands, restoring canopy-forming forests can regain their habitat and metabolic functions to levels similar to those of heathy forests.

Laboratory and mesocosm experiments examined the impact of single and multiple stressors related to both global and local pressures. The complexity of responses to multiple stressors was demonstrated in experiments examining the growth and physiological functioning of habitat-forming coastal plant and animal species, as well as community structure, of Atlantic ecosystems of rockweed and kelp. For example, in Portugal, where coastal upwelling is expected to weaken due to CC, the projected increase of temperature and decrease in nutrient levels is expected to have strong impacts on the growth and metabolic functioning of kelp species. In the UK, research identified how artificial light at night (ALAN) can surprisingly ameliorate the negative effect of a heatwave on important kelp species. In Norway, intertidal canopy-forming seaweeds and their communities were shown to be sensitive to coastal darkening and increased nutrient supply.

On the one hand, the results of fieldwork provide hope that, if local conditions are right, successful restoration of canopy-forming Fucales forests is possible and can provide functions similar to those of a healthy, existing forests. On the other hand, the results from Italy and Israel also indicate that some alternative/altered (non-Fucales dominated) benthic communities can provide similar functions as the original Fucales forests. However, work indicates that fully degraded, turf-barren communities provide very poor habitat for associated species and reduced metabolic functions. From a management perspective, protecting altered but highly functional communities can be viewed as alternative NBS if restoration of native species and communities is not possible. Our laboratory and mesocosm experiments underscore the importance of examining multiple stressors. The complexity of interactions among local and global stressors and their combined

impacts are essential to capture if we hope to advance the predictive capacity of models projecting the impacts of scenarios of climate change and conservation interventions.

1. Introduction

1.1. Impacts of climate change on species performance, community structure and ecosystem functioning

Considering global, regional and local impacts of climate change in conservation planning such as the development of NBS is a major societal and scientific challenge that was only fully recognized in the first decade of this millennium due to the mounting evidence of anthropogenic climate change impacts (e.g., Root and Schneider 2006, Pressey et al. 2007, Heller and Zavaleta 2009). Climate change represents a fast-moving target for marine conservation and requires flexible thinking on how to measure conservation success under rapidly shifting conditions and biodiversity (Rilov et al. 2020a). Climate change should also be considered in marine spatial planning (Santos et al. 2020), but adaptive conservation planning actions should be supported by extensive and relevant, science that is based on sound physiological, genetic and ecological studies (Rilov et al. 2019).

1.2. Conceptual framework

The concept of ecosystem functions is very broad and complex, and can include almost all biotic and abiotic processes occurring within an ecosystem (see extensive discussion in, Solan et al., 2012). Ecosystem functions are typically accepted as a general term that refers to the sum of all the processes occurring that transfer energy and mass within and among ecosystems or reservoirs. These include processes such as primary production, respiration, calcification and $CaCO_3$ dissolution that determine the accretion and loss of carbon from the organic carbon and inorganic carbon reservoirs of the ecosystem (Loreau et al. 2003, Naeem et al. 2009, Gravel et al. 2010), a reef being a good example. Some empirical studies suggested a positive relationship between diversity and functions (e.g. primary production), but the shape of the relationship (Naeem 2012) and the mechanisms behind it have been debated; does higher diversity simply increase the probability of inclusion of dominant species with particular traits (e.g. highly productive ones) in the local assemblage, or is it increasing the complementarity among species with different traits that improves the efficiency of resource utilization and ecosystem functions (Loreau et al. 2001). In reality, both mechanisms probably occur and their relative importance likely depends on the system, and may vary in space and time.

There is a general consensus that more species are needed to ensure a stable supply of ecosystem goods and services as spatial and temporal variability increases, and that certain combinations of species are complementary in their patterns of resource use and can increase the average rates of productivity and nutrient retention (Loreau et al. 2001, Hooper et al. 2005). As abiotic conditions can greatly influence that complementarity, climate change may play a pivotal role in altering ecosystem functions. At the same time, bio-invasions can reshuffle species compositions and interactions, and, in doing so, may considerably alter ecosystem functions as well.

1.3. Experimental approach

All Storylines that have measured in-situ ecosystem functioning of benthic communities have used an almost uniform experimental approach employing benthic metabolic chambers set on either macroalgae-dominated shallow reefs, seagrass or intertidal oyster reefs on mudflats. Most partners that tested macroalgae-dominated reefs used the method developed by IOLR (see, Peleg et al. 2020).

Mesocosm experiments on local benthic species assemblages were performed by some partners addressing climate change-related stressors relevant to the region. At least in terrestrial ecosystems it has been proven that the results of biodiversity-ecosystem functioning experiments are realistic (Gonzalez et al. 2020).Some partners also used laboratory experiments to test the thermal performance curves of key species of interest.

2. Storyline work

Eight partners and Storylines (four Mediterranean and four North Atlantic) were involved in the implementation of the objectives and activities organized in T3.1 (Fig 1). This section is sub-divided by the location where work was conducted.

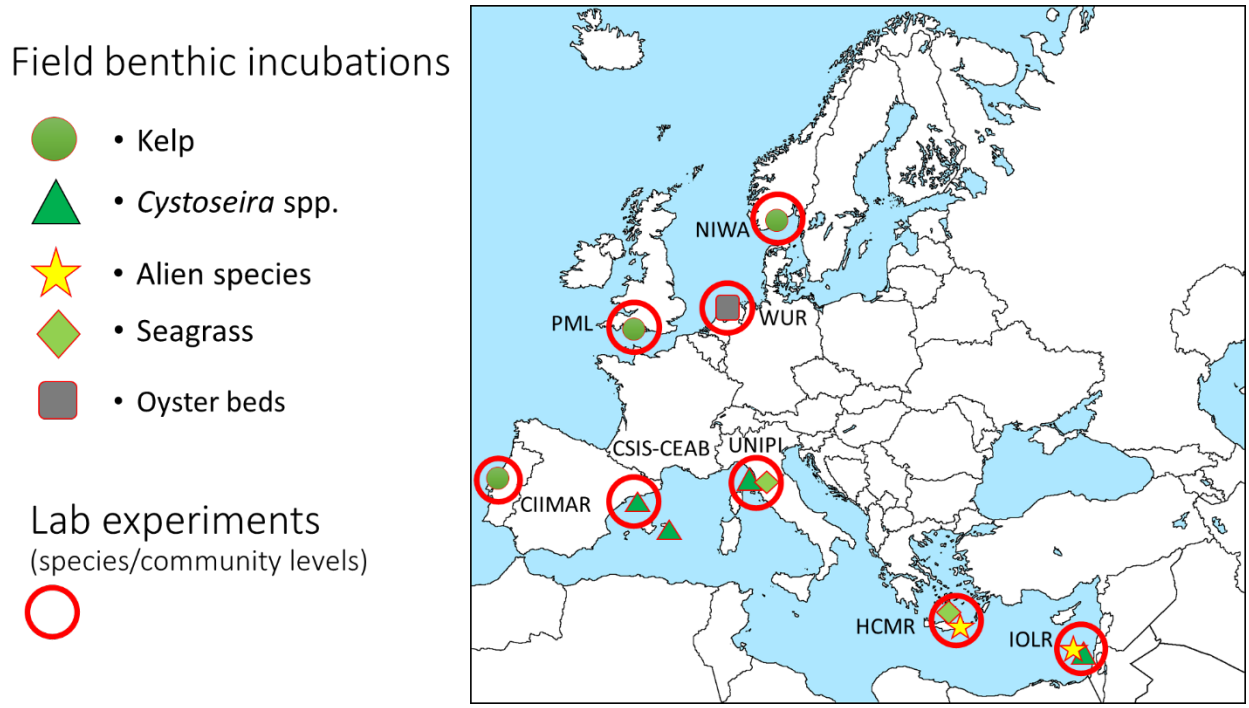

Figure 1 Map of participating storylines, ecosystems investigated and type of work done.

2.1 Israel: Present and future global risks and ecosystem functioning of macroalgae-dominated reefs in the Southeastern Mediterranean – a hotspot of ocean warming and bioinvasions (SL#34)

2.1.1 Introduction

The southeast Mediterranean Sea (SEM) or the Levantine Basin (Levant) represents the warm edge of most native Atlantic-Mediterranean species and is also a hotspot of invasions of thermophilic species coming mostly from the Indopacific through the Suez Canal (Rilov and Galil 2009). It is also a launching pad for the spread of many of these alien species throughout the Mediterranean Sea. The SEM is one of the hottest hotspots of the tropicalization process (Vergés et al. 2014a) as it is gaining tropical species through invasions but is also losing native species, presumably mostly those that are thermally sensitive due to ocean warming at the edge of their distribution (Yeruham et al. 2015, Rilov 2016, Albano et al. 2021). This two-pronged process leads to an extensive re-shuffling of the coastal communities (Edelist et al. 2013, Rilov et al. 2018) and, in some cases, to the creation of de-facto novel ecosystems. Linking reduced performance of native species and increased performance of alien tropical species to ocean warming requires experimental evidence. So does the assessment of the impacts of these shifts on ecosystem functions and services. For a handful of the alien species in the region, the ecological impacts have been well studied using controlled experiments. For example, caging and other experiments demonstrated that the tropical invasive rabbitfish, *Siganus rivulatus* and *S. luridus* can decimate macroalgal beds down to turf barrens (Sala et al. 2011, Vergés et al. 2014b). For most alien species, however, there is no such information and the impact of those species is mostly assumed either from observations, expert opinion, or via pure speculation.

Recent ecological studies from the Israeli coast have shown that the populations of the native sea urchin, *Paracentrotus lividus*, have collapsed to the point that this species has become extremely rare and ecologically extinct (Rilov 2016). Experiments have shown that this extinction was most probably driven by the fast-warming of the ocean and competition for food with rabbitfish (Yeruham et al. 2015, Yeruham et al. 2020). Other work has shown that native species (macroalgae and invertebrates) that are still abundant are at risk due to further ocean warming and ocean acidification (Guy-Haim et al. 2016, Guy-Haim et al. 2020, Amsalem and Rilov 2021) and that tropical alien species are more resilient to warming than their native counterparts (Rilov et al. 2022). Further, the entire community of the unique, biogenic ecosystem of vermetid reefs, and its functions are at risk from sea level rise (Rilov et al. 2021).

The focus of our Storyline 34 is on shallow reef communities on the Israeli coast that are currently overfished and highly dominated by alien species (Rilov et al. 2018). We specifically study macrophyte communities now dominated by turf due to overgrazing by the rabbitfish and where forests of native canopy-forming species from the *Cystoseira sensu-lato* (Fucales, Phaeophyceae) genera are now rare. One specific species that is more abundant, *Gongolaria rayssiae* is considered endemic only to Lebanon and Israel (Mulas et al. 2020) and forms the largest shallow water forests near IOLR in Haifa. There are also 86 known alien macroalgae in the Levant region (Israel and Einav 2017), some of them, such as the red, calcifying tropical

"shrub", *Galaxaura rugosa*, were documented to form large patches on the reefs (Rilov et al. 2018).

Macroalgal forests are globally recognized for their fundamental role as providers of ecosystem functions and services (Krause-Jensen and Duarte 2016, Macreadie et al. 2021, Duarte et al. 2022). These systems are important primary producers (Duarte et al. 2018, Duarte et al. 2022) involved in nutrient cycling (Human et al. 2015), energy flow (Queirós et al. 2023) and Blue Carbon production and sequestration (Krause-Jensen and Duarte 2016). They also provide refuge, nursery, foraging and breeding areas for many other species and, therefore, maintain a high biodiversity (Cheminée et al. 2013, Vergés et al. 2016, Teagle et al. 2017). To date, however, our knowledge on seasonal dynamics, thermal vulnerability and ecological role of both native and alien macrophytes is minimal in the fast-changing Levant basin.

In a recent study, an IOLR team was the first to use benthic incubation chambers on macroalgae in the Mediterranean Sea and to compare the biodiversity and metabolic functioning of endemic *Gongolaria*, alien *Galaxaura* and turf barrens communities during the spring season (Peleg et al. 2020). That work indicated that turf had the lowest diversity while that of the community associated with the native and alien shrub and similar species richness, but different structures and the alien-dominated community had a net autotrophic balance. This suggested that the alien species may provide high habitat provisioning functions but low carbon uptake functions, at least in the spring. Clearly, in most habitat-forming species, growth, biomass and ecosystem functions (e.g., habitat provisioning, carbon uptake) are not static, and seasonal and inter-annual variability in abundance and biomass can considerably alter the magnitude of those functions. This is especially true for seaweeds where strong seasonal changes are reported in both temperate and tropical areas (Ngan and Price 1980, Price 1989). In the Levant rocky intertidal, macroalgal seasonality was recently shown to be very strong (Rilov et al. 2020b), but very little is known on the seasonal dynamics of subtidal seaweeds. It is reasonable to assume that the alien seaweeds would have different seasonal dynamics compared to the native temperate to subtropical species, which can affect the annual carbon budget of the reef as a whole.

We also studied the thermal performance of the animals that are currently the major grazers of macroalgae on the shallow SE Levant reefs. This included the small native herbivorous crab that inhabit the algae, *Acanthonyx lunulatus*, and the invasive rabbitfish, *Siganus rivulatus*. After FutureMARES was organized, a new threat to the macroalgal communities was evolving in the SEM, that of the invasion of the large Red Sea urchin, *Diadema setosum*. This species invaded the Turkish and Greek coasts about two decades ago and has advanced south and east to Cyprus and Lebanon. In the last few years, the Red Sea urchin appeared on the Israeli and north African coasts (Zirler et al. 2023). In the past three years, the Red Sea urchin has shown signs of rapid increase in abundance on the Israeli coast and, as part of FutureMARES, efforts were started to i) monitor its presence, ii) investigate how different temperatures could influences the further spread of this species north and west and its potential viability under future, warmer, temperatures in the Levant, and iii) test the impact of this urchin on the reef community and functioning.

Our work was set to determine the current and future vulnerability of native and alien macrophytes, and the alien urchin, to climate change and test the macroalgal metabolic functioning as well as the functioning of their communities to determine whether the alien

macroalgae can offset some of the functions that could be lost by the loss of native canopy-forming algae due to both warming and overgrazing by the invasive rabbitfish as well as to determine the possible impact of the alien urchin on the reef community.

For that, we investigated (1) the seasonality of key native and alien macroalgal species focusing on both cover and biomass, (2) tested the thermal vulnerability of key native and alien macroalgae and some of their key grazers, (3) assessed the seasonal metabolic rates of those species to calculate their annual carbon budget, (4) measured the habitat and metabolic functioning of native vs. alien vs. turf dominated communities in different seasons, and (5) assessed the structure and functioning of the native canopy-forming *Gongolaria* community under different climate change scenarios.

Our approach was to (1) use ongoing monitoring work supplemented by targeted long-term surveys to document seasonal and interannual dynamics of native and alien macroalgal as well as the abundance of the invasive sea urchin, (2) use laboratory experiments to determine thermal vulnerability and metabolic rates of the target species, (3) use field incubations to assess community metabolism in different seasons, and (4) use mesocosm experiments to test the functioning of the native forest-forming species under simulated future ocean conditions.

2.1.2 Methods

2.1.2.1 Study area and target species

The shallow Mediterranean coast of Israel is generally characterized by relatively warm (14-32 °C), high salinity (38-40), low nutrient conditions (NO3- = 0-2 µM; PO4-3 = 0-0.1 µM). As a result of global warming processes, this region is undergoing fast warming and salinization at a rate of 0.5-1 °C/decade and +0.06-0.1 PSU/decade (Ozer et al. 2016, Ozer et al. 2022). Rocky reefs dominate most of the northern coast of Israel. At the shoreline, it is mainly characterized by vermetids reefs and the subtidal zone is dominated by bedrock and sandstone or limestone ridges.

An area of several km^2 near Haifa where sites that are part of the National Monitoring Program of the Mediterranean Sea run by IOLR (Fig. 2) was where we studied the target seaweed species (Fig. 3) and their associated assemblages: (1) *Gongolaria rayssiae* in its largest known forest near Tel Shikmona - site name SK-1 (~ 2m bottom depth); (2) The Atlantic newcomer brown algae *Lobophora schneideri* (Vieira et al. 2019) in the largest known patch on the Carmel Head Plateau – RD-1 (7m bottom depth); (3) The Lessepsian red seaweed *Galaxaura rugosa* (Hoffman et al. 2008), which is widely spread on shallow reefs in northern Israel (Rilov et al 2018), in a large meadow on the Shikmona ridge – SK-2 (12m bottom depth).

We also report on another canopy forming algae, *Sargassum vulgare*, that is quite rare along the Israeli coast but can still form small, discrete, patches in different areas on northern reefs at depths from 1-10 m. A patch was identified near RD-1 and started monitoring it in 2019 that we named RD-1-Sarg. This species thermal vulnerability was also assessed in the lab. Other sites that are monitored are SP-1 at 20 m (characterized mostly by turf algae) and SK-3 close to SK-2 that is also dominated by *G. rugosa*. At the community level, for logistical reasons, the community measurements of *G. rugosa* could not be executed at SK-2, thus we partly relied on previous work in a shallower site (Peleg et al 2020) for the discussion, and we included turf areas near SK1 for comparison.

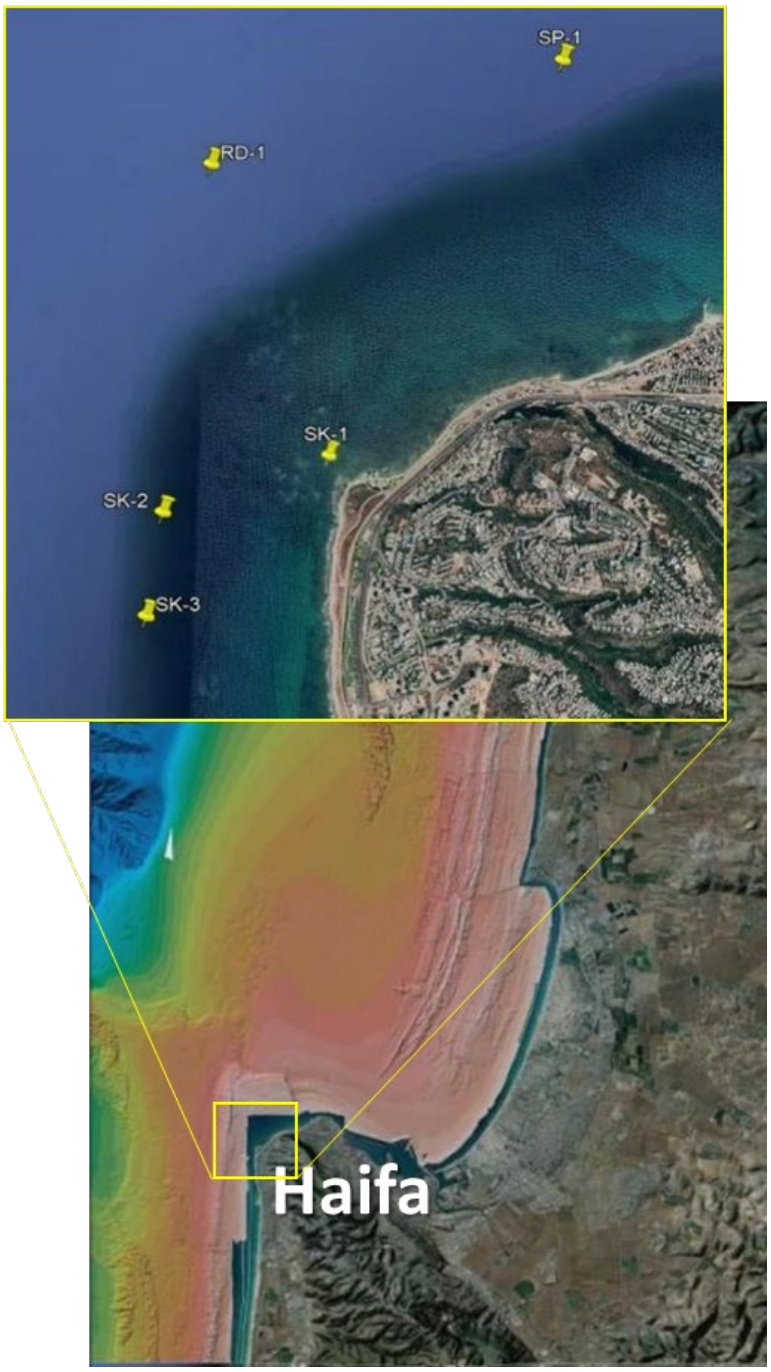

Figure 2 SL34 study area and sites (yellow pins on a GOOGLE EARTH inset) near Haifa. Bathymetric map was produced from data from multibeam acoustic surveys conducted by IOLR.

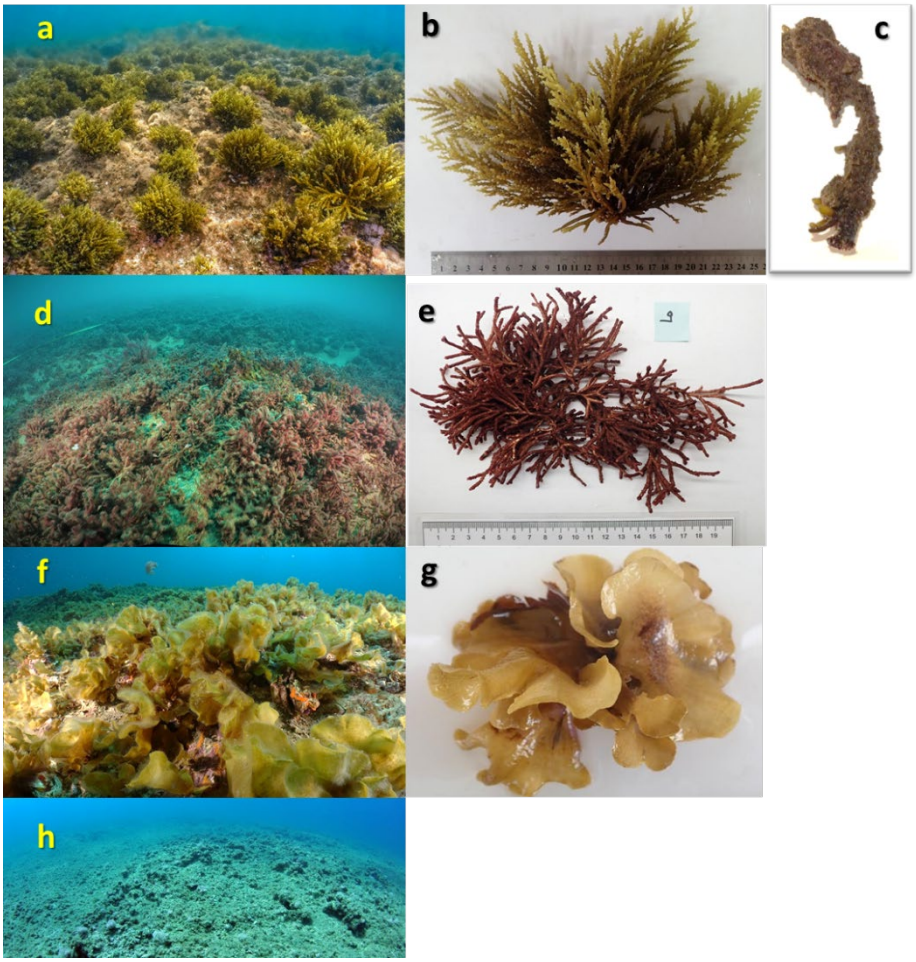

Figure 3 Study species and communities. Gongolaria rayssiae forest, plant and cauloid (a,b,c), Galaxaura rugosa patch and plant (d,e), Lobophora schneideri patch and plant (f,g) and a turf barren reef area (h).

2.1.2.2 Seasonal cover, biomass and community structure

We used two sources of data to assess seasonal dynamics of the target species. The seasonal cover of native and alien macroalgae has been assessed since 2013 by the Rilov lab as part of the National Monitoring Program run by IOLR. Cover is assessed along 30 m transects along which 15 random 50x50 photoquadrats are taken to assess benthic cover. These photos are later analysed for cover assessment using the online platform CORALNET.

Beyond that, for this specific study, during 2020 and 2021, we seasonally followed the seaweed percent cover and biomass using 5 random 25x25cm^2 quadrats positioned along a 30 m transect, except for fall and spring for *L. schnederi* and turf, for which the data were collected during the in-situ benthic chambers incubation experiment (0.126 m2 surface area, see below). Percent cover was assessed by photoquadrats, while all the associated communities were collected in 250 µm mesh-bags and transferred to the lab. For *G. rugosa*, we sampled only the tetrasporophyte, and we excluded the gametophytes (for more information about the phenology of the species see Garval 2015). Once transferred to the lab, we proceeded with the sorting, separating the target seaweed species from the other organisms (the associated assemblage). All the organisms were

identified to the lowest possible taxonomic level, and then collapsed into three main groups: dominant algae, other macroalgae and invertebrates. Coarse taxonomic resolution simplified biomass estimations. These were photographed, and fresh-weighted (wet weight, hereafter WW). Subsequently, samples were oven-dried at 60 °C for at least 48h or until the weight stabilized to measure the dry weight (DW), and finally burned at 500 °C for 4h to obtain the ash-weight (AW) and finally the ash-free dry weight (AFDW), which is the difference between DW and AW and represents the organic component of the algae. *Gongolaria* percent cover was also followed monthly with 50x50 m quadrats from January 2018 to May 2020 in the shallow SK-1 site to assess the growth season in more detail. During summer months (when only cauloids were present) sampling was often skipped due to wavy conditions in this wave-exposed shallow site.

2.1.2.3 Thermal vulnerability (thermal performance curves)

To assess the thermal vulnerability and optimum among native and alien macroalgal species, we measured their functioning under a wide range of temperatures to determine their Thermal Performance Curves (TPC) considering the gross oxygen production as response variable. For macroalgae and small invertebrates, we used the same ex-situ outdoor (allowing natural light conditions) incubation microcosm system (Fig. 4) described in detail in Guy-Haim et al. (2016) for macroalgae and also in Amsalem and Rilov (2021) and Rilov et al (2022) for invertebrates. The system consists of 11 thermobaths where temperature can be set between 8-40 °C. In our experiment, the temperature range was 15-35 °C or 17-37 °C with 2 °C intervals between treatment temperatures.

Figure 4 IOLR outdoor microcosm system.

Fresh specimens were collected from the field and transferred to the lab within a couple of hours. After rinsing and cleaning of epiphytes, we selected specimens with similar weight and size for the experiments. Each individual was photographed, weighed, inserted into 0.75-L glass jars and assigned to a specific treatment temperature (n = 3-6). We left the specimens to acclimate at ambient temperature for 5-7 days. Every 36-48h we manually replaced the seawater inside the jars with seawater that was warmed or cooled beforehand to the temperature set in the thermobath to reduce the amount of stress to the specimens. Water motion and stable temperatures were ensured by submerged pumps and aerators. After the acclimation period, we increased or decreased the temperatures by 0.5 °C every 12 hours, reaching the target values within 5 days. Subsequently, the seaweeds were kept at the target conditions for a further 5 days and then incubated. Photosynthesis and respiration rates for each specimen were measured by short incubations of 1-2 hours during daytime (at the solar noon) and nighttime (one hour after sunset), respectively. Dissolved oxygen (DO) was recorded at the onset and end of the incubation in each of the jars with a hand-held optode, WTW 3420 (mg O_2/L) and the difference between the initial and final concentrations were used to calculate the net photosynthesis and respiration. Finally, the gross primary production was calculated as the sum of daytime net photosynthesis

and nighttime respiration and divided by the wet weight biomass. In the native *Acanthonyx* crab, and the alien sea urchin, *Diadema setosum*, defecation rate was measured as an indication of feeding rate performance by counting the number of fecal pellets (crabs) or weighing the pellets (urchins) each day.

The measured and calculated rates were plotted against temperature and the best model characterizing the species was fitted to the data. We tested among different models allowing for negative values at both cold and warm extremes, and the best fitting one was chosen ranking by the lowest Akaike's Information Criterion (AIC). The optimal performance temperature (T_{OPT}) and the maximum critical temperature (CT_{MAX}) were calculated from the models using 'rTPC' package (Padfield et al. 2021). Derived TPC parameters were calculated from high resolution prediction (0.001 °C intervals) of the fitted model, such as activation (E) and deactivation energies (Eh). These latter values express the slope or rate of change in the rise and falling phases of a thermal performance curve before and after achieving the optimal temperature (Roth et al. 2019). To visualize the uncertainties and produce confidence intervals of estimated parameters, bootstrapping weighted non-linear least squares was applied to calculate 95% confidence intervals (CIs) (Padfield et al. 2021).

To examine the thermal performance of the invasive rabbitfish, *Siganus rivulatus,* we performed two long -term mesocosm experiments in the outdoor, flow-through system at IOLR (Fig. 5; see a more detailed description in section 2.1.2.6) during the winter and summer of 2017. Fish collection and acclimation: prior to each experiment, 170 specimens of *S. rivulatus* were collected manually from Shikmona coast and transferred immediately to the experimental tanks with running seawater. The acclimation was conducted in two stages: first - acclimation to the tank for two weeks. Second – gradual change in water temperature (according to each treatment) at a rate of 0.5°C a day. The fish will remain undisturbed for one week after target temperature was obtained for all tanks.

Figure 5 IOLR outdoor flow-through mesocosm system.

Experimental setup: the fish were divided into 5 treatments with different temperature regimes:

AMBIENT-	AMBIENT-	AMBIEN	AMBIENT+2	AMBIENT+4

Three replicates for each treatment, with a total of 15 tanks. Ten fish were placed in each tank. Prior to the beginning of the experiment the fish weighed and a sample of 20 specimens was dissected in order to measure the relative size of the gonad, intestine and liver. During the experiment, the fish fed with pellets composed of 95% grinded *Ulva* spp. and 5% corn flour. The experiments lasted 3 months. At the beginning, middle and end of each experiment, nine fish from each treatment (3 from each repeat) were randomly selected to undergo a series of tests as follows:

Respiration: fish were individually placed in a temperature-controlled respirometer (volume of 5 L) and incubated for 1 hour. The respirometers were rinsed with acid prior to the incubation and filled with filtered sea water, in order to reduce oxygen consumption by microorganisms. Oxygen level was measured before and after the incubation using an oxygen optode (Oxi3315, WTW). Adequate water mixing inside the chamber was ensured using an inner pump. All the data is standardized to the blank control measurements, test duration, water volume and the individual weight.

The thermal performance of the invasive sea urchin, *Diadema setosum*, was tested in a flow-through indoor mesocosm facility. This facility is generally similar to the outdoor mesocosm system but with only six units and artificial LED lights (Fig. 6).

Figure 6 IOLR indoor mesocosm system and the invasive sea urchin in the system.

2.1.2.4 Seasonal metabolic productivity of the algae

To compare seasonal dynamics in metabolic rates at the species level, in 2020-21 we collected five specimens from each of the study seaweed species in every season. All the individuals were transferred to an outdoor flow-through seawater water table within an hour from collection (seawater is filtered and coming from ca. 1-meter depth near SK-1). Within 5 hours from collection, we cleaned the individuals from epiphytes, and positioned them in labelled open 0.75L glass jars under running seawater after weighing and photographing them. Temperature was not controlled (i.e., ambient temperatures, as this was a flow-through system) and was measured at the beginning and at the end of each incubation. In order to maintain a constant temperature in the incubation jars during the incubation period, these were positioned within a plastic transparent bath receiving continuous fresh running seawater with high exchange rates.

After ca. 8-10 hours of acclimation, we initiated the incubations using a closed bottle respirometry technique (Biscéré et al. 2019). The specimens were incubated for ~ 1-2 hours, between 6:30 - 11 PM at night (at least one hour after the sunset) and between 11 AM and 2 PM of the following day within 24 hours of collection. DO and temperature (T) were measured at the beginning and end of each incubation, and we collected three water samples per jar after syringe filtration (0.45 µm GFF), for later measurements of dissolved inorganic carbon (DIC) (60 mL), pH, and total alkalinity (TA) (120 mL each). In both daytime and nighttime incubations, seawater controls (without algae) were included (n=3). Boundary layer effects at the beginning and end of the incubations were avoided by stirring the water in the jar with the oxygen probe until the readings stabilized, before recording the measurements. Water samples for lab analysis were taken after the oxygen measurements were recorded.

2.1.2.5 In-situ incubations

Metabolic rates of benthic algal communities (the native *Gongolaria*, the alien *Lobophora* and turf) were measured during the fall and spring except for *Lobophora*, which was measured during winter as well. It was not possible to conduct these measurements during the summertime due to wavy sea conditions. All the incubations were performed by SCUBA on days with clear skies, calm sea, and good visibility in five replicates in the shallow reef at SK-1 (~2m bottom depth) on turf and *G. rayssiae* communities in spring (April 2018) and fall (October 2017 and November 2020), and at RD-1 (~7m bottom depth) on *L. schneideri* community in winter (December 2017), spring (May 2019) and fall (October 2020). This part of the study did not include *G. rugosa* community, which was previously studied by Peleg et al. (2020) in a shallower site in the spring. However, turf barrens that represent a baseline for a fully degraded community (Connell et al. 2014, Rilov et al. 2018) were included. The incubation followed a protocol similar to the one described in detail in Peleg et al. (2020). Briefly, *in-situ* benthic incubations were performed using closed benthic custom-made dome-shaped (40cm diameter) chambers. Water circulation in the domes was maintained using submerged pumps that mimic the natural flow and reduce the risk for the formation of a boundary layer within the dome.

In each field campaign, we first conducted dark incubations under blackened domes (early morning) followed by light incubations inside clear domes during peak solar irradiance (between 11 AM-2 PM according to the season). After positioning the domes on the selected surface areas, we weighed them down by custom-made sleeve-like Lycra sandbags that also sealed their perimeters to prevent water exchange and dilution of the signal in the dome during the incubation. Following the dome deployment, water samples were collected from outside of the domes for initial ambient conditions (t0) using three 100 mL syringes. At the end of the dark incubations that lasted between 1-2 hours, water samples were taken from inside and outside the domes (t1). After water samples collection, the plots were left uncovered for approximately 10 minutes to re-acclimate the community to the ambient conditions, and then they were covered with clear domes and again sealed with the sandbags for the beginning of the light incubations. At the end of the light incubations, water was sampled again from inside and outside the dome with three 100 mL syringes (t2). Finally, the domes were removed, and the incubated biomass was collected into 0.250 µm mesh bags by scraping and using a manually operated suction sampler (MANOSS) (Chatzigeorgiou et al. 2013). The biomass bags were kept in water buckets and, within a few hours, transferred to the lab for sorting.

Immediately after sampling, the syringes with the water that was collected in t_0, t_1 and t_2, were brought to the boat during deeper incubations, or to the beach during shallow incubations, to be dispensed into vials or bottles for analysis of T, DO, pH, DIC, TA and nutrients. Samples for pH, DIC, TA and nutrients were filtered through a 0.45 µm GFF into appropriate storage containers for later analysis in the lab. Throughout each field campaign, measurements of Photosynthetically Active Radiation (PAR) were recorded with an ECO-PAR Seabird Electronics PAR-sensor or with a Hobo-Pendant light-temperature data logger.

2.1.2.6 Community mesocosm experiments

This part of the work started before FutureMARES but some of the analysis was done during the project, it was never published and contributes relevant information to the Storyline. The metabolic functioning of the native, endemic forest-forming macroalgae *Gongolaria rayssiae* community under past, present and future conditions of ocean warming and acidification conditions was tested in the outdoor, flowthrough mesocosm system at IOLR ('benthocosms', hereafter), on the shore of the Mediterranean Sea. The conceptual design of the benthocosm facility followed that of the Kiel Outdoor Benthocosms ('KOB', Wahl et al. 2015), but included several variations and adjustments necessary because of the distinct conditions of the Israeli Mediterranean shore, and their difference from the Baltic Sea conditions. The facility consists of 16 tanks, made of two-layer UV-resistant polyethylene (Dolav Plastic Products, Israel). The net water volume of each tank is 1500 L. A 4 cm layer of Polyurethane foam was applied to the outer tank surfaces, to increase insulation and limit heat conduction. Each tank is independently-controlled and serves as an independent experimental unit. The benthocosm facility, including the experimental tanks, controllers and equipment further detailed below, is set within a greenhouse with foldable walls, to prevent an artificial accumulation of rainwater, and to maximize insulation during the seldom occasions of wind storms. Under benign conditions the sides are rolled up for better ventilation. The greenhouse roof and walls are made of transparent UV-resistant 150µm polyethylene cover sheets, with maximal light penetration in the visible spectrum.

The benthocosm facility performs as an open, flow-through system. All tanks are constantly supplied with unfiltered seawater from the Mediterranean Sea. Seawater is pumped from a location found 100m offshore (1 m depth) to a 6000 L storage tank located on the IOLR roof. From there the seawater falls by gravity to the benthocosm facility. The flow rate was adjusted to 3000 L·day-1·tank-1 resulting in a residence time of approximately 12 hours, to allow continuous manipulation of temperature and pH levels and build-up of signals in chemical composition of seawater. Manipulation and monitoring of environmental parameters are computer controlled by an aquarium controlling system (two units of Profilux-3Nex and three units of Expansion Box, GHL Advanced Technology, Germany). Seawater from each tank is continuously pumped into a dedicated measurement cell (16 cells, GHL, Germany), where temperature, pH and salinity are continuously measured by sensors (platinum electrode PT1000, gel-electrolyte filled electrode, and conductivity electrode, respectively, from GHL, Germany).

The inlet flow rate is continuously measured by flow-sensor (GHL, Germany). Real-time temperature, pH and salinity of the ambient Mediterranean water are measured in an additional measurement cell. Ten Powerbar (Powerbar 6D-D, GHL, Germany) allow switchable power sockets for the different system components. All controllers are connected serially using the

Profilux Aquatic Bus (PAB, GHL, Germany). The PAB enables communication between the individual units, enabling the setup of the dynamic nominal value. The dynamic nominal value is a measured value from a specified sensor (e.g., the sensor measuring ambient temperature) transmitted to the other controllers, which then use it as a reference value for the delta treatment, i.e. relative to which a tank is warmed or cooled to a pre-set offset. This allows “treating” the system while admitting the stochastic, diel or seasonal fluctuations of the Eastern Mediterranean shallow subtidal water. The dynamic setting feature was specifically designed for the Kiel Outdoor Benthocosms (Wahl et al. 2015a).

Heating of each benthocosm tank was achieved by a 2000-Watt titanium heater (Titan-2000, Aqua-Medic, Germany), and cooling by a powerful customized chiller (14000 BTU, Tecumseh, France), both controlled by the aforementioned GHL controlling components. Seasonal, daily or convection-caused temperature fluctuations at natural frequencies and amplitudes are admitted to the tanks whether they run at the present-day or future temperature regime. pH was manipulated in the benthocosms by pumping the tank water (41 Watt, OPT-3000, Reef Octopus, China) to a tank-CO2 Reactor (OR-150, Reef Octopus, China) supplied with pure CO2 gas. Within each tank, a circulation pump (130 Watt, HY-10000W, Reef Octopus, China) produces currents to mimic water movements as close as possible to natural conditions and to distribute heat and acidified seawater homogeneously. Temperature, pH, salinity, oxygen and total alkalinity were measured throughout the tanks, and no gradients were observed. Temperature, pH and salinity were continuously measured in each tank and recorded at 10-minute intervals with a GHL Control Center software log. Temperature, pH and flow rate thresholds were set in the control software, and any deviations resulted in an alarm via SMS or e-mail notification.

To track sensor drift, discrete pH measurements were conducted daily inside the containers using a hand-held multi-probe (WTW MultiLine IDS 3420). Daily monitoring of DO (dissolved oxygen) was conducted using an oxygen optode with the WTW multi-probe. These daily measurements were carried out consistently around 12:00PM. The MultiLine sensors were calibrated using technical buffer solutions (WTW, Germany). GHL continuous measurements were compared to the discrete measurements, and calibrated daily accordingly, using GHL calibration fluids.

Experimental design: Two successive benthocosm experiments were performed during 2014-2015: from October 26 2014 to 1 April 2015 (Autumn-Winter), and from April 24 2015 to August 3 2015 (Spring-Summer), for durations of 155 and 100 days, respectively. The experimental design (Fig. 7) included five treatments: seawater with ambient temperature and ambient pH (AM), warming by 3ºC (ocean warming, OW), cooling by -2ºC (ocean cooling, OC, to reconstruct the cooler temperature regime during the 1970-80s, before the rapid warming of the 1990-2000s), acidification by -0.4 pH units (ocean acidification, OA), and combined warming by 3ºC and acidification by -0.4 pH units (ocean warming and acidification, OWA). Each treatment included three replications (5X3 treatments). An additional tank where no biota was added served as a procedural control.

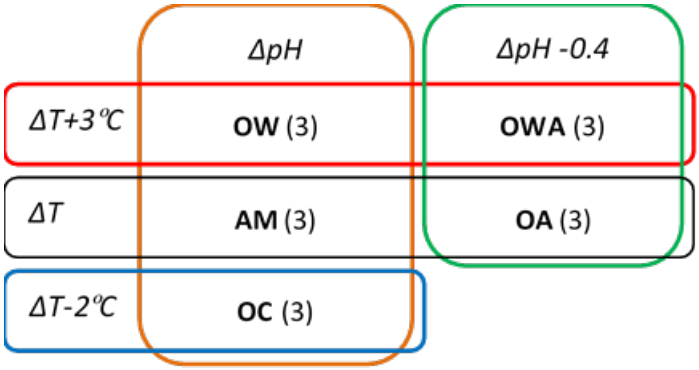

Figure 7 Experimental design diagram – a combination of temperature and pH treatments. ΔT and ΔpH are the ambient temperature and pH amplitudes, respectively. The replication level is presented in brackets.

At the onset of each experiment, dominant representatives of the Eastern Mediterranean rocky reef community were collected from a shallow subtidal reef (2-5 m depth) near the Israel Oceanographic and Limnological Research Institute, Haifa (32°49'32"N 34°57'26"E). These included the canopy-forming brown algae, *Gongolaria rayssiae*, the alien corticated calcareous red algae, *Galaxaura rugosa*, the herbivorous, mostly epiphytic, crab, *Acanthonyx lunulatus*, a carnivorous gastropod, *Collumbella rustica*, and a carnivorous (mostly invertivorous) fish, the ornamented wrasse, *Thalassoma pavo*. Large biogenic rocks were also collected from the natural substrate of the subtidal reef and placed in the experimental tanks as well to better simulate a reef environment. We used *G. rayssiae* as a foundation species in our experiments. The crab *A. lunulatus* feeds on *Gongolaria*, and resides between its branches. *C. rustica* is commonly found within the *Gongolaria* understory. The ornamented wrasse, *T. pavo*, predates on small gastropods and crustaceans, such as *A. lunulatus* and *C. rustica*. Both invertebrates and fish were collected from a *Gongolaria* forest. The invertebrates and rocks were manually collected using SCUBA, and the fish were collected using a seine net.

At the beginning of each experiment, all organisms were sorted, counted, fresh-weighed (g FW), photographed, and equally distributed between the 15 populated benthocosm tanks. Each tank included 12 plants (thalli) of *G. rayssiae* and 6 plants (thalli) of *G. rugosa*, clipped at their basal disk to upside down standing reusable plastic crates at 60 cm depth, 5 individuals of *A. lunulatus*, 5 individuals of *C. rustica*, and 2 individuals of *T. pavo* (only in the spring-summer experiment), roughly mimicking their natural relative abundances at the sampling site. For every species, all individuals were of the same size class. The macroalgae plants were individually tagged for monitoring their growth and function. The rocks were tagged, weighed and their surface area was calculated using photographic analyses by 123D software (Autodesk, USA). Continuous flow of non-filtered coastal waters supplied larvae allowing the arrival of new species into the benthocosm tanks throughout the experiments. The extra, 16th tank was used as a procedural control to compare the abundance and diversity of plankton and detritus, pumped into the tanks and naturally accumulating inside, and contained no pre-transplanted biota. Periphyton and fouling biota were allowed to grow on the tank walls, and were considered as an integral part of the community during the experiments.

Abundance, biomass and size. At the experimental endpoint, the supply of fresh seawater into the benthocosms was halted, and a thorough census was performed in each of the tanks. Motile organisms were captured using hand-nets. Periphyton and fouling organisms were gently scrapped off the algal branches, crates, tank bottom and walls. All organisms were sorted,

identified, counted, fresh-weighed (g FW), photographed, and stored at -80°C pending further analysis. The photos were later used to measure individual length using the image processing software ImageJ version 1.47t (https://imagej.nih.gov/ij/). To obtain algal length, the longest branch was measured from the holdfast. Crustacean size was measured by carapace width, and gastropod size was obtained by measuring shell length. The seawater within the tanks was filtered via a 125 µm mesh, and the feed was resuspended in 30 L filtered seawater and subsampled (100 ml) for a manual count of meroplankton using a stereoscope. Over the experimental period, sediment and detritus piled up at the bottom of the tanks. At the end of each experiment, after all organisms were removed, the sediment and detritus were siphoned from all 16 tanks, and their fresh weight (g FW), dry weight (g DW) and organic content (g AFDW) were measured for detritus biomass assessment. Where enough data was obtained, species-specific size class distribution was calculated.

Diversity indices, species origin and trait assignment. All organisms were identified to the lowest attainable taxonomical level. To estimate diversity indices, Richness (S), Evenness (J'), and Shannon-Weaver diversity index (H') were calculated using the taxa biomass. Established databases (AlgaeBase: http://www.algaebase.org/, WoRMS: http://www.marinespecies.org/) were searched to assign species origin (Mediterranean, Indo-Pacific, Other). Trophic levels, feeding habits, and structure (calcareous, non-calcareous) were assigned by searching EMODnet trait database (http://www.marinespecies.org/traits/) and relevant literature. Detritus and detritivores were assigned to trophic levels one and two, respectively, in parallel to the primary producers and primary consumers, after Odum and Heald (1975).

The ratio R_{FW} of a trait or functional groups was calculated as follows:

$$R_{FW} = FW_{group1}/FW_{group2}$$

where FW_{group1}, FW_{group1} are the total fresh weight of all taxa carrying a specific trait (e.g., calcareous *vs.* non- calcareous structure, indigenous *vs.* non-indigenous), or belonging to a specific functional group (e.g., basiphytes *vs.* epiphytes). Similarly, the ratio between taxa richness of functional group was calculated as follows:

$$R_S = S_{group1}/S_{group2}$$

Ecosystem functions. To asses whole community ecosystem functions at the treatment (tank) level benthocosm fluxes were assessed over one diurnal cycle (24 hours), 12-20 weeks into the experiment, on March 9-10 2015 and 6-7 July 2015 (Autumn-Winter and Spring-Summer experiment, respectively). In addition to the continuous recording of temperature, pH and salinity, discrete water samples were taken every two hours from the inlet (ambient seawater), the procedural control (lacking pre-set biota), and from one tank of every treatment (AM, C, W, A, WA). The samples were taken for analysis of DO, DIC, A_T, nutrients (NO_2^-, NO_2^-+NO_3^-, NH_4^+, PO_4^{-3}, $Si(OH)_4$) and Chlorophyll *a*.

Rates of net photosynthesis (P_n, in O_2 or CO_2), calcification (G) and biological processes affecting Chl. *a* content in the water column (F) were calculated using the following first order box model equations:

$$V \cdot \frac{dDO}{dt} = Q \cdot (DO_{in} - DO_t) - a \cdot K_{pO_2} \cdot (DO_t - DO_{sat}) + P_n$$

$$V \cdot \rho_{sw} \cdot \frac{dDIC}{dt} = Q \cdot \rho_{sw} \cdot (DIC_{in} - DIC_t) - a \cdot K_{pCO_2} \cdot \left(PCO_{2_t} - PCO_{2_{sat}}\right) + P_n - G$$

$$V \cdot \rho_{sw} \cdot \frac{dA_T}{2dt} = \frac{Q}{2} \cdot \rho_{sw} \cdot \left(A_{T_{in}} - A_{T_t}\right) + G$$

$$V \cdot \frac{dChl}{dt} = Q \cdot (Chl_{in} - Chl_t) - F$$

where, V is the benthocosm tank volume (1500 L), dDO, $dDIC$, dA_T and $dChl$ are the differences in dissolved oxygen (µmol·L^{-1}), dissolved inorganic carbon (µmol·L^{-1}), total-alkalinity (µmol·kg^{-1}) and Chl. *a* (µg·L^{-1}) concentrations between two consecutive measurements, dt (hours) is the time interval between measurements, ρ_{sw} is the density of seawater (kg·L^{-1}), Q is the flux of seawater at the tank inlet (L·h^{-1}), which is assumed to be equal to the flow rate at the tank outlet, DO_{in}, DIC_{in}, $A_{T_{in}}$ and Chl_{in} are the concentrations at the inlet (equal to the ambient seawater), DO_t, DIC_t, A_{T_t} and Chl_t are the concentrations in the tanks (and hence, tank outlet) at time t, a is the horizontal surface area of the benthocosm tank, K_{pO_2} and K_{pCO_2} are the piston velocities of O_2 and CO_2 in seawater (following Wanninkhof 2014), DO_{sat} and $PCO_{2_{sat}}$ are O_2 and CO_2 saturation levels at the measured temperature and salinity, and PCO_{2_t} is the partial pressure of CO_2 in the atmosphere. The possible biological processes affecting the Chl. *a* content in the water column (*F*) are light adaptation, grazing and filtration, mortality, and proliferation.

To evaluate a diel budget, the metabolic rates were integrated over daytime and night-time to calculate diel net photosynthesis ($P_{n_{diel}}(O_2)$, $P_{n_{diel}}(CO_2)$), night-time respiration ($R_{N\,diel}\,(O_2)$, $R_{N\,diel}\,(CO_2)$), daytime and night-time calcification ($G_{D_{diel}}$, $G_{D_{diel}}$) and filtration (F_{diel}):

$$P_{n_{diel}}(O_2) = \int_{t=sunrise}^{t=sunset} P_n(t)dt\ ,\ P_{n_{diel}}(CO_2) = \int_{t=sunrise}^{t=sunset} P_n(t)\,dt$$

$$R_{N\,diel}\,(O_2) = \int_{t=sunset}^{t=sunrise} R_N(t)dt\ , R_{N\,diel}\,(CO_2) = \int_{t=sunset}^{t=sunrise} R_N(t)dt$$

$$G_{D_{diel}} = \int_{t=sunrise}^{t=sunset} G(t)\,dt\ , G_{N_{diel}} = \int_{t=sunset}^{t=sunrise} G(t)dt$$

$$F_{diel} = \int_{t=sunrise}^{t=sunset} F(t)\,dt\ , F_{diel} = \int_{t=sunset}^{t=sunrise} F(t)dt$$

Diel carbon sequestration (organic and inorganic) was calculated as follows:

$$C_{seq_{diel}} = P_{n_{diel}}(CO_2) + R_{N\,diel}\,(CO_2) + G_{D_{diel}}(CO_2) + G_{N_{diel}}(CO_2)$$

where $G_{D_{diel}}(CO_2)$ and $G_{N_{diel}}(CO_2)$ are the additive inverse of $G_{D_{diel}}$ and $G_{N_{diel}}$.

Error bars for P_n, R_N, G_D and G_N were calculated for each data point using the first differential method with the analytical errors of all measurements involved in making these metabolic rate estimates (Topping 1972).

Water chemistry analysis. Water samples for A_T and DIC analysis were taken from the benthocosm inlet and outlet into 60 mL brown glass bottles with screw caps and stored at 4°C until analysis. Prior to refrigeration, DIC samples were poisoned with 30 µL (0.05% v/v) saturated $HgCl_2$ solution. A_T was determined by potentiometric Gran titration of ~22g subsamples, filtered through Sartorius 0.45 µm syringe filters using a Metrohm Titrino 785 Titrameter with a temperature corrected pH probe. A_T calculation employed the method described by Sass & Ben-Yaakov (1977). Measurements were calibrated using seawater CRMs from A. Dickson's lab (Scripps Institution of Oceanography, USA). The precision of these measurements was ±2 µmol·kg^{-1} (2 measurements per sample). DIC was extracted from the samples by acidifying them with phosphoric acid (H_3PO_4, 10%) using a custom, automated CO_2 extractor and delivery system (AERICA by MARIANDA) and high grade N_2 (99.999%) as a carrier gas connected on line with a LiCor 6252 IR CO_2 gas analyzer. Measurements were calibrated using seawater CRMs from A. Dickson's lab. The repeatability (mean±SD) of the measurements was 2.1±2.0 µmol·kg^{-1}.

Samples for Chlorophyll a were collected in 3 L plastic bottles that were immediately filtered onto Whatman GF/F glass fiber filters (25 mm), which were immediately wrapped folded in aluminum foil, frozen, and stored at -20°C for later extraction and measurement. Samples were extracted overnight in 5 mL of 90% acetone at 4°C in the dark. Chl. *a* concentrations were determined using a Luminescence Trilogy Spectrofluorometer with a 436 nm excitation filter and a 680 nm emission filter (Holm-Hansen et al. 1965). Samples for nutrient analysis were collected in 15 mL acid-washed plastic scintillation vials and placed immediately in a -20°C freezer pending analysis. Nutrient content was determined from 1–2 plastic scintillation vials using the segmented flow Seal Analytical AA-3 system described by Krom et al. (1991) within 3–6 months of collection. The limits of detection (twice the standard deviation of the blank) were 0.08 µM for nitrate + nitrite, 0.008 µM for phosphate, and 0.05 µM for silicic acid.

2.1.3 Results

2.1.3.1 Seasonal cover, biomass and community structure

The canopy-forming species *Sargassum vulgare* and *Gongolaria rayssiae* showed a very clear seasonal pattern with highest abundance (cover) in the winter and spring and a sharp drop in the warmer seasons (Fig. 8). They were only found in one of the five monitory sites at a time (Fig. 8). *Gongolaria* had very low cover in the deeper sites: RD-1 initially and SK-2 later on, but showed higher percentage in the cold months in the shallow forest site, SK-1. Growth, indicated as the formation and growth of branches from the base cauloid, initiated in February-March while branches were lost in early summer around June when temperatures went above 26 °C (Fig. 8) (Mulas et al. 2022). *Galaxaura* showed high, but fluctuating, cover in two sites SK-2, SK-3 with some indications in reduced cover during the colder months. Between 2013-2018 *Lobophora* have become dominant at the RD-1 site that was initially highly diverse in macroalgae species, and from there on showed extensive fluctuations in cover, that were partly biased by overgrowth by epiphytic species.

Mean cover values from the seasonal surveys of the three main study communities show again the highest values for *Gongolaria* in the spring while the two other species had high cover year-round except for *Galaxaura* in the spring (Fig. 9a).

Biomass of these dominant algae showed generally similar trends to percent cover (Fig. 9b), except for the low biomass of *Lobophora* in the autumn when cover was high (but thallus was flatter with less volume). Biomass of other macroalgae was much lower in the alien macroalgae patches vs. that of *Gongolaria* but was relatively high in spring in the *Galaxaura* patch when that of the *Galaxaura* itself was low. The biomass of other associated algae was high in *Gongolaria* plots (37% of the biomass in the spring) but lower in the alien macroalgae plots.

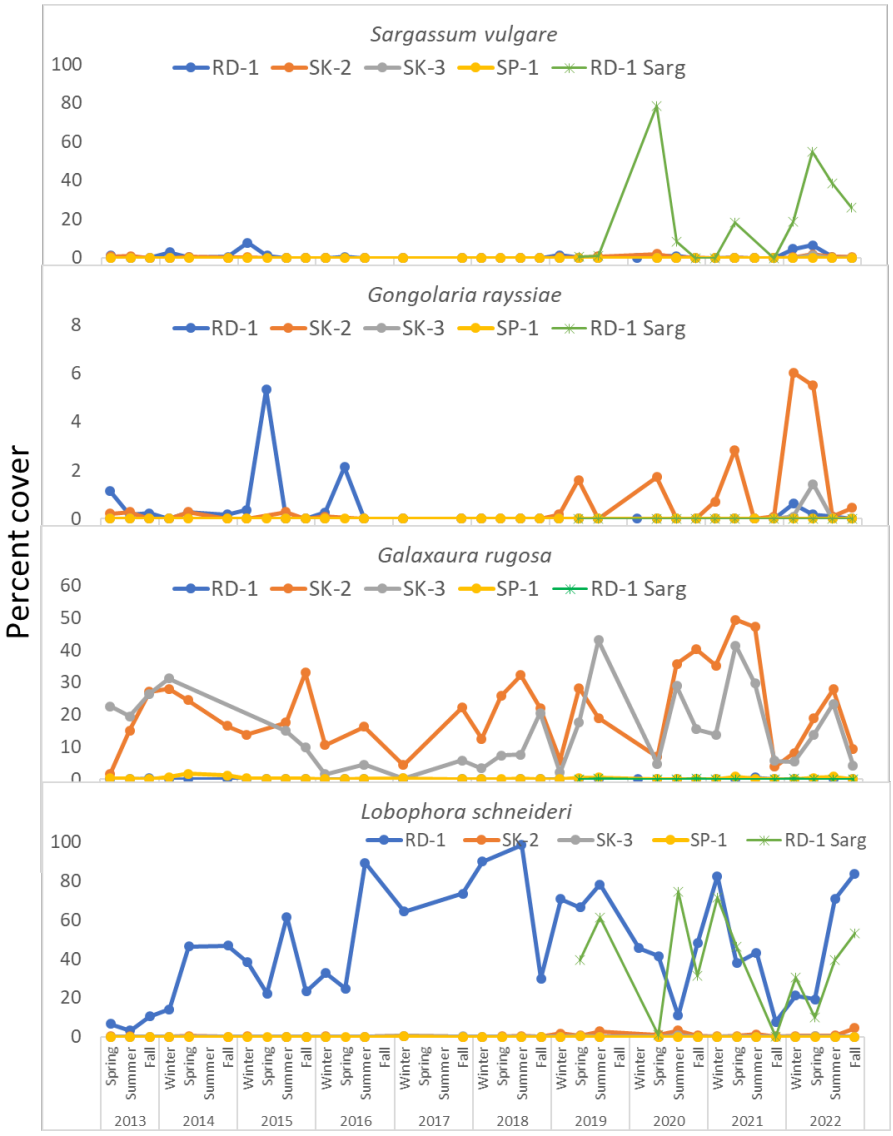

Figure 8 Seasonal dynamics in percent cover of the study species in the five main long-term monitoring sites (a) and the shallow Gongolaria forest site that was monitored monthly for more than two years

Associated invertebrate assemblage biomass had very high variability among replicates, and was high in the colder months (24%) in the *Gongolaria* forest and lowest in winter in *Lobophora* (14%) while it was higher in the fall (20%) in this alien species.

Finally, when comparing the community structure of the three communities based on the biomass of the associated taxa expressed as grams of wet weight per square meter, the nMDS and PERMANOVA analysis indicates a clear separation in structure among them (PERMANOVA, $p_{(perm)}$=0.001; Fig. 10). The *G. rayssiae* community was the only one with a clear separation between the assemblages in the cold and warm seasons.

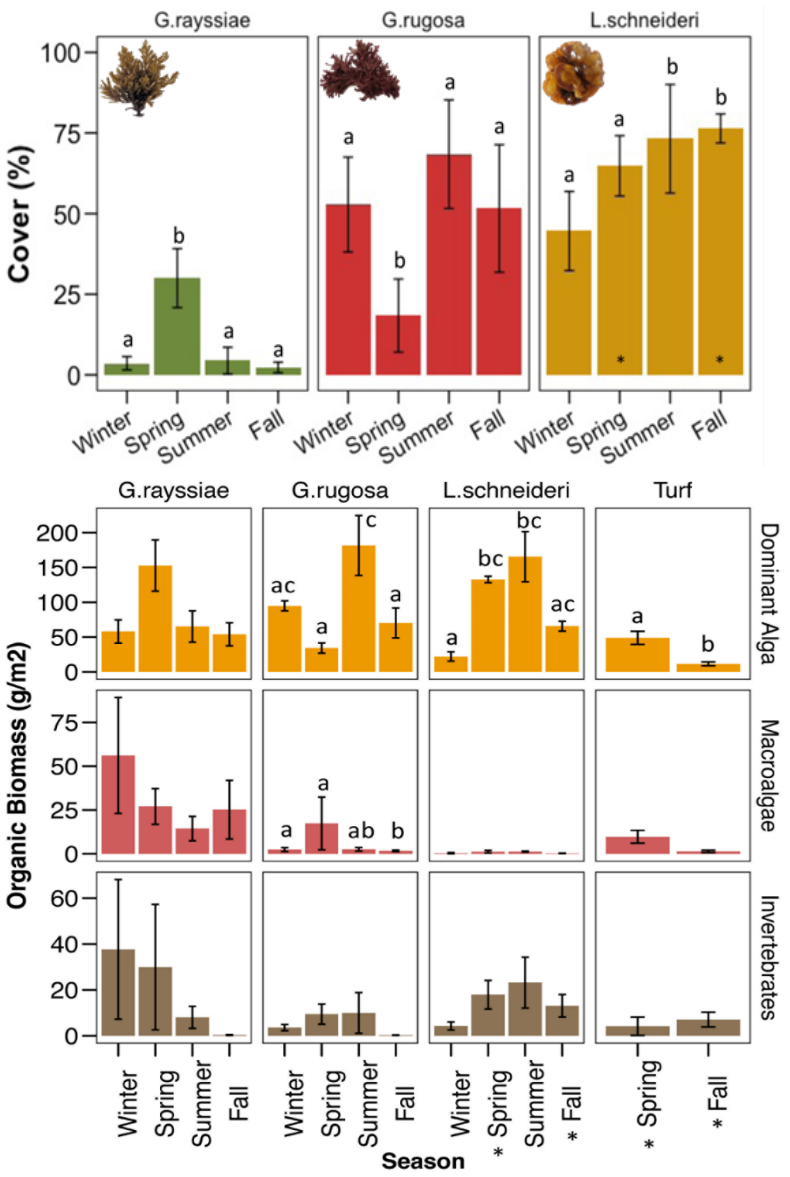

Figure 9 Seasonal means in cover (panel a) and biomass (panel b) of the main study species. The mean organic biomass, expressed as grams of AFDW per m², of the dominant seaweed, associated invertebrates and associated macroalgae species in each of the communities is shown (in b).

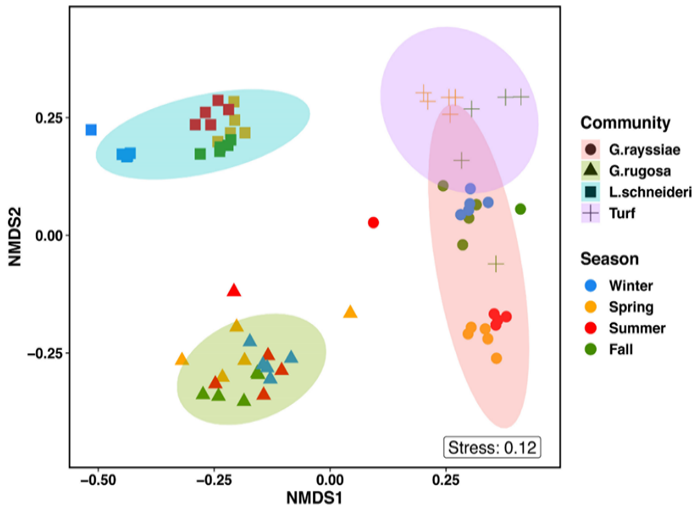

Figure 10 nMDS ordination of community similarity based on Bray-Curtis similarity square root transformed wet weight per square meter data of the four communities collected from 0.25x0.25 m².

Regarding taxa richness of each community, overall the *L. schneideri* community had the highest richness with the highest values in spring (11±1 taxa (±SD)) and fall (9±2 taxa (±SD)), while differences within the same community were found only in *G. rayssiae* between spring vs. fall (One-way ANOVA, $p < 0.001$) (Fig. 11).

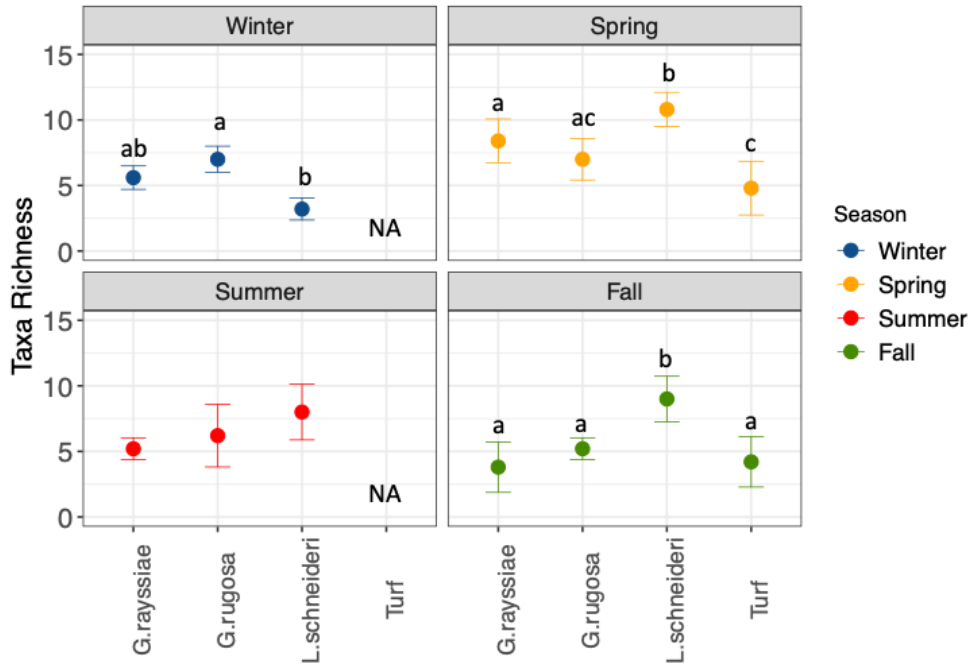

Figure 11 Taxa Richness per 0.25 m² calculated from the wet weight per square meter data matrix of the four communities collected from the quadrats. Data related to the turf and L. schneideri's communities in fall and spring were collected in 0.126 m².

2.1.3.2 Thermal vulnerability (thermal performance curves)

The thermal optimum for photosynthesis of the two native macroalgae, *Gongolaria* and *Sargassum*, was much lower than (below 25 °C) that of the two alien species (above 30 °C) (Fig. 12). Their critical maximum on the other hand was much closer to the optimum temperature in the alien macroalgae as compared to the two native species. The optimum temperature of the native herbivorous crab, *Acanthonyx lunulatus*, that lives within the macroalgae patches, was just below 30 °C (Fig. 13a), that of the Red Sea rabbitfish, *Siganus rivulatus*, was somewhere between 28-31 °C (Fig. 13c, d), while the feeding reduced considerably in the invasive urchin, *Diadema setosum*, only above 32 °C (Fig. 13b).

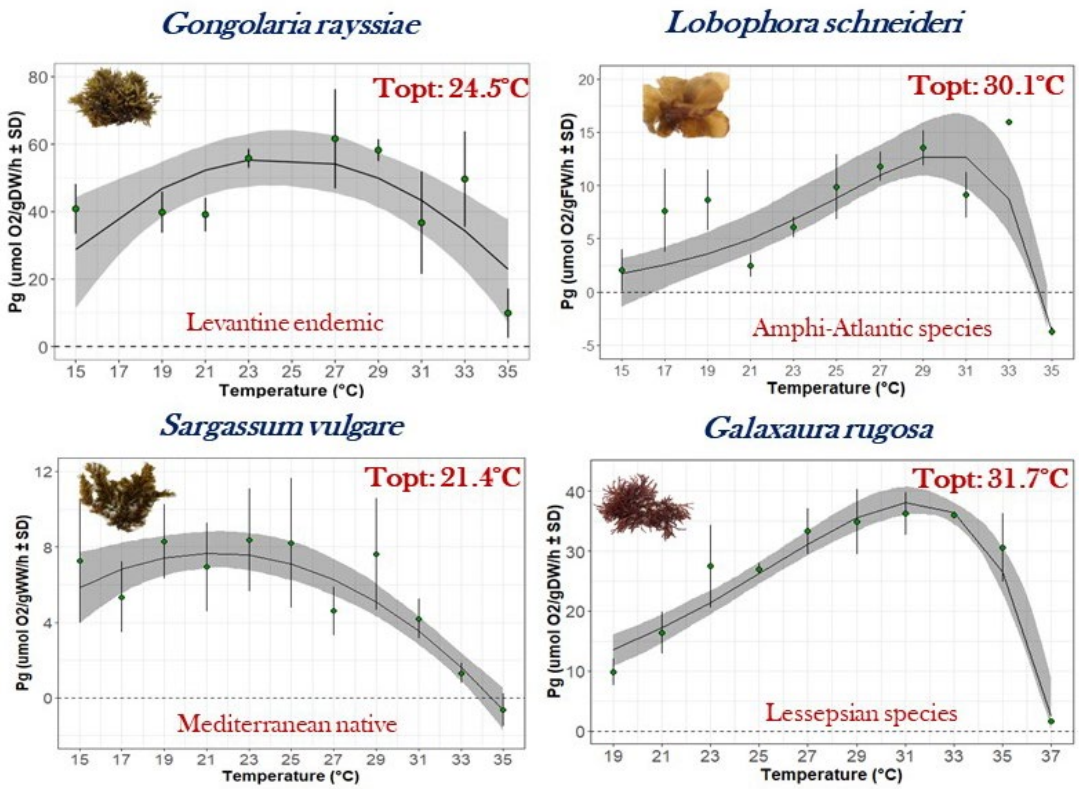

Figure 12 The thermal performance curve of gross photosynthesis (per gram wet or dry weight, depending on the species) for the four study macroalgae.

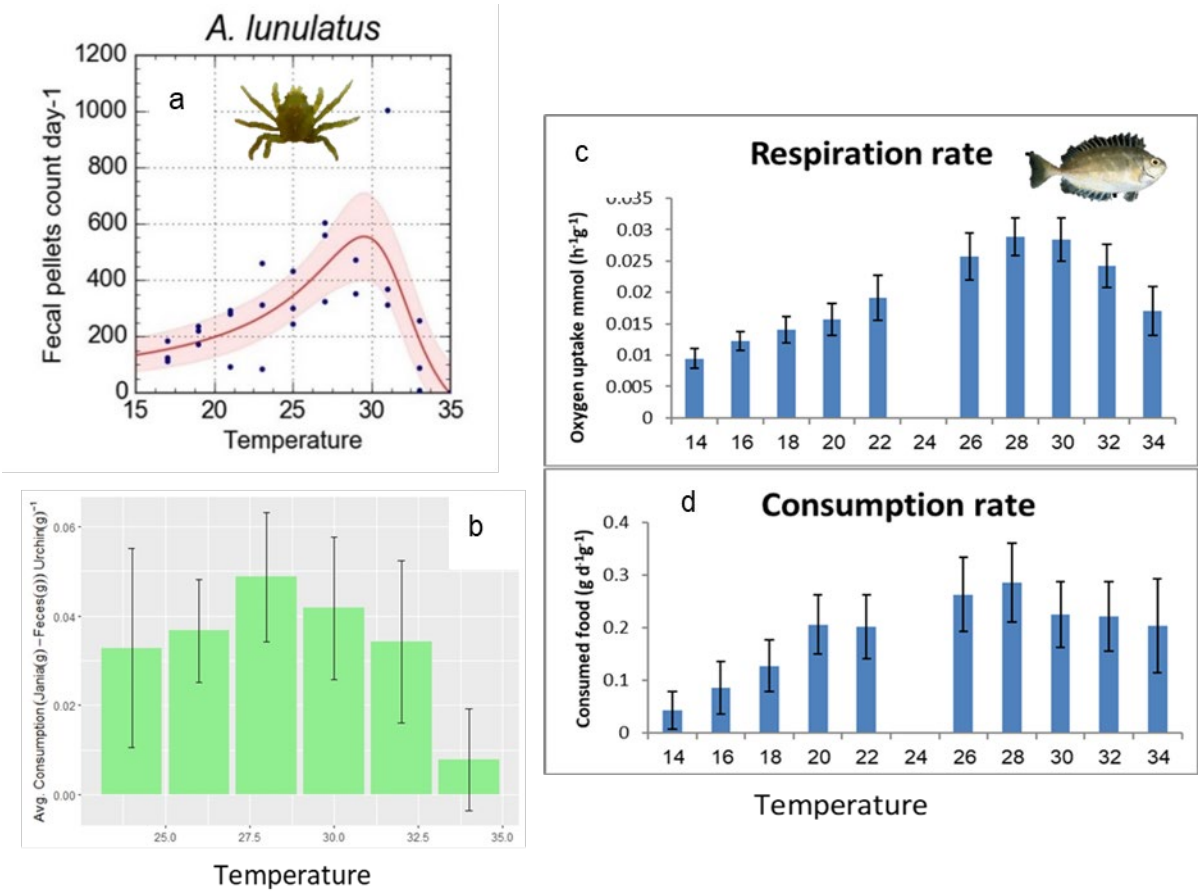

Figure 13 The thermal performance curve of native and alien macroalgae consumers. The native crab, Acanthonyx lunulatus (a) and the alien urchin Diadema setosum (b) where performance was measured by the production of fecal pellets, and the alien rabbitfish, Siganus rivulatus,based on respiration (c) and food consumption (d).

2.1.3.3 Seasonal productivity

Overall, the Atlantic newcomer *L. schneideri* had the highest net photosynthetic production in terms of DO (NPDO) (around 55 µmol O_2·g dw^{-1}·h^{-1}), among all species, except for spring (25±14 µmol O_2·g dw^{-1}·h^{-1}) (Two-way ANOVA, p<0.001; Fig. 14 A, D, G). The Indo-Pacific invader, *G. rugosa* had relatively stable values between 20-40 µmol O_2·g dw^{-1}·h^{-1} in all seasons, while the native *G. rayssiae* was highly productive (39±14 µmol O_2·g dw^{-1}·h^{-1}) only in spring (Fig. 14 A, B). Respiration rates as measured with DO (RDO) were relatively similar among species, except for slightly higher values in *L. schneideri* in summer and fall when it was almost three-fold the other two seaweed's rates. Net carbon production (NPDIC) and respiration (RDIC), showed overall similar trends when compared to the DO-based rates, except for *G. rugosa* (Three-way ANOVA, p<0.01) and *L. schneideri* which showed higher C uptake (One-way ANOVA, p < 0.01) and release in spring (Fig. 14 E) and summer (Fig. 14 H), respectively (Kruskal-Wallis test, p < 0.01).

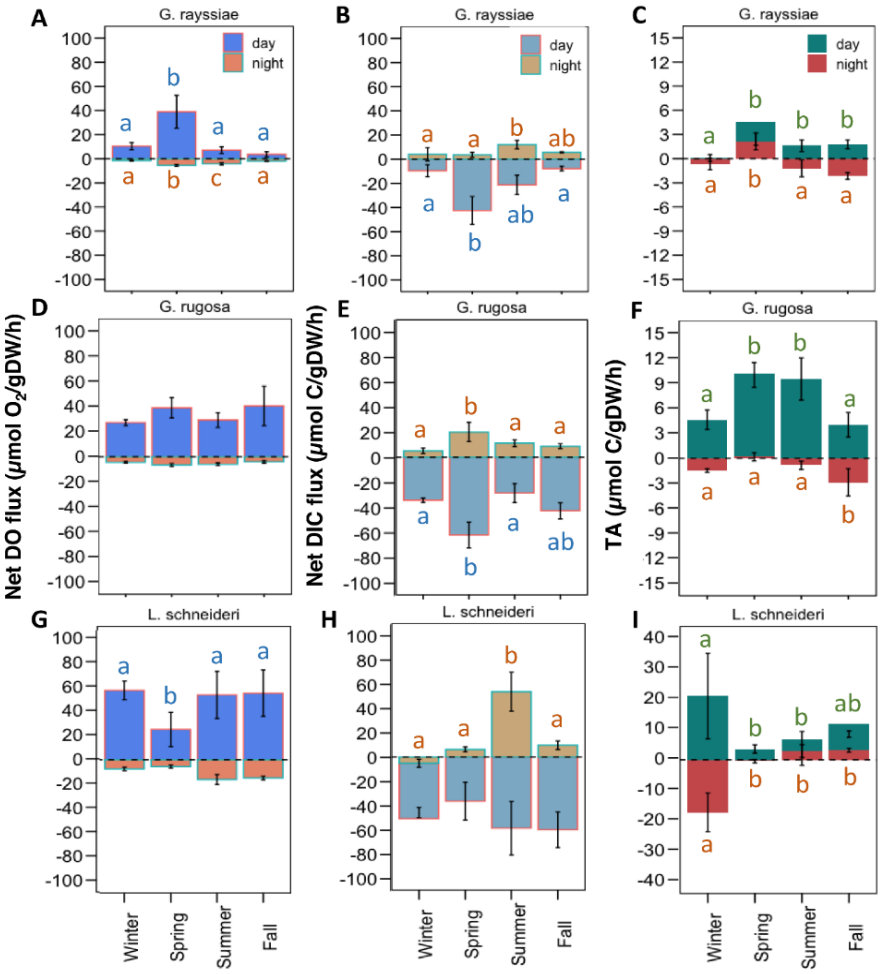

Figure 14 Ex-Situ single species incubations average metabolic rates measured in G. rayssiae, G. rugosa and L. schneideri seaweeds under day and nighttime conditions: Net Production (NP) and respiration (R) are measured as changes in (A) DO and (B) DIC adjusted f

Total alkalinity (TA) analysis (Fig. 14 C,F,I) indicated that: (1) In the non-calcifying *G. rayssiae*, alkalinity uptake/production rates were low with more production than uptake in most seasons except during spring (the growing season) when in both daytime and nighttime TA uptake was observed; (2) In the calcifying invader, *G. rugosa* we recorded high TA uptake during the daytime and low TA production during the nighttime, likely indicating calcification and $CaCO_3$ dissolution, respectively, with an overall net calcification; (3) In the non-calcifying newcomer *L. schneideri*, TA uptake dominated the daytime measurements as well as low rates of TA production during the nighttime, with particularly high values in winter. It should be noted that since both *G. rayssiae* and *L. schneideri* are non-calcifying, it is not clear what these recorded changes in TA signify, albeit that their rates are similar or greater in some seasons to those exhibited by *G. rugosa*. It is possible that calcifying organisms, such as foraminifera, remained attached to the thalli after our thorough cleansing of the seaweeds. Furthermore, $CaCO_3$ may have deposited chemically on the surface of the algae or intracellularly during light incubation, while during dark incubations, $CaCO_3$ may have been dissolved due to increase levels of CO_2 and reduced pH near the surface of the algae and intracellularly.

When considering gross primary production (GPPDO) rates, *L. schneideri* showed the highest values among the three seaweeds. Significant differences were recorded in winter and summer between *G. rugosa* vs. *L. schneideri* and with the latter vs. *G. rayssiae*, while in fall among G. rayssiae vs. the other two (One-way ANOVA, $p<0.0001$; Fig. 14 A, D, G). In contrast, a different trend was obtained when we considered the GPPDIC, where L. schneideri differed from both G. rugosa and G. rayssiae in summer, in spring we recorded statistical differences among L. schneideri vs. G. rugosa, and finally in fall *L. schneideri* vs. *G. rayssiae* (Two-way ANOVA, $p<0.01$).

Based on these data, we calculated the seasonal diel fluctuations of oxygen and carbon production and uptake rates for the three seaweed species (Table 1). *G. rayssiae* showed similar trends using both DO and DIC, with the highest rates recorded in spring (Two-way ANOVA, $p<0.001$). *G. rugosa* did not show significant seasonal fluctuations in terms of DO, while in terms of DIC, spring was different from winter (Two-way ANOVA, $p<0.01$). In *L. schneideri,* the lowest rate of diel O_2 production was recorded in spring, which was significantly different from summer (Two-way ANOVA, $p < 0.05$), but no differences were found in the DIC based rates. Considering primary productivity per area (Fig. 15), the overall highest levels were recorded in summer in *L. schneideri* (9±4 g $O_2 \cdot m^{-2} \cdot d^{-1}$ (±SD) and -2±1 g $C \cdot m^{-2} \cdot d^{-1}$ (±SD)). When comparing the species in each season based on DO, during winter the highest rate was recorded in *G. rugosa* (2.75 ± 0.29 g $O2 \cdot m^{-2} \cdot d^{-1}$ (±SD)) and the lowest in *G. rayssiae* (0.41 ± 0.13 g $O2 \cdot m^{-2} \cdot d^{-1}$ (±SD)). There was no difference in spring, while in summer and fall *G. rayssiae* was significantly lower than the other two (One-way ANOVA, $p < 0.001$). When comparing each species by seasons, *G. rayssiae* showed the highest photosynthetic rate in spring, which differed from fall (Kruskal-Wallis, $p <0.01$); *G. rugosa* productivity was higher in summer when compared to spring (One-way ANOVA, $p < 0.0001$), and *L. schneideri*'s was significantly higher in summer compared to all the rest (One-way ANOVA, $p < 0.01$) (Fig. 15 A). In terms of DIC, seasonal differences within the same species were generally subtler and not significant, except that in *L. schneideri* where summer rates were the highest and significantly different only compared to the winter ones (Two-way ANOVA, $p < 0.001$; Fig. 15 B). From species comparison, *G. rayssiae* showed a significant lower C uptake in summer than *L. schneideri*. Finally, we used these data to estimate the annual primary productivity of the three seaweeds in terms of O_2 production and C sequestration as shown in Table 1.

Table 1 Seasonal and annual oxygen production and C sequestration of the tested seaweeds. Net diel photosynthetic rates (NPP) are given as µmol O2 and C per grams of dry weight per day and per annum and biomass expressed as grams of dry weight per square meters

Value	**Units**	**Season**	**Species**		
			G. rayssiae	G. rugosa	L. schneideri
NPP O_2	µmol O_2 g dw^{-1} d^{-1}	Winter	124 ± 39	319 ± 33	690 ± 90
		Spring	562 ± 206	553 ± 118	344 ± 212
		Summer	89 ± 47	423 ± 88	730 ± 304
		Fall	33 ± 32	533 ± 212	629 ± 260
	mmol O_2 g dw^{-1} y^{-1}	Annual	26	69	79

NPP C	µmol C g dw^{-1} d^{-1}	Winter Spring Summer Fall	-93 ± 44 -594 ± 157 -249 ± 134 -72 ± 26	-296 ± 207 -717 ± 121 -303 ± 99 -310 ± 297	-840 ± 183 -502 ± 220 -471 ± 236 -655 ± 201
	mmol C g dw^{-1} y^{-1}	Annual	-28	-63	-33
Biomass	g dw^{-1} m^{-2}	Winter Spring Summer Fall	101.9 ± 40.8 211.8 ± 89.3 127.1 ± 67.8 106.3 ± 76.0	269.8 ± 61.1 93.2 ± 33.5 414.1 ± 187.6 204.6 ± 119.5	56.7 ± 7.2 241.9 ± 34.5 415.6 ± 78.9 126.5 ± 31.6

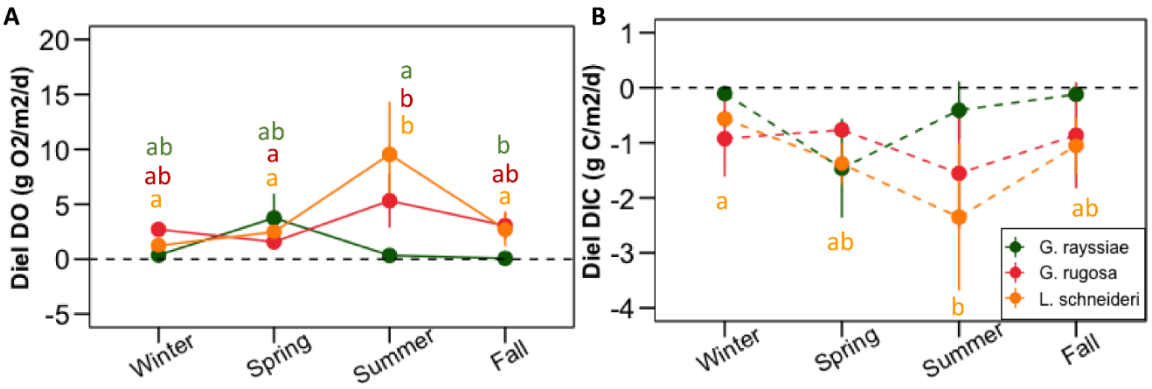

Figure 15 Seasonal diel metabolic rates of the three dominant Levantine basin seaweeds measured as changes in (A) DO and (B) DIC. Error bars represent standard deviations. The letters in the graphs represent significant differences between the same species at diff

2.1.3.4 In-situ incubations

The seasonal net production and dark respiration rates show that the *G. rayssiae* community varied between highly autotrophic (NP>R) during spring and trophic balance (NP~R) in fall (Fig. 16). In contrast, the *L. schneideri* community shifted between autotrophy in winter, trophic balance in spring and heterotrophy (NP<R) in fall, while turf showed a low autotrophy balance in spring to then switch towards a low heterotrophy in fall. Both *G. rayssiae* and *L. schneideri* communities are sources of total alkalinity during both daytime and nighttime with the highest rate exhibited by the *L. schneideri* community during winter and the next highest by *G. rayssiae* community during fall, while within the turf we recorded a high variability tending towards calcification in spring and dissolution in fall.

Gross primary productivity based on Oxygen change (GPP_{DO}) was calculated by adding the values from the light (NP_{DO}) and dark incubation (R_{DO}) (Fig. 16). Production was much higher in spring compared to fall in the *G. rayssiae*'s community, and in *L. schneideri*'s was positive in winter and spring and negative (heterotrophic) in fall. Among communities, in spring *G. rayssiae*'s was much more productive than the other two, while in fall the only differences were between turf and the other two (One-way ANOVA, $p < 0.01$). Production indicated by carbon (GPP_{DIC}) showed a matching (opposite) trend. NP_{DIC} showed significant seasonal differences between spring and fall in all the three communities and additionally between fall and winter for *L. schneideri*. Finally, during light and dark incubations, all three communities showed a net $CaCO_3$ precipitation (calcification) in the different seasons, except for some minor dissolution in fall in *L. schneideri* and a higher one in turf-barrens in spring, under dark conditions.

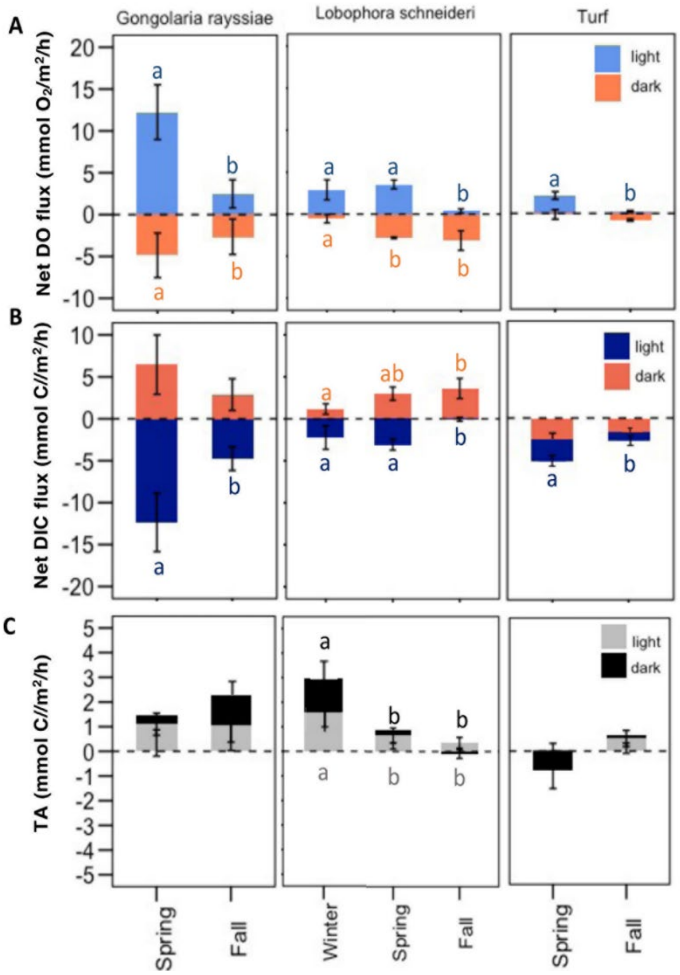

Figure 16 Seasonal metabolic rates of G. rayssiae, L. schneideri and turf communities measured at SK1 (G. rayssiae and turf) and RD1. (A) NP in terms of dissolved oxygen (DO), (B) NP in terms of dissolved inorganic carbon (DIC), (C) Total Alkalinity flux (TA).

Daily rates of community metabolism were calculated from the integration of GPP, R and G along the diurnal cycle (considering the cycle of illumination). Overall, the *G. rayssiae* community was significantly more productive than the other two communities in spring, while in fall, although almost 6 times less efficient, it was the only community among the three to show positive diurnal rate values (149.53 ± 35.30 (±SD) and 27.27 ± 40.42 (±SD) mmol O_2 m^{-2} d^{-1}, respectively) (Two-way ANOVA, $p < 0.05$) (Fig. 17 A). The carbon uptake/release data showed similar trends. *L. schneideri* showed autotrophic balance in spring and winter, while in fall

oxygen consumption and C production were recorded, meaning heterotrophic balance. Finally, during spring, the turf community exhibited net oxygen production and DIC uptake, while in fall there was a net oxygen consumption with almost 10-fold C intake (Fig. 17 A, B).

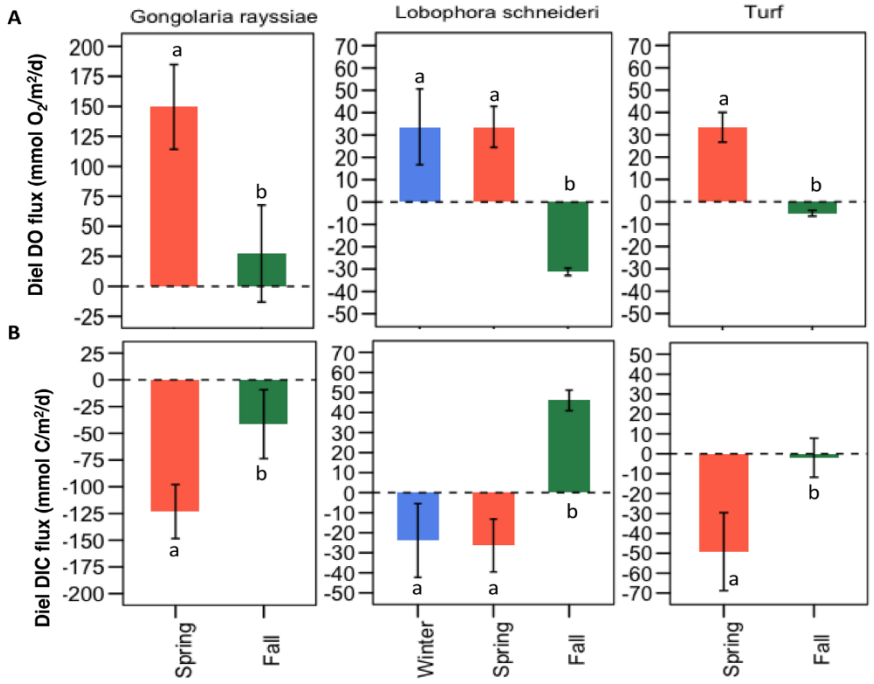

Figure 17 Seasonal diel metabolic rates of G. rayssiae, L. schneideri and turf communities measured at SK1 (G. rayssiae and turf) and RD1. (A) Diel NP in terms of dissolved oxygen (DO), and (B) dissolved inorganic carbon (DIC). Error bars represent standard deviations. Significant differences within the same community are reported with letters ($p < 0.05$). Note: the y-axes are different.

2.1.3.5 Mesocosm experiments

We are showing here only a fraction of the results stemming from this large experiment that are most relevant to the Storyline. Because the benthocosm is an open system which allows recruitment of algal propagules and larval recruitment, the experiments ended with many more species in the community (around 30 on average, Table 2) than at the start of the experiments (5). Many of these species were aliens. However, the community diversity indices indicated that taxa richness (S), evenness (J') and Shannon-Wiener diversity (H') were higher in the summer than in the winter (Table 2, 2-way ANOVA, $p<0.01$) but did not differ significantly between treatments (2-way ANOVA, $p>0.05$).

Table 2 Taxa richness (S), Evenness (J') and Shannon-Weiner diversity index (H') in the benthocosm treatments at the experimental endpoint, in the winter and summer (values represent averages ± SD, n=3).

	Autumn-Winter			Spring-Summer		
Treatment	S	J'	H'(loge)	S	J'	H'(loge)
AM	29.3±1.5	0.54±0.15	1.80±0.52	34.7±2.1	0.72±0.05	2.55±0.22
OC	31.0±2.0	0.43±0.04	1.47±0.15	33.3±1.2	0.71±0.05	2.47±0.17
OW	33.0±4.4	0.60±0.01	2.09±0.09	32.7±3.5	0.69±0.05	2.41±0.23
OA	30.3±1.2	0.47±0.14	1.59±0.47	32.0±1.0	0.74±0.04	2.57±0.12

OWA	34.7±1.2	0.56±0.11	1.99±0.41	34.3±4.2	0.67±0.13	2.38±0.50

The majority of the biomass of the basiphytic algae in the benthocosm experiments stemmed from the algae that were transplanted in the benthocosms at the beginning of the experiment (*G. rayssiae*, *G. rugosa*), while all the epiphytic biomass settled independently within the benthocosms throughout the experiments (e.g., *Dictyota spp*, *Polysiphonia* sp., Fig. 18). Three-way ANOVA on the effect of algal growth form (basiphyte *vs.* epiphyte), season and treatment, revealed a significant effect of the growth form, season, and their combinations. The highest relative growth of epiphytic algae was obtained under the combined treatment of warming and acidification during the winter, where non-calcifying epiphytes heavily settled on *G. rayssiae* and *G. rugosa* (Fig. 18).

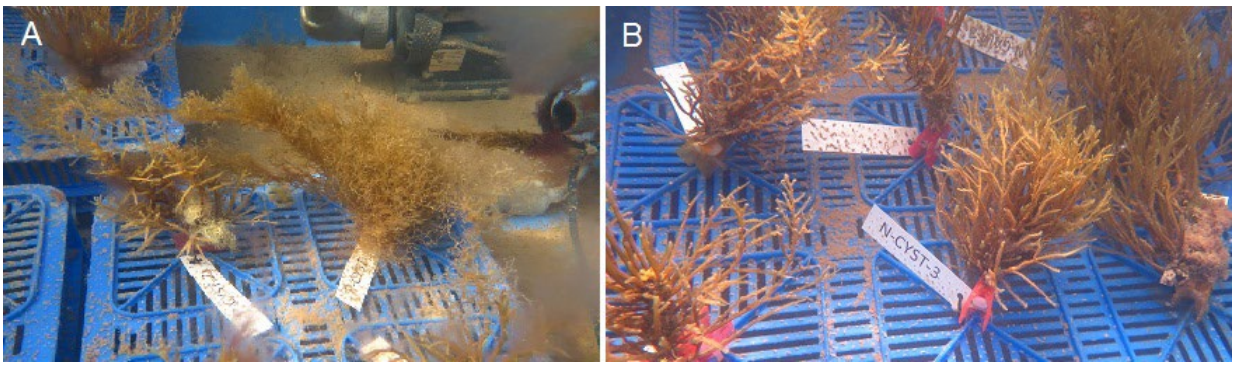

Figure 18 A. Epiphytic Dictyota spp. completely covered the basiphyte G. rayssiae under combined warming and acidification, whereas under cooling (B) macroepiphytes were scarce.

The total biomass of calcareous and non-calcareous taxa was significantly different between seasons (Fig. 19, 2-way ANOVA, $p<0.05$). The ratio between calcareous and non-calcareous taxa (Table 2) differed significantly between seasons and treatments (2-way ANOVA, $p<0.05$). In the winter (Fig. 20 A), the average ratio was <1 under all treatments except warming, where it was even. In the summer (Fig. 20 B), this ratio was >1 in all treatments apart from the cooling treatment. The post-hoc Tukey HSD test revealed significantly higher calcareous: non-calcareous ratio in the warming *vs.* cooling treatments. The acidified treatments had the lowest ratio in the winter, and the highest in the summer (Table 3).

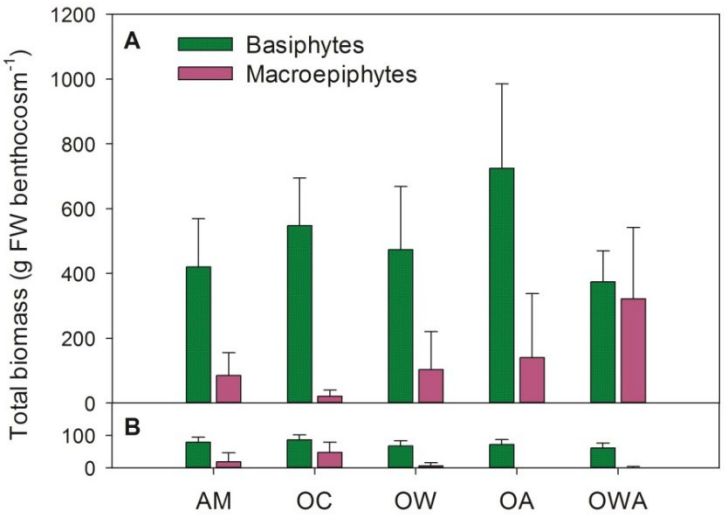

Figure 19 Average total algal biomass of basiphytes and macroepiphytes (g FW) per benthocosm tank under five treatments. A. winter 2015, B. summer 2015. Error bars denote standard deviation (n=3).

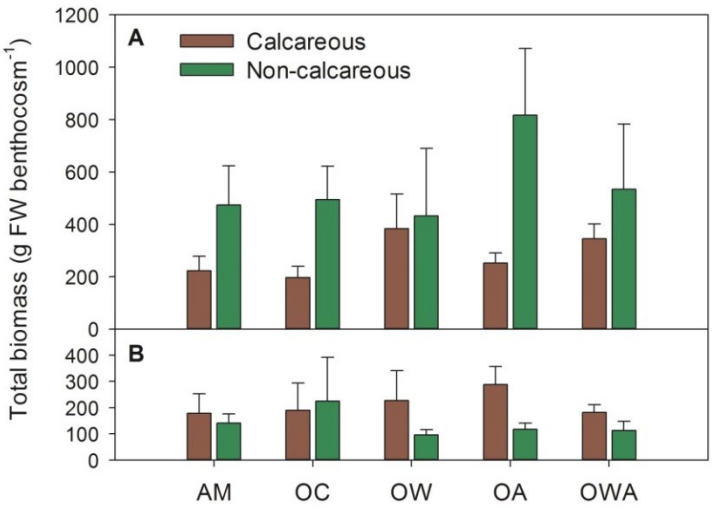

Figure 20 Average total biomass of calcareous and non-calcareous taxa (g FW) per benthocosm tank under five treatments. A. Winter 2015, B. Summer 2015. Error bars denote standard deviation (n=3).

Table 3 The ratio between the total biomass of calcareous and non-calcareous taxa in the benthocosm treatments (values represent averages ± SD, n=3).

Treatment	Autumn-Winter	Spring-Summer
AM	0.48±0.07	1.42±0.92
OC	0.40±0.02	0.94±0.28
OW	1.01±0.32	2.26±0.76
OA	0.34±0.15	2.49±0.65
OWA	0.79±0.49	1.71±0.54

Ecosystem functions. In the winter, the most productive system was the warmed benthocosm (Fig. 21A, C), whereas in the summer, the acidified benthocosm was the most productive in terms of oxygen production (Fig. 21 B), and the cooled benthocosm was the most productive in terms of dissolved inorganic carbon uptake (Fig. 21 D). In the winter, all treatments except the combined warming and acidification, had a positive oxygen budget (Fig. 21 A) and negative inorganic carbon budget (Fig. 21 C), indicating that these systems were autotrophic, whereas under combined warming and acidification the system was heterotrophic. In the summer, the calculated oxygen budget indicates that under warming the system was heterotrophic (Fig. 21 B), whereas the inorganic carbon budget indicates that only under combined warming and acidification the system was heterotrophic (Fig. 21 D).

Diel net calcification (Fig. 22) was positive in all treatments and seasons, except a slightly negative diel budget in the summer under the combined warming and acidification (Fig. 22 B). Nighttime dissolution was observed under all treatments except the cooling treatment in the winter, where nighttime calcification was measured (Fig. 22 A). In both winter and summer, the highest net diel calcification rates were measured in the cooling treatment.

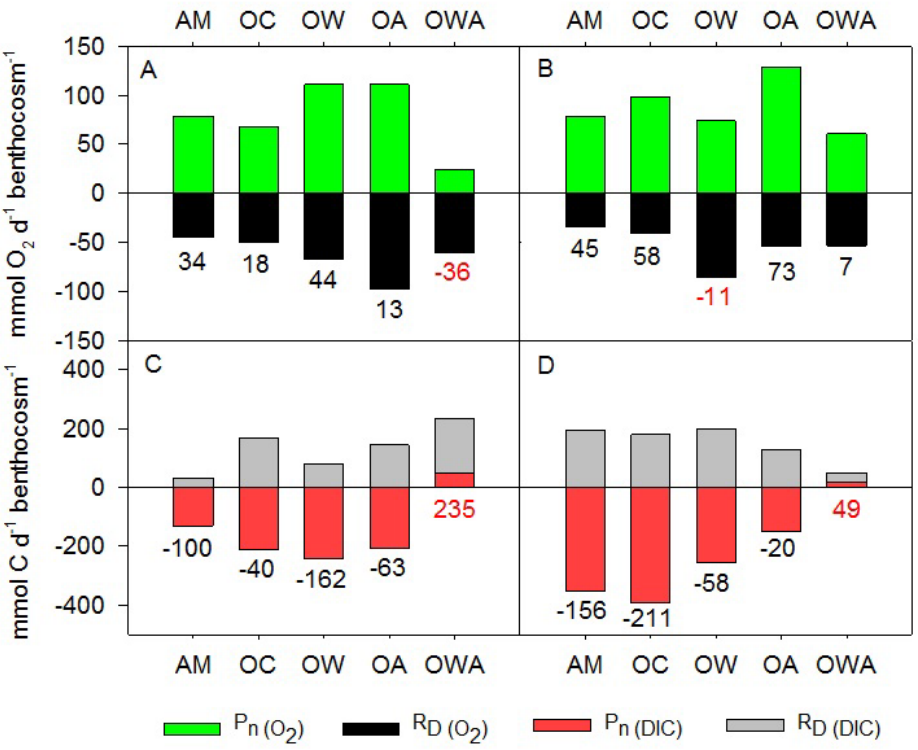

Figure 21 Diel net production (Pn) and night-time respiration (RN) as a function of dissolved oxygen (A, B) and dissolved inorganic carbon (C, D) in the benthocosms, in winter 2015 (A, C) and summer 2015 (B, D). The diel budgets of oxygen and carbon are noted in the numbers below the bars: autotrophic budget is marked in black, heterotrophic budget is marked in red.

In both winter and summer, the total diel sequestered carbon (Fig. 23) was negative, indicating a carbon sink, under all treatments except the combined warming and acidification, where a positive budget was measured - indicating a carbon source.

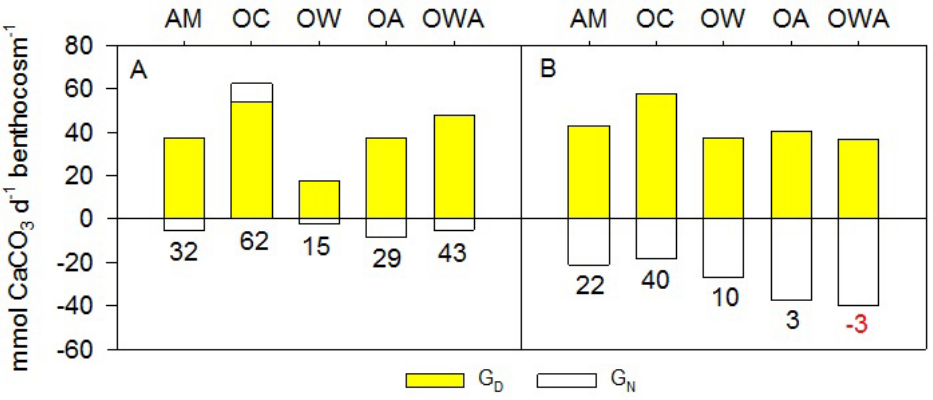

Figure 22 Daytime calcification (GD) and night-time calcification (GN) in the benthocosms, in winter 2015 (A) and summer 2015 (B). The diel budgets are noted in the numbers below the bars: net calcification is marked in black, net dissolution is marked in red.

Figure 23 Total sequestered dissolved inorganic carbon, as a result of photosynthesis, respiration, calcification, and dissolution in the benthocosms, in winter 2015 (A) and summer 2015 (B). Negative values indicate carbon sink, positive values indicate carbon source.

2.1.4 Discussion

Seasonality

Our results from the field sampling indicated a very strong seasonality of the native canopy-forming algae (i.e., *Gongolaria rayssiae* and *Sargassum vulgare*) which have a very short growth season (growing and branching). Growth occurs from late winter to spring or early summer after which most (*Gongolaria*, left only the cauloid) or all (*Sargassum*) of their biomass has disappeared. This is in contrast to the tropical alien species invading from the Indopacific (*Galaxaura rugosa*) and Atlantic (*Lobophora schneideri*), which varied much less in cover and biomass along the year. Specifically, we demonstrated that,

at high temperatures, the two non-indigenous species, *G. rugosa* and *L. schneideri*, attained their peak biomass during the summer, when temperatures can reach up to 32°C, while the endemic foundation species, *G. rayssiae*, reached its peak biomass in spring (SST~21°C), and similar trends were consistent when considering the percent cover. The lowest value for *G. rugosa* was in spring, following the coldest months of the year as was also previously shown by Garval (2015). These seasonal trends fit well with the thermal performance of the species. Perhaps not surprisingly, the two Mediterranean native canopy-forming macroalgal species had much lower optimal (photosynthetic rates) temperatures, below 25 °C, than that of the two tropical aliens with an optimum above 30 °C. Based on their TPC and the fact that the Israeli coastal water already warmed by about 3°C in the past few decades (Rilov 2016, Ozer et al. 2022) we can also assume that the tested canopy-forming, native, brown seaweeds' growth season has already shrunk considerably compared to the past.

Furthermore, these results suggest an adaptation of the invasive species to the low nutrient conditions that prevail in Israeli coastal waters (Rahav et al. 2018, Rahav et al. 2020), especially during the summertime, when the alien algae attain the highest biomass, while the endemic species have their peak in spring. Nutrient levels in the southeastern Levant coastal waters are generally higher during the spring and much lower during the summer. This may be the result of reduced nutrient loads from submarine groundwater discharge during the summer directly onto the shallow reefs in northern Israel compared to spring (Rahav et al. 2020, Kolker et al. 2021).

Our calculations show that, under present conditions, the annual standing stock (Blue Carbon potential) of the two invaders seems to be 1.5-1.8 times higher than the that of the endemic *G. rayssiae*. Furthermore, the associated invertebrate biomass was highest in winter and spring in *G. rayssiae*, and during summer and fall in *L. schneideri*. This difference could be attributed

to the different peak cover and biomass of the two seaweeds: when at its branchless stage between summer and early winter, *G. rayssiae* offers less surface and complexity to hide within or under, while the rosette shape of *L. schneideri* creates a flat canopy under which other organisms can hide all year round.

From the consumers' side, the native grazer crab, *Acanthonyx lunulatus*, had a slightly lower optimum temperature for feeding (near 29 °C) compared to the two invasive Red Sea grazers: the former invader, the rabbitfish *Siganus rivulatus*, and the much more recent invader, the urchin, *Diadema setosum*. This suggests that the native species already is a less effective consumer during the peak summer season when temperatures reach between 31-32°C (compared to 29 °C, several decades ago). The alien species, however, can handle these summer temperatures but may be stressed under future temperatures that, according to the downscaling models for the region developed in WP2, are projected to be close to 4 degrees higher than today under the SPP5-8.5 scenario (Fig. 24).

Functionality

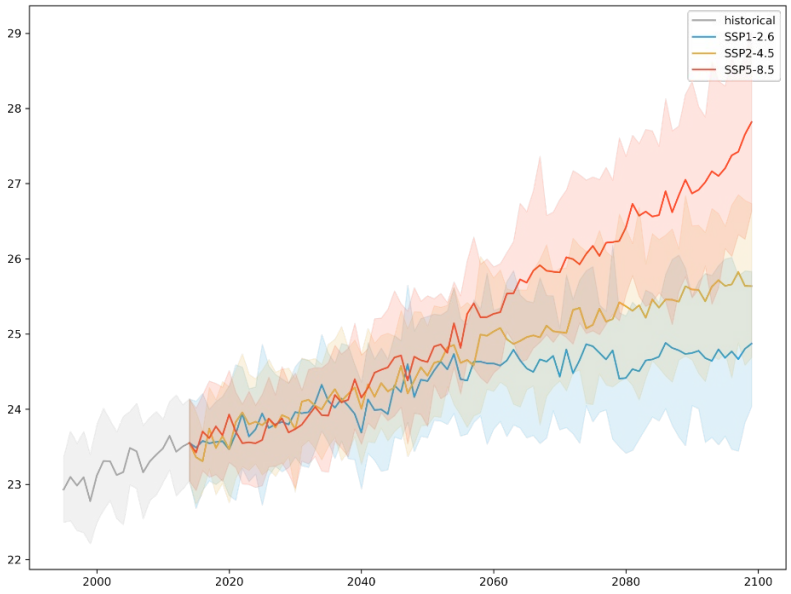

Figure 24 Mean temperature for the Israeli Mediterranean territorial waters under the different SPP scenarios as predicted by the downscaling models developed in WP2 for the end of the century.

According to Littler (1980), the morphology and functionality of macroalgae co-evolved. Based on conventional morphological groups, the main investigated species have very different morphologies: the native endemic *G. rayssiae* belongs to the "thick blades and branches" form, *G. rugosa* to the "articulated" form and *L. schneideri* to "sheet/blade-like" form. The "thick blades and branches" group allocates a greater proportion of energy to structural vs. photosynthetic tissues, exhibiting lower metabolic rates and lower net production per g dry weight (Littler 1980, Ho et al. 2021). A similar trend has been identified for the "articulated" form, while the "sheet/blade-like" shape minimizes the shading, their thinner-walled cells produce less shade of the photosynthetic apparatus so that together with a larger exposed surface area they are a more photosynthetically efficient group (Littler 1980). This might explain the highest efficiency of *L. schneideri* among the three studied species, both in the hourly measurements and in the calculated daily rates. In fact, overall *L. schneideri* showed the highest primary productivity in terms of DO except in spring, when its hourly rates were two-fold lower than the other two species. When assessing the functions in terms of carbon, we obtained similar patterns, with significant differences only in summer between *L. schneideri* and *G. rayssiae*.

The very different morphologies of the three study species probably also explain the very different community structure associated with these species. Our data indicated that species richness was comparable among species (and even higher within the alien species) but the

identity of the species and/or their relative abundance/biomass was considerably different. In that sense, all three species support rich albeit different assemblages when fully grown. This indicates that the alien species does not offer the same habitat functionality as the native habitat-forming species but still support a rich community compared to a turf community that dominates the reef today, a finding similar to what was show in the spring season by Peleg et al. (2020).

Single species annual metabolic rates were converted into unit of surface area where rates for L. schneideri, G. rugosa and the native G. rayssiae reached 83, 186 and 46 g $C \cdot m^{-2} \cdot y^{-1}$, respectively. These results were comparable with rates obtained from other studies conducted on *Cystoseira* s.l. species in the Mediterranean Sea stressing the importance of studying and quantifying the rates of these dominant macroalgae in different locations (Ballesteros, 1990a, 1990b, 1992). The results also suggest that, in isolation, the alien species could potentially compensate, or over-compensate for the productivity and carbon uptake of the native species that is at risk of collapse due to further ocean warming, a collapse that may seriously compromise the viability of the local populations. A collapse in *Gongolaria* may mean a global extinction as it is endemic only to the coast of Lebanon and Israel (Mulas et al. 2020).

Compared to the *ex-situ* metabolic functions measured in the laboratory for the different algal species, *in-situ*, the final net production or C uptake (sequestration) in the seaweed community was expected to be different because it is the result of the metabolism of the entire assemblage The assemblage can include the simultaneous metabolic rates of many different associated species, including consumers, in different abundances within the community under natural environmental conditions (i.e., not in a jar in the lab). Diel rates of the *G. rayssiae* community measured *in-situ* in spring were ca. 5 time greater than its autumn rate, when only the cauloid is present, which is consistent with the single-species lab incubations. Interestingly, the invasive *L. schneideri* community exhibited positive net production (autotrophic balance) in spring and winter, similar to the turf community net production in spring. In the autumn, however, both communities were in heterotrophic balance. In contrast, the diel primary productivity of the same Atlantic invader measured in species-level laboratory incubations, did not differ between winter, autumn and spring. Thus, the heterotrophic balance obtained from the community incubations in the autumn could be explained by its relatively lower biomass compared to the higher abundance of invertebrates, which was greater compared to winter and spring (20% vs. 14% and 12%, respectively). Despite this, it is interesting to note that the net production recorded in-situ in winter (34±17 mmol $O_2 \cdot m^{-2} \cdot d^{-1}$) was similar to the calculated single species ex-situ results for that season (ca. 36.7 mmol $O_2 \cdot m^{-2} \cdot d^{-1}$) suggesting that the combined *in-situ* algal community productivity was sufficiently large to offset the respiration of the heterotrophic components of the community. The results of this study confirmed the finding of Peleg et al. (2020) that the current dominating low-laying turf barren community (Rilov et al. 2018), formed mainly by rabbitfish overgrazing (Sala et al. 2011, Yeruham et al. 2020), has very low habitat and metabolic functionality compared to both native and alien macrophyte-dominated communities in the SEM.

The future of native forests under climate change

Shifting traits under future conditions. Our mesocosm experiment showed that the native, endemic, forest-forming macroalgae and its associated assemblage will be strongly affected by future ocean conditions of warming and acidification in both their dominant traits and metabolic functioning. Although the univariate diversity indices did not indicate any significant change, species composition in terms of origin and functional groups differed considerably between treatments. Thus, the evident parity in the diversity indices is the outcome of a

balance between the loss and gain of species, rather than a genuine stasis in the species diversity. This finding also implies that the univariate species-based indicators are not good indicators of a change in dynamic ecosystems. The gap between species-based indices (i.e., richness and biodiversity) and trait-based indices lays in the basic assumptions behind them. The null assumption in using species-based indices as ecosystem indicators is that the functional differences between species are unimportant and, thus, the overall numerical or biomass abundance of organisms in a community might be better predictors than any of the measures that incorporate traits (Gagic et al. 2015). Alternatively, the null assumption using trait-based indices is that the complementarity of different traits in the community may be important for the functioning of the ecosystem (Garnier et al. 2004, Vile et al. 2006) and, thus, the abundance of different trait levels or their richness in the community is the best predictor of its functionality (Schumacher and Roscher 2009, Mouillot et al. 2011). Similar to Gagic et al. (2015), the univariate species-based indices in the benthocosm experiments were non-informative, whereas the trait-based information, detailed below, provided a better mechanistic description of the processes structuring the communities.

Both seasonal and experimental warming enhanced the abundance of calcareous species (and the ratio between calcareous and non-calcareous species). Calcification is a temperature-enhanced metabolic process (Silverman et al. 2007), typically increasing with warming. However, negative calcification responses (i.e. decreased calcification rates or dissolution) to warming were recorded in various marine calcifiers, e.g. corals (Silverman et al. 2007), molluscs (Talmage and Gobler 2011), and macroalgae (Guy-Haim et al. 2016). These declines in calcification can be attributed to warming beyond the species-specific physiological tipping point (beyond Topt), following general metabolic breakdown. In the benthocosm experiments, warming had positive effects on both autotrophic and heterotrophic calcifiers in the winter, whereas, in the summer, negative effects were measured only in the autotrophic calcifiers. The main autotrophic calcifier in the experimental community was *G. rugosa*, that rapidly deteriorated in the summer (with noticeable signs of bleaching and decay) in all treatments except ambient. As ambient temperature reached 32 °C, right above the Topt determined by the TPC, and beyond which there is a sharp decline in functioning, this may have biased the summer results. The growth of other autotrophic calcifiers, e.g. CCA, was enhanced with warming, but did not contribute much to the community biomass because of their low biomass. An overall positive effect of the calcifying heterotrophic species to warming can be associated with both increased metabolic rates and the increase in the dominance of NIS, further discussed below.

The increase in heterotrophic calcifiers under OA treatments in the summer was intriguing and may be related to both direct and indirect positive effects of this treatment on this group. Calcifying species are generally considered more susceptible to OA than non-calcifying species as acidification can impair their capacity to produce calcified skeletons (Kroeker et al. 2010). However, while most calcifiers are affected adversely by OA, the production and growth of non-calcifying autotrophic species (e.g., algae) may be facilitated by CO_2 enrichment (Connell and Russell 2010). Indeed, in the benthocosm experiments, the total biomass of non-calcifying autotrophs increased with acidification, mainly in the winter. The main non-calcifying autotroph, the foundation species *G. rayssiae*, had higher growth rates in the winter and presented slower deterioration in the summer under OA. Although counter-intuitive (as calcifying species are overall more susceptible), the increase in heterotrophic calcifiers during summer can, therefore, be explained by the provision of food and habitat facilitated by OA. Recently, it was found that the abundance of a calcifying herbivorous gastropod, vulnerable to low pH levels, is 134% greater in a CO_2 vent site under near-future pH levels (Connell et al.

2017). In the benthocosm experiments, both herbivores and detritivores, largely being calcifiers, potentially benefitted from the increasing autotrophic biomass (in the winter), or its shedding (in the summer), as a source for food and/or due to its pH buffering capacity (in the winter), thus becoming more abundant under OA. Clearly, when tested within a community (and not by themselves as has been done in most OA experiments), species that might be sensitive to low pH can actually benefit from it. Hence, both the benthocosm results described here and the recent CO_2-vents evidence, emphasize the need to understand the ecological processes, apart from population-specific adaptation (see Deliverable 3.2) that buffer the negative effects of environmental change.

Synergistic interactions between warming and acidification, in which the response to the combined stressors was stronger than to the individual stressors, were found in different organisms (e.g., Talmage and Gobler 2011). Meta-analyses revealed that the combined OWA caused significant negative effects on calcification, reproduction, and survival, and a significant positive effect on photosynthesis (Kroeker et al. 2013). Nevertheless, these synergistic OWA responses were recorded in single-species experiments that excluded species interactions, potentially buffering OWA impacts. In the benthocosm settings, where OWA was tested for the first time on benthic communities and their biodiversity, OWA did not demonstrate negative synergistic effects. Rather, the results imply complex indirect effects, resulting from species interactions under the OWA treatment, where acidification facilitated the growth of non-calcifying autotrophs and warming enhanced metabolic rates, resulting in an overall significantly positive effect on calcifying heterotrophs. Here, again, species interactions are proven to be more influential than single-species responses to climate change in determining community responses.

OWA effects on ecosystem functioning. Over the past decades, the ecological discourse has shifted its focus from the structural to the functional role of biodiversity in ecosystems, as society might be more likely to take action to preserve biodiversity if it could be shown that there was some direct economic gain by doing so (Costanza et al. 1997, Worm et al. 2006). Subsequently, climate change research is rapidly moving into investigating ecosystem functioning and services (Mooney et al. 2009). The majority of community studies has utilized trophic or functional groups as indicators for ecosystem functioning, assuming various BEF connections (e.g., Edwards and Richardson 2004, Parmesan 2006, Kroeker et al. 2011). Yet, some of these relationships are not well-established, especially under multiple-stressor conditions. Our study has assessed OWA effects on both benthic biodiversity and ecosystem functions, and not just by assessing change in traits but by directly measuring biogeochemical fluxes.

In the winter, all treatments, except the combined warming and acidification, had a positive oxygen budget and a negative inorganic carbon budget, indicating an autotrophic balance, whereas the system was heterotrophic under combined warming and acidification. In the summer, the calculated oxygen budget indicates that under warming the system was heterotrophic, whereas the inorganic carbon budget indicates that only under combined warming and acidification the system was heterotrophic. These overall ecosystem fluxes were fully reflected in the functional (trophic) traits of species in the transformed communities, where heterotrophic versus autotrophic biomass increased under the combined warming and acidification. Such shift to heterotrophic balance was also observed in pelagic ecosystems under warming, mainly due to increased bacterial activity, as their metabolic processes show higher temperature sensitivity than autotrophic processes causing population acceleration with warming (Vázquez-Domínguez et al. 2007, Riebesell et al. 2009). The *in-situ* incubations also

show the shift to a less autotrophic or even a heterotrophic functioning at the warmer months (autumn in our experiments) of the native (*Gongolaria*) and alien (*Lobophora*) communities, respectively. These two lines of evidence indicate that warming leads to a functional shift towards a heterotrophic balance by altering metabolic rates and by facilitating NIS. The ecosystem-level implications of this shift are considerable and are discussed in detail below.

Diel net calcification was positive in all treatments and seasons, except a slightly negative diel budget in the summer under the combined warming and acidification. Night-time dissolution was observed under all treatments except the cooling treatment in the winter, where night-time calcification was measured. In both winter and summer, the highest net diel calcification rates were measured under cooling treatment. These lines of evidence suggest that biogeochemical cycles in the system have already shifted considerably in the past few decades. The diel net dissolution measured under OWA, albeit small, is of major concern as it implies the deterioration of SEM biogenic reefs in the near-future. Similar concern was raised for coral reefs by Silverman et al. (2009).

During both winter and summer, the total diel carbon uptake (sequestered) was negative, indicating carbon sink in all benthocosm treatments except the combined warming and acidification where a positive budget was measured - indicating a carbon source. Overall, these findings indicate that under OWA, coastal reef communities in the SEM may experience considerable shifts in their functions (and derived services).

In terrestrial ecosystems, Gagic et al. (2015) tested how well diversity indices and a trait-based approach predicted ecosystem functioning using datasets of bees, beetles and worms. They found that trait-based indices consistently provided greater explanatory power than species richness or abundance. Similarly, the experimental benthocosm findings described here suggest that the common, univariate diversity indices are not appropriate as indicators for ecosystem functioning, especially in invaded systems, and under climate change. Instead, both functional traits and direct biogeochemical measurements of system fluxes should be used in future studies as ecological indicators of the well-being of coastal marine ecosystems.

Conclusions and NBS perspectives

The observational and experimental work presented here demonstrates that native forest-forming Fucales species on coastal reef macrophyte communities on SEM reefs are strongly seasonal. They have a very short growth season of 3-5 months from late winter to early summer, when they have high cover, biomass, productivity and functionally as both habitat providers and contributors to the carbon cycling. The seasonality of many studied western Mediterranean *Cystoseira* s.l. species show that branches shed in these species at the end of summer or in in winter, for example in *Ericaria* (=*Cystoseira*) *zosteroides* (Ballesteros 1990) or *Gongolaria* (=*Treptacantha*) *barbata* (Falace and Bressan 2006), suggesting that summer is not a stressful season yet in this colder part of the Mediterranean basin. By contrast, on the SEM reefs, the alien, NIS, macroalgae are present in high cover and biomass through much of the year, and they are highly productive year-round, and at least individually can maintain high carbon uptake capacity in the warmest months. We have also shown that both the native produces and consumers have much higher vulnerability to high temperatures than the tropical alien producers and consumers and that the native macroalgae, which explain their success in this fast-warming region. These results raise a great concern for the future viability of the habitat-forming *Gongolaria rayssiae* endemic, which, based on its current phenology, thermal performance and the mesocosm experiment, probably already have a shrunken growth season compared to the period before the warming, and this season will shrink more and increase the risk for the existence of these species even further. The latest addition to this community is

the invasive sea urchin, *Diadema setosum*, which, as our experiments demonstrated, can eastly cope with current and future summer temperatures and may, thus, pose great risk to the macrophyte community on these reefs. Finally, the fact that the alien algae are present and highly productive year-round, and provide habitat for a rich associated community should provide some reassurance for the future productivity of the shallow reefs in this region under the accelerating climate crisis. Can some tropical NIS macroalgae even be viewed as benefactors to the ecosystem in a region where thermally-sensitive native species with important functions are in danger or lost together with their services due to warming? Can protecting these NIS habitats be viewed as an NBS in a climate change hotspots where much of the native biodiversity is lost due to warming?

This perspective is promising but should be viewed with caution at this stage. Our in-situ measurements of the entire community showed that the net balance of the alien *Galaxaura rugosa* community (measure only in the Spring by Peleg et al. 2020) and at that of *Lobophora schneideri* in the fall (summer was not assessed) can be net heterotrophic, probably due to the presence of many invertebrates that increase overall respiration rates and can thus tip the community metabolic balance. Such measurements should be monitored further in different locations, seasons and over several years to get a fuller picture of the present and future capacity of the reefs to provide habitat for other species and also serve as carbon sink and thus a support for Blue Carbon potential.

Our findings are highly relevant to a broad range of coastal systems beyond the Israeli coast, as the SEM can be viewed as the “canary-in-the-coal-mine” for what will occur in the rest of the Mediterranean in the coming decades. This is because the temperatures experienced now on the Israel coast in summer will soon be prevalent in numerous other Mediterranean regions, and many of the invaders present on this coast today will continue to rapidly spread west and north. It is highly likely that the novel, highly transformed, ecosystems currently present in the SEM will become established elsewhere in the basin.

2.2 Italy: Carbon metabolism of benthic assemblages on pristine and urban rocky shores of the Tuscan Archipelago (SL#28)

2.2.1 Introduction

Marine forests formed by brown macroalgae, such as Laminariales and Fucales, have long being recognized to play a key role as habitat formers, sustaining biodiversity and ecosystem functioning (Steneck et al. 2002, Pessarrodona et al. 2022) and providing important ecosystem services, including coastal protection, nutrient cycling and nursey (Steneck et al. 2002, Beaumont et al. 2008, Bertocci et al. 2015). More recently, kelp forests have been also identified as potential Blue Carbon habitats (Filbee-Dexter and Wernberg 2020) and their conservation and restoration envisioned as NBS to climate change. However, canopy-forming macroalgae are highly sensitive to extreme climatic events (e.g., marine heatwaves, storms) and anthropogenic disturbances (e.g., enhanced sediment and nutrient loading) and collapse of their populations have been documented globally (Benedetti-Cecchi et al. 2001, Smale and Wernberg 2013, Wernberg et al. 2013, Strain et al. 2014, Krumhansl et al. 2016).

Brown algae belonging to the complex *Cystoseira* sensu lato (genera Cystoseira C. Agardh, Ericaria Stackhouse and Gongolaria Boehmer) form intertidal and shallow subtidal forests along Mediterranean rocky shores (Benedetti-Cecchi et al. 2001, Bulleri et al. 2002, Tamburello et al. 2012, Illa-López et al. 2023b). Nonetheless, these communities are declining throughout the basin as a consequence of human alteration of environmental conditions and species interactions. In particular, excessive grazing by herbivores such as sea urchins and the native fish, *Sarpa salpa*, in the western Mediterranean can cause the shift from macroalgal forests to encrusting coralline macroalgae (i.e., marine deserts) (Benedetti-Cecchi et al. 1998, Bulleri et al. 2018a, Illa-López et al. 2023a). Furthermore, excessive nutrient loading can promote the dominance of algal turf (Gorman et al. 2009, Strain et al. 2014).

Such decline in brown algal forests has promoted conservation strategies such as the establishment of Marine Protected Areas (MPAs), but, due to the low dispersal of zygotes of most *Cystoseira* s.l. species (i.e., over a few tens of cm) (Riquet et al. 2021), natural recovery is difficult in areas far from extant populations. This has raised interest towards active restoration strategies (Susini et al. 2007, Falace et al. 2018, Verdura et al. 2018). Nonetheless, positive feedbacks may stabilize these alternative states, making the reverse shift to the macroalgal forest very unlikely (Elsherbini et al. 2023). Under these circumstances, understanding the ecological value of alternative habitats, generally regarded as degraded, is paramount in order to plan sound conservation strategies.

In the NW Mediterranean, marine forests are present along most of the islands of the Tuscan Archipelago while they have been replaced by algal turfs on the mainland coast of Tuscany (Tamburello et al. 2012). Here, we compared the functioning of macroalgal forests composed of *Ericaria brachycarpa* at Capraia Island with that of assemblages dominated by algal turfs and by the red alga, *Halopithys incurva* along the coast of Livorno. In particular, given the current interest in macroalgal forests as potential carbon sinks (Filbee-Dexter & Wernberg 2020), we assessed productivity and carbon turnover between macroalgal assemblages at pristine versus urban rocky reefs.

2.2.2 Methods

Capraia Island is located about 30 miles off the mainland coast of Tuscany, in the Northern Tyrrhenian Sea. This island is included in the Tuscan Archipelago National Park and can be considered pristine due to very limited urban development and lack of industrial activities (Tamburello et al. 2012). Rocky reefs around the island are characterized by the dominance of macroalgal canopies formed by *Ericaria brachycarpa*, at 1-15 m depths (Fig. 25). Reefs along the coastline of the city of Livorno are exposed to inputs of sediments, nutrients, organic and inorganic pollutants (Tamburello et al. 2012) and characterized by the presence of *Halopithys incurva* and by turf-forming macroalgae, including filamentous (e.g., *Ceramium* sp., *Sphacelaria* spp.), articulated coralline (e.g., *Ellissolandia elongata, Jania rubens*) and coarsely branched species (e.g., *Chondria* spp e *Laurencia* spp.) (Tamburello et al. 2012, Ravaglioli et al. 2021b) (Fig. 25).

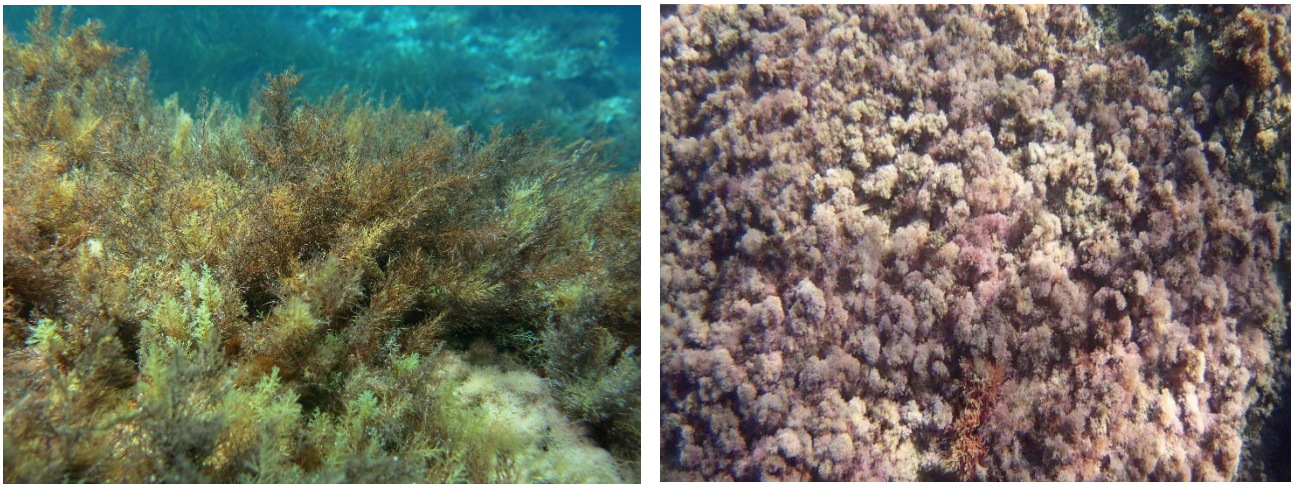

Figure 25 Macroalgal assemblages dominated by Ericaria brachycarpa at Capraia Island (left) and algal turfs/Halopithys incurva at Livorno (right).

In July 2021, two sites were selected, 2-4 km apart, at Capraia Island (43° 03' 57" N, 9° 48' 56" E; 43° 01' 34" N, 9° 50' 23" E) and along the coast of Livorno (43° 31' 08" N, 10° 18' 34" E; 43° 30' 41" N, 10° 18' 41" E). The productivity and carbon metabolism of benthic communities were estimated using the benthic incubation method developed by Peleg et al. (2020). This consists of dome-shaped chambers (~17 L; 0.4 m in diameter; area of 0.126 m^2), made of either transparent or dark Plexiglass (2 mm thick) for light and dark treatments, respectively (Fig. 26a, b). Domes were deployed on the bottom at a depth of 3-5 m. Sleeve-shaped Lycra bags filled in with sand were positioned all along the circumference of the dome to sealing it to the bottom and, hence, to reduce water exchange with the surrounding seawater. Aquarium pumps, powered by 12V batteries and activated by a magnetic switch, were used for enhancing recirculation of water inside the domes, thus minimizing the formation of a boundary layer and mimicking natural water flow. Pumps were connected to domes with plastic tubes. Temperature (°C) and light (lumens/ft2) were measured using loggers (HOBO® Pendant, Onset Computer Corporation) applied to the top of the batteries (Fig. 26).

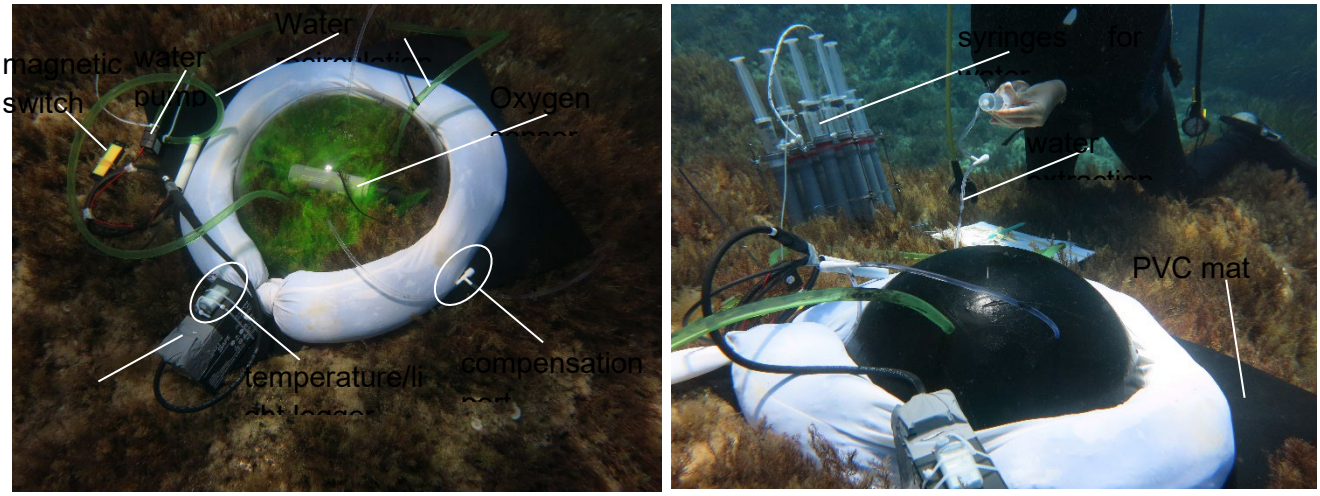

Figure 26 Transparent (left) and dark (right) domes deployed on rocky bottoms.

To assess possible seasonal shifts in functioning, measurements were carried out at each of the two sites selected along the island and urban coasts in July 2021 and February 2022, but at only one site for each condition in April 2022. Three plots were incubated at each site for each sampling event. Domes were positioned over plots characterized by a ~ 100% cover of the bottom by either *E. brachycarpa* or turf/*H. incurva*. Measurements were performed between 10.00 am and 14.00 pm and each of the light and dark incubation of the plot lasted ~1 hour. Oxygen concentration and pH within domes were recorded on site using HOBO Dissolved Oxygen (U26-001) and pH Loggers. Water samples for analysis of total alkalinity (TA), dissolved inorganic carbon (DIC) and nutrients (100 ml each) were taken before and at the end of each light/dark incubation period using plastic syringes. Water analyses were conducted at the Institute for Oceanographic and Limnological Research (IOLR) in Haifa (Israel), following the protocol described in Peleg et al. (2020). In addition, a total of 10 ml of 0.16 g fluorescein L SW^{-1} was injected into each dome at the beginning of each incubation to assess the level of water exchange in the case the domes were not completely sealed to the bottom.

Metabolic rates were calculated using the difference between the initial and final concentrations of DO, DIC and TA. Data from the light incubations were used to estimate net community production (NCP) and those obtained under dark conditions to estimate community respiration (CR). Gross primary production (GPP) was calculated from NCP and CR measurements. When NCP and CR were estimated from DIC measurements, the contribution of calcification and $CaCO_3$ dissolution (G) to the differences in total DIC was accounted for by subtracting the change in total alkalinity divided by two. G was calculated for both light and dark separately, where positive and negative values indicate calcification and dissolution, respectively. The net trophic state of the two habitats was compared in terms of their diel carbon balance. To this end, we calculated the diel GPP, CR and G rates, assuming that the GPP and Glight vary sinusoidally with light during the daytime (12 hr photoperiod) and that CR and Gdark are constant throughout the diurnal cycle (Marsh Jr 1970, Yates and Halley 2006). For the summer sampling event, after each incubation, all the macroscopic organisms present inside the domes were collected using a paint scraper, inserted into a plastic bag and transported to the laboratory for analysis of species composition and abundance. Samples were immediately transported to the laboratory, where a 0.85 M solution of $MgCl_2$ was added to each bag for 10 min in order to facilitate the detachment of animals from the macroalgae. Specimens were then rinsed in seawater onto an 80-µm sieve and fauna transferred to a 70%

alcohol solution for preservation, until identification. Mobile invertebrates were then identified to the lowest possible taxonomical level and individually counted.
Apart from the main habitat-formers (e.g. *E. brachycarpa* at Capraia Island and, when present, *H. incurva* at Livorno), macroalgae were classified into broad morphological groups, including: filamentous, foliose, and articulated corallines. After blotting with paper, their wet weight was measured with a precision scale. The dry weight of each species or morphological group was measured after samples were kept in oven muffle at 60 °C for 24 hours.

Statistical analyses
Data were analyzed separately for each season, using linear mixed models with the lmer package, v. 1.1-26. The habitat (pristine versus urban) was treated as a fixed effect, while the site was included in the random part of the model. Since only one pristine site was sampled in spring, the model for this season included the habitat as a fixed effect, but only the replicates in the random part. Type III Analysis of Variance with the Satterthwaite's method was used to test for fixed effects included in the model by means of the 'anova' function. Model assumptions were visually checked by means of Q-Q and fitted versus residual plots. All analyses were performed in R studio v. 2022.07.2.

2.2.3 Results

Diel O_2 fluxes were higher in benthic assemblages at pristine than urban sites in winter, while there were no differences in summer and spring, although there was a tendency for urban sites to have slightly higher fluxes in those warmer months (Table 4; Fig. 27).

Total DIC fluxes did not differ between habitats consistently among seasons and they were always negative because of a prevalence of production over respiration, indicating an autotrophic metabolism (Table 4; Fig. 28). Calcification was always prevailing over $CaCO_3$ dissolution and, despite low fluxes, it was higher at the urban than at the island site in spring (Table 4, Fig. 28).

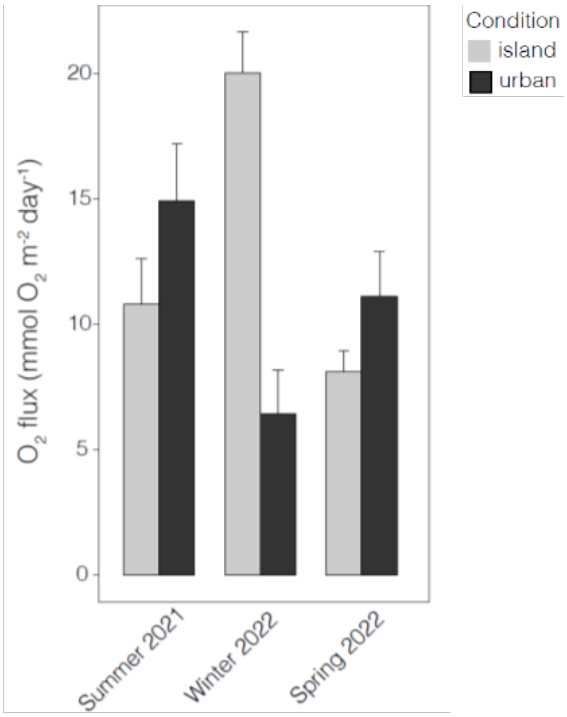

Figure 27 Diel O_2 fluxes on island and urban rocky reefs in summer 2021, winter and spring 2022

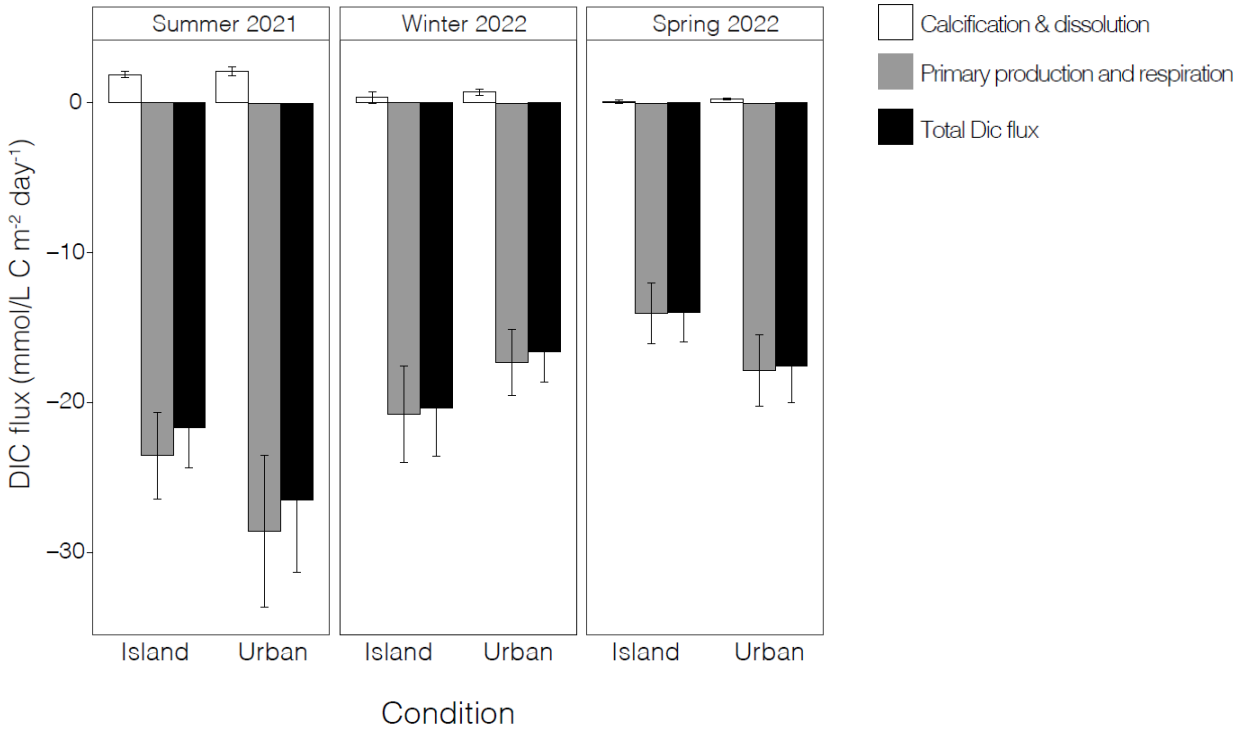

Figure 28 Total DIC fluxes and relative contribution of production/respiration and calcification/dissolution on island and urban rocky reefs in summer 2021, winter and spring 2022

Table 4 Summary of Type III ANOVA on the effects of habitat on diel O2 and total DIC fluxes, production/respiration and calcification/dissolution

O_2 flux		Summer 2021			Winter 2021/2022			Spring 2022		
Source of variation	df	MS	F	P	MS	F	P	MS	F	P
Habitat	1	33.720	2.11	0.283	555.84	38.788	<0.001	11.327	1.647	0.264
Total DIC flux		Summer 2021			Winter 2021/2022			Spring 2022		
Source of variation	df	MS	F	P	MS	F	P	MS	F	P
Habitat	1	70.215	0.914	0.358	43.128	2.410	0.152	15.93	1.394	0.289
Production/Respiration		Summer 2021			Winter 2021/2022			Spring 2022		
Source of variation	df	MS	F	P	MS	F	P	MS	F	P
Habitat		76.494	0.899	0.362	35.203	1.695	0.222	18.317	1.584	0.262
Calcification/Dissolution		Summer 2021			Winter 2021/2022			Spring 2022		
Source of variation	df	MS	F	P	MS	F	P	MS	F	P
Habitat	1	0.051	0.270	0.630	0.402	0.821	0.383	0.080	22.431	<0.01

There were no significant differences between pristine and urban habitats in the total number of individuals or in the species richness of Anellids, Molluscs, Crustaceans and other taxa found in incubated plots in summer (Table 5, Fig. 29). There was a trendency for the total

number of individuals belonging to other taxa to be higher in pristine than urban habitats (Fig. 29).

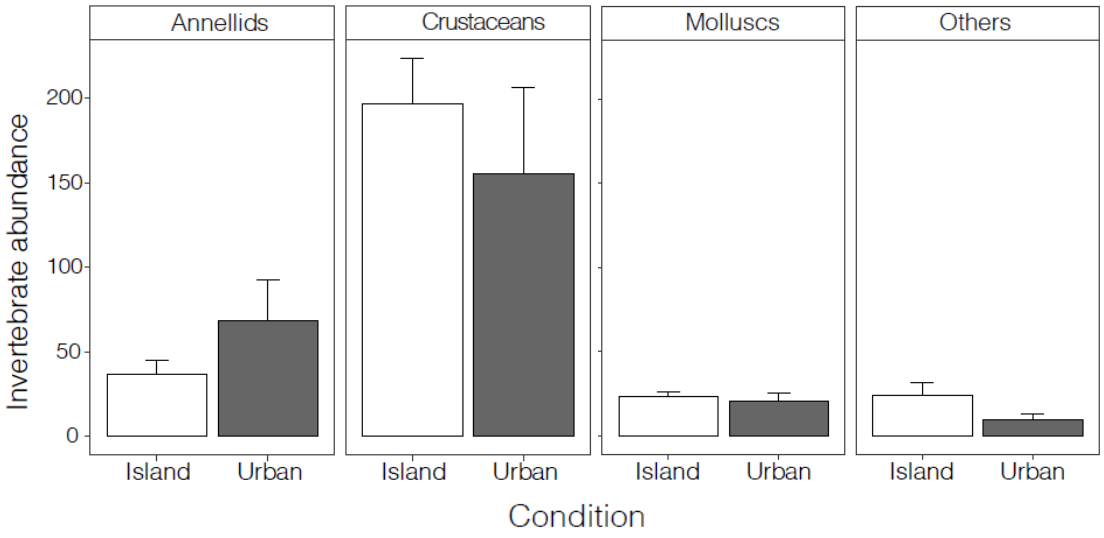

Figure 29 Number of individuals of Anellids, Crustaceans, Molluscs and Other taxa on island and urban rocky reefs in summer 2021, winter and spring 2022

Table 5 Summary of Type III ANOVA on the effects of habitat on the total number of individuals and species richness of Anellids, Molluscs, Crustaceans and other taxa

Anellids		Total ind. number			Species richness		
Source of variation	df	MS	F	P	MS	F	P
Habitat	1	932.72	0.977	0.379	35.349	0.777	0.428
Molluscs		Total ind. number			Species richness		
Source of variation	df	MS	F	P	MS	F	P
Habitat	1	9.814	0.189	0.686	0.538	0.049	0.835
Crustaceans		Total ind. number			Species richness		
Source of variation	df	MS	F	P	MS	F	P
Habitat	1	5043	0.712	0.419	82.029	1.268	0.323
Other taxa		Total ind. number			Species richness		
Source of variation	df	MS	F	P	MS	F	P
Habitat	1	588.00	3.552	0.084	2.083	0.691	0.422

2.2.4 Discussion

Diel fluxes of total DIC, as well as the contribution of production/respiration and calcification/dissolution, of benthic communities formed by the red seaweed, *H. incurva* and algal turfs along an urbanized stretch of the coast of Tuscany did not differ from that of communities associated with the canopy-forming fucoid, *E. brachycarpa*, along the coast of Capraia Island in the Tuscan Archipelago. This lack of difference was consistently observed among times of sampling. Only in winter was there a greater O_2 production by benthic

communities at pristine compared to urban sites. Similarly, there were no remarkable differences in the structure of associated invertebrate assemblages in terms of species richness and total abundance of individuals in plots that were incubated at pristine versus urban sites in summer.

To the best of our knowledge, this is the first study showing that *Cystoseira s.l.* communities are actually autotrophic and, hence, represent a carbon sink. Indeed, although species belonging to this genus are included in the European Red List of Habitats and protected under several legal frameworks, including the European Habitats Directive 1992 EU Regulation 1967/2006 and the Barcelona Convention (1976), there is little information on their functioning. Thus, our findings strengthen arguments for their protection.

Our study also indicates that communities at both pristine and urban sites, beyond differences in species identity, have a similar structure and functioning. In particular, they are both characterized by an autotrophic metabolism and, hence, function as carbon sinks. A previous study carried out along the Mediterranean coast of Israel found that communities formed by the native Gongolaria (=*Cystoseira*) *rayssiae* were autotrophic, while those formed by algal turfs and expanding tropical shrubs dominated by red calcifying alga, *Galaxaura rugosa*, were heterotrophic (Peleg et al. 2020). In our study, benthic assemblages at urban sites were dominated by a mix of turf-forming species and *Halopithys incurva*, a species able to develop large thalli (up to about 20 cm in size) which are generally overgrown by another red alga, *Jania rubens* (Ravaglioli et al. 2021a). Due to the large biomass and architectural complexity of the thallus and to the presence of the epiphyte, *H. incurva* appears to provide a habitat comparable to that formed by *C. brachycarpa*, sustaining a diverse assemblage of invertebrates.

Under these circumstances, urban benthic assemblages appear to be functionally equivalent to those found at pristine sites. Thus, our results suggest that, despite being commonly regarded as not worthy of conservation, benthic assemblages at urban areas which are not degraded up to an extent where they are composed exclusively by turf-forming species, can play an important role in sustaining biodiversity and ecosystem functioning. This has several important implications in terms of both our fundamental understanding of the biodiversity and functioning of temperate rocky reefs and policies for their conservation and restoration.

First, we should likely move from the concept of a sharp dichotomy between marine forests and algal turfs. Our study suggests that, despite that these two states could represent alternative basins of attraction of the system, benthic communities in rocky reefs can be present along a gradient that goes from the pristine (i.e., the forest) to the extremely degraded state (i.e., algal turfs).

Second, in the case in which the main Mediterranean canopy-forming macroalgae belonging to genus *Cystoseira* s.l. are replaced by other architecturally complex species, the consequence for the biodiversity and functioning of the whole community could be minor. Thus, these communities, also by virtue of their large spatial extent and functioning as carbon sinks, could be worth protection to prevent further degradation.

Third, plans to restore *Cystoseira* at relatively degraded sites might not produce large improvements in the diversity of the whole community, as well as in their functioning. This does not imply, by any mean, that practices for the conservation and restoration of marine forests formed by *Cystoseira s.l.* should be weakened, but rather that their benefits and costs should be fully evaluated against the *status quo*.

2.3 Italy: Seagrass meadows as refugia for sea urchin larvae under ocean acidification (SL#28)

2.3.1 Introduction

Global climate changes, due to rising anthropogenic CO_2 emissions, are causing unprecedented alterations to marine ecosystems (Doney et al. 2009, Kroeker et al. 2013). Ecological impacts of climate changes are generally the result of an interplay between physiological impairment and altered species interactions (Gilman et al. 2010, Kroeker et al. 2017, Sunday et al. 2017, Bulleri et al. 2018b). Many coastal communities are organized by hierarchical interactions in which facilitation by foundation species, such as corals, salt marsh plants, mangroves seagrasses and kelp, are of primary importance. Thus, understanding their role in regulating the response of associated species to climate changes is paramount to devise sounded conservation and restoration strategies.

Anthropogenic ocean acidification (OA) has been widely demonstrated to negatively affect calcifying organisms by impairing their capacity to maintain carbonate structures and altering acid-base regulation (Kroeker et al. 2010). Sea urchins are considered to be particularly vulnerable to OA because they calcify in both their planktonic larval stage and benthic adult life (Byrne et al. 2013, Dworjanyn and Byrne 2018, Byrne and Hernández 2020). Similarly to other calcifying taxa, their early development stages appear to be more sensitive to OA compared to adults, likely representing a major bottleneck for sea urchin populations under future climate scenarios (Lamare et al. 2016). Previous laboratory studies reported reduced growth, delayed development and increased body abnormality of larvae exposed to constant low pH conditions, likely due a trade-off between the maintenance of core activity (acid-base regulation) and skeletal integrity and growth (reviewed by Byrne & Hernández, 2020). On the other hand, sea urchin larvae inhabiting natural fluctuating pH environments, such as upwelling regions, intertidal pools and CO_2 vents, appear to be more tolerant to future OA, as a result of a complex interplay of biotic (e.g., parental acclimation, phenotypic plasticity) and abiotic (e.g., food availability) factors at play (Uthicke et al. 2016, Byrne and Hernández 2020, Karelitz et al. 2020). Within this context, understanding how the responses of sensitive species to OA could be influenced by local environmental variability is key to identify climate refugia and devising sound mitigation strategies (Kapsenberg and Cyronak 2019).

Coastal areas are generally characterized by diel fluctuations in seawater carbonate chemistry, mainly driven by metabolic activities of primary producers (Falkenberg et al. 2021). In particular, habitat-forming species, such as seagrass meadows and macroalgal forests, can generate marked daily fluctuations in pH, with increases up to a full unit during the day (Hendriks et al. 2014, Pacella et al. 2018, Pfister et al. 2019, Ricart et al. 2021). Hence, vegetated habitats may represent a climatic refugia for resident calcifying organisms, by either enhancing their adaptive capacity to fluctuating environment or temporally reducing exposure to low pH (Falkenberg et al. 2021). In addition, these habitat-forming species have been widely shown to benefit or, at least, to be unaffected by enhanced CO_2 concentration predicted by the end of the century (Koch et al. 2013), having thus the ability to persist and continue to deliver benefits under future climate conditions (Bulleri et al. 2018b).

The evaluation of the role of vegetated habitats as refugia under OA has generated contrasting results (Kapsenberg and Cyronak 2019). Available research shows that biogenic fluctuations of seawater chemistry could be beneficial to calcifiers if the benefit at daytime, when the

photosynthetic activity of macrophytes decreases CO_2 concentration and increases pH, outweighs enhanced stress conditions during the night, driven by community respiration (Cornwall et al. 2013, Camp et al. 2016, Wahl et al. 2018b, Young et al. 2022). Therefore, it has been argued that vegetated habitats could mitigate the impacts of OA on stress-sensitive species if they sustain significant and prolonged higher pH conditions compared to surrounding areas (Krause-Jensen et al. 2016, Kapsenberg and Cyronak 2019). Although the idea of macrophytes acting as OA refugia has recently garnered considerable attention within the scientific community, little is known about the effects of biogenic pH fluctuations on the early development stages of calcifying organisms. A few recent studies on bivalve larvae still reported inconsistent outcome among species, with the majority of biological processes unresponsive to fluctuating seawater chemistry (Frieder et al. 2014, Clark and Gobler 2016, Kapsenberg et al. 2018). In these studies, however, pH change was chemically induced and, thus, it remains unclear how realistic, gradual fluctuations of seawater pH and carbonate chemistry imposed by biological processes could influence the early development stages of vulnerable species under future climates.

Here, we performed a mesocosm study to assess whether the seagrass, *Posidonia oceanica*, through its metabolic activity, could mitigate the negative effects of OA on larval development and growth of the calcifying sea urchin, *Paracentrotus lividus*. Sea urchin larvae were exposed to ambient and low pH conditions, either in tanks with *P. Oceanica* plants or without plants. Early development stage and total body length were assessed on pluteus (72 h post-fertilization) and echinopluteus (~3 weeks after fertilization) larvae, respectively, under different experimental conditions. Specifically, we hypothesized that i) plants of *P. oceanica* that are expected to be unaffected by OA (Hall-Spencer et al. 2008) would temporally increase seawater pH and shift its carbonate chemistry, through their photosynthetic activity (Hendriks et al. 2014), at both ambient and low pH conditions and ii) these biological fluctuations of carbonate system would decrease and increase the percentage of larval abnormal development and their total body length, respectively, under OA scenarios.

2.3.2 Materials and methods

2.3.2.1 Sea urchin and plant collection and preparation

To test for temporal generality, the experiment was run twice over two spawning periods of the sea urchin, *Paracentrotus lividus*, in May and November 2021 (adults are mature from October to June). Unfortunately, for the second run, most of the larvae were lost before their development to echinopluteus phase due to issues during laboratory procedure and, thus, the total body length of echinoplutei was assessed only in the first run. Specimen of *P. lividus* were collected at depths of ~ 2-3 m south of Livorno (Antignano, Italy, 43°29′17.39″N, 10°19′33.17″E), on 30th May and 17th November 2021. The urchins were rapidly transferred to the aquarium of Livorno and kept in a large holding tank with filtered seawater until the start of the experiment.

Large rhizome fragments of *Posidonia oceanica* were sampled by divers from well-preserved meadows at a depth of ~ 5 m, located off the coast of Livorno (43° 28’ 45.005’’ N, 10° 17’ 30.001’’ E), on 28th May and on 17th November 2021. Plant fragments, bearing a number of vertical shoots, were rapidly transported in coolers to the mesocosm facility located at the aquarium of Livorno. Plant fragments of similar size and shoot number were carefully selected and attached to the bottom of four plastic cages filled with small cobbles. Two cages were then randomly placed in two large (500 L) and independent tanks, filled with filtered fresh seawater from a nearby area. Two other independent tanks were filled with fresh seawater and

maintained without *P. oceanica* plants. Each tank was then assigned to each of the four combinations of pH (ambient vs. low pH) and *P. oceanica* plants (present vs. absent). Each tank with and without *P. oceanica* plants was illuminated by three (two Silvermoon Reef Blu 895 and one Silvermoon Marine 895) and two (one Silvermoon Reef Blu 895 and one Silvermoon Marine 895) LED lamps, respectively, which allow the simulation of light diel fluctuation. Irradiance level was ~ 100 µmol photons m-2 s-1 both within the canopy and in tanks without plants. Seawater temperature was independently controlled in each tank by a chiller (Teco TK 500) and maintained at a constant temperature of ~ 19.5°C and ~ 17.5 °C for the first and second experimental runs, respectively, in line with temperatures recorded in the field at the time of plant collection. Plants were allowed to acclimatize to laboratory conditions for ~ ten days during both experiments. CO_2 was bubbled into the sumps of tanks assigned to low pH, controlled by an automatic CO_2 injection and pH-controlled feedback system. The low pH treatment simulated values expected by the end of the century under the RCP 8.5 scenario. During the first experimental run (June), pHNBS was monitored several times a day during the experiment, using a portable pH meter (Hach HQ2100). The average values (± SE) at ambient pH were 8.270 ± 0.003 and 8.17 ± 0.007 with or without *P. oceanica* plants, respectively. At low pH, the average values were 7.79 ± 0.008 and 7.75 ± 0.013 with or without *P. oceanica* plants, respectively (Fig. 30a). For the second experimental run (November), pHNBS was continuously monitored with HOBO data loggers along the course of the experiment. The average values (± SE) at ambient pH were 8.15 ± 0.001 and 8.08 ± 0.003 with or without *P. oceanica* plants, respectively. At low pH, the average values were 7.84 ± 0.001 and 7.61 ± 0.002 with or without *P. oceanica* plants, respectively (Fig. 30b). For the first experimental run, salinity was measured weekly using a conductivity meter and total alkalinity samples were collected weekly from each aquarium and measured using an automated potentiometric titration with a Methrom 848 Titrino plus system and applying the Gran method. For the second experimental run, which lasted only four days, salinity was measured every two days and total alkalinity samples were collected once during the experiment. Carbonate system variables were then calculated from measured pH, total alkalinity, temperature and salinity values using the seacarb R package (Table 6).

Table 6 Carbonate chemistry variables (mean □ SE) measured in each tank exposed to different experimental conditions (T1= Run1, T2= Run2; ApH = ambient pH, LpH = low pH; +P =with P. oceanica, -P = without P. oceanica). AT: total alkalinity; pH; Temp: temperature; Sal: salinity; pCO2: the partial pressure of CO2 in seawater; Ωcalc: the saturation state of seawater for calcite; Ωarag: the saturation state of seawater for aragonite; HCO3-: the bicarbonate ion concentration; CO32-: the carbonate ion concentration.

Treatment	A_T (µmol kg^{-1})	pH	Temp (°C)	Sal (PSU)	pCO_2 (µatm)
T1, ApH, +P	2676 ± 7	8.30 ± 0.01	19.33 ± 0.09	36.7 ± 0.1	214 ± 5
T1, LpH, +P	2742 ± 5	7.87± 0.01	19.48 ± 0.10	36.9 ± 0.1	729 ± 16
T1, ApH, -P	2774 ± 5	8.17 ± 0.01	19.6 ± 0.12	36.7 ± 0.1	327 ± 7
T1, LpH, -P	2847.5± 9	7.75 ± 0.01	19.42 ± 0.15	37 ± 0.1	1048 ± 36
Treatment	Ω_{calc}	Ω_{arag}	HCO_3^- (µmol kg^{-1})	CO_3^{2-} (µmol kg^{-1})	
T1, ApH, +P	8.16 ± 0.1	5.31 ± 0.06	1840 ± 10	346 ± 4	
T1, LpH, +P	3.91 ± 0.1	2.55 ± 0.04	2343 ± 8	166 ± 3	
T1, ApH, -P	6.86 ± 0.1	4.46 ± 0.05	2075 ± 12	290 ± 4	
T1, LpH, -P	3.17 ± 0.1	2.07 ± 0.10	2525 ± 11	134 ± 4	
Treatment	A_T (µmol kg^{-1})	pH	Temp (°C)	Sal (PSU)	pCO_2 (µatm)
T2, ApH, +P	2669	8.17	37	17.3	317.1
T2, LpH, +P	2731.5	7.82	37	17.5	837.5
T2, ApH, -P	2769.5	8.12	37	17.7	376.6
T2, LpH, -P	2837	7.61	17.5	37	1478.4
Treatment	Ω_{calc}	Ω_{arag}	HCO_3^- (µmol kg^{-1})	CO_3^{2-} (µmol kg^{-1})	
T2, ApH, +P	6.2	4.0	2034.1	262.3	
T2, LpH, +P	3.3	2.1	2396.5	139.1	
T2, ApH, -P	6.0	3.9	2150.9	256.5	
T2, LpH, -P	2.2	1.4	2610.7	94.5	

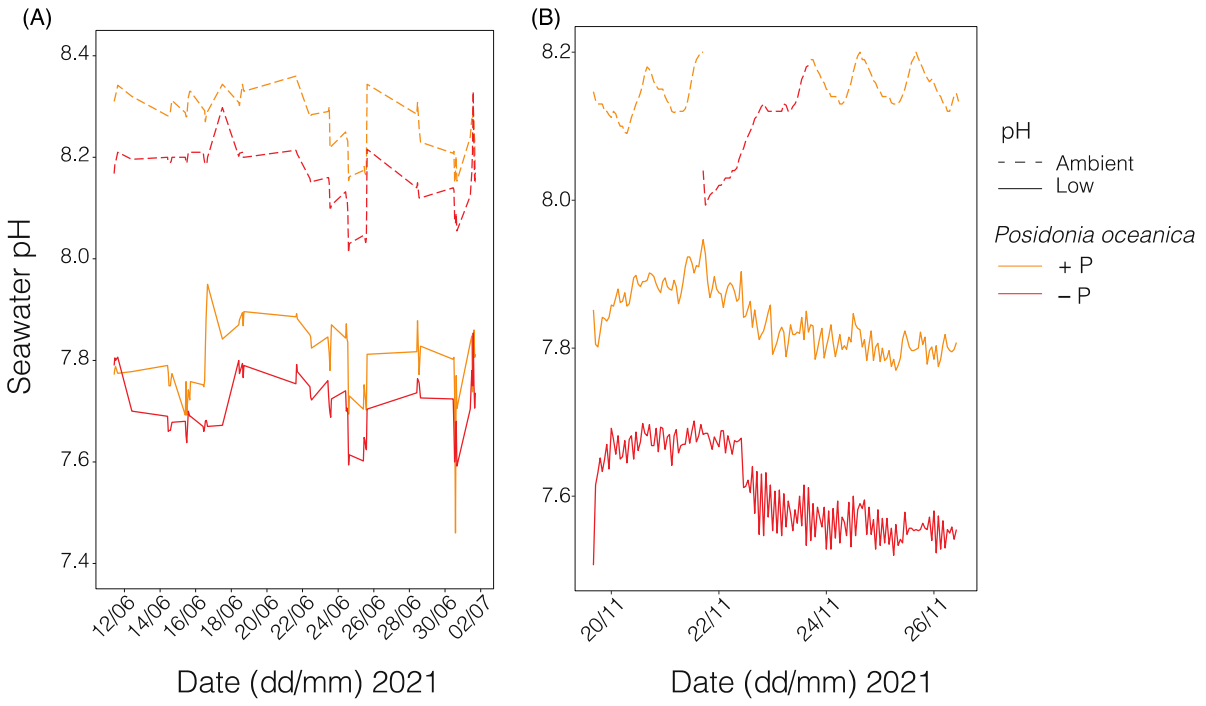

Figure 30 Time series of (A) daily seawater pH values for different combinations of pH (ambient and low) and Posidonia oceanica (+P and -P), measured during the first run (June 2021), and (B) hourly seawater pH for different combinations of pH (ambient and low) and Posidonia oceanica (+P and -P), measured during the first run (June 2021), and (B) hourly seawater pH for different combinations of pH (ambient and low) and Posidonia oceanica (+P and -P), measured during the second experimental run (November 2021). pH measurements were obtained by using three high-resolution HOBO data loggers, two of which were deployed in the two tanks exposed to low pH treatments (solid lines) throughout the experiment, while the third sensor was alternated between tanks with and without P. oceanica plants maintained at ambient pH (dotted lines).

2.3.2.2 Spawning and fertilization procedure

Spawning in adults of *P. lividus* was induced within five days of collection by injecting 0.5 mL of 0.5 M KCL. Eggs were collected into beakers of 100 mL with filtered seawater. Sperms were collected and stored in 1.5 mL Eppendorf tubes and conserved at 4°C. Gametes were visually checked for quality in term of sperm motility and egg shape and colour. Spawned eggs were washed with filtered seawater, pooled into a 1L beaker and, then, inseminated by using a final sperm concentration of 105 sperm Lm^{-1}.

To assess the effects of experimental treatments on the abnormal development of pluteus larvae, embryos were transferred into 50 mL modified falcon tubes and either suspended within *P. Oceanica* canopies or maintained at the same height in tanks without plants, for 72 hours (Fig. 31). The falcon tubes were closed with 0.45 µm mesh caps to restrict loss of embryos but allowing maximum water exchange. Six falcon tubes were randomly allocated to each tank.

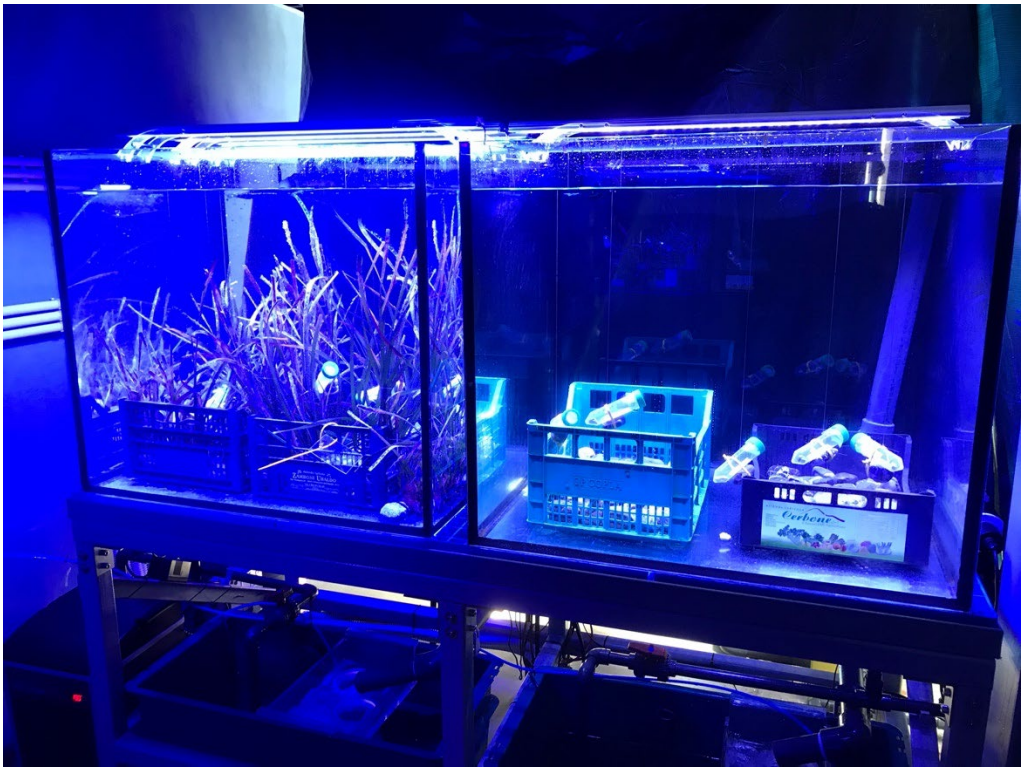

Figure 31 Larvae into falcon tubes either suspended within P. oceanica canopies or maintained at the same height in the tanks without plants.

At the end of the experiment (72 h), tubes were retrieved from the tanks and transported to the laboratory. Larvae were filtered out of the tubes, transferred to 1.5 mL Eppendorf tubes and fixed with 4% buffered paraformaldehyde for later measurements. After 24 h, larvae were transferred into petri dishes and observed in an inverted optical microscope. One hundred larvae were counted for each replicate tube and developmental abnormalities recorded. In particular, larvae at pluteus stage, pyramid-shaped and with fully developed arms were considered normal, while abnormal development at the stages of blastula, gastrula or plutei were considered malformed larvae (Fig. 32 a, b).

To evaluate the effects of experimental treatments on the total body length of echinoplutei, embryos were kept in 3L aquaria with filtered seawater and maintained at a constant temperature of ~ 18°C for ~ 3 weeks. During this period, seawater was changed every 2 – 3 days and larvae were fed with microalgae twice a week. After 20 days, larvae were transferred into 24 falcon tubes and randomly allocated to the four experimental tanks (6 falcon tubes for each tank), as described above. Larvae were maintained under different experimental conditions for ten days. At the end of the experiment, tubes were retrieved from the tanks, transported to the laboratory and fixed in paraformaldehyde as described above. All larvae were photographed using a Leica DMi1 microscope fitted with an MC120-HD digital camera. The total arm length of larvae was then measured using the free software Image J (Fig. 32 c).

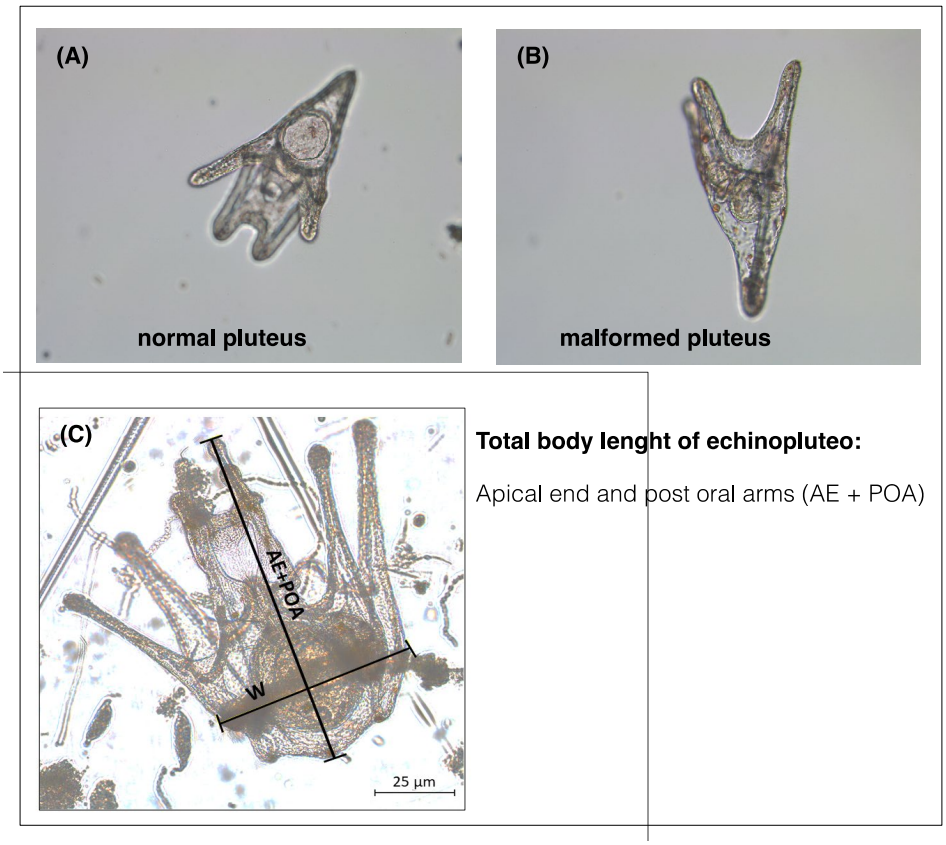

Figure 32 Examples of (A) a normal larva with fully developed arms and (B) a malformed larva at pluteus stage after 72 h development in experimental tubes; (C) total body length of an echinopluteus larva measured as the total length of apical end plus post oral arms.

2.3.2.3 Statistical analyses

For the percentage of abnormal development of pluteus larvae, the effects of pH, *P. oceanica* plants and time were analysed using a generalized linear mixed model (GLMM), assuming a gaussian distribution. The factor pH (ambient vs. low) and *P. oceanica* (+P vs. -P) were included in the fixed part of the model as predictor variables. In addition, the factor experimental run (run1 vs. run2) was added in the fixed part of the model to test for the temporal consistency of experimental runs. The factor tank was added in the random part of the model to take into account that replicated tubes were grouped within each tank. The total body length of echinopluteus larvae was analysed using a GLMM, including pH and P. oceanica as fixed factors and tank as a random effect. The GLMMs were run using glmmTMB R package. Post-hoc comparisons were performed with R function emmeans for the significant interaction terms. Model assumptions were checked using the R package DHARMa.

2.3.3 Results

2.3.3.1 Larval development and growth under experimental conditions

There was a significant interaction between pH and P. oceanica on the percentage of abnormal development of pluteus larvae, regardless of time (Table 7, Fig. 33). At low pH, larvae growing within *P. oceanica* canopies displayed a significant reduction in the percentage of abnormal development compared to those growing without plants while, at ambient pH, there were no differences in the percentage of abnormal larvae between *P. oceanica* treatments (Fig. 33).

Table 7 Results of Generalized Linear Mixed Models (GLMMs) used to assess the effects of pH (ambient = ApH, low = LpH), P. oceanica (+P, -P) and Time (Run1, Run2) on the percentage of abnormal larval development.

*Coefficients and standard errors (SE) for pH, P. oceanica and time are reported for the fixed effects, while estimates of variance (□2) and standard deviation (SD) per tank are reported for the random effects. *P < 0.05, **P < 0.01, ***P < 0.001.*

Effect	Abnormal development
Fixed effects	Estimate (SE)
Intercept	56.66 (3.03)***
+P	-4.99 (4.29)
LpH	24.83 (4.28)***
Run2	-11.99 (4.29)**
+P x LpH	-12.66 (6.06)*
+P x Run2	4.33 (6.06)
LpH x Run2	2.99 (6.06)
+P x LpH x Run2	-0.66 (8.57)
Random effects	σ^2 (SD)
Tank	4.7e-08 (0.0002)
Residual	5.5e+01 (7.4)
	Post-hoc contrasts (Yes x Run2)
	ApH: +P = -P
	LpH: +P < -P***

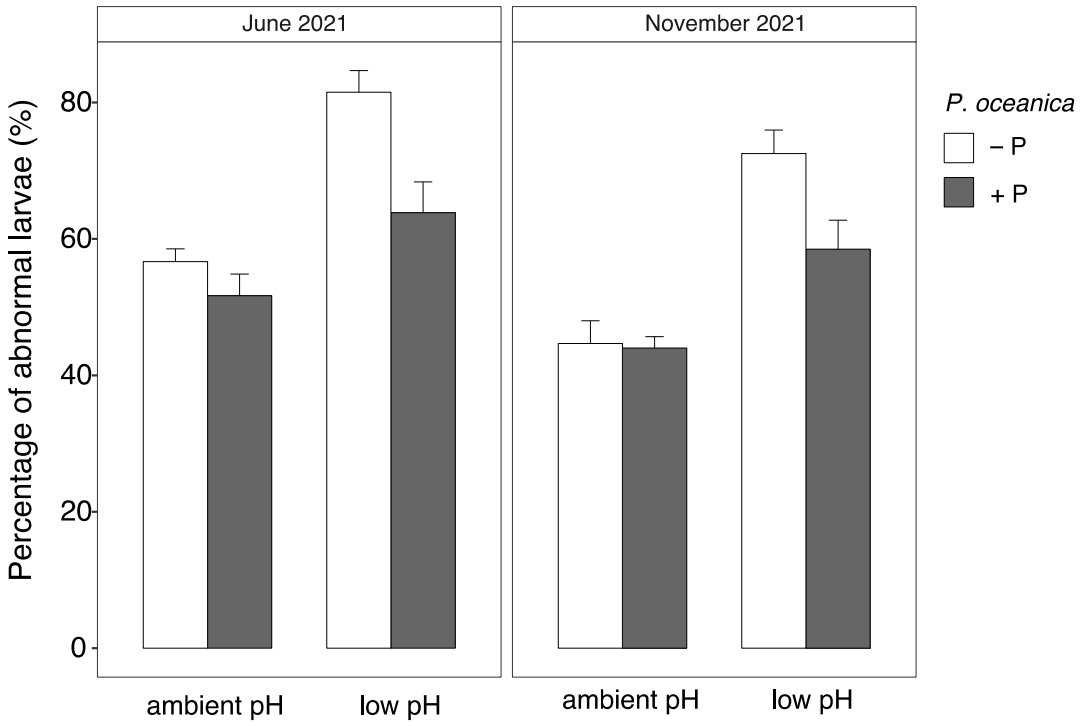

Figure 33 Percentage of abnormal development of pluteus larvae (mean ± SE) growing with or without P. oceanica plants under ambient and low pH conditions, for both experimental runs.

There was also a significant interaction between pH and *P. oceanica* on the total body length of echinopluteus larvae (Table 8, Fig. 34). At low pH, the total body length of larvae growing within *P. oceanica* plants was significant higher compared to those maintained without plants while, at ambient pH, there were no differences in the larval body length between *P. oceanica* treatments (Table 8, Fig. 34).

*Table 8 Results of Generalized Linear Mixed Models (GLMMs) used to assess the effects of pH (ambient = ApH, low = LpH) and P. oceanica (+P, -P) on the total body length of echinopluteus larvae. Coefficients and standard errors (SE) for pH and P. Oceanica are reported for the fixed effects, while estimates of variance (±2) and standard deviation (SD) per tank are reported for the random effects. *P < 0.05, **P < 0.01, ***P < 0.001.*

Effect	Total body length
Fixed effects	Estimate (SE)
Intercetta	92.5 (3.9)***
+P	2.7 (5.6)
LpH	-29.7 (5.6)***
+P x LpH	33.3 (7.9)***
Random effects	σ^2 (SD)
Tank	6.1e-08 (0.0002)
Residual	8e+01 (8.932)
	Post-hoc contrasts
	(Yes x LpH)
	ApH: +P = -P
	LpH: +P > -P

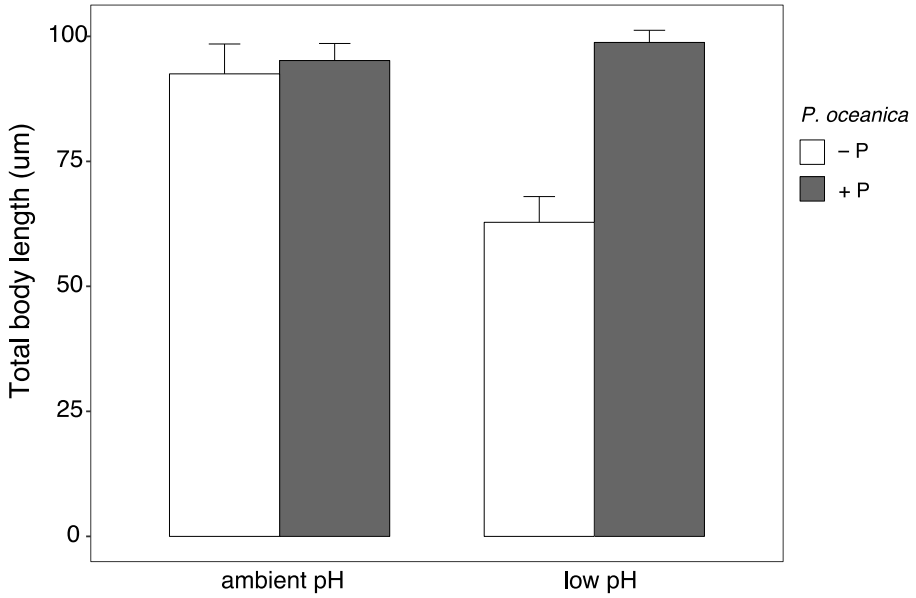

Figure 34 Total body length (mean ± SE) of echinopluteus larvae growing with or without P. oceanica plants under ambient and low pH conditions, for the first experimental run.

2.3.4 Discussion

Posidonia oceanica, by altering seawater chemistry through their photosynthetic activity, mitigated the negative impacts of ocean acidification on the larval development and total body length of the sea urchin, *Paracentrotus lividus*. At low pH, larvae growing within *P. oceanica* canopies displayed a significant decrease and increase in the percentage of abnormal development of plutei and in the total body length of echinoplutei, respectively, compared to those developing without plants.

Ocean acidification has been widely shown to adversely affect different life-cycle stages of sea urchins (Byrne et al. 2013, Lamare et al. 2016, Byrne and Hernández 2020), by altering physiological processes due to hypercapnia and impairing calcification (Byrne & Hernández, 2020). In particular, planktonic urchin larvae seem to be the most vulnerable to OA (Byrne *et al.*, 2013; Lamare *et al.*, 2016), thereby representing a key life-history stage in determining

future population dynamics and distributions. In our study, larvae growing at low pH without plants displayed a significant increase in the percentage of malformed larvae during the first three days of development, as well as a decrease in the total body length of echinoplutei during the final development stage before to settle (~ three weeks). Our results are in line with previous studies, with reduced size and altered body morphology at low pH reported for a wide range of sea urchin larvae under controlled laboratory conditions (reviewed by Byrne et al., 2013; Byrne & Hernández, 2020). Stunted larvae growing at low pH have been suggested to depend on energetic constraints associated to impaired digestion, alteration of metabolism and disruption of extracellular acid-base regulation as well as reduced availability of seawater carbonate minerals under OA scenario (Byrne et al., 2013; Byrne & Hernández, 2020). Since arm length and larval skeleton are positively correlated to feeding success and swimming ability of larvae (Byrne & Hernández, 2020), the negative impacts of OA on larval size and body morphology will lower their performance, likely compromising success of the pelagic life stage under future conditions.

The effects of OA on stress-sensitive species can be, however, influenced by local environmental conditions upon which climate change manifests (Kapsenberg et al. 2018, Kapsenberg and Cyronak 2019). Recent studies have shown that calcifying organisms (mainly sea urchins), inhabiting fluctuating pH environments, such as upwelling regions, tidal pools and CO_2 vents, enhanced their physiological tolerance to OA across different life stages, as a result of phenotypic plasticity and/or parental acclimation (Kapsenberg and Cyronak 2019, Byrne et al. 2020, Karelitz et al. 2020). Therefore, exposure to seawater chemistry variability has the potential to modulate calcifiers sensitivity to OA and enhance their adaptive capacity (Kapsenberg & Cyronak, 2019). In many coastal areas, vegetated habitats, such as seagrass meadows and macroalgal forests, can modify the intensity of OA exposure for resident calcifying organisms, through their metabolic activities (i.e., photosynthesis and respiration), which can remove and add seawater CO_2 concentrations (Falkenberg et al. 2021, Ricart et al. 2021). For example, the photosynthetic activity of seagrasses, including *P. oceanica*, has been reported to increase pH levels across different spatial and temporal scales compared to non-vegetated habitats (Hendriks et al. 2014, Pacella et al. 2018, Ricart et al. 2021). This change in seawater chemistry could act as OA refugia for stress-sensitive species, by temporally reducing exposure to harmful conditions, although this benefit may vary with seasons, hydrodynamic conditions and macrophyte density and biomass (Krause-Jensen et al. 2016, Falkenberg et al. 2021).

To date, the biological effects of pH variability on calcifying marine invertebrates remain somewhat elusive, with non-generalizable responses among taxa and life stages (Kapsenberg & Cyronak, 2019). For example, macrophyte-driven biogenic pH fluctuations have been shown to increase calcification of adult mussels under OA scenario, by shifting most of their calcification activity during daylight hours of high pH (Wahl et al. 2018a). In contrast, experiments on larvae of different bivalve species found that pH fluctuating of ~ 0.3 units around ambient and low pH conditions did not mitigate the negative impacts of reduced pH on larval development and survival (Frieder et al. 2014, Kapsenberg et al. 2018). Therefore, it has been argued that biogenic pH fluctuations could potentially act as OA refugia for stress-sensitive species if high pH values can be maintained for a period of biological significance compared to unvegetated areas (Krause-Jensen et al., 2016; Kapsenberg & Cyronak, 2019).

Here, in line with our hypotheses, we found that *P. oceanica* plants increased pH values and the carbonate saturation state at both ambient and low pH treatments compared to tanks without plants. These changes in seawater chemistry likely provided a temporal refugia for sea

urchin larvae exposed to low pH, as the percentage of larval abnormal development and their total body length significantly decreased and increased, respectively, in tanks with *P. oceanica* compared to those without plants. In particular, the abnormal development of plutei and the total body length of echinoplutei growing at low pH within *P. oceanica* plants were comparable to those recorded at ambient pH. To the best of our knowledge, this is the first study experimentally investigated the biological impacts on seawater chemistry fluctuations on different development stages of sea urchin larvae. The contrasting results between our work and those found in previous experiment with bivalve larvae could be due to variations in OA sensitivity among early life stages of calcifying taxa. Alternatively, it could be the result of the different methods used to manipulate pH fluctuations as, in the aforementioned studies, pH changes were chemically (not biologically) induced (Frieder et al., 2014; Kapsenberg et al., 2018) and may not be comparable to fluctuations of pH and associated carbonate chemistry imposed by biological processes.

The role of vegetated habitats, such as seagrass meadows and macroalgal forests, in rescuing stress-sensitive species from increasingly adverse conditions due to climate change has recently garnered considerable attention to identify potential climate refugia and devised sounded mitigation strategies, such as restoration or conservation plans (Bulleri et al. 2018b, Kapsenberg and Cyronak 2019, Falkenberg et al. 2021). Here, we show that the presence of *P. oceanica* plants, by raising pH and associated carbonate saturation state through their metabolic activity, can buffer the negative effects of OA on the calcifying larvae of the sea urchin, *P. lividus*. Thus, the results of our study add to recent evidence that macrophyte-driven substantial biogenic fluctuations can be managed as nature-based solution against climate-driven loss of biodiversity under future climates (Wahl et al., 2018; Falkenberg et al., 2021).

Importantly, a benefactor species should be able to withstand adverse future conditions, without major changes in structural traits, such as morphology or density, that could undermine its ability to rescue other species (Bulleri *et al.*, 2018). *P. oceanica*, like other macrophytes, is predicted to benefit, or to be unaffected by chemical changes in seawater driven by enhanced CO_2 concentrations, having thus the ability to persist and deliver benefits to associated organisms under future OA scenario.

2.4 Greece: seagrasses and macroalgal meadows, soft/rocky bottom (SL#27)

2.4.1 Introduction

The Northern Karpathos and Saria MPA is located in the Dodecanese islands (Greece), Eastern Mediterranean Sea, and covers an area of about 154 km^2. Saria is a small island separated from Karpathos by a narrow sea strait less than 100 m wide. The MPA is included in the list of Natura2000 sites (GR4210003) and hosts a rich biodiversity and many endemic species (flora and fauna, including birds). Populations of several charismatic marine species such as the Mediterranean monk seal (*Monachus monachus*), the dolphin *Tursiops truncates* and the marine turtles *Caretta caretta* and *Chelonia mydas* are present in the MPA. Tristomo Bay is an enclosed highly productive fishing area in the MPA with extensive *Posidonia oceanica* and *Cymodocea nodosa* meadows surrounded by hard substrate. The bay hosts thriving populations of the bivalves *Arca noae* and *Pinna nobilis*. The number of non-native species, such as *Caulerpa taxifolia* and *Halophila stipulacea,* are increasing in the area; however, *P. oceanica* has been proven so far, a good competitor maintaining the ecosystem balance.

These habitats provide a range of services, such as: a) provisioning services (i.e. dead leaves can be used in industry and agriculture); b) regulation and maintaining services (i.e. seawater is purified by filtration, the leaves reduce water turbidity, offer shelter and nursing habitat, protect the seabed from erosion and support nutrient cycling and oxygenation; and c) cultural services (preservation of the underwater cultural heritage, diving tourism, marine environmental education).

The area has a significant archaeological value due to the 7th-10th century AC settlements that are present, while the Ephorate of Underwater Antiquities performs field research as there are remains which are yet to be studied. The Management Agency of Dodecanese Protected Areas (formerly Management Agency of Karpathos-Saria) was established in 2002, and its primary objective is the management, protection and conservation of the species and habitats of the MPA.

Climate change may impact in different ways the seagrass meadows and the associated benthic assemblages. Firstly, the region is relatively close to the Suez Canal, which is the main point of entrance for invasive alien species (IAS) in the Mediterranean (Corsini-Foka et al. 2015). Thus, the islands of Karpathos and Saria are characterized by the high prevalence of marine IAS, which form dense populations. Examples of such IAS are the seaweed *Halophila stipulacea*, the lionfish (*Pterois miles*) and the invasive long-spined sea urchin (*Diadema setosum*). *H. stipulacea* does not seem to compete with *P. oceanica* since the two species are ecologically very different; however, the temperature increase poses a potential threat at the naturally occurring meadows of *P. oceanica* which, in turn, could be substituted by *H. stipulacea*, one of the “100 Worst Invasive Alien Species in the Mediterranean” (Lowe et al. 2000). Despite the capability of *P. oceanica* plants to acclimate to temperature changes, it has been predicted that even under a relatively mild greenhouse-gas emissions scenario, this species might face functional extinction by the middle of this century (Winters et al. 2020). In addition, changes in the sea currents imposed by climate change may impact the gene flow and connectivity of the *P. oceanica* meadows with other meadows in the Eastern Mediterranean, since population connectivity is strongly influenced by environmental factors such as oceanic currents, depth profiles, changing water flows and gyres (McMahon et al. 2018).

Furthermore, Tristomo gulf is a naturally occurring semi-enclosed gulf in the region, protected from wave action that may act as a climate refugium in terms of warming for several species; it is considered as the most important marine site in Karpathos (Adamantopoulou et al. 2000). There is also very limited anthropogenic activity in Tristomo gulf, therefore it can act as a hotspot for preservation and conservation of several marine species, from schools of fish to the critically endangered noble pen shell (*Pinna nobilis*) and the Noah's Ark shell (*Arca noae*).

The present experiment aims to compare the community structure and functionality a) between hard bottom communities and soft bottom macrophyte communities and b) between native and invasive macrophyte soft bottom communities. The vegetated hard bottom communities included only turf (no macroalgae were present), while the unvegetated hard bottom communities were completely bare due to overgrazing. The macrophyte soft bottom communities included the native *Cymodocea nodosa* and the invasive *Halophila stipulacea* seagrasses. Macrophyte meadows have a strong potential as carbon sinks (Marx et al. 2021), therefore we assessed community productivity and carbon turnover between communities dominated by native versus invasive species.

2.4.2 Methods

During the present study, field in situ incubation experiments were performed in the area of Mononaftis in northern Crete. This site was selected as a more convenient option for performing the experiments and it has the same environmental characteristics with the storyline area. Four different benthic habitats were selected (Fig. 35): 1) one soft vegetated with the invasive macrophyte *Halophila stipulacea*, 2) one soft vegetated with the native macrophyte *Cymodocea nodosa,*3) one with vegetated (turf) hard substrate and 4) one with non-vegetated (barren) hard substrate. Three replicates per habitat were performed.

Incubation chambers were constructed as shown in Figure 35 using a plastic bag of known volume that was attached on a piece of plastic pipe on the bottom. The chamber was fixed on the substrate using either a fast-drying epoxy filler for underwater application (hard substrate) or a belt with diving weights attached (soft bottom). The incubation bag was equipped with an oxygen and a lux logger attached to a fishing float that also helped maintaining the upper position of the plastic bag. The bag had also a tube for collecting water samples during the experiment (Fig. 36A).

The incubation chambers were initially covered with a black bag for about two hours to simulate the dark conditions (respiration only) and then uncovered and left during two additional hours simulating the light phase (Fig. 37). Water samples were collected at the beginning of the experiment, after the dark phase and after the light phase. The water samples were used to estimate nutrients (PO_4, NH_4, NO_3, NO_2, SiO_2), Particulate Organic Carbon (POC), Total Inorganic Carbon (TIC) and Total Organic Carbon (TOC). In addition, pH, salinity and alkalinity were measured in the water samples. Oxygen, temperature and light intensity (lux) were continuously monitored using the loggers. After the end of the experiment macrophytes within the soft substrate incubation chambers were collected in order to estimate their biomass as wet, dry (70°C for 8 hours) and ash (500°C for 4 hours) weight. Turf biomass was not estimated since it was not dense enough to be collected from the hard substrate surface. In addition, macrobenthos samples were collected from the experimental chambers (Fig. 37) using a manually operated suction sampler (MANOSS) (Chatzigeorgiou et al, 2013) for the vegetated hard substrate and plastic corers for the soft substrate, and their abundance and biomass (wet weight) were recorded per taxonomic category.

After the end of the experiment 5ml of a KH_2PO_4 solution of known concentration (0.25M) were added in the incubation bag and carefully mixed (Apostolaki et al., 2010). Then a sample of 500 ml was collected and the final PO_4 concentration was estimated in order to estimate the total volume of water into the incubation bag.

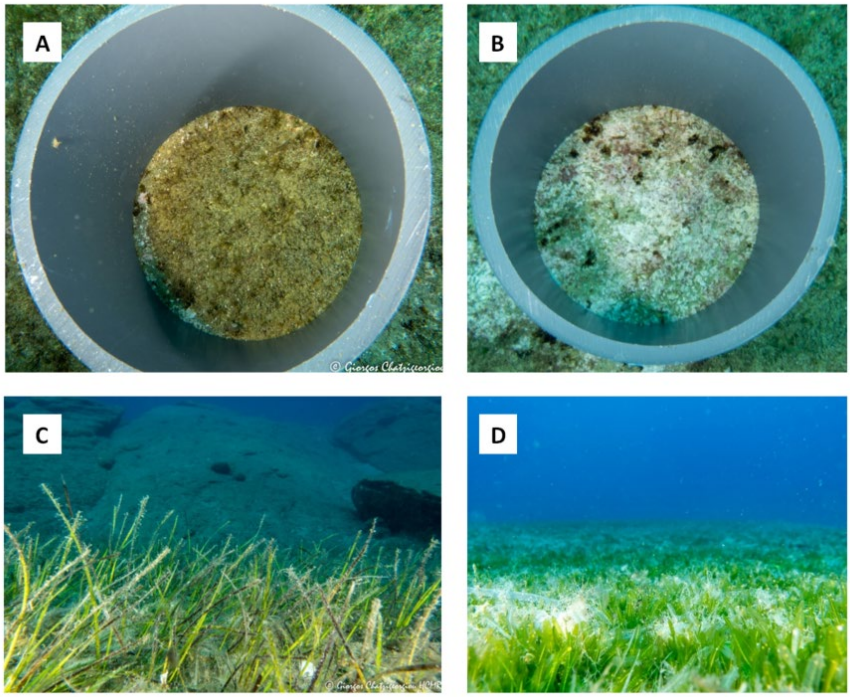

Figure 35 The different habitats used for the incubation experiments. A) hard substrate vegetated (turf), B) hard substrate non-vegetated, C) soft substrate Cymodocea nodosa and D) soft substrate Halophila stipulacea.

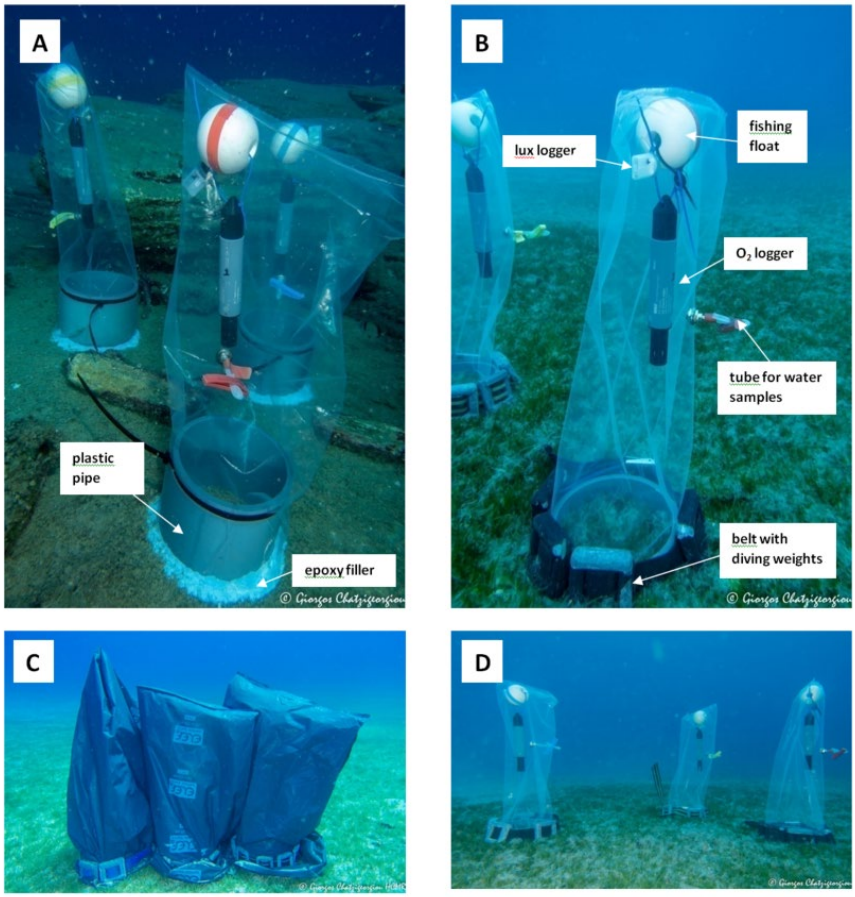

Figure 36 Field incubation experiments A) hard substrate, B) soft substrate, C) dark phase, D) light phase.

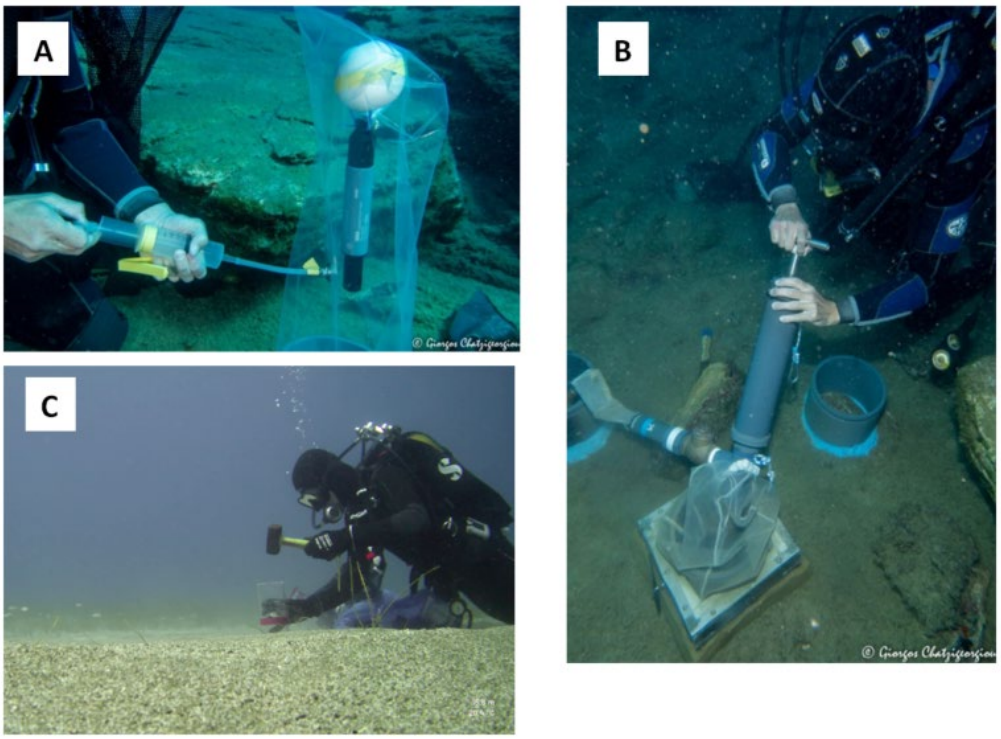

Figure 37 A) collection of water samples, B) collection of macrobenthos samples from hard substrate using the MANOSS suction device, C) collection of macrobenthos samples from soft substrate using corers.

2.4.3 Results

The concentration of phosphates (PO_4) and nitrates (NO_3) is higher in the seawater surrounding both the vegetated and non-vegetated hard bottom habitats in comparison to soft bottom macrophyte habitats (Fig. 38). More specifically, nitrates in vegetated hard substrates are significantly higher during the whole experiment (zero, dark, light) than all the other habitats (ANOVA - zero: F=4.18, p=0.047; dark F=8.36, p=0.008; light F=18.57, p=0.001). Ammonium (NH_4) is lower in the soft *Cymodocea* habitat in comparison to all other habitats, while vegetated hard substrates have significantly higher NH_4 concentration (Anova F=7.97, p=0.009). Seawater from soft bottom substrates with macrophytes is in general poor in nutrients, although the invasive *Halophila stipulacea* has higher concentration of nitrates (NO_3) and ammonium (NH_4) in comparison to the native *Cymodocea nodosa*. The soft substrate macrophytes habitats have constant concentrations in nutrients during the dark and light phase of the experiment (ANOVA p>0.05). Phosphates (PO_4) in the hard substrate habitats, especially in vegetated ones - are gradually reduced during the experiments during both the dark and the light phases of the experiment, although differences are not statistically significant (ANOVA F=2.18, p=0.194).

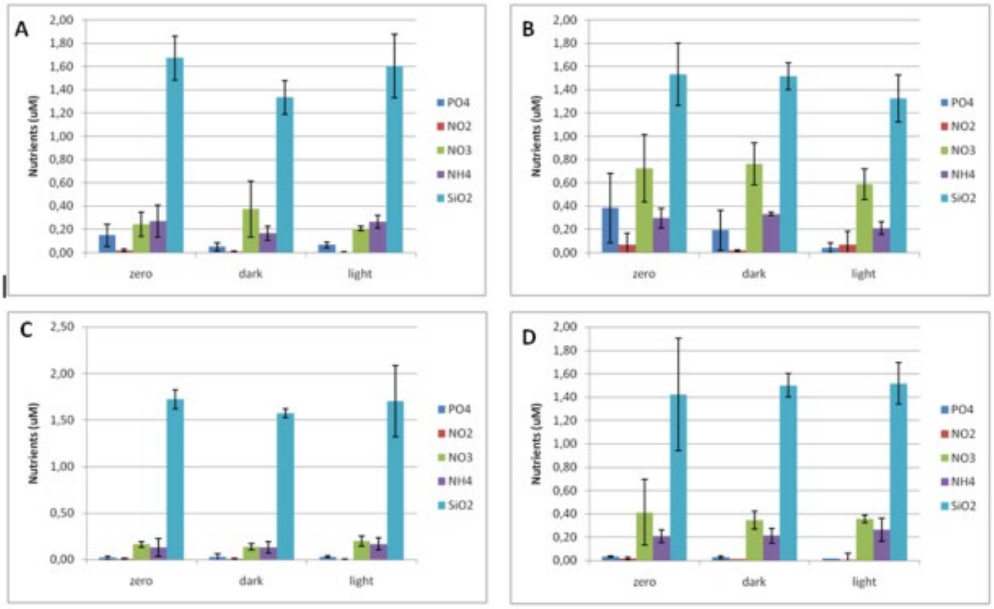

Figure 38 Concentration of nutrients (µM) PO4, NH4, NO3, NO2, SiO2 in seawater samples collected during the beginning of the experiment (zero), after the dark phase (dark) and after the light phase (light) in the A) non-vegetated hard substrate, B) vegetated hard substrate, C) soft substrate Cymodocea nodosa and D) soft substrate Halophila stipulacea. Error bars represent standard deviation.

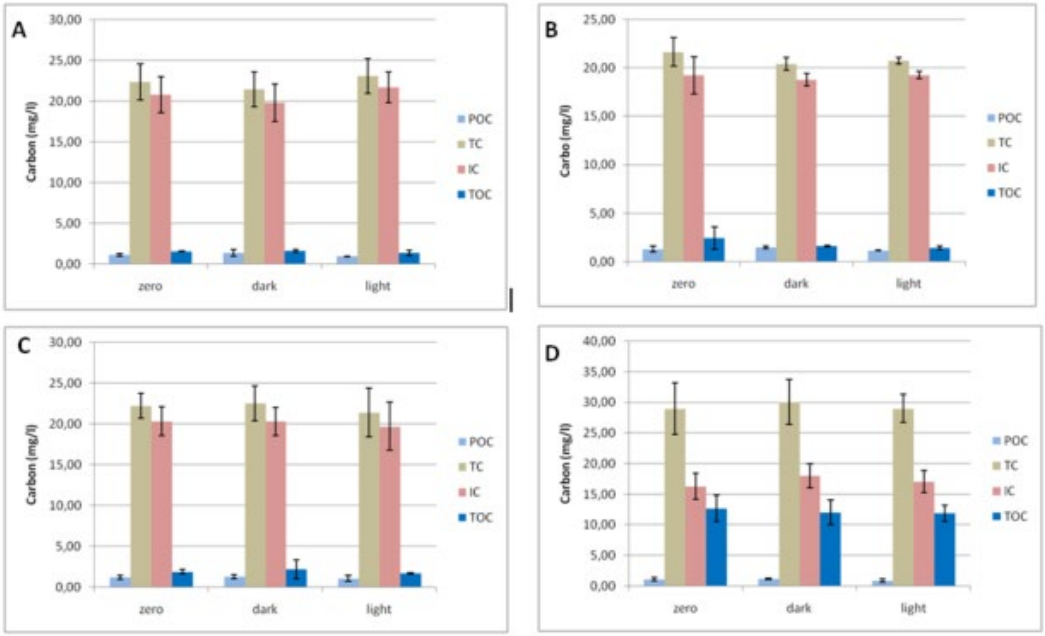

Figure 39 Concentration of carbon as Particulate Organic Carbon (POC), Total Carbon (TC), Inorganic Carbon (IC) and Total Organic Carbon (TOC) in seawater samples collected during the beginning of the experiment (zero), after the dark phase (dark) and after the light phase (light) in the A) non-vegetated hard substrate, B) vegetated hard substrate, C) soft substrate Cymodocea nodosa and D) soft substrate Halophila stipulacea.

In hard substrates, both vegetated and not, as well as in the native *C. nodosa* areas, the inorganic carbon is considerably higher and constitutes the most significant proportion of the total carbon in seawater (Fig. 39). On the contrary, in the invasive *H. stipulacea* soft substrates the total organic carbon (and therefore the total carbon as well) is significantly higher (almost

5 times) than all the other substrates and remains like that during both the dark and light phases (ANOVA zero: F=59.64, p<0.001; dark F=59.10, p<0.001; light F=176.87, P<0.001).

Oxygen concentration remains constant (reduction rate = 0 mg/l) during the dark phase in non-vegetated and vegetated hard substrate habitats (ANOVA F=2.46, p=0.137). On the contrary, in soft substrates with *C. nodosa*, oxygen is slightly reduced during the dark phase (reduction rate = 0.001 mg/l), and this is more intense (reduction rate = 0.002 mg/l) in the *H. stipulacea* chambers (Fig. 40). During the light phase, oxygen is increased for all habitats. Non-vegetated and vegetated hard substrate habitats have a lower rate (increase rate = 0.002 mg/l) and are similar between them, in comparison to macrophyte soft substrate habitats. The rate of oxygen increase in *C. nodosa* is double than the hard substrates (increase rate = 0.004 mg/l). *H. stipulacea* has an even higher increase rate (increase rate = 0.005 mg/l), which is significantly different from all other habitats (Anova F=9.60, p=0.005).

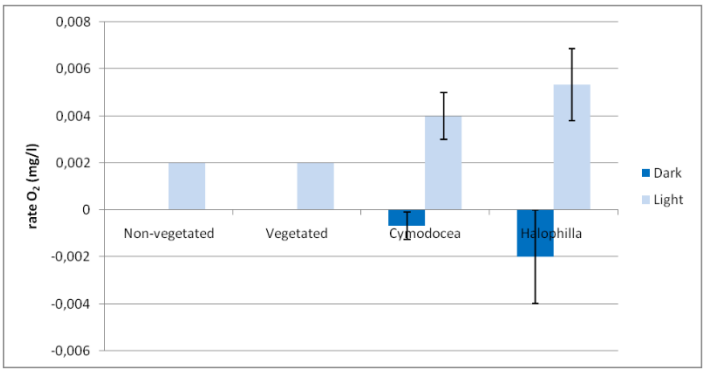

Figure 40 Oxygen reduction rate (dark) or production rate (light) as monitored during the in-situ experiment in the four habitats (non-vegetated hard substrate, vegetated hard substrate, soft substrate Cymodocea nodosa and soft substrate Halophila stipulacea).

Community net primary production (NPP_{O2}) based on oxygen fluxes (Fig. 41) is significantly higher in both macrophyte communities in comparison to hard substrate communities (ANOVA: F=15.80, p<0.001) as it was also confirmed by the Tukey's pairwise comparisons. The hard substrate habitats have similar NPP_{O2} between them, as is also the case for the two soft substrate habitats. Community respiration (CR_{O2}) is significantly higher in the *H. stipulacea* macrophyte communities in comparison to both hard substrate communities (ANOVA: F=7.61, p=0.010) as it was also confirmed by the Tukey's pairwise comparisons. Gross primary production (GPP_{O2}) is higher for both macrophyte communities in comparison to hard substrate habitats; however, differences were not statistically significant (ANOVA, F= 3.59, p=0.066).

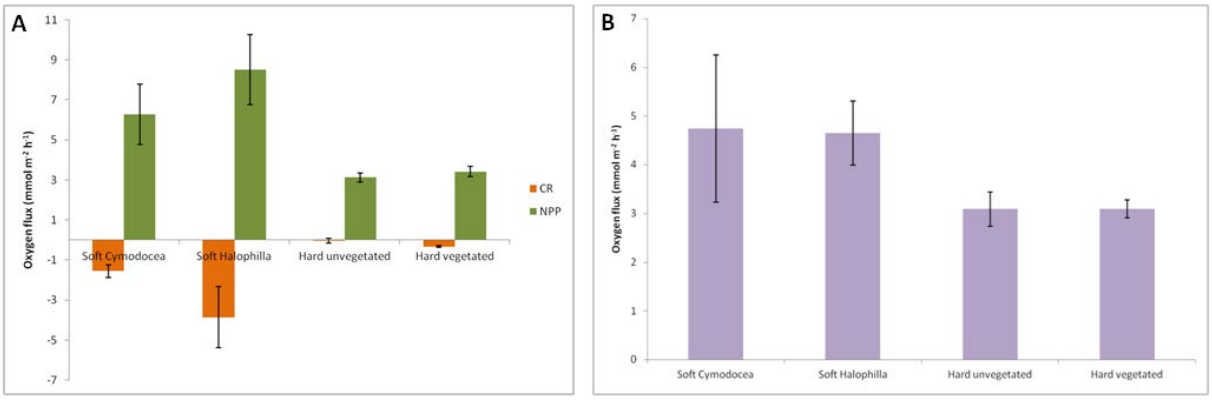

Figure 41 Community metabolic rates in the four habitats (soft substrate Cymodocea nodosa, soft substrate Halophila stipulacea, non-vegetated hard substrate and vegetated hard substrate indicated by A) community net

primary production (NPPO2) and community respiration (CRO2) and B) gross primary production (GPPO2) based on oxygen fluxes estimated during in situ incubations. Error bars correspond to standard deviation (SD).

Community fluxes based on DIC showed high variability and therefore differences although visible were not statistically significant. Community net primary production based on the DIC flux (NPP_{DIC}) (Fig. 42) was higher in the hard-non-vegetated substrate (with positive values), however differences with other habitats were not significant (ANOVA F= 0.73, p=0.562). NPP_{DIC} values obtained in both macrophyte habitats were negative, indicating a reduction in DIC concentration and prevalence of production over respiration in those autotrophic communities. By contrast, community respiration based on the DIC flux (CR_{DIC}) was higher in the soft substrate *Halophila* habitat, however differences were as well not statistically significant (ANOVA F= 1,00, p= 0,440).

Macrophyte (seagrass) biomass (Fig. 43 A) was found at similar levels between the two species, for wet weight (ANOVA F=0.08, p= 0.787), dry weight (ANOVA F=0.90, p= 0.396) and ash weight (ANOVA F=4.31, p= 0.107). *H. stipulacea* had a slightly lower wet weight and a higher ash weight in comparison to *C. nodosa*, however differences were not significant.

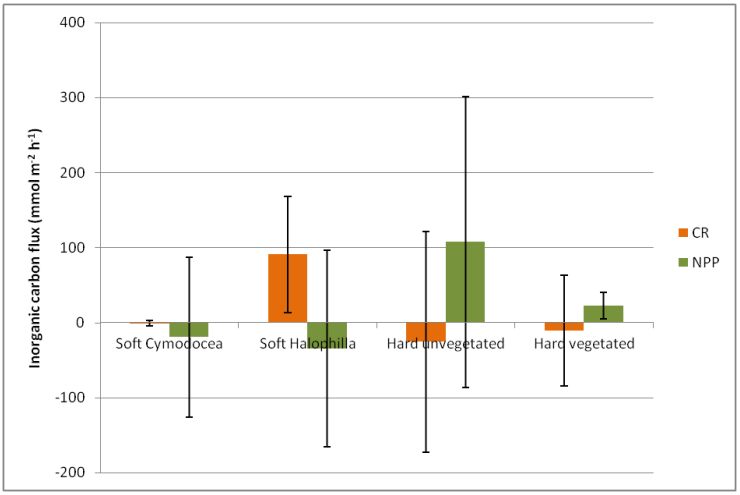

Figure 42 Community metabolic rates in the four habitats (soft substrate Cymodocea nodosa, soft substrate Halophila stipulacea, non-vegetated hard substrate and vegetated hard substrate indicated by community net primary production (NPPDIC) and community respiration (CRDIC) based on inorganic carbon fluxes estimated during in situ incubations. Error bars correspond to standard deviation (SD).

The abundance and the biomass of the macrobenthic communities were clearly lower in the hard vegetated substrate (Fig. 43 B), however due to the increased variability between the replicates

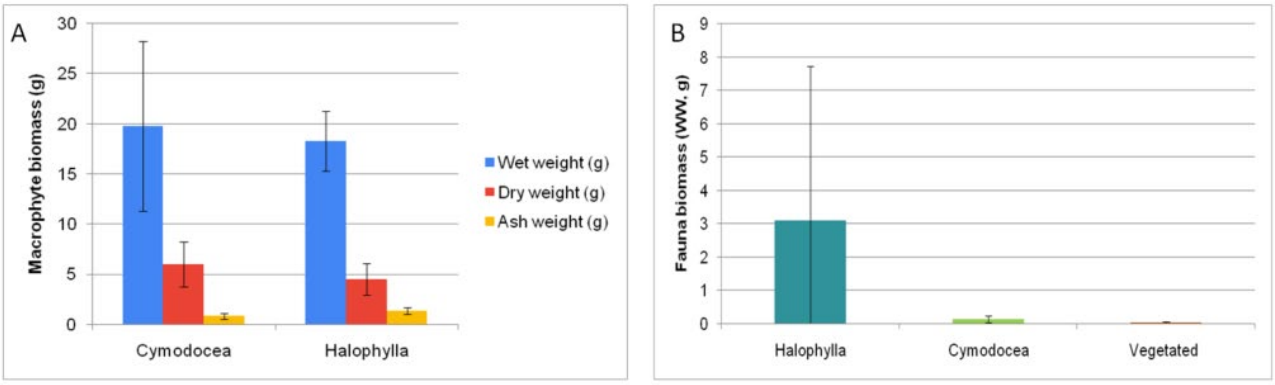

Figure 43 A) Macrophyte biomass for Cymodocea nodosa and Halophila stipulacea inside the incubation chambers as wet, dry and ash (weight). B) Total fauna biomass (wet weigh, g) for soft Halophila stipulacea, soft Cymodocea nodosa and hard vegetated substrates inside the incubation chambers.

of the soft substrate differences were not significant (ANOVA F= 1.27, p=0,346). Only 6 out of the 14 taxonomic groups were present in hard bottoms with Polychaeta being the most abundant group (Fig. 44 A). The non-native *H. stipulacea* hosts higher abundances and higher biomass(Fig 44 B) of macrofauna in most taxonomic categories. Only Gastropoda are more abundant in the native *C. nodosa* communities.

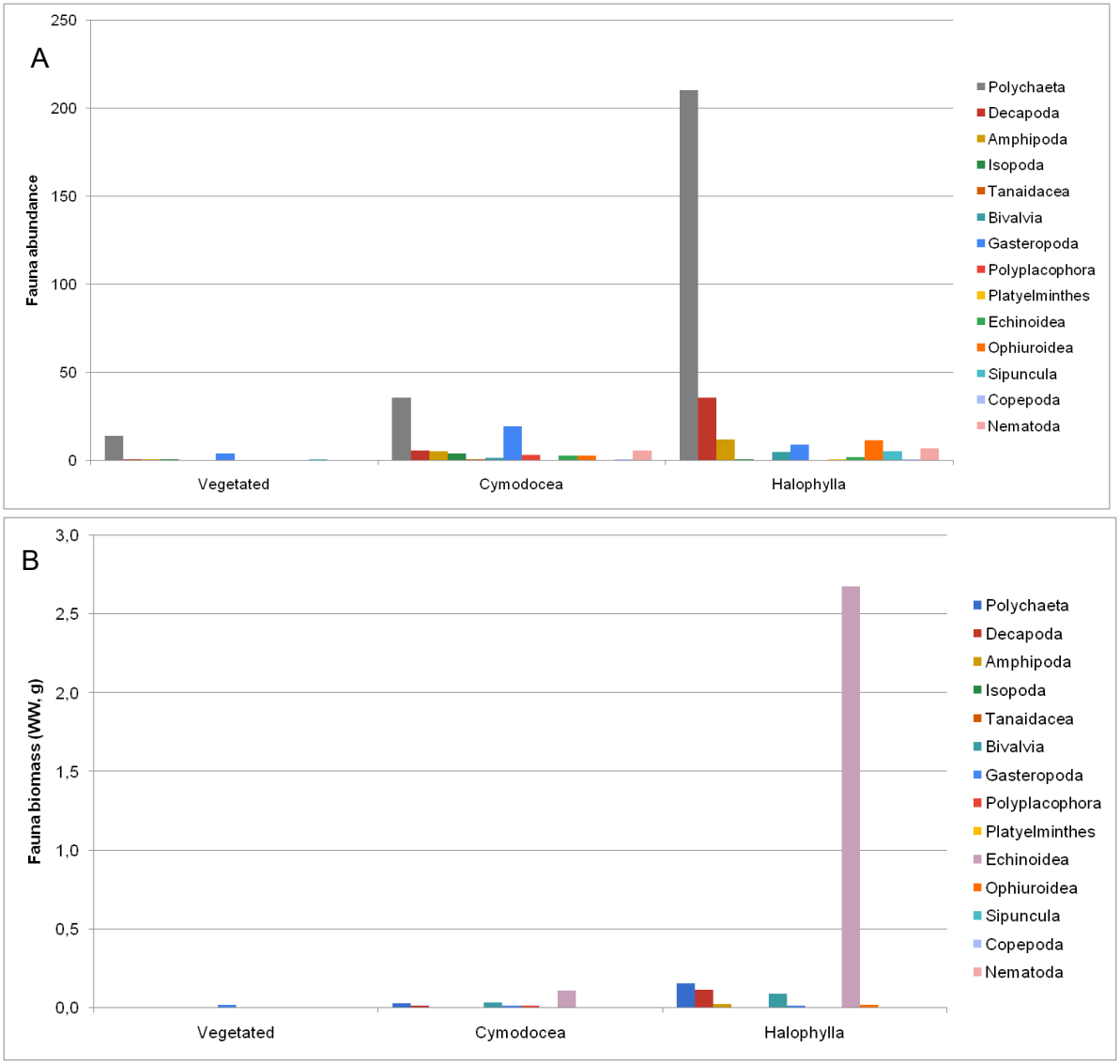

Figure 44 A) Abundance and B) biomass (wet weight, g) of the macrobenthic communities inside the incubation chambers of the vegetated hard substrate, the Cymodocea nodosa and the Halophila stipulacea soft substrate experiments.

2.4.4 Discussion

Seagrass habitats, such as the ones examined in the present study, are characterised as some of the most important ecosystems in the biosphere by supporting fisheries production, mitigating CC and improving water quality (Boutahar et al. 2022). However, seagrass meadows are currently at risk due to human disturbances and CC. *Cymodocea* meadows such as the ones that present in our Storyline area have high productivity and are rich in biodiversity. They form important nursery grounds for several species of fish (Verdiell-Cubedo et al. 2007) and they are hosting ample invertebrate species such as polychaetes, amphipods, isopods, decapods and molluscs (Brito et al. 2005). However, *Cymodocea nodosa* is usually threatened by mechanical disturbance such as trawling, pollution, competition with other seagrass species and alien species invasions (Short et al. 2010, Boutahar et al. 2022). Therefore, the aim of this study was to examine the productivity and functioning of a native species meadow (*C. nodosa*) in comparison to an alien macrophyte species meadows (*Halophila stipulacea)*, as well as in comparison to hard substrate habitats which are characterised by a reduced or complete absence of vegetation in this particular region.

Habitats of soft substrates with seagrass appeared to be less rich in seawater nutrients when compared to hard substrates with restricted or no vegetation. This is probably due to the fact that one of the most important functions of marine macrophytes is the absorption of nutrients including phosphorus and nitrogen from seawater, either by direct uptake or though the symbiotic bacteria found on their roots (Brix 1997). Similarly, community net primary production and gross primary production were higher in both macrophyte communities in comparison to hard substrate communities, while *Halophila stipulacea* had higher community respiration (based either on O_2 or DIC fluxes) than all habitats. In addition, the non-native *H. stipulacea* hosted the highest abundances and biomass of macrofauna in most taxonomic categories. As Winters et al (2020) indicated in their review, Polychaeta, Amphipoda and Decapoda are among the most abundant groups in *H. stipulacea* meadows, and this is in accordance with our findings during the present study.

The work in this Storyline found that hard substrates, both vegetated and non-vegetated, as well as the native *C. nodosa* areas, were richer in inorganic carbon, while the invasive *H. stipulacea* soft substrates had a significantly higher organic carbon content. This is in agreement with what Apostolaki et al. (2019) had indicated regarding the considerable storing capacity of carbon and nitrogen of the exotic *H. stipulacea* that reaches a 2-fold higher C stock than non-vegetated areas and *C. nodosa* meadows. Therefore, the introduction of *H. stipulacea* in native ecosystems may actually contribute in the increase of carbon sequestration in the Eastern Mediterranean (Apostolaki et al. 2019).

Oxygen reduction and oxygen increase rates are the highest for *H. stipulacea* in comparison to the native species meadows. Bare and low vegetation sites were even less productive regarding oxygen during their photosynthetic period. There is recent evidence that the invasive *H. stipulacea* populations are able to shift their thermal niche, suggesting a rapid adaptation towards the lower thermal regimes in the Eastern Mediterranean (Wesselmann et al. 2020). *H. stipulacea* seems to have the capacity to cope with colder thermal conditions by displacing its thermal niche downwards, instead of just broadening its amplitude, which is already exceptionally broad (Wesselmann et al. 2020). A recent study indicated that under the most severe climate change scenario the meadows of *C. nodosa* could be reduced by 20 - 46%, while *H. stipulacea* seems well adapted under these climate change scenarios in the future Mediterranean Sea (Chefaoui et al. 2018). Therefore, climate change might result in a significant change regarding the composition of macrophyte communities that thrive in the Mediterranean Sea and specifically in the area of Storyline #27.

2.5 Spain: macroalgae forest restoration (SL29)

2.5.1 Introduction

Marine macrophytes, including seaweeds and seagrasses, are the main drivers of primary production in coastal regions (Mann 1973). Specifically, large brown seaweeds have the ability to form dense stands over large areas, creating what is commonly known as marine forests (Wernberg and Filbee-dexter 2019). These forests underpin entire ecosystems by generating large amounts of oxygen and accumulating organic matter via photosynthesis (Pessarrodona et al. 2022). These marine forests also provide habitat and shelter for numerous organisms (Cheminée et al. 2013, Teagle et al. 2017) and are particularly important for human societies, delivering a wealth of ecosystem functions and services (Eger et al. 2023).

Despite this recognition, human impacts have driven widespread changes and losses of marine forests (Krumhansl et al. 2016). A common consequence of impacts is the replacement of highly complex and structured marine forests for small, mat-forming algae (Vergés et al. 2014b). These shifts can cause alterations in some ecosystem functions and processes as, for example, modifications in food webs and energy flows (Vergés et al. 2019) (Vergés et al., 2019) or changes in biodiversity and primary production (Rocha et al. 2015). Several studies have demonstrated that several years are needed for the recovery of some marine ecosystems (Jones and Schmitz 2009) and, in numerous cases, they cannot recover even after the removal of the initial impact. To that end, active restoration actions appear should be considered as a good tool capable to reverse the loss and degradation of ecosystems (Suding et al. 2015).

In terrestrial environments, besides the vegetation structure and species diversity, restoration efforts also aim for the rehabilitation of functions and services, to ensure that the ecosystems deliver again the benefits and services they previously provided or have the potential to provide (Suding et al. 2015). Therefore, from the perspective of ecological restoration we are interested to assess the restorations of functions in restored communities, by measuring the metabolism of a complete restored community compared to degraded areas and more intact/healthy ones. In this study, we aimed to determine the recovery of ecosystem processes such as primary production and respiration after the restoration of a marine forest. We evaluated the community metabolism of a restored forest using *in situ* benthic incubations, in spring and autumn. We compared the restored forest results with a degraded site and a healthy forest (used as a reference site). Estimations of metabolic rates were based on both oxygen and carbon fluxes. With all this information, we seek to understand to what extent active marine restorations are able to recover parts of the ecosystem functions and services.

2.5.2 Materials and methods

1. Study site

We focused our study on a restoration action that took place in 2011 in the Bay of Maó (Menorca, NW Mediterranean Sea), where the reintroduction of a structural and foundation species (*Gongolaria barbata*) led first to the recovery of the population (Verdura et al. 2018, Gran et al. 2022) and later to the recovery of the associated macroalgal community and the overall functionality (Galobart et al. 2023). We compared the metabolism (i.e. primary production and respiration) of the restored forest (39° 52' 47.65" N, 4° 18' 28.46" E) with a healthy and mature *G. barbata* forest located ca. 50 km north (40° 2' 4.46" N, 4° 8' 14.03" E), which represents one of the only two remaining populations of *G. barbata* in the island and was the donor population of the restoration. We also studied the metabolism of a degraded

site located nearby the restored forest (39° 52' 43.78" N, 4° 18' 33.56" E), but without the presence of the structural or any other canopy forming species.

Benthic incubations were replicated in two seasons, spring and autumn (April 2022 and October 2021; respectively). At each season, we conducted the incubations during three consecutive days in a calm and constant weather window that ensured consistent environmental conditions. We measured every day the *in-situ* water temperature, salinity, above surface irradiance, pH and dissolved oxygen prior to the incubations to account for any sudden change in water and atmosphere conditions that may influence the incubation outcomes.

2. Field setup

The field setup was followed and adapted from Peleg et al. (2020). The incubation design consisted of a dome-shaped chamber (ca. 17.5 L, 0.42 cm in diameter) with a rigid "skirt" of 4 cm at the base. We used transparent and black, opaque methacrylate chambers for light and dark treatments. Light treatments allowed us to estimate community net primary production, while dark treatment accounted for community respiration. Chambers were connected to an automated external pump that circulated the water at a rate of 240 L h^{-1}. The pump was powered by a 12 V battery made waterproof and was operated through a float switch. During the incubations, chambers were carefully sealed using Lycra bags (175 x 25 cm) filled with sand collected at the surroundings of each site and placed below and above the chamber skirt.

For each site (i.e. degraded, restored forest and forest), we randomly deployed 6 replicate incubation chambers. Light incubations were always conducted around midday, guaranteeing a period of much light availability. Prior to the incubations, we placed the chambers over communities for a period of 30 minutes to allow all the organisms acclimatise to new light conditions. We incubated the communities for 1 h 30 min (averaged time 1h 32 ± 6 min). At the beginning and end of each incubation, water from inside the chambers was slowly sampled through a tube and a sampling port using 100 mL polyethylene syringes. We sampled a total of 200 mL at each chamber for field and laboratory analysis.

3. Sea water measurements and chemical analysis

We determined initial and final concentrations of dissolved oxygen, pH and total alkalinity (TA) for each incubation. Dissolved oxygen and pH were immediately measured in the field using temperature corrected probes (Hach sensION+ DO6 and Hach sensION+ pH1 – 5052T, respectively). Oxygen and pH probes were calibrated to 100% of O_2 before everyday fieldwork and to 4, 7 and 10 calibration fluids, respectively. Water samples for TA were kept in 100 mL amber bottles, at 4ºC and in dark conditions until analysis. TA was determined within a maximum of four days via potentiometric titration with an automated open cell titrator (665 Dosimat, Metrohm, Switzerland) using 50 g of sample and 0.1 N HCl. Calibration of TA analytical procedure and HCl concentration was done using a 100 µeq kg^{-1} $NaHCO_3$ solution. Last, we calculated TA concentrations following the method in Sass & Ben-Yaakov (1977).

4. Metabolic rates

4.1 Oxygen flux

Community net primary production (NCP_{O2}) was estimated by the difference between the final and initial dissolved oxygen concentration in light incubations, while community respiration

(R_{O2}) was likewise estimated but using the dissolved oxygen concentration from dark incubations. Rates were normalised by area, volume and time according to the formula:

$$NPP_{O2}\ or\ R_{O2}\ (mmol\ O_2 \cdot m^{-2} \cdot h^{-1}) = \frac{([O_2]_{final} - [O_2]_{initial}) \cdot V}{(A \cdot t)}$$

Where *[O_2]* is the dissolved oxygen concentration (mmol O_2 · L^{-1}), *V* is the volume of the chamber (~17.5 L), *A* is the area enclosed in the chamber (42 cm in diameter; ~ 0.1384 m^2), and *t* is the duration of each incubation (hours). Community gross primary production (GPP_{O2}) was then calculated according to the formula:

$$GPP_{O2}\ (mmol\ O_2 \cdot m^{-2} \cdot h^{-1}) = NPP_{O2} + |R_{O2}|$$

4.2 Dissolved inorganic carbon flux

Community net primary production and respiration were also calculated considering the dissolved inorganic carbon variations (NPP_{DIC} and R_{DIC}, respectively). Concentrations of dissolved inorganic carbon (DIC) at the start and end of each incubation were calculated from pH and TA measures, and corrected by *in situ* temperature and salinity (Dickson et al. 2007) using the "seacarb" R package (Gattuso and al 2023). The constants K1 and K2 from Lueker et al. (2000) were applied in the calculations. NPP_{DIC} and R_{DIC} rates (light and dark incubations, respectively) were calculated following the same formulas as for the oxygen flux but with the initial and final DIC concentrations.

2.5.3 Results

During the 3-d spring incubations, water temperature was 20.04 ± 2.8 ºC, salinity was 36 ppm, surface light irradiance was 22,119 ± 155 µmol photons m^{-2} s^{-1}, dissolved oxygen was 7.30 ± 0.50 mg O_2 L^{-1} and pH was 8.23 ± 0.03. During autumn incubations, water temperature was 23 ± 2.4 ºC, salinity was 40 ppm, surface light irradiance was 18,251 ± 140, dissolved oxygen was 6.21 ± 0.46 mg O_2 L^{-1} and pH was 8.24 ± 0.03.

1. Oxygen flux

Community net primary production (NPP_{O2}) varied significantly by site and by the interaction between site and season ($p < 0.0001$ and $p < 0.0003$, respectively), with high NPP_{O2} values found in the forest in spring and in the restored forest in autumn (5.38 ± 1.01 and 5.08 ± 0.43 mmol $O_2 \cdot m^{-2} \cdot h^{-1}$, respectively) (Fig. 45). When comparing sites, NPP_{O2} of the degraded site differed from the ones found in the restored forest and the forest in both seasons, with consistently low NPP_{O2} values (0.87 ± 0.5 and 1 ± 1.03 mmol $O_2 \cdot m^{-2} \cdot h^{-1}$ in spring and autumn, respectively) (Fig. 45). Contrastingly, community respiration (R_{O2}) did not vary significantly in different sites or seasons, nor in the interaction between them (all $p > 0.05$, Fig. 45).

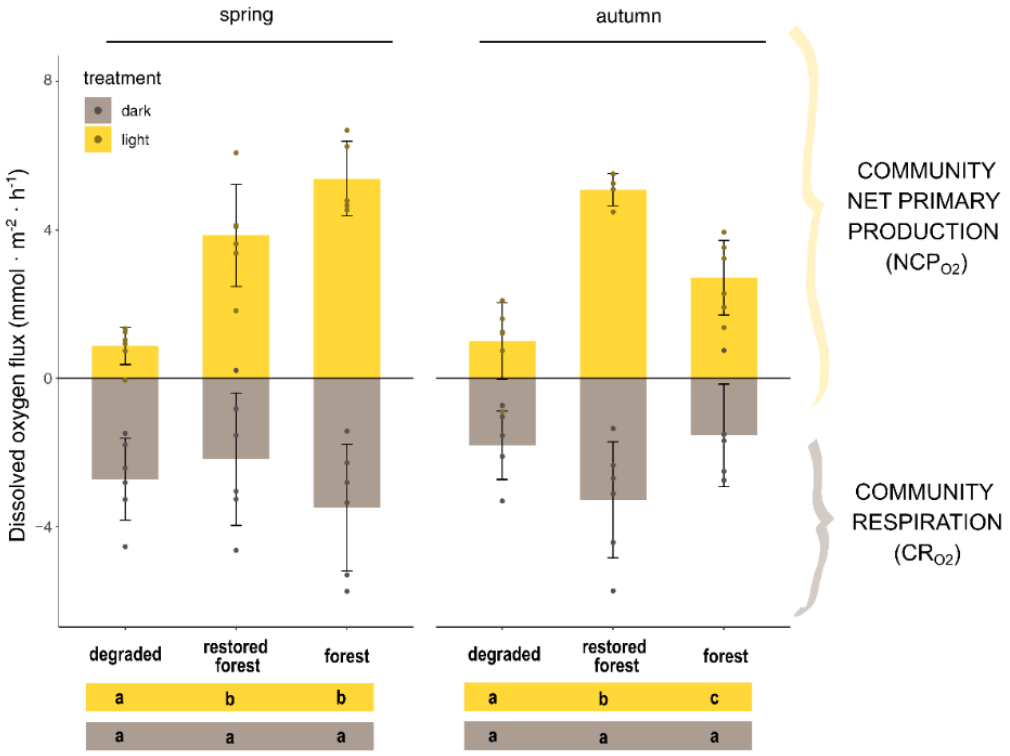

Figure 45 Community metabolic rates in the three studied sites (degraded, restored forest and forest) under light and dark treatments. Community net primary production (NPPO2) and respiration (RO2) was estimated in spring and autumn via oxygen evolution in 1 h 30 min incubations. Dissimilar letter under plots indicate significant differences (Bonferroni post-hoc pairwise test within 95% confidence intervals). Error bars correspond to standard deviation (SD).

Gross primary production (GPP_{O2}) was also significantly affected by site and the interaction between site and season ($p < 0.0001$ and $p = 0.0002$, respectively). In particular, GPP_{O2} of the degraded site was significantly different from the values obtained in the forest in spring and from the restored forest in autumn (Fig. 46). Despite this, here again, the degraded site was the one showing the lower GPP_{O2} values (3.59 ± 1.19 and 2.81 ± 1.57 mmol $O_2 \cdot m^{-2} \cdot h^{-1}$ in spring and autumn, respectively) (Fig. 46). The higher GPP_{O2} were obtained in the forest in spring and in the restored forest in autumn (9.89 ± 1.69 and 8.99 ± 1.75 mmol $O_2 \cdot m^{-2} \cdot h^{-1}$, respectively).

F

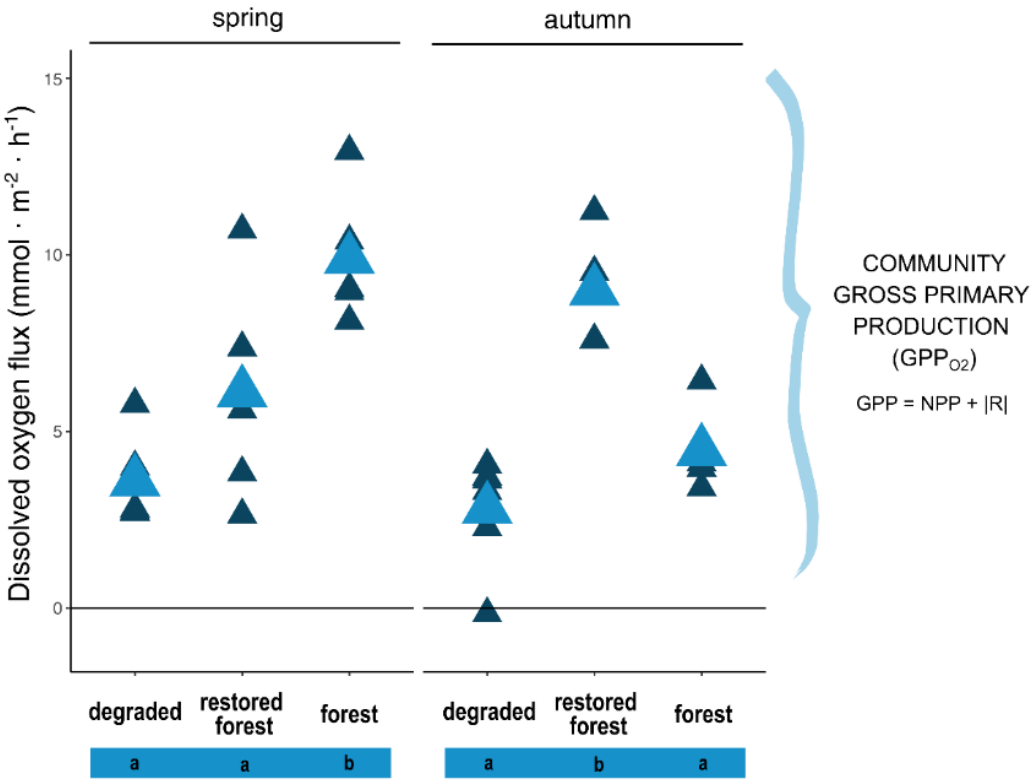

Figure 46 Community gross primary production (GPPO2) in the three studied sites (degraded, restored forest and forest) estimated via oxygen evolution in 1 h 30 min incubations in spring and autumn. Dissimilar letter under plots indicate significant differences (Bonferroni post-hoc pairwise test within 95% confidence intervals).

2. Dissolved inorganic carbon flux

Results related to the dissolved inorganic carbon (DIC) flux are reported from spring data, autumn data are not yet analysed. We found differences between the initial and final pH in all sites and in both light and dark incubations (Fig. 47). The pH was significantly augmented in the light incubations with a greater increase in restored forest and forest sites compared to degraded sites (Fig. 47). In contrast, pH significantly decreased in dark incubations, but showed a similar reduction at all sites (Fig. 47). Total alkalinity (TA) did not vary during incubations either in light or dark treatments nor at different sites (all $p > 0.05$, Fig. 47), with the exception of TA from dark incubations in the restored forest, which was significant ($p = 0.041$).

Community net primary production based on the DIC flux (NPP_{DIC}) varied between sites ($p = 0.025$), with significant differences between the degraded and the forest sites (Fig. 47). NPP_{DIC} from the restored forest showed high variability and no differences with the degraded and the forest site were found. All 6 NPP_{DIC} values obtained in the forest were negative (corresponding to a reduction in DIC concentration), while the restored forest and the degraded site presented both positive and negative results (5 out of 6 and 3 out of 5 negative NPP_{DIC} values,

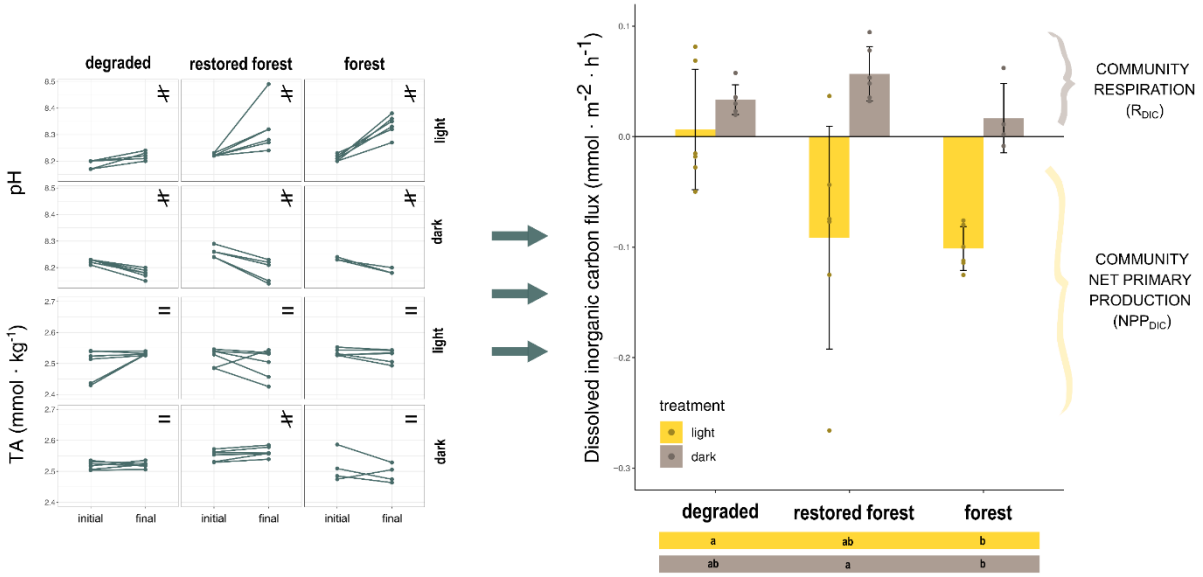

Figure 47 Initial and final measures of pH and total alkalinity (TA) during light and dark incubations at the three studied sites. Community net primary production (NPPDIC) and respiration (RDIC) was estimated in spring via dissolved inorganic carbon (DIC) evolution. Dissimilar letter under plots indicate significant differences (Tukey test within 95% confidence intervals). Error bars correspond to standard deviation (SD).

respectively). Last, community respiration (R_{DIC}) varied in relation to site, but the differences were marginally significative (p = 0.049)

2.5.4 Discussion

Our results show that, at all sites, gross community primary production (GPP) was higher than community respiration (CR), meaning that these sites accomulated organic matter in excess and, thereby acted as sinks of inorganic nutrients and CO_2 from the surrounding water.

The evaluation of the functioning of these important habitats, their potential productivity and the recovery of the oxygen and carbon cycles will result in a more holistic understanding of the restoration success and provide a long-term perspective. The results from the restored forest suggest that community net primary production has likely increased after 10 years from the restoration action since its production values are similar to those found in healthy and well-established forests dominated by the same structural species. The net gain of primary production after restoration is expected to be transferred to higher trophic levels, thus benefiting other associated invertebrate and fish species.

2.6 Portugal: Experimental approach to explore the functional effects of a weaker upwelling in kelp forests (SL21&23)

2.6.1 Introduction

Rocky coastal habitats support extensive and diverse macroalgal communities of structurally complex seaweed species with high ecological relevance known as marine forests (Wernberg and Filbee-dexter 2019). These communities are characterized by large habitat forming seaweeds (Dayton 1975) such as kelps or other species with similar functional properties, e.g. subtidal large canopy-forming species of the genus *Cystoseira*, *Fucus*, *Saccorhiza* and *Sargassum* among others (Coleman and Wernberg 2017, Wernberg and Filbee-dexter 2019). Marine forests create highly complex 3-dimensional submerged canopies which provide refuge for multiple species of mammals, crustaceans, fishes, other seaweeds and epibiota, together founding highly diverse assemblages (Mann 1973, Steneck et al. 2002). In addition, these communities have important socio-economical value as they create fishing grounds that support coastal fishing industries across the world (Smale et al. 2013, Bertocci et al. 2015). Besides these ecosystem-supporting and provisioning services, marine forests play an active role in mitigating the effects of climate change on a broad scale (Krause-Jensen and Duarte 2016). Indeed, marine forests, namely those formed by kelps, are thought to be among the most productive systems on Earth (Steneck et al. 2002) and fundamental in the carbon fixation balance of coastal areas. Marine forests net primary productivity may reach > 3000 g C m^{-2} $year^{-1}$ and the global primary productivity of this biome was projected to be around 1,521 TgC y^{-1} (Gao and McKinley 1994).

In the current scenario of climate change, marine forests, especially those characterized by cold affinity species like kelps, are facing increasing pressures from climate-driven stressors (Harley et al. 2012, Smale 2020). Anthropogenic activities are triggering ocean temperature increases (about 1°C on average since pre-industrial time) and the Intergovernmental Panel on Climate Change is expecting average global warming of sea surface temperatures (SST) between 1.5 and more than 4°C at the end of the century (IPCC 2019). Facing these increasingly stressful environments, organisms could physiologically acclimatize or adapt by producing more tolerant phenotypes over generations. Once certain thresholds are surpassed, organisms will need to migrate or face local extinction if the timing or speed of the stressors does not allow for acclimatization and adaptation (Parmesan 2006). Sessile ectothermic species with cold-water affinity like kelps are particularly affected by temperature increase which regulates the rate of enzymatic reactions and subsequently metabolic rates (Gerard 1997, Allakhverdiev et al. 2008). For instance, the increase in temperature is associated with the increase of respiration rates (Larkum et al. 2003) and when the increase of temperature is moderate, photosynthetic capacity is also promoted. However, beyond certain thresholds, temperature increases may reduce the maximum rate (Vmax) and substrate affinity (Km) of key enzymes such as RuBisCO leading to reduce photosynthetic capacity (Davison 1991). Moreover, supra-optimal temperatures can lead to protein denaturation and impairment of damage-protection systems which irreversibly affect the integrity of the photosynthetic apparatus (Takahashi and Murata 2008). Those adverse effects on photosynthesis and other metabolic rates ultimately result in reduced growth (Kübler and Davison 1995, Biskup et al. 2014) affecting in turn the population dynamic by reducing species abundance and overall assemblage productivity as well as eroding the resilience of the systems that will be more sensitive to other stressors, such as herbivory

In the north of Portugal, the presence of the Iberian upwelling system creates a sort of "boreal refuge", bringing cold and nutrient-rich seawater inshore and stimulating the occurrence of cold-water affinity species at relative low latitude, including highly productive and diverse kelp assemblages (Tuya et al. 2012). Although most eastern boundary upwelling systems around the world are expected to increase in intensity as the upwelling favorable winds tend to increase (Bakun 1990), in the case of the NW Iberian upwelling system, it is predicted that it will weaken in the near future due to the intense surface heating leading to higher stratification (Sydeman et al. 2014, Sousa et al. 2020). This will not only lead to an increase in seawater temperature but also to a decrease in nutrient input (Sousa et al. 2020). In the last decades, growing evidence of species distribution shifts in this area has emerged (Lima et al. 2007, Díez et al. 2012, Fernández 2016, Pineiro-Corbeira et al. 2016, Casado-Amezúa et al. 2019). Some cold-water affinity seaweed species are retracting their southern distribution ranges, reducing abundance or being locally conned to small areas where the conditions are more suitable, such as rias (Viejo et al. 2011, Duarte et al. 2013). Similarly, the southern distribution range of kelp is also contracting, and empirical evidence suggests that this phenomenon will continue as the intensity of the NW Iberian upwelling system decreases, resulting in warmer water and reduced nutrient availability (Tuya et al. 2012, Fernández 2016, Franco et al. 2018, Casado-Amezúa et al. 2019). Because upwelling dynamics drives the condition of kelp forests in these coastlines, it is critical that we gain a greater understanding of how current and future environmental will affect not only the structure but also the functioning of these coastal assemblages.

In the context of FutureMARES Task 3.1, we explored the combined effects of seawater warning and nutrient depletion on the structure and functioning of seaweed semi-natural assemblages. The individual and combined effects of climate change stressors, as well as their consequences on seaweed-dominated ecosystems, are still not well understood and highly variable, contingent upon the local environmental context (Wernberg et al. 2012). We used a mesocosms experiment to assess single and combined impacts of elevated temperature and nutrient depletion on the functioning of semi-natural assemblages, unravelling the potential effects of future weak upwelling scenarios. Our experimental units were semi-synthetic communities created with rock-pool boulders covered with natural algal assemblages dominated by perennial species and some canopy species, all collected from the same shore and habitat. This approach enables to assess the effects of a combination of environmental drivers while working with realistic assemblages of species. Our experimental responses included individual and whole assemblage level effects, such as fronds growth, photosynthetic performance (using Pulse amplitude modulated (PAM) fluorometer) and primary productivity of both individual species and the whole experimental units. By combining individual and assemblage level responses we aimed to provide insights on how single species performance contributes to community level responses, helping to unravel the underlying mechanism behind stress responses (Maxwell and Johnson 2000, Tait et al. 2017). We expected that both elevated temperature and nutrient depletion would negatively affect the performance and productivity of the species and assemblages. There is some evidence that nutrient concentration may affect temperature tolerance in Laminaria species (Gerard 1997, Gao et al. 2013). Hence our hypothesis is that both drivers (temperature and nutrients) will have synergistic effects on the structure and functioning of the communities.

2.6.2 Methods

To test for individual and combined effects of nutrient depletion and high temperatures, experimental assemblages were exposed to four different treatments consisting of two

temperature levels: 15°C & 19°C (hereafter, T15°C and T19°C) and two different nutrient concentrations: nutrient depletion & nutrient replacement (hereafter, Nut- and Nut+). 15°C is a rounded annual average seawater temperature in the NW Iberia coastal area, and 19°C as an average temperature predicted by the IPCC RCP 8.5 scenario “business as usual”. Nutrient levels were chosen according to values typically experienced in the area due to the strong variability in nutrient concentrations induced by the NW Iberian upwelling system (See details on treatment methodology below).

The experimental setup consisted of 5 replicated assemblages per treatment for a total of 20 mesocosm units, each holding a volume of seawater of 60 l. Nitrate values were on average 25.42 mg/l (± 5.36) and phosphate values on average 2.6 (± 0.8) in the nut + treatment. In the Nut- treatment, nutrients concentration was kept at 1.6 (± 0.42) for nitrates and 0.032 (± 0.01) for phosphates. These concentrations were little lower compared to those used by Franco et al (2018) in their experiments with *L. ochroleuca* but are in line with the natural concentration of nutrients in the area of study during summer with and without upwelling conditions (J. Franco & F. Arenas per. comm., Brito et al. 2020). The temperature ranged between 14.9 and 15.1 in the 15°C treatment and between 18.9 and 19.1 in the 19°C treatment (mean temperatures ± SE = 15.02 ± 0.15; 18.9 ± 0.02).

Fronds of *Laminaria ochroleuca* and *Chondrus crispus* were individually tagged at the beginning of the experiment using numbered plastic tags attached with cable ties. Individual growth was estimated by estimating fresh weight (FW) of each individual frond at the start and at the end of the experiment. Growth rates (g FW d^{-1}) were calculated as the difference between final and initial fresh weight of each frond divided by the experiment duration in days. For the two large and at species used in the experiment (*Laminaria ochroleuca* and *Chondrus crispus*), in vivo chlorophyll-*a* fluorescence of photosystem II was also measured using a portable pulse amplitude modulated fluorometer (Junior-PAM, Walz®).

2.6.3 Results

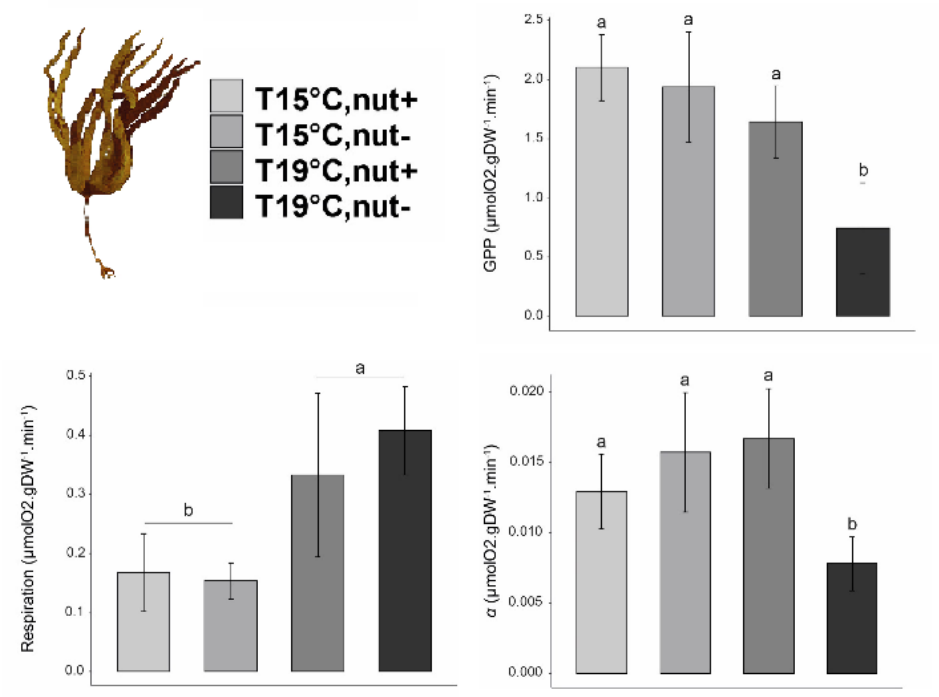

Figure 48 Mean of P-I curves parameters for Laminaria ochroleuca measured at the end of the experiment. Values are presented as means ± SD (n=5). P-values from two-way ANOVA ($p \leq 0.05$). If interaction was significant, Tukey post-hoc test was performed to detect differences between groups. Different letters denote for significant difference.

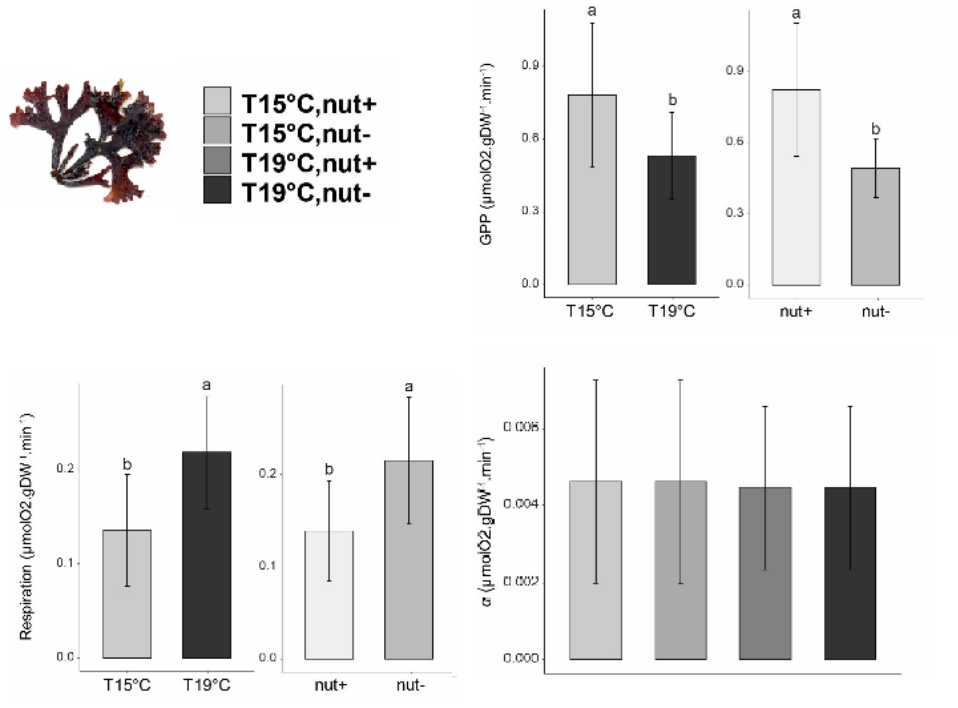

Figure 49 Mean of P-I curves parameters for Chondrus crispus measured at the end of the experiment. Values are presented as means ± SD (n=5). P-values from two-way ANOVA ($p \leq 0.05$). If interaction was significant, Tukey post-hoc test was performed to detect differences between groups. Different letters denote for significant difference

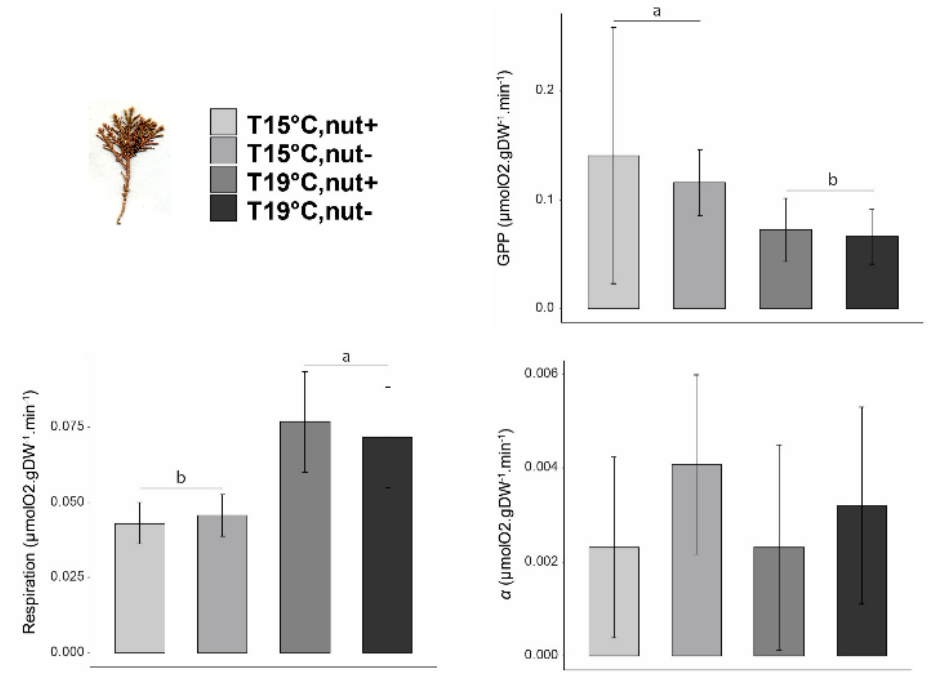

Figure 50 Mean of P-I curves parameters for the turf measured at the end of the experiment. Values are presented as means ± SD (n=5). P-values from two-way ANOVA (p ≤ 0.05). If interaction was significant, Tukey post-hoc test was performed to detect differences between groups. Different letters denote for significant difference.

Regarding GPP (gross primary productivity), values for *Laminaria ochroleuca* ranged between 2.44 and 0.26 µmolO_2 gDW^{-1}min^{-1} and were the highest among the components tested in our assemblages (Fig. 48). Temperature and nutrient had a significant interactive effect on the kelp maximum productivity (ANOVA, F1,16 = 5, p = 0.04). Under high nutrient supply, no differences were detected between temperatures (overall mean ± SD = 1.87 ± 0.36 µmolO2 gDW^{-1}min^{-1}). However, in the nutrient depletion treatment the temperature had a significant negative effect and at 19°C GPP values were lower than those measured at 15°C (mean ± SD = 0.745 ± 0.38, and 1.937 ± 0.46 µmolO_2 gDW^{-1}min^{-1} respectively) representing a 60% decrease compared to 15°C nutrient enriched treatment (Fig. 48). In the case of *Chondrus crispus*, GPP was negatively affected by nutrient availability with lower values measured in the nut- compared to the Nut + treatment. Also, higher temperatures affected the fronds where GPP values were significantly higher for plants exposed to 15°C compare to the one exposed to higher temperature (mean ± SD = 0.98 ± 0.36 and 0.65 ± 0.20 µmolO2 gDW^{-1}min^{-1}, respectively). Values of productivity for the turf significantly decreased with temperature with an average at 15°C of 0.13 µmolO2 gDW^{-1}min^{-1} (± 0.08) versus 0.07 µmolO2 gDW^{-1}min^{-1} (± 0.02) at 19°C (Fig. 42). GPP of the communities decreased significantly in the nut- treatment when exposed to 19°C compared to the rest of the treatments (Fig. 44), indicating a significant interaction between temperature and nutrients (ANOVA, Temp x Nutrient interaction F1,16 = 4.8, p = 0.043)

Respiration rate significantly increased with temperature for all the three components examined. In the case of *Laminaria ochroleuca* individuals, respiration rates increased by two folds with a mean respiration rate of 0.161 µmolO2 gDW^{-1}min^{-1} (± 0.061) when exposed to 15°C and 0.344 µmolO2 gDW^{-1}min^{-1} (± 0.12) at 19°C. *Chondrus crispus* respiration rate was significantly higher at higher temperature but also higher in the Nut- treatment (Fig. 44). Respiration significantly increased when plants were exposed to 19°C (mean ± SD = 0.219 ± 0.05 gDW^{-1}min^{-1}) compared to those exposed to 15°C (mean ± SD = 0.135 ± 0.05 µmolO2

$gDW^{-1}min^{-1}$). Regarding the nutrient treatment, respiration rates also increased in the nut- treatment (mean ± SD = 0.215 ± 0.07 µmolO2 $gDW^{-1}min^{-1}$) compare to nut+ (mean ± SD = 0.139 ± 0.05 µmolO2 $gDW^{-1}min^{-1}$). In the case of the turf, respiration rates were significantly higher at 19°C (mean ± SD = 0.075 ± 0.015 µmolO2 $gDW^{-1}min^{-1}$) compare to the ones recorded at 15°C (mean ± SD = 0.044 ± 0.006 µmolO2 $gDW^{-1}min^{-1}$) (Fig. 45). The communities experienced significantly higher respiration rates when exposed to elevated temperature (ANOVA, Temperature F1,16 = 4.8, p = 0.042). Respiration of seaweeds exposed to 15°C was on average 0.324 µmolO2 $gDW^{-1}min^{-1}$ (± 0.06) whereas seaweeds exposed to 19°C displayed average respiration rates of 0.387 µmolO2 gDW− 1min− 1 (± 0.06). No other significant effects were detected (Fig. 45).

Regarding the ability of the different components to use light under limiting conditions (alpha in P-E curves), individuals of *Laminaria ochroleuca* showed a significant decrease in α when exposed to low nutrient concentration and elevated temperature (ANOVA, F1,16 = 16.62, p = 0.001). No significant effects were detected in the case of the turf and of *Chondrus crispus* for the parameter alpha although the interaction was just marginally not significant, and we observed were some trends toward significance with a decrease of the values in nut- when plants were exposed to high temperature. The values of α (alpha) for the whole community didn't show any significant effects of treatment.

2.6.4 Discussion

Growth is a useful response to assess the deleterious effects of environmental stressors because it integrates many biochemical and physiological effects and ultimately is linked to individual fitness (Pineiro-Corbeira et al. 2019). In the case of the kelp *Laminaria ochroleuca*, results showed that when nutrients were available, temperature treatments did not affect the growth rate of this species. Indeed, *L. ochroleuca* is considered a warm-temperate Lusitanian species (Smale et al. 2015) and known as one of the most heat-tolerant species of the genus. In fact, the species has its southernmost limit of distribution in Morocco, where the water temperature can reach more than 20°C (Izquierdo et al. 2002, Bartsch et al. 2008, Benazzouz et al. 2014). Previous studies have demonstrated that *L. ochroleuca* is capable of exhibiting optimal growth rates when exposed to long-term temperatures as high as 19°C (Franco et al. 2018). Moreover, the ecotype from north Portugal exhibits positive growth rates after short term exposure to 27°C, demonstrating its ability to withstand supra- optimal temperature (Pereira et al. 2015). Finally, fronds used in this study were collected in the rockpools from the intertidal zone, where they are subject to a high range of physical stress and as a result prone to withstand sub-optimal conditions better than the individuals from the subtidal zone (Biskup et al. 2014).

Our observations regarding the growth of the two species measured were mostly in line with the results found for the metabolic rates assessment. In particular, for *Laminaria ochroleuca*, the reduction of growth, productivity and alpha indicated a lower fitness when both stressors were interacting. These results are consistent with previous studies, which have suggested a decrease in eco-physiological performance with decreasing nutrient concentration and increasing temperature in *Laminaria* species and other canopy forming seaweeds (Gerard 1997, Colvard and Helmuth 2017). Colvard & Helmuth (2017) have demonstrated that *Fucus vesiculosus* growing in nutrient-enriched water had higher Pmax at high temperature than the ones lacking nutrients, suggesting that accessibility to nutrients increases thermal tolerance of this algae. In fact, nutrient limitation is recognized to negatively affect plants capacity to synthesize essential molecules such as chlorophyll, decreasing the PSII density and size (Gerard 1997), which ultimately impacts photosynthesis and growth (Wiencke and Bischof

2012). The decrease of fitness when combined with high temperature might have resulted from increased metabolic rates, leading to higher nitrogen consumption, a requirement that cannot be met in a nutrient- deprived environment. Therefore, nutrient-limited plants will show quicker signs of alteration of eco-physiological performances as they hardly meet their nutrient requirement to maintain the good functioning of their metabolism (Davison 1991; Colvard and Helmuth 2017). Furthermore, Gerard (1997) showed that the increase of protein content in non-nitrogen limited plants exposed to high temperatures could also be associated with the production of heat shock protein, promoting tolerance to high temperatures with increasing nutrient availability (Gerard, 1997) and could partly explain the observed tolerance of the canopy species to high temperatures when exposed to sufficient nutrient availability.

As indicated above, assemblage level response followed a similar pattern as the canopy species response, with a similar significant decrease of productivity under low nutrient concentration and elevated temperatures. The elevated temperature significantly increased the respiration rates for all the components of the assemblages and the whole assemblages themselves. As the temperature increased within the tolerance range of the species, the rate of enzyme-catalyzed reactions increased, resulting in a faster metabolism and ultimately higher respiration rates (Davison 1991). Primary productivity did not follow this increase of respiration rates, and the negative effects were exacerbated by nutrient depletion. Temperature effects had similar results to those observed by Tait et al. (2013) in mesocosms, where naturally formed assemblage experienced increasing respiration rates with rising temperatures. Our results also show that the increase in respiration rate was not followed by increasing GPP, like previously suggested in other marine autotrophs (Koch et al. 2013, Olabarria et al. 2013). However, this mismatch of respiration and GPP rates is a consequence of a reduced NPP when assemblages are exposed to higher temperature (Tait and Schiel 2013), and in our experiment when assemblages experienced high temperatures and low nutrient conditions.

Kelp species have been reported to be the main contributor to community production, with a substantial reduction in the assemblages' primary productivity when canopy species were removed (Schiel and Foster 2006, Davies et al. 2011). Additionally, response of natural assemblages to experimental drivers have been shown to be modulated by the nature of the canopy forming species, pinpointing the importance of canopy species contribution to assemblage response (Olabarria et al. 2013). In accordance with these previous studies, our results suggest that the overall effects of environmental changes on community productivity are expected to be highly dependent on the kelp fitness rather than other components with lower contribution to the productivity of the assemblage. Furthermore, sub-canopy species are highly dependent on the amount of shade created by the canopy (Flukes et al. 2014) and could be subjected to photodamage if this protection happens to disappear (Figueroa and Korbee 2010, Beardall et al. 2014), potentially aggravating the putative effects of weak upwelling conditions at the community level. The resilience to nutrient depletion of the turfs also suggests that species currently with a small ecological contribution could get advantage over canopy forming species, potentially promoting shifts to turf-dominated assemblages (Filbee-Dexter and Wernberg 2018).

Surface temperature of the oceans has increased globally over the past decades; however, this increase is far from being homogenous, and the North Atlantic seems to warm faster than other regions (Huang et al. 2017, Chan et al. 2019). In coastal areas influenced by eastern boundary upwelling systems (EBUS), those warming rates are partially buffered by cold upwelled deep seawater (Seabra et al. 2019). Coastal ecosystems of north Portugal benefit from the NW Iberian upwelling system, which brings cold and nutrient-rich waters and reduces

nearshore seawater warming (Mackas et al. 2006). Extensive kelp forests thrive in these conditions, holding diversity rich and productive communities. However, the warming of the upper layer of the ocean is leading to an increase in the thermal stratification of the water column and a decrease in upwelling intensity in this region (Sydeman et al. 2014, Sousa et al. 2020), lessening the efficiency of the upwelling in lifting nutrient-rich deep waters into the photic zone. Our understanding of the ecological impacts of changes in upwelling intensity is limited, rendering our capacity to foresee the future of these biologically rich and productive ecosystems (García-Reyes et al. 2015). Our experiment assessing primary productivity and respiration rates using incubations and fluorescence measurements provides valuable insights on community response to relevant upwelling associated drivers and allows to identify the contribution of each component to the general observed response.

2.7 Effects of darkening and eutrophication on macroalgal forests in Norway (SL1-3)

2.7.1 Introduction

Norwegian coastal macroalgal ecosystems support high biodiversity and provide a wide array of ecosystem functions and services, including support of coastal fisheries. They are significant carbon sinks and offer opportunities to mitigate and adapt to climate change. However, these shallow ecosystems are influenced by both terrestrial and ocean processes, and their high productivity, as well as deteriorated state, can in part be attributed to high nutrient run-off from land (Nixon 1988, Barbier et al. 2011, Cloern and Jassby 2012). The Skagerrak and North Sea have densely populated catchment areas where human activities have resulted in changes in water quality and in marine species distribution. Additionally, these regions experience effects of climate change, such as ocean warming and species displacements (Perry et al. 2005, Beaugrand et al. 2014, Rinde et al. 2017), and ocean darkening (Frigstad et al. 2023).

Storylines 1-3 examines how the interplay between climate-related stressors and terrestrial nutrient control effects macroalgal ecosystems. Perennial macroalgal ecosystems (kelp and rockweed beds) are anticipated to be directly sensitive to warming, coastal darkening and increased nutrient supply. These processes will directly impact the productivity of the algal species and their associated fauna, causing complex, non-intuitive ecosystems responses.

Ocean darkening and eutrophication are two related but distinct phenomena, and both may be intensified by climate change. Ocean darkening refers to the process by which the ocean's surface becomes darker due to the accumulation of suspended particulate matter and dissolved organic matter. The concentrations of suspended organic material have increased in Skagerrak and the North Sea over the last three decades (Aksnesa and Ohman 2009, Dupont and Aksnes 2013, Frigstad et al. 2023) and are associated to increased riverine input and run-off from land. Ocean darkening can have negative impact on macroalgae by reducing the amount of available light, and thereby affecting the performance of key species through impacts on their physiology, growth, survival etc.

Eutrophication, on the other hand, refers to the process by which excess nutrients, primarily nitrogen and phosphorus, enter the water and stimulate the growth of habitat-forming algae (rockweed and kelps), as well as opportunistic filamentous algae. Among the multifactorial stressors driving the ongoing regime shifts from communities dominated by perennial kelp to filamentous algae on the south and west coasts of Norway, eutrophication has been identified as one of the most important processes (Christie et al. 2019).

Exploring the level and direction of the impacts of these stressors individually and combined, will provide much-needed knowledge on macroalgal communities performance and functioning in the face of CC.

Our approach was twofold. First, mesocosm experiments were conducted to test the effects of two factors, nutrient enrichment and ocean darkening, on the performance and functioning of shallow, rocky shore macroalgal communities. Second, field incubations were conducted to explore community metabolism of kelp communities with and without epiphytic loading.

For the mesocosms, our main objective was to study whether nutrient enrichment and darkening would have a significant effect on 1) the macroalgal community structure and function and 2) the performance and survival of key habitat-forming macroalgal species. Here we present a synopsis of the mesocosm study and its results (2.7.2-2.7.4) and provide a (2.7.5)

short introduction to a field incubation; the protocol that were used and some preliminary results as the full analysis still needs to be completed.

2.7.2 Mesocosm methods

The mesocosm experiments were carried out at NIVA's Marine Research Station Solbergstrand (59°37'N, 10°39'E) by the outer Oslofjord (southeastern Norway), using 12 large outdoor concrete basins, each containing 12 m^3 of seawater (Fig. 51). The surface area of the mesocosms is 4.8 x 3.7 m, and the deepest part is 1.3 m deep at high tide. Diverse rocky shore macroalgal ecosystems were established 18 days before the experiment started by transplanting rocks with rockweeds (two species; *Fucus serratus* and *Fucus vesiculosus*) and their associated fauna, from the shallow rocky shoreline outside the research station. The rockweeds were distributed evenly between and within each of the basins, among four tidal levels until full coverage was reached. The tidal levels are formed as stairs in the shoreline part of each basin, and *F. vesiculosus* was placed at the two upper tidal levels, and *F. serratus* at the two lower tidal levels, due to their natural zonation along the tidal gradient.

Figure 51 Overview of the 12 outdoor mesocosm basins at Solbergstrand, close to Oslo, Norway, including information of the design of the allocated treatments in this study, i.e. C-controls, N-nutrients, D-darkening, and the combination of darkening and nutrient enrichment (DN).

To analyse the impact of the treatments on the photosynthetic performance of sugar kelp (*Saccharina latissimi*), we introduced 5 individual sugar kelps attached to a rope at the deep end of each mesocosm basin in early May 2021. These plants had been collected by diving at a nearby location the same day. We also tested the use of green gravel (seeding sugar kelp sporelings onto small rocks) and introduced juvenile sugar kelps into each of the basins, but these were unfortunately rapidly lost due to grazing by snails. Similarly, several attempts to add *Zostera marina* plants to small enclosed soft sediment boxes placed at the deepest parts of the basins were unsuccessful. All of those plants were rapidly lost due to grazing or disturbance by snails/crabs, even when the rhizomes were fastened to BESE-mats (as used earlier to facilitate eelgrass restoration in outer Oslofjord, Gagnon et al. 2021).

The mesocosms receive a continuous flow of 4 m^3/hour of seawater from 1 m depth in the fjord. Each basin is equipped with a wave machine and tidal regulation mimicking the natural tidal cycle, and contained loggers for temperature and salinity. For further description and use of the mesocosms, see Bokn et al. (2003), Christie et al. (2020), and Kraufvelin et al. (2020).

The experiment lasted 132 days and was initiated mid-May (11.5.2021) and ended mid-September (20.9.2021). The twelve mesocosms were arranged in a fully factorial design where

the two factors (nutrients and darkening) could be tested separately and in combination with proper (n=3) replication. The four treatments were randomly distributed among the mesocosms; three mesocosms did not receive any nutrient enrichment or darkening treatment and served as controls (C), three mesocosms were allocated for nutrient enrichment (N), three were assigned to darkening treatment (D), and the remaining three mesocosms received nutrient enrichment and darkening treatment in combination (ND). The experimental set-up is shown in Figure 51.

2.7.3 Mesocosm treatments

Nutrient enrichment

Nutrients were applied to the mesocosms with automatic dosing equipment to achieve 32 µmol L^{-1} nitrogen and 2 µmol L^{-1} phosphorus above background fjord levels. The nutrients were added as a mixture which consisted of 14.3 mol N as NH_4NO_3 and 0.9 mol P as H_3PO_4 and a N/P mol ratio of 16/1 (Kraufvelin et al. 2006a). The treatment levels correspond to concentrations recorded in eutrophic areas locally (Kristiansen and Paasche 1982) and globally (Cloern and Jassby 2012), Similar levels have been used in previous mesocosms studies (Bokn et al. 2003, Kraufvelin et al. 2006a, Kraufvelin et al. 2006b, Kraufvelin et al. 2020). Chemical analyses of water samples taken from the basins at the start and towards the end of the experiments confirmed that the target treatment levels were achieved. We managed to have similar nutrient levels (NH4, PO4, NO2-, NO3- and total P) for the control and darkening treatments (Δ µg/l <5). Nutrient enrichment (NH4, PO4, NO2-, NO3-, total N and total P) was documented for the combined treatment of darkening and nutrient, as well as for nutrient only. The darkening treatment showed elevated levels of total nitrogen. It is unlikely that this is due to any nitrogen compounds in the lignin used to mimic darkening. The concentration of ammonium, nitrate and nitrite was, however, not elevated, indicating that the increased level of nitrogen must have been of low bioavailability. Lignin's low bioavailability makes it a useful biomarker of terrigenous dissolved organic matter (Opsahl and Benner 1997), as well as a useful tracer of ocean circulation (Hernes and Benner 2002). Hence, lignin should be a good choice to achieve light limitation without adding bioavailable nutrients.

Darkening

Lignin is a complex organic polymer found in plant cell walls, helping to provide rigidity and support of the plant. Due to its high resistance to degradation and dark color causing light absorbance, it's suitable for simulating ocean darkening. We aimed to double the light attenuation (i.e. how quickly the light availability decreases from the surface through the water column) in the darkening treatment compared to ambient levels. Lignin was applied with automatic dosing equipment (30 mg/L lignin giving approx. 1 ($^{m-1}$) absorption at a443 nm in end-concentration above ambient background levels). Control of the absorption was undertaken weekly in each basin to confirm the darkening level (Fig. 52). Additionally, Kd PAR (the diffuse attenuation coefficient for photosynthetically active radiation) was determined three times during the timeline of the experiment to relate a443 to Kd PAR.

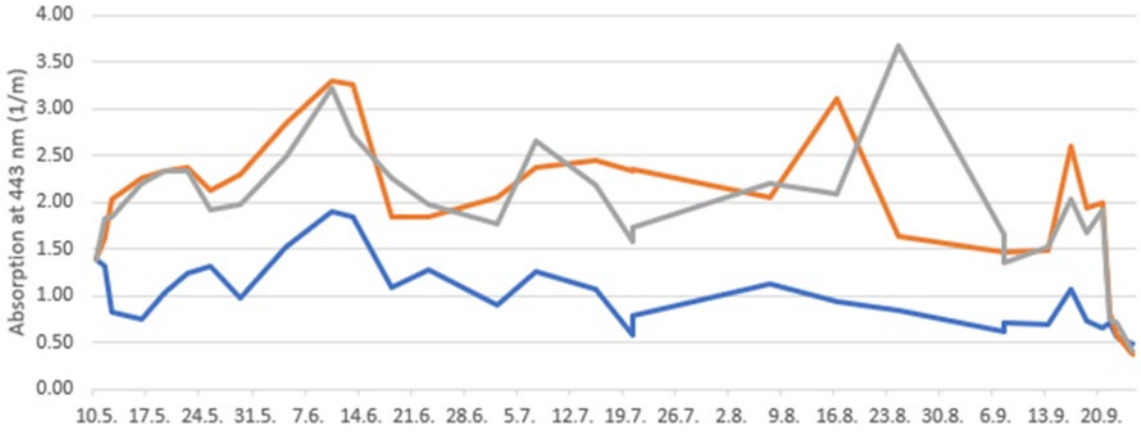

Figure 52 Plot showing variation in absorption (mean values) at Abs-443 during the course of the experiment for the control (blue line) and darkening treatments with lignin (orange line) and with darkening (lignin) and nutrients combined (grey line). Dates when measurements were done are shown on the x-axis.

2.7.4 Mesocosm - Sampling and measurements

Photosynthetic performance

The photosynthetic activity in the thalli of *F. serratus* and *S. latissimi* was measured in situ with a submersible pulse amplitude modulated (PAM) fluorometer. The measurements were undertaken on n=3 sporophytes from each species in every mesocosm basin, to assess how habitat-forming macroalgal species, living in the lower littoral and upper sublittoral zone, respond to the different levels of irradiance and nutrient load. We made the measurements continuously and darkened plants in parallel to be able to carry out the measurements under as similar lighting conditions as possible. Algal fronds were dark-adapted for 190 sec. using a "Dark Leaf Clip Diving L-C" (Walz) to which the fiber optic of the fluorometer was applied and maintained to perform each measurement. The initial fluorescence (F0) was first induced by a low irradiance of red measuring light, followed by a single saturating light pulse giving the maximal fluorescence (Fm). Variable fluorescence (Fv) was calculated as the difference between Fm and F0, while the optimal quantum yield was calculated as Fv/Fm.

Rockweed community changes

The cover and diversity of macroalgal species was assessed 1 and 3 months after the experiment was initiated. The scraped areas were surveyed using one frame (20x20) per tidal levels/stair, for all basins, 1 and 3 months after the initiation of the experiment. The unscraped areas were surveyed with 2-4 frames per tidal level, per basins at the same time periods.

Community changes of fauna associated with *Fucus serratus*

A branch of rockweed *Fucus serratus* was sampled from each mesocosm basin and sealed in a plastic bag, washed in freshwater, sieved at 250 µm mesh size, and later analyzed under magnification in the lab. The individual organisms associated with the seaweed were assessed to the lowest possible taxonomic resolution, and the abundance of fauna was related to the weight of the sampled rockweed. Furthermore, the grazing level of each rockweed plant was assigned to one of the three categories low, moderate, or high, based on signs of grazing as illustrated in Fig. 53.

Figure 53 The grazing level of each of the rockweed plants was assigned to one of the categories low, moderate, and high, as illustrated in these photos showing increasing grazing pressure from left to the right.

C:N ratios of macroalgal tissue

The carbon to nitrogen ratio is an indicator of the nutritional quality of the macroalgae. In general, macroalgae with lower C:N ratios are considered to be of higher nutritional quality, as they contain more nitrogen per unit of carbon. Access to ample nutrients may lead to lower C:N ratios in the algae, as they are able to allocate more resources to nitrogen rich compounds such as proteins and amino acids. Similarly, light conditions may also affect the C:N ratios. When macroalgae are exposed to high levels of light, they may photosynthesize more, and allocate more resources to carbon rich compounds, resulting in higher C:N ratios. Plant tissue were sampled from *F. serratus* (n=3) and *S. latissima* (n=3) sporophytes from all basins towards the end of the experiment for determination of C and N content.

Statistical analysis

To explore similarities and differences of the fauna communities associated to the rockweed *Fucus serratus* between treatments, non-metric multidimensional scaling (NMDS) and permutational multivariate analysis of variance (PERMANOVA) were applied (Anderson et al., 2008). The analysis was done in R (version 4.2.1, R core team 2022, using the packages vegan (Oksanen et al. 2022) and adonis2 respectively (McArdle and Andersen 2001). To explore how much of the variance in the structure of the fauna communities could be explained by treatment and the level of grazing pressure, we fitted the variables onto the ordination using the vegan function envfit. The NMDS was done with the function metaMDS. We used nested ANOVA's (with basin nested in treatment) to test for any treatment effects on several responses such as number of species and number of individuals of the rockweed fauna, photosynthetic performance, and snail abundance. Two-way ANOVAs, with and without interaction or blocking variable (i.e. basin) was used to test the impact of treatment and the individual grazing level of the rockweed plants on abundance of individuals and number of species of the fauna community associated with *Fucus serratus*.

2.7.5 Mesocosms - Results

Rockweed community changes

There was a rapid response of the rockweed community within one month in unscraped plots, i.e. the nature-like rockweed communities. The coverage of rockweeds (*F. serratus* and *F. vesiculosus*) was lower when exposed to nutrients compared to the controls, but the difference was not significant for *F. serratus* (low tidal zone). There was a significant impact of treatment on *F. vesiculosus* coverage in the high tidal zone. Darkening had no impact on *F. serratus* coverage (Fig. 54). Nutrients promoted the coverage of filamentous algae, and the effect of treatment was significant for the upper tidal level.

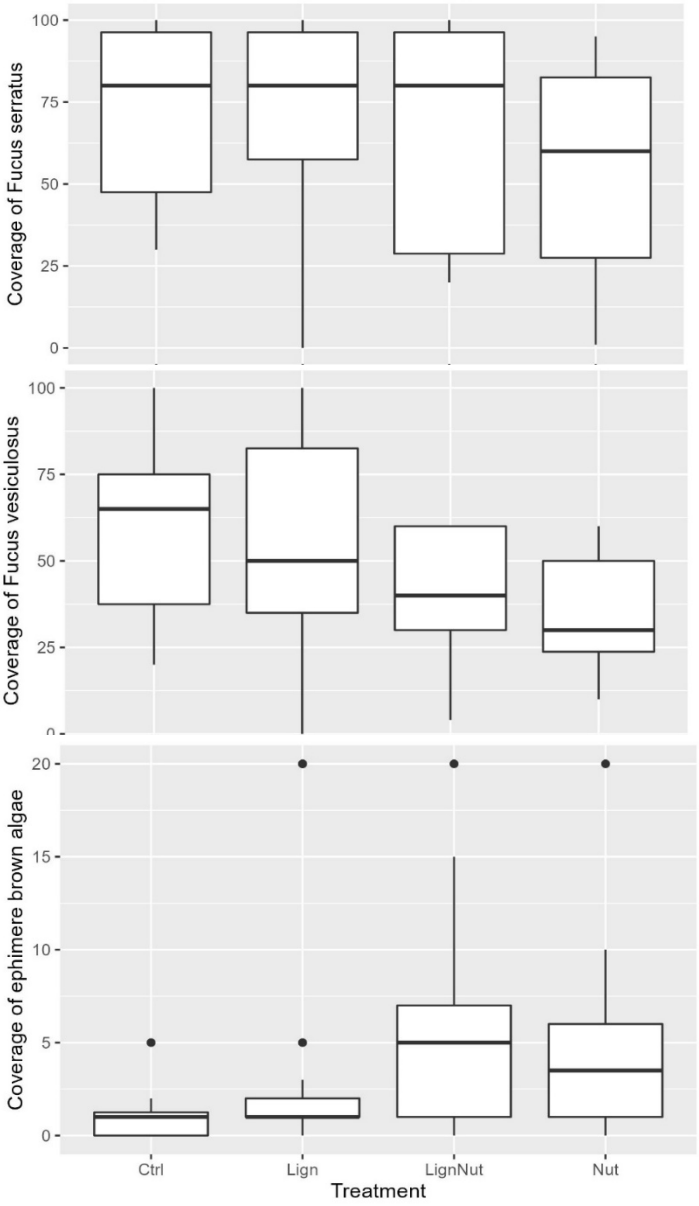

Figure 54 The coverage of Fucus serratus (upper panel), F. vesiculosus (middle) and of filamentous algae (lower panel) in unscraped plots one month after treatments initiated in the mesocosm under four levels of treatments; Control, Nutrients, Darkening (Lignin), and the combination of nutrients and darkening.

After three months, there continued to be more ephemeral filamentous brown algae in the scraped plots in the basins treated with nutrients (Fig. 55), but the impact was not significant when including all tidal levels in the analysis (p=0.07). In the unscraped plots the treatment effects differed between the upper and the lower tidal level with respect to occurrence of filamentous algae (Fig. 56), with increased abundance of filamentous algae in the treatments including nutrients, only in the upper tidal level. There were no significant differences in the abundance of grazing snails among the basins. *Fucus serratus* recruited, though in low numbers, to the scraped plots in all basins except for the basins receiving nutrients where the was no recruitment at all. Hence, nutrients alone seem to hamper settlement of *F. serratus*. Looking at only the two deepest tidal levels in the basins, *F. serratus* coverage in the scraped plots was significantly lower in basins treated with nutrients compared to the basins treated with darkening alone and darkening and nutrients combined (Fig. 57). In the unscraped plots, both of the darkening and nutrients alone, caused a decrease in coverage of F. s*erratus*, whereas the combination of darkening and nutrients had no impact (Fig. 57). This indicated an antagonistic effect on *Fucus* coverage when the two factors were combined.

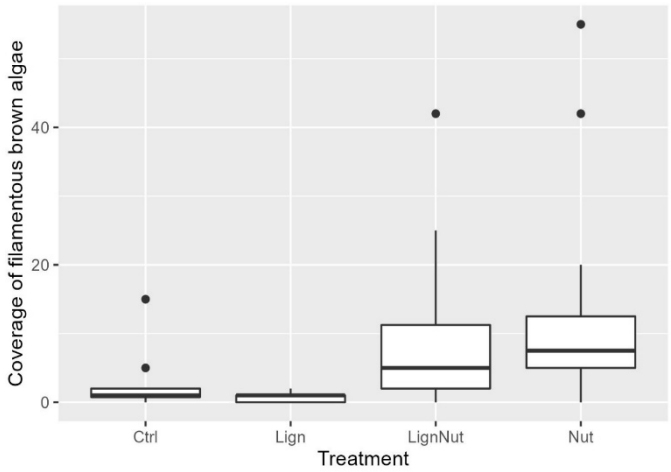

Figure 55 The coverage of filamentous brown algae in scraped plots three months after treatment, in the mesocosm under four levels of treatments; Control, Nutrients, Darkening (Lignin), and the combination of nutrients and darkening.

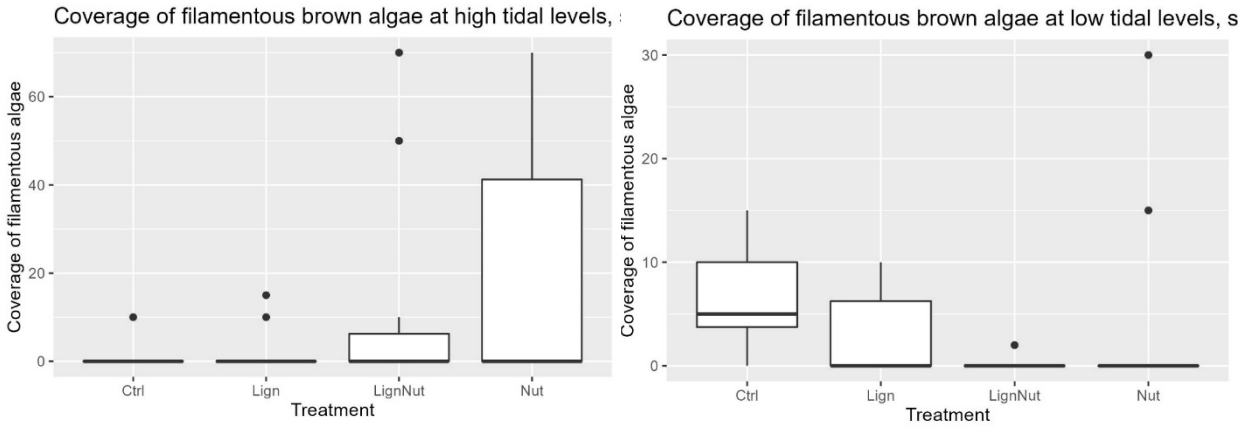

Figure 56 The coverage of filamentous brown algae in unscraped plots three months after treatment, in upper (left panel) and lower (right panel) tidal zone in the mesocosm under four levels of treatments; Control, Nutrients, Darkening (Lignin), and the combination of nutrients and darkening.

Community changes of fauna associated with *F. serratus*

A total number of 11,330 individual animals were found associated with *Fucus serratus* sampled from the mesocosms, encompassing 23 species. We found between 7 and 16 species

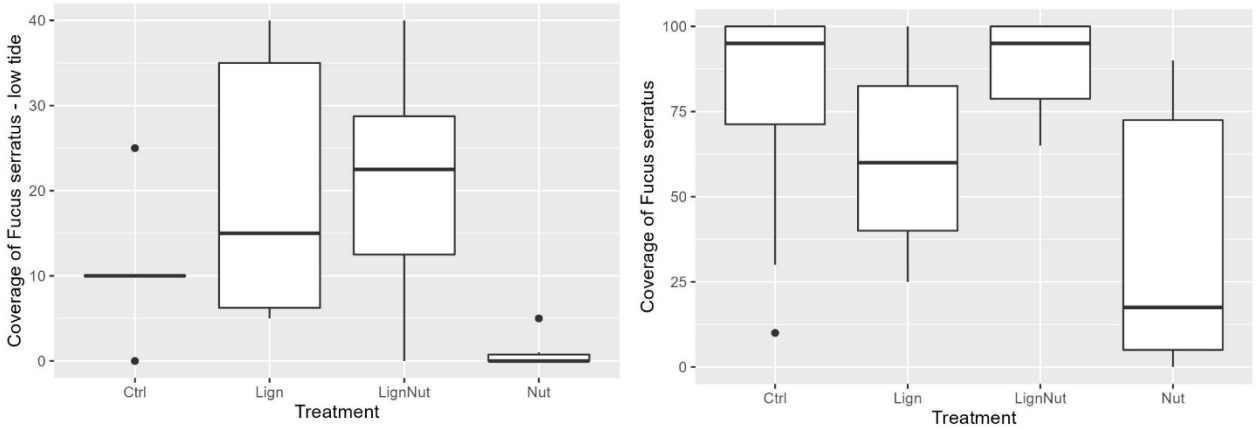

Figure 57 The coverage of Fucus serratus in scraped plots (left panel) and unscraped plots (right panel) three months after treatment at the two lower tidal levels, in the mesocosm receiving four levels of treatment; Control, Nutrients, Darkening (Lignin), and the combination of nutrients and darkening.

per *F. serratus* sample. The most abundant species were the isopods *Jaera albifrons* and *Idothea granulosa*, the snail *Littorina obtusata* and juvenile mussels. There were also relatively many amphipods of the group *Stenothoidae* and *Jassa*. Large individuals of *Gammarus* were also common.

Darkening reduced the number of individual invertebrates as well as the number of species associated with *F. serratus* (Fig. 58). The difference between treatments was significant for number of species (p=0.01) but not significant for number of fauna individuals. Adding nutrients to basins with darkening treatment caused a further reduction in number of species, but fauna abundance was at the same level as with darkening only. Nutrient and control treatments had similar number of species and number of individuals. For both biodiversity responses, the two-way ANOVA without any interaction or blocking variable (i.e. basin) performed best based on AIC. Darkening and nutrients combined caused a reduction by 3.1 in the number of fauna species compared to the controls. Darkening alone did not cause a significant reduction in the number of species compared to the controls. The combined impact of darkening and nutrients had significantly fewer species (-3.4) than when adding nutrients alone, indicating a synergistic impact of the stressors. The darkening treatment had fewer species than nutrient treatments, but the difference was not significant.

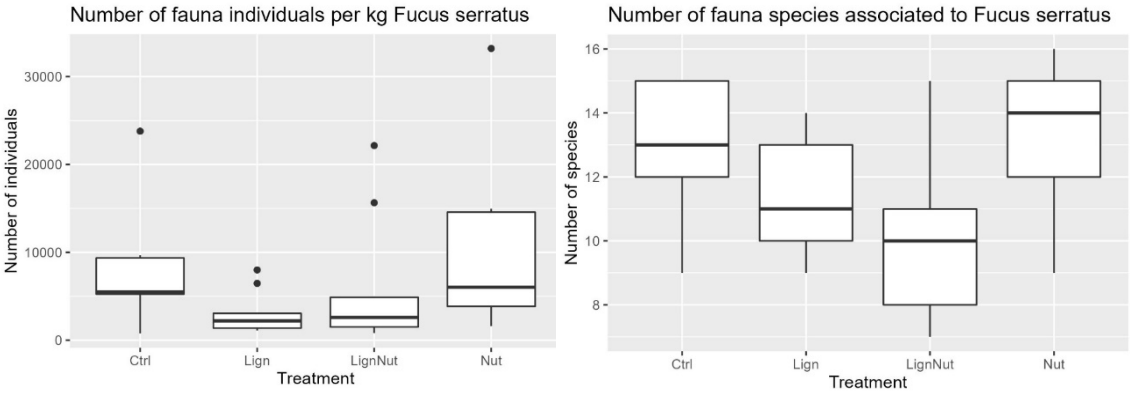

Figure 58 Number of fauna individuals (per kg, left panel) and number of species (right panel) associated to Fucus serratus sampled from mesocosms under four levels of treatments; Control, Nutrients, Darkening (Lignin), and the combination of nutrients and darkening.

We found a significant effect of treatment on fauna community associated to *F. serratus* (PERMANOVA, p=0.003, Fig. 59), 3 months after the initiation of the experiment. There was also an impact of the grazing level of the individual rockweed plants. However, the latter effect was not significant (PERMANOVA, p=0.07). The pattern of dissimilarity between the communities receiving the different treatments also indicates a synergistic impact of darkening and nutrients. The community established in the basins with the stressors combined was more different from the controls than the communities in basins treated with only one of the stressors.

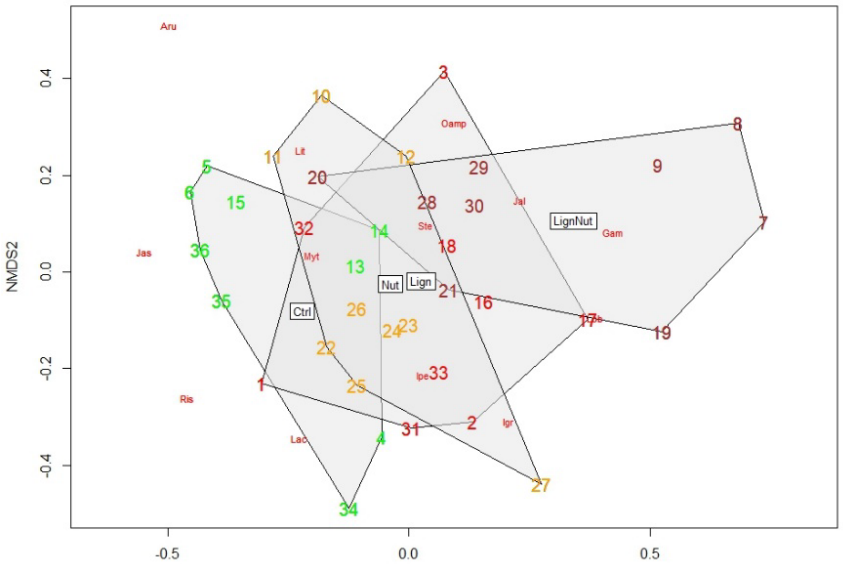

Figure 59 NMDS plot of the fauna community associated with Fucus serratus in the mesocosm receiving four levels of treatment; Control, Nutrients, Darkening, and the combination of nutrients and darkening.

Grazing pressure and photosynthetic performance of rockweed and sugar kelp

The PAM measurements indicated a positive effect of nutrients on sugar kelp *Saccharina latissima* photosynthetic performance (measured after 70 days). Nutrient enhancement had no impact on rockweed photosynthetic performance, although darkening significantly reduced *F. serratus* photosynthetic performance (after 80 days). Hence darkening impacted the photosynthetic performance of this species even at the shallow depth levels studied in the mesocosms.

During the course of the experiment, varying grazing pressure from snails were found on the kelp fronds, causing heavy reduction of the area of individual fronds or dislodgement of whole plants. After 76 days, half of the initial 60 kelps introduced to the basins were heavily grazed or dislodged. A higher grazing impact was found in the control basins compared to basins with nutrient enrichment or darkening (One-way ANOVA, $p<0.005$).

A positive effect of darkening on the grazing resistance was found for *S. latissima.* In darkened basins, 73% of the kelp were still in good health after 76 days compared to 53% healthy kelp in basins with nutrient enhancement and darkening combined, and 46% in basins with nutrient enrichment. The darkening effect was not significant but could be related to the significantly higher C:N ratio of the individuals from the darkening treated basins compared to the basins receiving nutrients, and hence a lower nutritional value for the grazers compared to the nutrient treatments (Fig. 60).

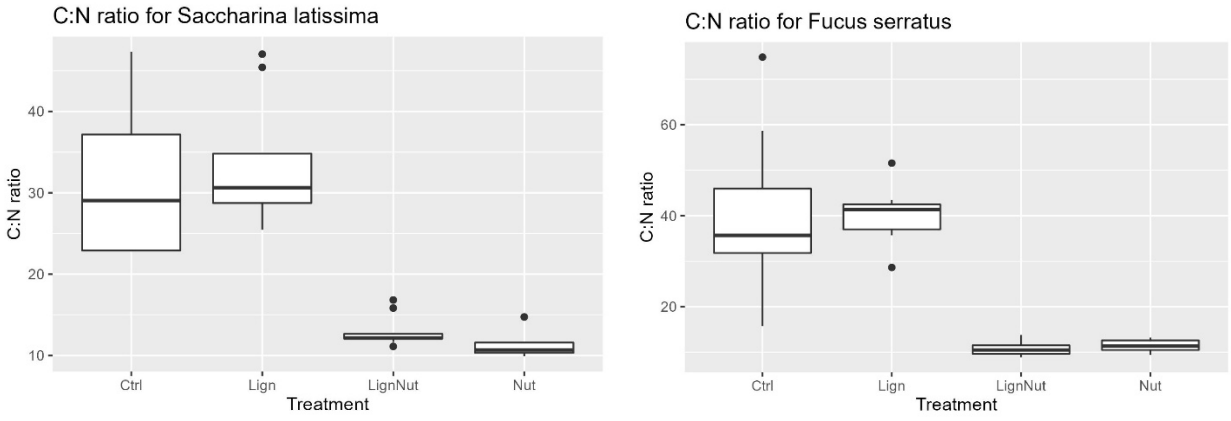

Figure 60 C:N ratios for Saccharina latissima and Fucus serratus sampled from the mesocosm receiving four levels of treatment; Control, Nutrients, Darkening, and the combination of nutrients and darkening.

2.7.6 In situ field incubations

Photorespirometry experiments were carried out to explore the difference in the function and production of sugar kelp beds in good biological condition compared to kelps heavily fouled by filamentous algae and encrusting bryozoans (Fig. 61). The experiment was a joint effort between NIVA, CIIMAR and IOLR.

Figure 61 Suger kelp bed without fouling (left) and with filamentous algae overgrowing the kelp (right)

Two sites at the Skagerrak coast, southern Norway (58°N, 8°E) were selected for conducting the incubations. The experiments were undertaken by SCUBA divers over two consecutive days in August 2022. Four replicate chambers were deployed at each site at 2-4 m depth. The incubation followed a similar light/dark cycle and water sampling protocol as described in Ch. 2.1.1.4 but with a different chamber design developed by CIIMAR. The customized chambers were flexible and had an open bottom. The bottom-frame of the chambers consisted of PVC with a foam-covered underlayer and with a strong polyethylene sleeve covering the PVC frame and extending well beyond the frame. Heavy sandbags were placed on the frame, providing a tight seal against the bedrock, and preventing water exchange with surrounding water bodies. Cylindrical, transparent polyethylene bags formed the flexible incubation chambers. After a chamber was deployed and the macroalgal community inside was gently organized inside the frame, the bag was manually closed at the top. Positive buoys were attached at the top to secure an upright position in the water column. The flexibility of the bag allowed the kelp and macroalgae inside to move freely as wave energy were transmitted through the soft walls of the bag allowing water motion and mixture within the bag.

To determine whether photosynthetic rates varied due to natural variability in light levels and the biological state of the kelp community, photosynthetically active radiation irradiance (PAR) was measured during the incubations with a PAR sensor (Odyssey® Waterproof PAR Logger) mounted outside the chamber in an upward direction. HOBO® data loggers were used for measuring oxygen concentration/fluxes and water temperature, allowing for calculating net primary productivity and respiration inside the incubation chambers. The chambers were first incubated in the dark for at least an hour followed by a light phase (Fig. 62). The dark phase was created artificially by draping a textile cover over the chamber. The volume of the incubations bag was estimated by using the fluorescein method and by calculating the volume of a cylinder. When incubations terminated, the bedrock within the PVC frame were gently scraped and all macroalgae and associated species were carefully collected into a textile bag. Samples were frozen until processing at the laboratory.

Figure 62 Pictures showing the incubation chambers during dark (upper left) and light (upper right) phase and diver preparing for sampling (bottom).

Preliminary results from metabolic calculations indicate a low net community production (NCP) for the kelp community characterized by heavy epiphyte loading, however these results are based only on calculations from two chambers, and without consumers included. *S. latissima* was the greatest contributor to the algal biomass in both chambers (>50%), followed by the typical understory species *Corralina officinalis* (>13%) and *Furcellaria lumbricales* (>15%). Filamentous algae only made up a small proportion of the biomass (<1%), presumably due to their feathery structure. The remaining samples will be analysed and a complete overview of the community structure and metabolic rates for the two habitat types will be presented in the scientific literature.

2.7.7 Discussion

We found a significant impact of nutrient enrichment and darkening on several aspects of the habitat-forming macroalgal communities common in Norwegian coastal waters. This includes reduced coverage of the habitat-forming rockweeds (*Fucus serratus* and *F. vesiculosus*), changes of the associated fauna community in the rockweed *F. serratus*, reduced photosynthetic performance of *F. serratus* (only for darkening) and *Saccharina latissima* (only for nutrients), and survival of *Saccharina latissima,* a key habitat-forming kelp species. The impact on the macroalgae community varied between the upper (the two uppermost stairs within the mesocosm basins) and lower tidal levels (the two bottom stairs), and between

treatments. Furthermore, the results indicate both *synergistic* (species diversity and community structure of the fauna associated to *F. serratus*) and *antagonistic* effects (coverage of *F. serratus*) on the ecosystem.

The reduced coverage of rockweeds in basins treated with nutrients could be due to the increased levels of nitrogen in the rockweeds tissue and hence a higher nutrition value of the algae for the grazers. The C:N levels were significantly reduced in *F. serratus* plants sampled from mesocosms treated with nutrient enhancement. Similar top-down control of macroalgae by grazers are well documented for rocky shore communities (e.g. Lubchenco 1978; Menge et al. 1997). We could not document any significant differences in the abundance of snails between the treatments, but it is challenging to get precise estimates of snail abundance when the occurrences of juvenile snails are high, and the individuals are difficult to observe and count. Also, the abundance of snails could have differed among basins before we estimated their abundance and recorded reduced rockweed coverage. Hence a numerical response of the snails could have occurred unnoticed. However, we observed a general increase in the abundance of snails in all basins over time, likely because of lack of predators, resulting in heavy grazing of the rockweeds in all basins at the end of the experiment. This is in contrast with the results from earlier experiments in the mesocosms which included predators and maintenance of the rockweeds (Kraufelin et al. 2020).

Differences in the rockweed ecosystems response between tidal levels, could be due to differences in the physiology of the two rockweed species, as well as differences in the environmental conditions between the tidal levels. *F. vesiculosus* is adapted to live in the upper tidal and *F. serratus* in the lower tidal and upper subtidal zones. The two zones experience differences in light conditions as well as differences in stressors such as heat, desiccation, salinity etc. with more stressful conditions in the upper tidal. Hence, additional stress could have more severe impact on the rockweed species inhabiting this level and explain why the most severe reduction in rockweed coverage occurred at this level. The reduction in coverage of rockweeds in the high tidal level (i.e. *F. vesiculosus*) in basins treated with nutrients could also be related to an increase in abundance of filamentous brown algae. Hence the loss of the rockweed could be due to competition with the filamentous algae.

The impact of stressors on photosynthetic performance differed between the two habitat-forming species, *F. serratus* and sugar kelp *S. latissima.* The different response to darkening could be caused by contrasts in the species adaptation to light, as sugar kelp are adapted to live in deeper and hence darker environment than the rockweed, which occur in shallow areas. Sugar kelp grows mainly in the winter season (January until May/June, Kain 1971). A hypothesis that can explain the reduced photosynthetic performance of sugar kelp as a result of nutrient enhancement could be that the enrichment causes an increased physiological stress for this species.

Darkening seemed to promote recruitment of *F. serratus* in the scraped plots in the lower intertidal zone, whereas the basins receiving nutrient enhancement tended to have reduced rockweed recruitment. In the more natural *F. serratus* rockweed community (i.e. the unscraped plots), the coverage of rockweed was reduced in the darkening treatment and the nutrient enhancement treatment but not when the two stressors were combined (similar to controls). This antagonistic impact of the combined stressors could be explained by a negative impact on faunal abundance and diversity, and reduced grazing pressure on plants.

Darkening resulted in a reduction in the number of faunal individuals associated with *F. serratus*, whereas darkening and the combined impact of darkening and nutrient enhancement

reduced the number of species associated with this rockweed species. In contrast, nutrient enhancement alone had no impact on fauna abundance and species diversity. Darkening and nutrient enhancement had a significant impact on the faunal community associated with *F. serratus, and* the pattern of dissimilarity between the assemblages also indicated a synergistic impact of the stressors. The negative impact of darkening could be explained by reduced photosynthesis and primary production rates of the rockweed, and hence less food for the fauna assemblage. The synergistic negative impact could be related to a cumulative impact of multiple stressors, crossing some threshold level, and hence increasing the negative impact on the ecosystem.

In conclusion, the mesocosm experiments demonstrate that the rockweed species *Fucus vesiculosus* and *Fucus serratus*, are both sensitive to coastal darkening and increased nutrient supply. Furthermore, the stressors reduce faunal abundance and species diversity of the community associated to *F. serratus*, through synergistic negative impact. The results indicate complex, non-intuitive ecosystem responses that cannot be understood without doing experimental studies in complex ecosystems as done in this study and made possible by the large scale mesocosm facilities. Preliminary results from the incubation study indicate a negative impact of filamentous algae on the kelp community production rate. Hence, an increasing trend of coastal darkening and nutrient enrichment will further promote the presence of filamentous algae as demonstrated in the mesocosm experiments, and thereby contribute to regime shifts towards a dominance of filamentous algae or fouled rockweed and kelps.

2.8 Assessment of ecosystem functioning of Pacific oyster reefs and determining thermal requirements of flat oysters early life stages used for ecosystem restoration in Dutch waters (SL 10)

2.8.1 Introduction

The restoration of habitat-forming species is a Nature-based Solution (NBS) that is being applied throughout the world's oceans to halt the loss of biodiversity, combat climate change and help sustain the provision of ecosystem services (Steven et al. 2020). Native flat oyster (*Ostrea edulis*) beds, once a major component of the North Sea covering > 25,000 km^2, largely disappeared from the region in the late 19th century due to a combination of overfishing, habitat degradation, introduction of invasive species and appearance of parasitic organisms. In the late 20th century, commercial farming of the Pacific oyster (*Crassostrea gigas*) began in the Wadden Sea from where the species spread and has by now established large populations throughout the region (Diedrich et al. 2005).

Habitats created by oyster beds support biodiversity by providing natural refugia, substrate and feeding grounds for many co-existing species. Moreover, by filtering phytoplankton, oysters play a key role in nutrient cycles of shelf seas and can mitigate poor water quality caused by excess nutrients (eutrophication). Also, deposition of suspended particulate matter from the water column is relevant, especially when increased storminess can elevate suspended particulate matter. Oyster reefs along coasts can also function as wave barriers that grow with sea level rise and reduce coastal erosion which will help with adapting to sea level rise and weather extremes. Finally, the shell formation and silt capture of oysters may contribute to carbon sequestration (Blue carbon). These important roles of oyster beds have long been recognised and large-scale restoration efforts are now underway to help safeguard future biodiversity and various provisioning, supporting, regulating and cultural ecosystem services for humans.

Effects of climate change in the North Sea region are sea level rise, coastal erosion, general temperature increases, changes in stratification patterns and hence in timing and amount of primary production, and more weather extremes such as heat waves and severe storms in summer. Changes in primary production will impact the carrying capacity of the North Sea for extensive shellfish beds. Changes in the timing of the spring bloom (generally linked to the timing of onset of stratification) can interfere with food availability at times of spawning. Oysters have specific tolerance ranges for temperature. If temperatures shift substantially the habitats with suitable temperatures are likely to shift. These changes will not only affect the sessile juveniles and adults but also impact the survival and settlement success of the pelagic larvae to bottom habitats.

Objective

The objective of this work was to determine in-situ habitat provisioning (support for biodiversity) and carbon cycling (respiration, net calcification, nutrient fluxes and carbon uptake capacity, Fig. 63) for introduced Pacific oyster reefs in the intertidal zone compared to nearby mudflats. This work (1) performed incubations in the field and in the laboratory to determine calcification and oxygen consumption rates, (2) quantified organic matter in the sediment at different distances from a reef and (3) measured biodiversity on artificial and natural oyster reefs.

Futhermore, work in SL10 aimed to quantify vital rates and thermal performance curves (TPCs) of larval *O. edulis* to better understand the impacts of temperature on the potential recruitment success in ecosystem restoration sites within the North Sea. For this, larvae were reared at two fluctuating temperature regimes (low 20–21°C, *versus* high 20–24°C) and growth, development, survival and settlement success were measured. In addition, TPCs (oxygen consumption rates (MO_2) and swimming behaviour) of all three larval life-stages (D-shape, umbo and pediveligers) were measured and their acute thermal preference range was determined.

The first larval study revealed that the larval thermal preference was between 25 and 30°C which corresponded with optimum temperatures for MO_2 and locomotion. Based on the large difference between these optimum temperatures and naturally occurring summer temperatures of the North Sea (16–22°C), *O. edulis* larvae were also reared at unnaturally high stable temperatures, i.e. 25 and 29°C and their vital rates were assessed. This was done in an attempt to optimize hatchery protocols to improve yields for a growing demand of hatchery-reared spat used in ecological restoration within the North Sea.

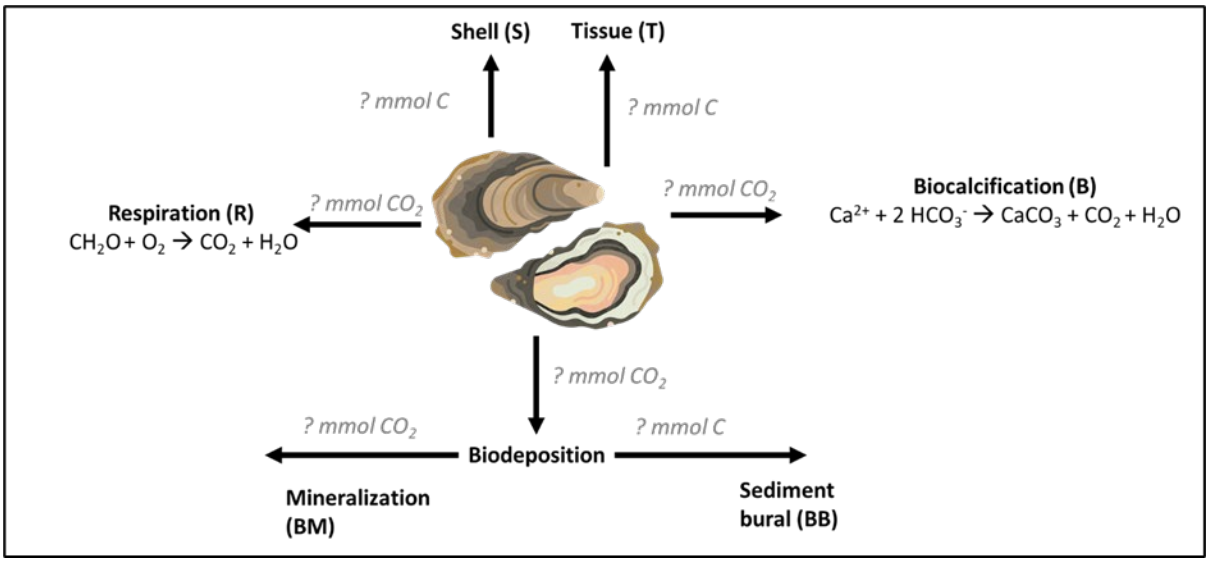

Figure 63 Carbon sequestration potential = shell formation + tissue production + feces production – biogenic calcification – respiration – mineralized feces

2.8.2 Methods

2.8.2.1. Assessment of Pacific oyster reefs

In-situ incubations for carbon cycling

To determine if oyster reefs are either a carbon sink or source, in-situ incubations experiments were performed at night on natural reefs of Pacific oyster (*Crassostrea gigas*) in the Oosterschelde estuary (The Netherlands) in the summer (June/July) and autumn (September) of 2021 and 2022. Respiration and calcification rates were calculated based on measured changes in oxygen, alkalinity, DIC and nutrients using benthic incubation chambers (henceforth called CUBEs in reference to their cubical design) designed by the Royal Netherlands Institute for Sea Research (Stratmann et al. 2018). CUBES were deployed on patches of oysters (n=14) and bare sediment (n=7, Fig. 64). The CUBEs had a volume of 125

L and were equipped with a stirring plate to ensured homogeneous mixing of the water. Furthermore, a rosette with six 35-mL sampling syringes on top of the CUBEs allowed water samples to be taken at set intervals. Oxygen was measured continuously whereas water samples were taken at 5 time periods during the experiment (0, 100, 200, 300 and 491 ± 20 min (mean ± sd)). The first and the last sampling was taken by hand whereas the other three times were sampled automatically. To obtain enough water for all measurements, two syringes were lanced simultaneously. The final sampling time differed depending on the moment the CUBE emerged from of the water due to the ebb tide. All water samples were filtered through a 0.2 µm syringe filter. Samples for DIC concentration analysis were stored in 5ml headspace vial and preserved by adding 5 µL 0.24 mol L^{-1} $HgCl_2$. For alkalinity analysis, 45 ml water was preserved by adding 45 µL 0.24 mol L^{-1} $HgCl_2$. For nutrient analysis, 1 ml was stored by placing it in a -20°C freezer. At the end of the incubation, all oysters were removed and the sediment sieved over a 1 mm sieve. The benthic macrofauna was stored in formalin. To determine the biomass of the oysters, the live top layer was separated from the dead layer under the sediment and both were stored in a -20°C freezer. Biomass was determined by removing all oyster flesh, dry it at 70 °C till weight constantly and combusted it at 450 °C to determine their ash-free dry weight in grams.

In 2022, lab incubations were also performed to correct field observations for fluxes from the sediment. In total eight incubations chambers were used to measure oxygen continuously and take water samples at set intervals, as done in the field. Three chambers received 1 oyster each. Three chambers were filled with sediment from the field and two chambers contained water only.

Year	Month	Oyster	Control	Lab incubation
2021	July	2	1	No
	September	4	2	No
2022	June	4	2	Yes
	September	4	2	Yes

Figure 64 Overview of in-situ incubation locations at a natural Pacific Oyster reef in front of the Royal Netherlands Institute for Sea Research in Yerseke (The Netherlands).

Biocalcification

Net calcification (G in µmol $CaCO_3$ h^{-1}) can be estimated using the alkalinity anomaly technique (Smith and Key 1975) based on the fact that total alkalinity (TA) decreases by 2 equivalents for each mole of $CaCO_3$ precipitated, using the following equation:

$$G = -\frac{(\Delta TA * v)}{(2 * \Delta t)}$$

Where ΔTA is the variation of total alkalinity during incubation (µmol L^{-1}), v is the net chamber volume (l), and Δt is the incubation time (h). Excretion of ammonium by the oysters during the incubation causes an increase in TA by 1 mol TA per mole of ammonium excreted, leading to an underestimation of calcification fluxes. Total alkalinity is however also impacted by other processes. Assuming that (1) the assimilation and remineralization of 1 mol of NH_4^+ (ΔNH_4^+) respectively leads to a decrease and an increase of 1 mol of TA, (2) the assimilation and remineralization of 1 mol of NO_3^- + NO_2^- ($\Delta(NO_3^-$ + $NO_2^-)=\Delta NO_x$) respectively lead to an increase and a decrease of 1 mol of TA, and (3) the assimilation and remineralization of 1 mol of PO_4^{3-} (Δ PO_4^{3-}) respectively lead to an increase and a decrease of 1 mol of TA, calcification rate (G^* in µmol $CaCO_3$ L^{-1}) can be estimated using the following equation (Gazeau et al. 2015):

$$G^* = \frac{\Delta NH_4^+ - \Delta TA - \Delta NO_x - \Delta PO_4^{3-}}{2}$$

But to get net calcification we need to correct for time and volume. The equation can be modified as follow to get G in µmol $CaCO_3$ h^{-1}:

$$G^* = \frac{(\Delta NH_4^+ - \Delta TA - \Delta NO_x - \Delta PO_4^{3-}) * v}{2 * \Delta t}$$

Respiration

Underwater respiration (R, µmol DIC h^{-1}) in each incubation chamber was calculated according to the following equation:

$$R = -\frac{(\Delta DIC * v)}{\Delta t * 10^3} - G^*$$

Where G^* is the net $CaCO_3$ flux in the incubation chamber (µmol $CaCO_3$ h^{-1}), is the net chamber volume (l), is the incubation time (h), and is the change in the total inorganic carbon concentration (µmol DIC L^{-1}), background respiration values from “control” chambers without oysters where subtracted prior to reporting this value.

Biodeposition

Oysters are filterfeeders which can bring carbon rich phytoplankton towards the sediment through excretion of feaces and pseudofeaces (Fig. 65). When this is buried it can act as carbon storage. We measured the amount of organic matter stored at different depths in the sediment (0-5, 10-15, 20-25, 30-35, 40-45 cm) and at differenct distances from oyster reefs (1, 2, 4, 6 and 10m). This was done by taking sediment cores around reefs up to 45cm depth and slicing them in 5-cm segments before storage in a jar. Organic matter was determined by freeze drying the sediment and combusting at 450 °C to determine loss on ignition (LOI). Five

samples were used to determine the amount of organic carbon and total nitrogen using a CHN-analyser (Flash EA 1112 Series).

Biodiversity

Ten years ago, artificial oyster reefs were placed in the Oosterschelde estuary (Walles et al. 2016). To determine the development of the artificial reefs biodiversity, *Magellana gigas* was measured on artificial and natural reefs in winter 2020 using catch-per-unit-effort in a fixed quadrat of 50 by 50cm. This method did not work for mobile species such as crabs that were able to escape the quadrat, resulting in an underestimation of the species richness and abundance. Therefore, we switched to the use of eDNA. Water, sediment and epifaunal samples were taken on and at different distances from artifical and natural reefs (Fig. 66). Two transects were sampled per reef type. At each location, 1-L water samples were collected in triplicates and subsequently filtered over a 1.2µm nitrocellulose membrane. The filters were stored in DNA/RNA shield and stored at -20°C until processing in the lab. Samples were thawed on ice and DNA was extracted using the Qiagen Blood&Tissue kit following the tissue protocol. PCR and sequencing has been done for the samples collected in tidal pools from artificial and natural reefs. The 313bp Folmer region of the COI barcode was amplified using primers designed by Leray et al. (2013) in a thermocycler with the following settings: 98°C for 3 min, 35 cycles of 98°C for 8s, 56°C for 8s, 72°C for 15s and finally 72°C for 3 min. Amplified samples were prepared for sequecing using the LSK-SQK113 kit by Oxford Nanopore Technologies.

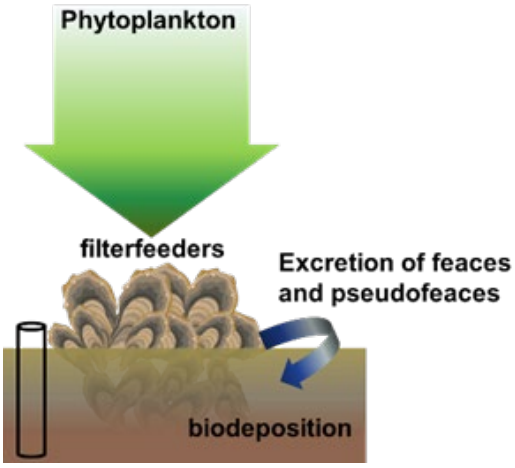

Figure 65 schematic overview of biodeposition

Furthermore, sediment samples were collected in combination with benthic sediment cores. The sediment samples are used for eDNA analysis, whereas the benthic cores are meant to groundtrough the eDNA sampling, by checking which species can be found and if they are also found in the eDNA analysis. The benthic cores were 10cm in diameter. Samples were taken up to 30cm depth. The sediment was then flushed over a 1 mm sieve and all residual organisms were stored in a jar. In the lab, these jars were fixed with ethanol. All species were named and counted after which they were pooled and mixed to a substance from which an DNA sample could be taken.

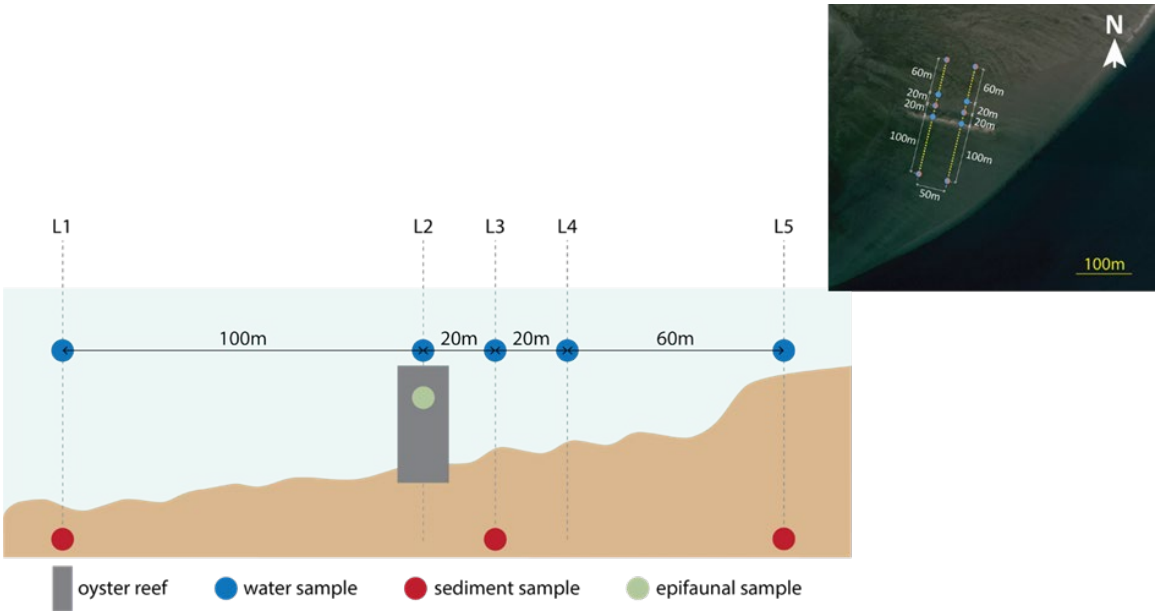

Figure 66 Overview of eDNA sampling around natural and artificial reefs. Two transects were sampled per reef type.

2.8.2.2. Thermal performance of flat oyster larvae

Broodstock conditioning and larval release

Broodstock (n = 38) were from the NIOZ in-house *O. edulis* population, which was collected on the east coast of the island of Texel (Jacobs et al. 2020). Temperature of seawater for broodstock was increased from 12 to 20°C within 4 weeks to induce gonad ripening and spawning. A sieve with a 100 µm mesh size was fitted below the outflow of the broodstock container. Released larvae were transported with the waterflow and collected in the sieve and then used for experiments.

Rearing of the experimental larval batch

Larvae were reared (initial density 10 larvae/ml) in conical flow-through seawater tanks (50 L, n = 6) with constant aeration at 28 PSU and at a low fluctuating temperature (n = 3) between 20 and 21°C (mean: 20.6 ± 0.1°C; SCHEGO titanium heater, Germany) and a high fluctuating temperature (n = 3) between 20 and 24°C (mean: 21.4 ± 0.1°C; IKS Aquastar Industrial, Germany). In the low fluctuating treatment, temperature change was not time-controlled while in the high fluctuating treatment, temperatures were 20 and 24°C during the night and day, respectively. Larvae were fed with an algae mixture (Stichting Zeeschelp, the Netherlands) at a cell concentration of 40.000 algal cells/ml. Subsamples from each larval tank were taken and larvae were counted and measured to determine survival, development into competent pediveligers for settlement, and growth. Larval length (n = 25) was averaged for each replicate tank and time point. Pediveligers were classified as competent for settlement when both the foot and eyespot were visible. Alive larvae that had not developed into competent pediveligers were transferred to a clean rearing tank at their respective treatment condition and a subsample of the competent pediveligers was used to determine settlement success (see below). The remaining competent pediveligers were pooled and transferred to larger settlement tanks without further inspection for this study.

Settlement success and post-settlement size

Competent pediveligers for settlement were transferred to a 200 µm sieve which was hung in a separate rearing tank (n = 3) at the respective temperature treatment. The inflowing water and food supply was placed above the sieve. Grind-up oyster shells (300 µm, microbrisure, Entre Mer et Terre, France) were placed in the sieve as settling material. The tanks were shaded and left undisturbed for 10 days after which larvae were counted and their behavior was assessed. Larvae were categorized either as settled, crawling, swimming or dead which corresponded to individuals that i) had attached firmly to the oyster shells, ii) had not yet attached firmly to the oyster shells, iii) were predominantly swimming, or iv) had an open shell and were not moving, respectively. The length of settled larvae was measured (n = 7–20 per replicate tank) under a microscope and averaged for each replicate tank.

Thermal coping ranges

Thermal preference, swimming speed and mean directional change rate

A horizontal thermal gradient was used to determine acute thermal preference range and thermal influence on swimming behavior of D-shape, umbo and pediveligers (Wiggins and Frappell 2000). The gradient consisted of a glass tube (40.1 ml volume, 51 cm length, 1 cm Ø) embedded in a water bath within an u-shaped aluminium block with LED lighting along the left and right horizonal planes. The ends of the aluminum block were connected to a Peltier device or a heating unit. Temperatures were set using a custom-built electronic controller and the linear gradient between 16 and 30°C established within 30 min. Larval position within the gradient could be viewed through the opening on the top of the aluminium block. A camera (Galaxy S8, Samsung) was installed above the gradient that took images of the gradient at a rate of one per hour throughout each experimental run. In addition, after 1 hour, 1-min videos were taken at 5 locations along the gradient which corresponded to 17, 20, 24, 27 and 30°C. Individuals of D-shape, umbo and pediveligers were evenly distributed throughout the glass tube using a syringe connected to aquarium tubing (n = 3 per life-stage). Larvae were left to move throughout the gradient for three hours after which the temperature was measured every 2 cm along the gradient using a digital thermocouple thermometer. Control runs (n = 2 per life-stage) with a uniform temperature (20°C) throughout the thermal gradient were conducted to test whether the design of the gradient apparatus had an influence on the larval distribution. Subsamples of larvae were taken at the end of each experimental day to confirm developmental stage and measure larval length (n = 25) under a microscope.

Images captured at the start (0 h) and end (3 h) of each experimental run were used to determine the acute thermal preference range of larvae by counting the number of larvae in 2 cm-sections along the gradient. Numbers of larvae in consecutive sections were summed to determine the temperature range where 50% of the test-population occurred after the 3 h-exposure (Alter et al. 2017). The average of this temperature range was used to test for differences in the temperature range between treatments and life-stages. Videos taken 1 hour after the larvae were introduced into the gradient were used to determine swimming speed and swimming directionality. The 1-min videos were analyzed by automatedly tracking the distance traveled by larvae between every frame (0.03 s) using the plugin TrackMate for Image J (FIJI) (Ershov et al. 2021). The median swimming speed (µm*sec^{-1}) was corrected for larval size by dividing it by larval length (body length (BL)*sec^{-1}). The mean directional change rate is the

angle between two links of the swimming path in succeeding frames averaged across the entire track length (Meijering et al. 2012). This value was inverted and the lowest inverted directional change rate was added to each data point and termed swimming directionality in order to achieve positive values to which performance curve models could be fit. Median swimming speeds and swimming directionality of larvae (n = 12–39) of each life-stage were averaged for each temperature (n = 5).

Oxygen consumption rate

Oxygen consumption rate was measured in D-shape, umbo and pediveligers (n = 5–9). Subsamples of larvae were taken at the commencement of each experiment to confirm developmental stage and measure larval length (n = 25) under a microscope. Oxygen consumption rate trials were conducted in a temperature-controlled room at 17, 20, 24, 27, 30 and 33°C. Two temperatures were tested at the same time and four temperatures were tested in one day. Hence, trials with all six temperatures were accomplished over a period of two days. Pre-experiments showed that $\dot{M}O_2$ did not change significantly within two days of development. Ultra-pure seawater was preconditioned to each of the six temperatures and an unknown number of individuals were transferred from the rearing tanks to the respiration chambers, providing an acute exposure of the individuals to the new temperature. Trials commenced immediately after respiration chambers were hermetically sealed under water. Respiration chambers were 2-ml glass vials with screw caps (PreSens, Germany) that were placed on a sensor dish reader (PreSens, Germany). The sensor dish reader measured the oxygen content within each chamber at a rate of four readings per minute. Larvae swim frequently and stirred the water such that a mechanical stirring mechanism was considered unnecessary. Lights were switched on during trials and all experiments were conducted during the day. Percentage air saturation (O_2sat) was measured until oxygen dropped below 70% O_2sat which took approx. 3–5 h. Pre-experiments had shown that critical oxygen levels were below 25% O_2sat for all veliger life-stages. After the experiments, individuals were preserved in 4% formalin and subsequently counted (density = 308 ± 13 ind/ml). Pre-experiments had shown that these densities did not influence individual $\dot{M}O_2$. Sensors were calibrated in air saturated seawater for 100% O_2sat and in sodium sulfite-saturated seawater for 0% O_2sat. Three chambers without larvae served as blanks to account for background respiration. Oxygen consumption rates (in pmol*h^{-1}*ind^{-1}) were calculated from the linear decrease in % O_2sat in each respiration chamber according to:

$$\dot{M}O_2 = \frac{FO_2}{t} \times (P_B - P_S) \times \beta_{O_2} \times Vol \times 0.2093$$

where FO_2 is the change in fractional oxygen concentration over time, t (sec), P_B is the barometric pressure (kPa), P_S is the saturation vapor pressure of water (kPa), β_{O2} is the capacitance of water for oxygen, *Vol* is the chamber volume minus the larvae volume (L, assuming 1 g wet mass equals 1 ml) and 0.2093 is the fractional concentration of oxygen in water (Alter et al. 2017). Individual weights were estimated from measured larval length according to Labarta et al. (1999).

Predicting performance and statistical analysis

We fitted exponential curves to data on larval lengths across developmental time of *O. edulis*. For larval lengths from each rearing tank we fitted the model

$$yt = a \times exp^{k \times t}$$

where *yt* is the larval length (µm) at time *t*, *t* is the number of days since larval release, *a* is the larval length at *t* = 0, and *k* is the growth constant.

For data on swimming speed, swimming directionality and $\dot{M}O_2$, TPCs were fitted to predict the thermal optima for each parameter. First, data from all three replicate tanks were averaged. Then, TPCs were fitted (*rTPC, nls.multstart*) using nonlinear least squares (NLSS) regression according to Padfield et al. 2021. In brief, out of 24 different TPC models, five models were selected ("Gaussian_1987", "Joehnk_2008", "Oneill_1972", "Pawar_2018", "Weibull_1995") and fitted to data. These five models were chosen because we were interested in the optimum temperature and those models included that parameter in their formulation. Subsequently, the five models were weighted based on the smallest Akaike information criterion correcting for small sample size and the temperature at which swimming speed, swimming directionality and $\dot{M}O_2$ was maximal was estimated using the weighted model (Padfield et al. 2021).

Differences in larval sizes between larval release dates were tested with a non-parametric one-way analysis of variances (ANOVA) (*ARTool*) because homogeneity of variances (Levene's test) was significant. A two-way repeated measures ANOVA was used to test for differences in larval length of the three life-stages at time points of experimental runs. Kaplan-Meier analysis was conducted for data on *O. edulis* cumulative survival and development of competent pediveligers. Larvae that survived and larvae that developed into competent pediveligers were treated as right-censored observations. A two-way ANOVA was used to test if proportions of larvae were statistically different in settlement behaviors between the two rearing temperatures and a two-way repeated measures ANOVA was used to test if rearing temperature and time affected post-settlement larval length.

Differences between the distributions of larvae with and without being exposed to a thermal gradient were tested using Chi-square tests. This was followed by examining the differences in average acute thermal preference range between life-stages and treatments using a two-way ANOVA. The influence of life-stage, treatment and exposure temperature on swimming speed, swimming directionality and $\dot{M}O_2$ data (*ln*-transformed) was tested with three-way ANOVAs.

Curve fitting and statistical analyses were conducted using R (version 4.2.0). Normality and homogeneity of variances were assessed using the Shapiro-Wilkinson test and Levene's test, respectively. A probability of less than 0.05 was considered as significant. Bonferroni host-hoc tests were used to detect significant differences between the levels of the variables when independent variables were significant.

2.8.2.3. Hatchery rearing of flat oyster larvae and spat

The methods are published in Alter et al. (2023). In brief, broodstock conditioning, release and rearing of larvae and spat of *O. edulis* was performed according to standard hatchery practices at the hatchery Stichting Zeeschelp, Kamperland, the Netherlands in August 2022. Boodstock (*n* = 70) were housed in one flow through tank containing a sieve at the outflow to collect released larvae that were transported with the water flow. The seawater was heated to 25.3 ±

0.1°C at a salinity of 30 ± 1 PSU and constantly aerated. Released larvae were collected from the sieve each day and larvae from one day were used for experiments.

Larval phase

Larvae (5 ± 1 ind/ml) were reared in conical flow through tanks (180 L capacity, 20 renewals/day, *n* = 6). Seawater was filtered (0.02 µm), had a salinity of 30 ± 1 PSU and was heated to the treatment temperatures of 25°C (25.3 ± 0.1°C, range 24.6–25.7°C, *n* = 3 tanks) and 29°C (28.5 ± 0.0°C, range 28.3–28.6°C, n = 3 tanks). The live micro-algae diet for rearing the larvae consisted of *C. neogracile* (40%), *I. galbana* (25%), *P. lutheri* (25%), and *R. lens* (10%) and was held constant at an excess density of 40,000 cells/ml. Larvae were transferred to new tanks every other day, whereby they were sieved over a mesh size of 150 µm, 180 µm and 250 µm on day 2, 6 and 9, respectively. Larvae that fell through the mesh size were discarded. A subsample of larvae which remained on the mesh was counted and their anterior-posterior length was measured (*n* = 12 larvae per tank for 6 tanks, subsequently averaged per tank) under a microscope (Olympus CKX41) to determine growth and development into competent larvae for settlement which was considered as larval survival. Individual larvae were considered suitable for settlement ('competent') when eye spots and the foot were present, and they had reached a minimum size of 300 µm.

Spat phase

On day 9 post release (dpr), competent larvae were harvested for determination of spat survival and growth. On that day, a batch of larvae was taken from each tank, divided into two groups and transferred into 12 settlement tanks in total. A group reared at a particular temperature as larvae was further maintained at that temperature (*n* = 3) while the second group (n = 3) was transferred to the other temperature, i.e. 25°C when larvae were reared at 29°C and *vice versa*. Different amounts of larvae were taken from the larval tanks because different amounts of competent larvae were available on 9 dpr. This resulted in different stocking densities among replicates within the settlement tanks. A total of 50,000 competent larvae was taken from each of two out of the three larval tanks at both temperatures resulting in a stocking density of 8 ind/ml in the settlement tank. From the third larval tank only 44,500 competent larvae at 25°C and 29,500 competent larvae at 29°C were taken which resulted in stocking densities in the settlement tanks of 7 and 5 ind/ml, respectively. Settlement tanks consisted of PVC pipes (20 cm Ø) with a mesh bottom (200 µm) hung into a flow through tank in which the inflowing water and food supply was placed above the sieve. The food ration during the early benthic phase was similar as used for the larvae, but was increased to a density of 60,000 algae/ml. Grind-up oyster shells (200–400 µm, microbrisure, Entre Mer et Terre) were placed in the sieve as settling material. Sieves were cleaned with seawater every day. After two weeks, subsamples (*n* = 10) of the spat from each tank were counted and their anterior-posterior length and dorsal-ventral height were measured (*n* = 20) under a stereo microscope (Leica MZFLIII) to determine survival and growth. Sizes of spat were averaged for each replicate tank (*n* = 3).

Statistical analysis

Repeated measures two-way analysis of variances (ANOVA) was used to detect differences in larval size between rearing temperatures during the larval phase. A *t*-test was used to test for differences in larval survival as well as amount of larvae reaching competence on 9 dpr between rearing temperatures. Two-way ANOVAs were used to test for differences in spat size and spat survival with larvae and spat rearing temperatures as explaining variables.

Statistical analyses were conducted using R (version 4.2.0). Normality and homogeneity of variances were assessed using the Shapiro-Wilkinson test and Levene's test, respectively. A probability of <0.05 was considered as significant. Bonferroni host-hoc tests were used to detect significant differences between the levels of the variables when independent variables were significant.

2.8.3 Results and discussion

2.8.3.1 Assessment of Pacific oyster reefs

In-situ incubations for carbon cycling

The oxygen profiles indicate a gradual decline in DO of less than 20% over a ~8-hour incubation period for bare sediment (control) whereas incubated oyster patches displayed an oxygen depletion of ~50-100% depending on the oyster biomass (Fig. 67). In summer oxygen depletion occurred rapidly whereas DO depletion was linear and occurred more slowly in autumn. Due to oxygen depletion, calcification declined during the incubation (Fig. 68). When only looking at all autumn measurements in 2021 and 2022, calcification was in the range of 5-10 mmol $CaCO_3$ $CUBE^{-1}$ h^{-1} m^{-2}. Respiration was in the range of ~15 mmol DIC $CUBE^{-1}$ h^{-1}.

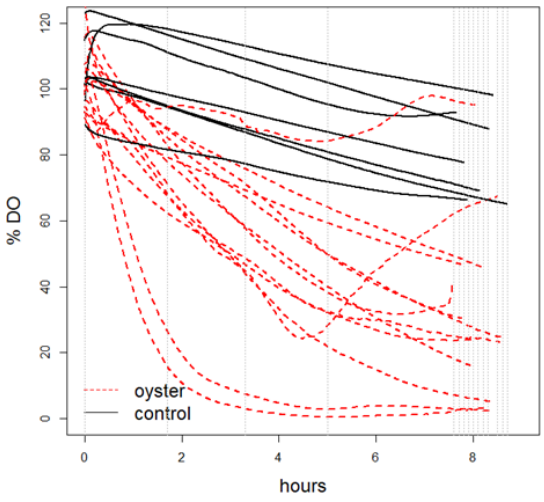

Figure 67 Oxygen depletion of 21 incubations. Two oyster incubations where leaking. Sampling intervals are indicated with the vertical dashed lines.

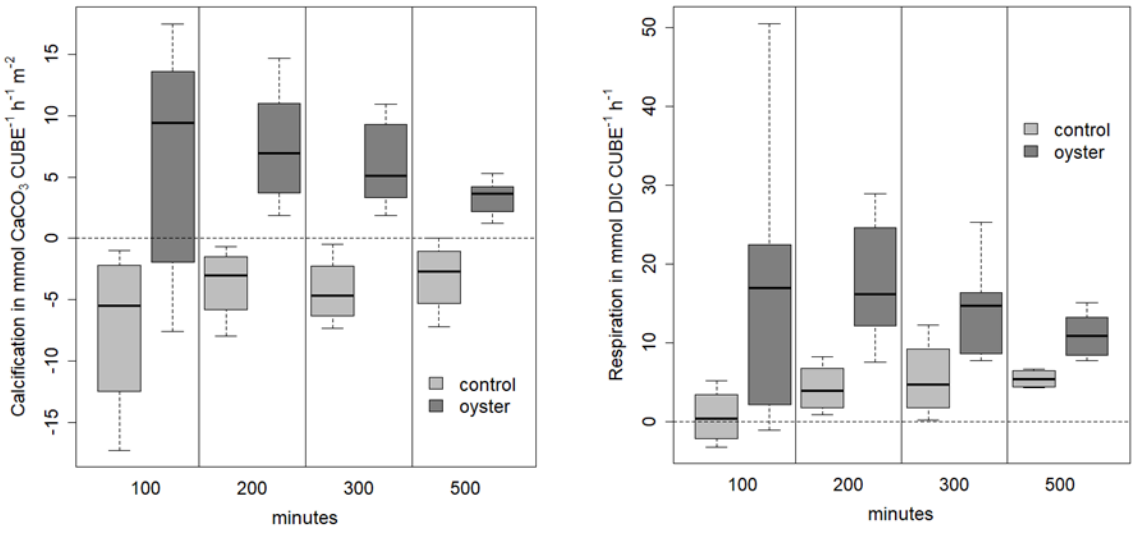

Figure 68 Calcification (left) and respiration (right) for all incubations performed in autumn (2021 and 2022 combined), 100, 200, 300 and 500 minutes after the start of the incubation.

Biodeposition

The top sediment layer is mobile due to sediment deposition, resuspension and sediment transport, whereas the deeper layers reflect the long-term storage of carbon into the sediment. Overall the percentage of organic matter increased with depth. There was not a clear change with distances (Fig. 69). Organic matter still needs to be converted to the amount of organic carbon.

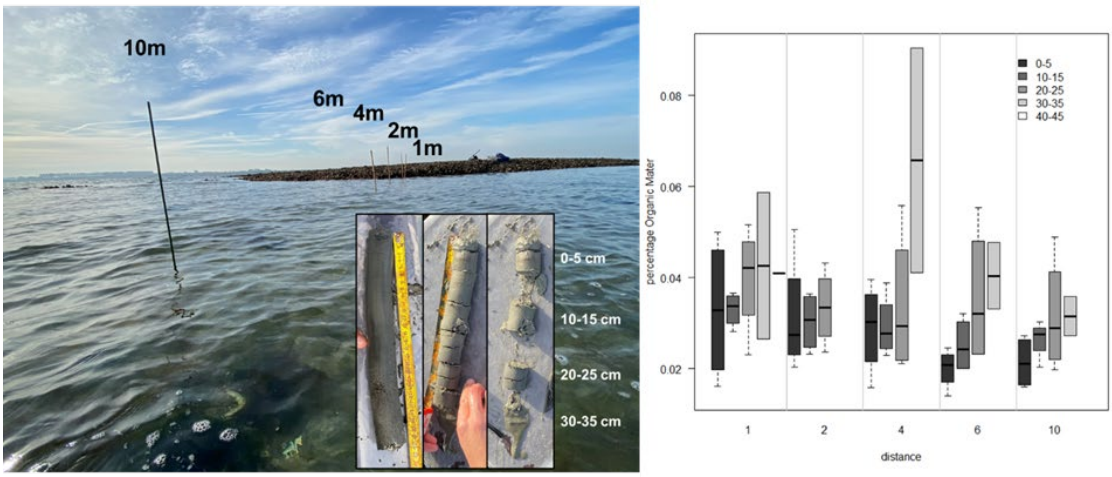

Figure 69 Overview of sediment sampling (left) and percentage organic matter of the sediment at different depths in the sediment and different distances from the reef (right).

Biodiversity

Biodiversity on artificial and natural oyster reefs was compared through metabarcoding of eDNA from water samples collected in tidal pools. Sequencing results show a slight difference in relative abundance of species-specific reads between samples from artificial and natural reefs. The difference in community composition was mainly caused by the relatively high

abundance of the snail *Peringia ulvae* and the worm *Nephtys hombergii* on the artificial reefs, which are developing species and the sponge *Halichondria panicea* on the natural reefs which grows much more slowly.

Some mobile species such as *Carcinas maenas* and *Hemigrapsus takanoi* can be detected with the current experimental pipeline, but the setup needs optimization to improve the results. For example, primers specifically designed for mobile target taxa can help to identify these particular animals. Also, a different barcode region may result in better detection of mobile species. This is ongoing work.

Water samples from other locations along the transects, as well as the sediment samples are still being processed.

2.8.3.2. Thermal performance of flat oyster larvae

Larval batch releases and sizes

The broodstock first released larvae 44 days after the temperature was increased from 12°C, at 19.6°C. Over a total period of 61 days, oysters released larvae on 14 days. Summer temperatures of the North Sea are between 16 and 22°C, indicating that the thermal environment of the North Sea is sufficient to induce spawning.

Vital rates

Developmental time from release to reaching competence for settlement was seven days longer at the low compared to the high fluctuating treatment (Fig. 70). Yet, larval length at D-shape, umbo and pediveliger life-stages were similar between treatments ($p > 0.05$; Fig. 70). Cumulative survival of larvae until settlement was low and was not influenced by rearing treatment ($p > 0.05$, Fig. 71A). The survival was 4.2 ± 2.1 and 8.5 ± 1.5 % at the low and high fluctuating temperature treatments, respectively. The percentage of larvae that developed into competent pediveligers was 4.2-fold lower in the low *versus* the high fluctuating treatment ($p < 0.001$, Fig. 71B). After 10 days in the settlement tank, length of spat was similar between treatments ($p > 0.05$, Fig. 72A). Yet, 5.5-fold more larvae ($p < 0.001$) had settled and 0.8-fold fewer larvae were dead ($p < 0.001$) in the high fluctuating treatment compared to the low fluctuating treatment (Fig. 72B).

In the wild, it has been estimated that approx. 2.5 and 10% of *O. edulis* larvae survive until settlement at 18 and 22°C, respectively, and of those that survive approx. 1% successfully settle to benthic habitats (Korringa 1946). Our results showed that for larvae developing in temperatures representing the lower end of their thermal performance curve (20–21°C) for locomotion and MO_2, a slight increase in mean temperature (0.9°C increase) or an increased magnitude of temperature fluctuation (3°C) resulted in a more than 5-fold higher settlement success. Hence, in order to better estimate the recruitment potential within the restoration site in a present and future climate it is important to monitor and thus gain information of the local thermal variability to date to project it for the future as not only magnitude but also duration and periodicity of the thermal variability can influence vital rates (Vasseur et al. 2014). Climate driven intensification of temperature fluctuation would most likely increase growth and survival in *O. edulis* population but the impacts of these changes in thermal environment on later life stages remains to be tested (c.f. Xing et al. 2014).

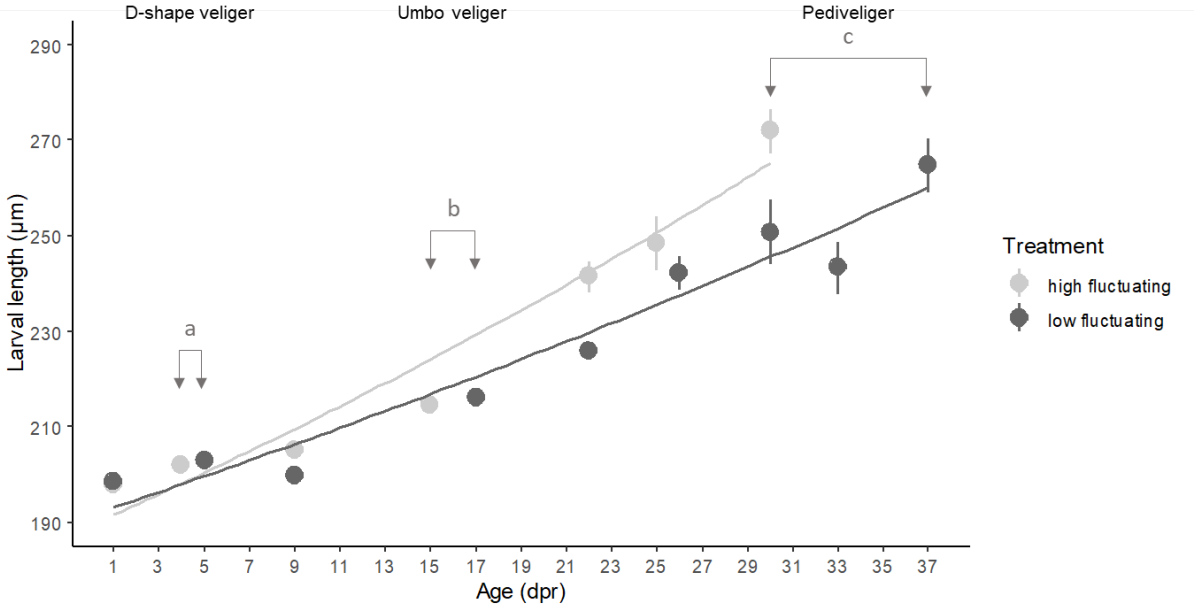

Figure 70 Ostrea edulis *larval length (µm) during pelagic development (days post release (dpr)) when reared at low (20–21°C, dark grey symbols) and high (20–24°C, light grey symbols) fluctuating treatments. The arrows indicate timepoints at which experiments with the three life-stages were conducted. Note that these are offset on the x-axis for each life-stage between treatments because of longer developmental times in the low fluctuating treatment. Different* lowercase letters *indicate significant differences in larval length between life-stages.*

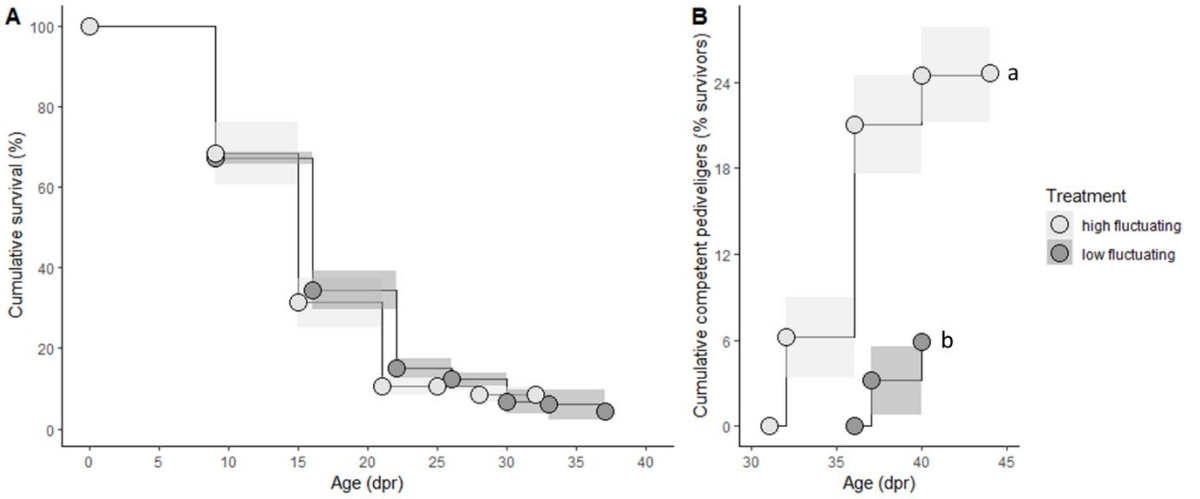

Figure 71 Ostrea edulis cumulative survival (%) during larval development (A) and cumulative development of competent pediveligers (% survivors, B) over time (days post release (dpr)) at low fluctuating (dark grey symbol, 20–21°C) and high fluctuating (light grey symbol, 20–24°C) temperatures. Different lowercase letters *indicate significant differences between rearing treatments. The mean (solid lines) ± 95% confidence interval (shaded) is shown, n = 3.*

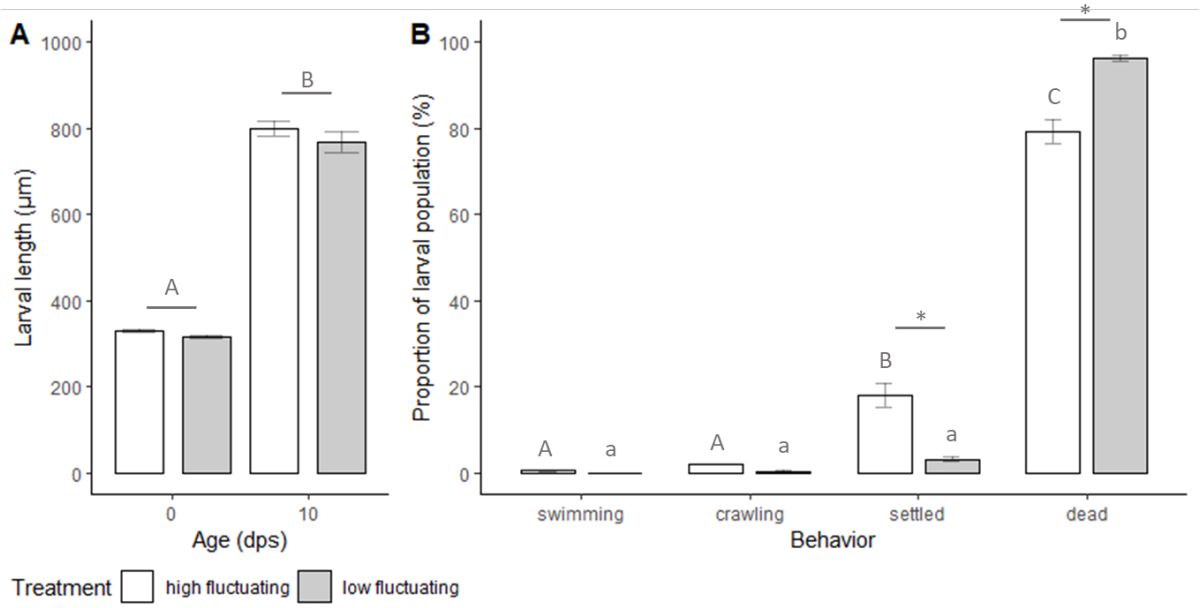

Figure 72 Shell length (µm) (A) and behavior (B) of proportion (%) of Ostrea edulis pediveliger test population (B) after 10 days within settlement tanks (dps). Pediveligers were reared at low (20–21°C, grey bars) and high (20–24°C, open bars) fluctuating temperatures. In A, different capital letters indicate significant different larval sizes across time. In B, different capital and lowercase letters indicate significant differences between behaviors within the high and low fluctuating treatments, respectively. Asterisk indicates significant differences between treatments for both settled and dead larvae. Values are mean ± SE, n = 3.

Acute thermal preference range and TPCs

The mean temperature of the acute thermal preference range was higher in pediveligers reared in the high fluctuating treatment compared to D-shape veligers in that treatment ($p < 0.05$) as well as pediveligers at the low fluctuating treatment ($p < 0.05$, Table 9).

At each life-stage, swimming speeds were similar between treatments ($p > 0.05$) and at the high fluctuating treatment, swimming speeds were also similar between life-stages ($p > 0.05$). At the low fluctuating treatment, however, swimming speed across exposure temperatures decreased from D-shape to pediveligers ($p < 0.01$; Fig. 73A-C). Based on TPCs, swimming speed was predicted to be highest at ≥ 30°C for D-shape and umbo veligers at both treatments and 29.9°C and 28.4°C for pediveligers in the low and high fluctuating treatments, respectively (Fig. 73A-C). Swimming directionality was influenced by the interaction between treatment and life-stage as well as life-stage and exposure temperature ($p < 0.05$; Fig. 73D-F). Directionality was predicted to be highest at 27.2 and 25.2°C in D-shape veligers, 26.8 and 29.3°C in umbo veligers, and 28.4 and 29.5°C in pediveligers in the low and high fluctuating treatments, respectively (Fig. 73D-F). $\dot{M}O_2$ increased with life stage and were significantly higher in larvae reared in high compared to the low fluctuating treatment in all life-stages across all exposure temperatures ($p < 0.05$, Fig. 74). TPCs predicted maximal $\dot{M}O_2$ for umbo veligers at or above 33°C and pediveligers at 29.2°C for both thermal rearing treatments. For D-shape veligers, $\dot{M}O_2$ was predicted to be maximal at 28.9 and 32.8°C for larvae reared at low and high fluctuating temperature, respectively (Fig. 74).

These high thermal optima for swimming performance and $\dot{M}O_2$ suggest that growth rates, survival and settlement success of *O. edulis* larvae will potentially further increase when larvae are reared at temperatures higher than 20–24°C. In addition, when given a choice of temperatures, larvae preferred 26 to 30°C (note that higher temperatures were not tested). In agreement, when reared at stable temperatures in 5°C increments between 15 and 30°C, size at settlement, settlement success and food intake were highest at 30°C (Robert et al. 2017). Yet, while food intake was linearly correlated with temperature, increments in size at settlement and settlement success were smaller between 25 and 30°C in comparison to increments between lower temperatures (Robert et al. 2017). This suggests that larvae were approaching their thermal optimum between 25 and 30°C which agrees with TPCs from the present study.

Table 9 Average, minimum, maximum and the width (mean ± SE) of the temperature range where 50% of the total test-population (individuals) of D-shape, umbo and pediveliger of Ostrea edulis *gathered after three hours when exposed to temperatures between 16 and 30°C within a thermal gradient. Larvae were reared at a low (20–21°C) and high (20–24°C) fluctuating temperature treatment. Different* lowercase letters *indicate significant differences between life-stages within the high fluctuating treatment.* Asterisk *indicates significant differences between treatments for pediveligers.*

	Temperature range (°C)				Number of runs (*n*)	Individuals (ind/*n*)
	average	minimum	maximum	width		
Low fluctuating						
D-shape veliger	28.7 ± 0.3	27.2 ± 0.5	30.0 ± 0.0	2.8 ± 0.5	2	703 – 798
Umbo veliger	28.3 ± 0.7	26.6 ± 1.3	30.0 ± 0.0	3.4 ± 1.3	3	543 – 760
Pediveliger	27.9 ± 0.1*	25.7 ± 0.2	30.0 ± 0.0	4.3 ± 0.2	3	222 – 399
High fluctuating						
D-shape veliger	27.8 ± 0.3[a]	25.6 ± 0.6	30.0 ± 0.0	4.4 ± 0.6	3	467 – 662
Umbo veliger	28.6 ± 0.1[ab]	27.1 ± 0.3	30.0 ± 0.0	2.9 ± 0.3	3	165 – 918
Pediveliger	29.4 ± 0.0[a]*	28.8 ± 0.0	30.0 ± 0.0	1.2 ± 0.0	3	228 – 537

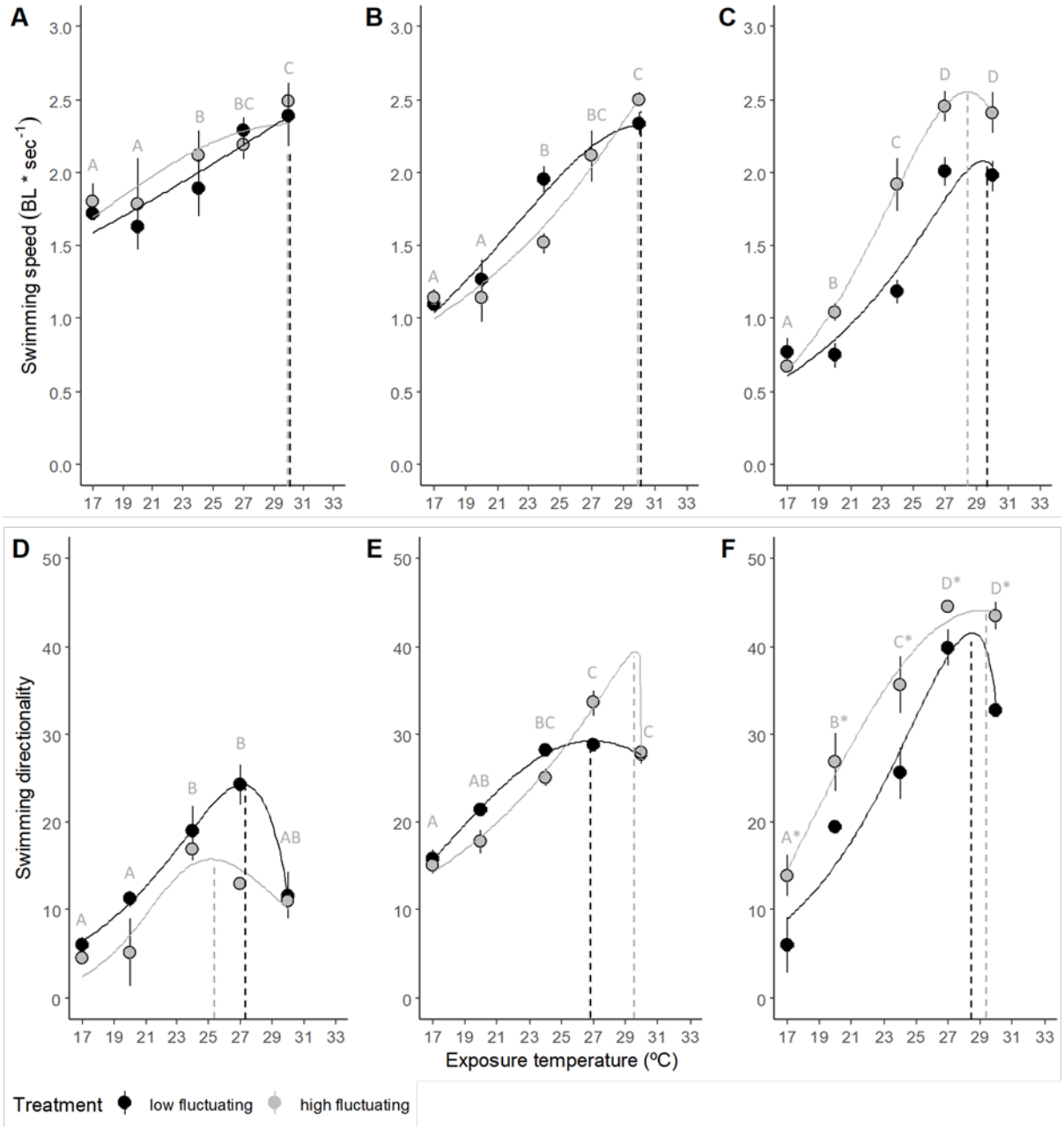

Figure 73 Median swimming speed (body length (BL) sec-1, A-C) and swimming directionality (D-F) of D-shape veliger (A, D), umbo veliger (B, E) and pediveliger (C, F) of Ostrea edulis across different exposure temperatures (°C). Larvae were reared at low fluctuating 20–21°C, black symbols) and high fluctuating (20–24°C, grey symbols) temperatures. Different capital letters indicate significant differences between exposure temperatures. Asterisks indicate significant differences between treatments. Thermal performance curve models were fitted to data. Values are mean ± SE, n = 3.

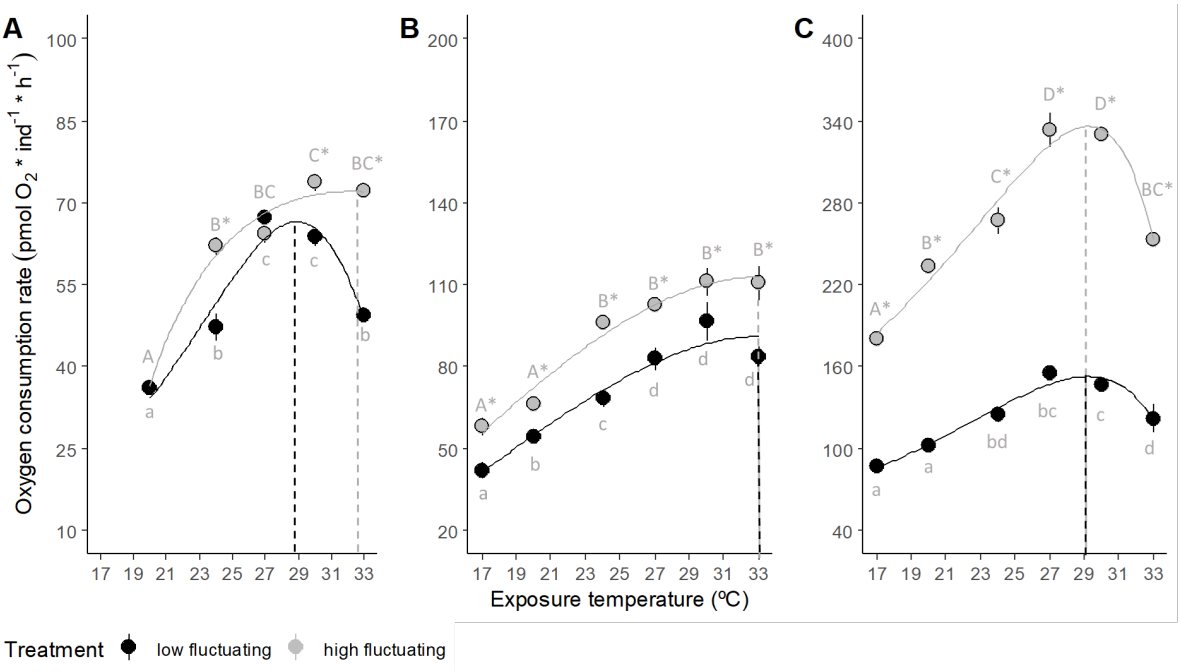

*Figure 74 Oxygen consumption rate (pmol O2*ind-1*h-1) (ṀO2) of D-shape veliger (A), umbo veliger (B) and pediveliger (C) of Ostrea edulis at different exposure temperatures (°C). Larvae were reared at low (20–21°C, black symbols) and high fluctuating (20–24°C, grey symbols) temperatures. Within each panel (A-C), different* lowercase *and* capital letters *indicate significant differences in $\dot{M}O_2$ between exposure temperatures within the low and high fluctuating temperature treatment, respectively.* Asterisks *indicate significant differences between rearing treatments at a given exposure temperature. Note the difference in y-axis scale between panel A-C. Thermal performance curve models were fitted to data. Values are mean ± SE, n = 3.*

2.8.3.3. Hatchery rearing of flat oyster larvae and spat

Detailed results and discussion can be found in Alter et al. (2023). For clarity, temperature conditions during the larval and spat phase are stated as a fraction. For example, 25/29°C refers to 25°C during the larval phase and 29°C during settlement, metamorphosis and the spat phase.

Larval and spat survival and sizes

Larval survival was similar between 25 and 29°C ($p > 0.05$, Table 1, Fig. 75A). The highest percentage of larval settlement competence was 28.4 ± 4.4% at 25°C and 25.6 ± 2.7% at 29°C, which occurred at 10 dpr at both temperatures. Spat survival was neither influenced by larvae nor spat rearing temperature (p > 0.05, Fig. 75B). Averaged across all temperature treatments, spat survival of competent larvae was 38.3 ± 4.8%. Although the mean survival of spat was not significantly different between treatments, the 29/25°C treatment showed a high range in the percentage values of spat that survived the first 14 days after settlement (37–85%) compared to those for the other three temperature treatments (30–40% for 25/25°C, 22–40% for 25/29°C, and 25–44% for 29/29°C; Fig. 75B). Larval length was similar (p > 0.05) between temperature treatments until 10 dpr, at which time point larvae reared at 29°C were 3% larger compared to those reared at 25°C ($p < 0.01$, Fig. 76). The average growth rate of larvae during the pelagic phase at 25 and 29°C was 10.4 ± 1.4 µm/day and 12.3 ± 1.2 µm/day, respectively. After two weeks in the settlement tanks, spat length was influenced by larval temperature ($p < 0.05$) and spat temperature ($p < 0.001$). Spat length was largest in treatment 25/ 29°C and spat from treatment 29/ 29°C and 25/25°C were significantly smaller (p < 0.05 for both, Fig.

77A). Spat height was influenced by spat temperature only ($p < 0.01$). For this measure, spat from treatment 25/29°C was 22% larger than spat from treatment 25/25°C ($p < 0.01$, Fig. 77B).

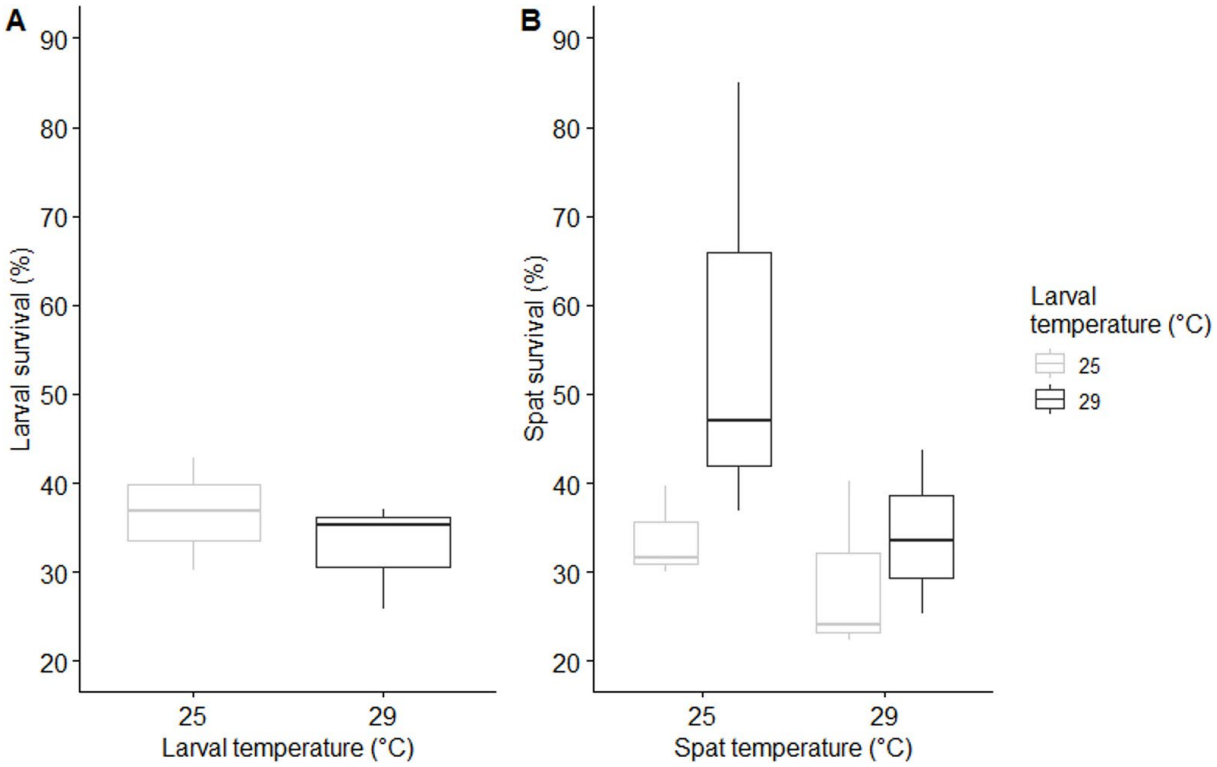

Figure 75 (A) Percentage (%) of larvae that survived the first 14 days post release from the broodstock and (B) percentage (%) of spat that survived the first 14 days post settlement, when reared at 25◦C (grey box) and 29◦C (black box). Differences between survival were not significant.

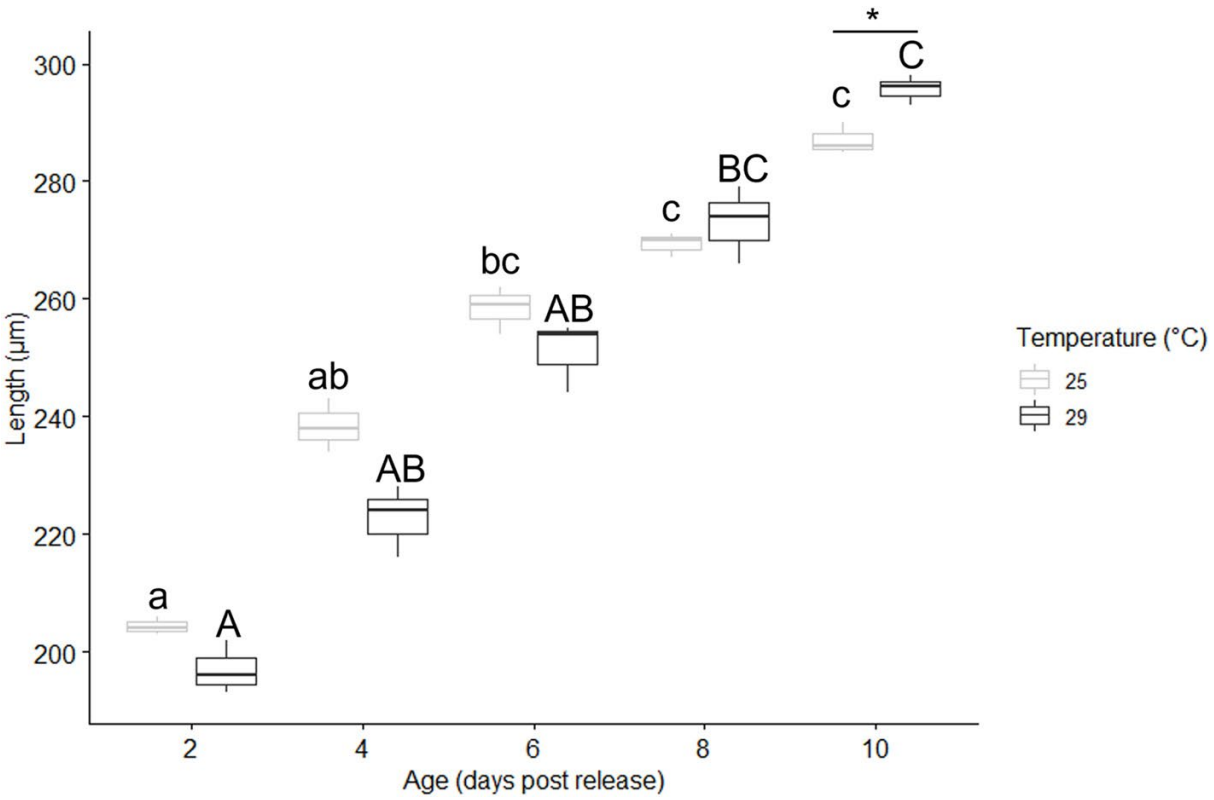

Figure 76 Larval length (µm) during the pelagic phase when reared at 25◦C (grey box) and 29◦C (black box). Different lower-case (25◦C) and upper-case (29◦C) characters indicate significant differences between the various ages (days post release) for each of the two treatments separately. Asterisk (*) indicates a significant difference between the two temperature treatments at ten days post release from the broodstock.

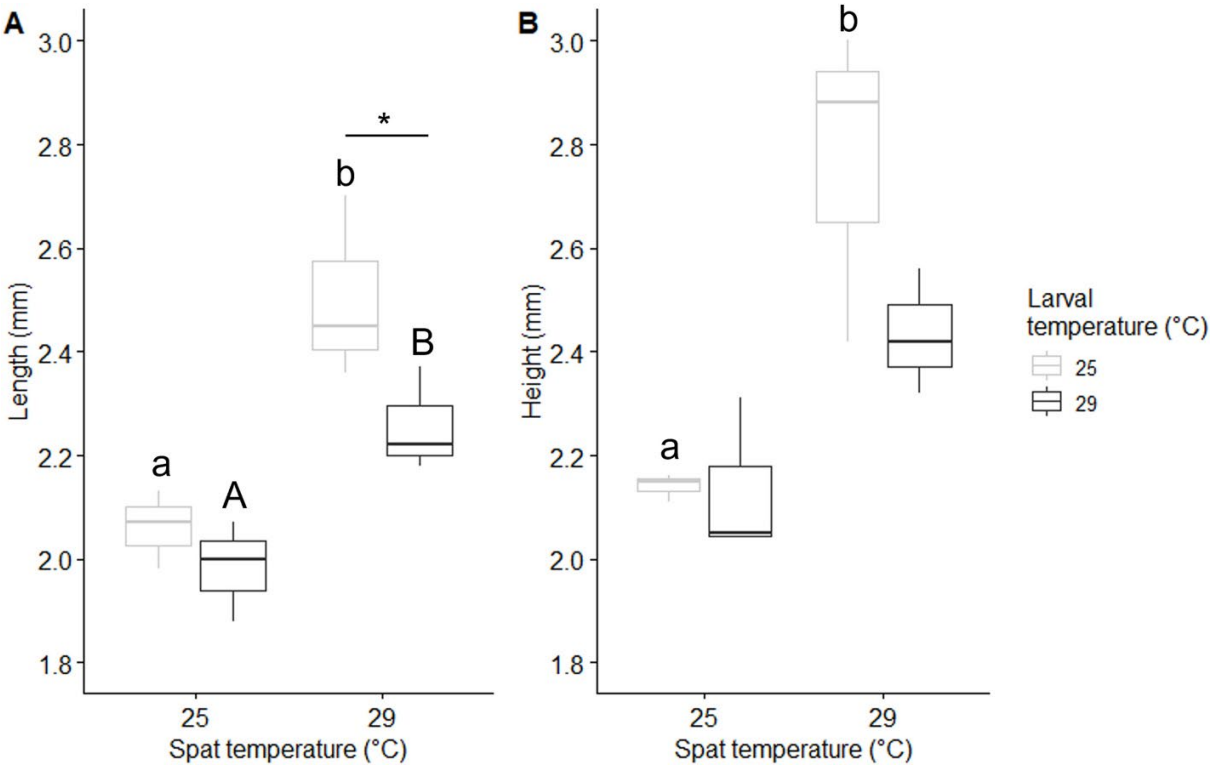

Figure 77 Larval sizes as (A) length (mm) and (B) height (mm) of spat after being reared at 25◦C and 29◦C for 14 days, preceded by rearing during the pelagic larval phase at 25◦C (grey box) and 29◦C (black box). Different lower case (25◦C) and upper case (29◦C) characters indicate significant differences in spat size for each larval

temperature treatment separately. Asterisk (*) indicates a significant difference in spat size within the given spat temperature.

When *O. edulis* experienced the lower temperature (25°C) during the larval phase, spat grew faster at the higher temperature (29°C) compared to stable temperatures throughout the two life-stages. For species with complex life-stages, larval experiences can influence post-metamorphic fitness, such as growth and survival of juveniles and adults (reviewed in Pechenik 2006). The effects are usually investigated with regards to nutritional stress during critical periods before metamorphosis, yet other environmental stressors are rarely investigated (Pechenik, 2006). Bivalve larvae often grow best at temperatures well above those which they would experience in nature and those between 25 and 32°C have been stated as optimal for larvae of the oysters *O. edulis, Crassostrea rhizophorae* and *Magellana gigas* (Helm et al. 2004, Rico-Villa et al. 2008, Robert et al, 2017). These studies, however, did not investigate carry-over effects on the benthic life-stage performance. It may be that larval exposure to 29°C was energetically suboptimal compared with exposure to 25°C so that, once transferred to 29°C at settlement, large larval energy reserves coupled with a more rapid passing through metamorphosis and a higher food intake post-metamorphosis may have boosted rapid early spat growth resulting in largest spat within this treatment group. Metamorphosis is an energetically costly process during which larvae deplete their energy storage of as much as 65% (Rodriguez et al. 1990, Videla et al. 1998, Whyte et al. 1992). After morphological and physiological changes occurred, spat commence feeding again but its rate may not immediately be sufficient for early post-metamorphic growth, resulting in further dependence on stored energy (Whyte et al. 1992). Food intake is positively correlated with temperature in both life stages, yet early spat (determined until 4 days post-metamorphosis) ingested 30% more algae whereas larvae ingested only 10% more algae at 30°C than at 25°C (Robert et al., 2017). In addition, experiments with 4 mm spat showed that upon transfer to a 6°C increase, metabolic costs of spat did not change, and filtration rates increased continuously throughout the three-week experimental period, while a transfer to a 6°C decrease resulted in reduced metabolic costs but also reduced filtration rates which in the long term were partly compensated (Beiras et al. 1995). Hence, upon transfer from the lower to the higher temperature, competent larvae in the present study might have had a metabolic advantage during the short-term exposure over those that were reared continuously at the higher temperature. Our results show that after rearing *O. edulis* larvae at a temperature commonly used for other oyster species within hatcheries (25°C) and a transfer of competent larvae to 29°C results in rapid early spat growth which yields a market sized product (2–4 mm) within the next two weeks (Utting and Spencer 1991, Helm et al. 2004). It is noteworthy, however, that exposure to temperatures as high as 29°C become disadvantageous for feeding and thus growth in adult *O. edulis* (Eymann et al. 2020). This time point, when further rearing at high temperatures results in reduced instead of enhanced growth of juvenile oysters, still needs to be determined. In addition, it further remains to be tested if early spat experiences to high temperatures during the first two weeks post settlement influence later life stages just as it was seen for larval experiences on spat in the present study.

Conclusion

Based on the results obtained so far, we cannot answer the question if oyster reefs are a sink or source of carbon as some data still need to be processed. The percentage of organic matter increased with depth suggesting burial of organic matter, however, an effect of the reef was not observed as there was no clear change with distance from the reef. We found a difference

in community composition between artificial and natural reefs. This difference was mainly caused by the relatively high abundance of fast-developing species on the artificial reefs and slow-growing animals on the natural reefs. This indicates that, after 10 years, the succession has not reached its climax state at the artificial reefs.

A major bottleneck to creating self-sustaining oyster beds is the successful development and settlement of larvae to bottom habitats, processes largely governed by temperature. In aquaculture, bivalve larvae, including those of *O. edulis*, are reared and grow best at temperatures well above those which they would experience in nature (Helm et al. 2004). Across ecologically relevant temperatures, however, a mechanistic understanding of larval performance is lacking. To better understand how temperature fluctuations in the field could impact the success of oyster restoration, we reared oyster larvae at two thermal regimes that overlapped, yet differed in thermal variability by 3°C but only by 0.9°C in their mean temperature. The small difference in temperature resulted in significant and relevant impacts on vital rates, as well as TPCs, especially in the last larval life-stage. The results suggest that *O. edulis* benefitted from the periodically high temperatures by increasing metabolism and swimming performance which translated into more rapid development and higher settlement success.

Previous research showed that increasing the temperature from the commonly used hatchery temperature for *O. edulis* of 22 to 25°C yields much higher larval survival and settlement success (Robert et al. 2017). By further adjusting the temperature at settlement, these parameters can be further optimized. Calculations are necessary to determine which temperature combination, i.e. larval phase at 25°C with a spat phase of 29°C which resulted in larger spat, or a larval phase at 29°C with a spat phase at 25°C which may lead to increased survival when stocking densities are low, is most cost effective for hatcheries. Either temperature combination yielded an oyster size at which they are suitable for release into restoration sites within two weeks, resulting in a hatchery period of as little as three weeks. These optimized hatchery protocols contribute to a more predictable and efficient production of flat oyster spat.

Acknowledgements

We thank Emiel Brummelhuis, Jennifer Chin, Douwe van den Ende, Arjen van der Kamp, Tilman Meyer and Wouter Suykerbuyk of Wageningen Marine Research, Sophie Valk of Marine Animal Ecology - Wageningen University and Dick van Oevelen and Anton Tramper of the Royal Netherlands Institute for Sea Research for their contribution to the fieldwork and experiments.

2.9 Impact of marine heatwaves (MHW) and artificial light at night (ALAN) on kelp in Hoe Bay, UK (SL#10/11)

2.9.1 Introduction

In addition to a long-term progressive increase in the ocean's temperature, more intense localized warming events have also been increasingly recorded, named Marine Heatwaves (MHWs) (Frölicher et al., 2018, Oliver et al., 2018, 2019). MHW are described as discrete and prolonged irregularly warm water local events, resulting from different temporal and spatial scale processes (Hobday et al., 2016). With an increase in their occurrence, frequency and intensity (Russo et al., 2014, Straub et al., 2019, Filbee-Dexter et al., 2020), such events have also caused great impacts on several marine communities (Smale et al. 2019), including high conservation value ecosystems, such as Kelp forests.

Kelp forests play an important ecological role, being one of the photosynthetic marine organisms with the highest rates of primary production and thus important blue carbon sinks, and acting as ecosystem engineers by serving as shelter for a huge diversity of marine organisms in varied coastal zones (Teagle et al. 2017, Wernberg et al. 2019). Several effects of MHWs have already been recorded on these organisms, from physiological levels (e.g. Pessarrodona et al. 2018, Fernández et al. 2021); to greater scale changes (reviewed in Smale 2020), and widespread declines in their abundance (Krumhansl et al. 2016). Studies using simulated heatwave scenarios have also been conducted, with equally negative effects observed (e.g. Nepper-Davidsen et al. 2019, Sánchez-Barredo et al. 2020, Britton et al. 2020, Umanzor et al. 2021).

Besides temperature, the physiology, and consequently the distribution of these organisms is also dependent on other environmental factors, such as inorganic carbon and light (Steneck et al. 2002). The combined effect of temperature and inorganic carbon, in the form of CO_2, has been widely addressed, in studies of ocean warming and ocean acidification (Brown et al. 2014, Iñiguez et al. 2016, Provost et al. 2016, Qiu et al. 2019, Fernández et al. 2021), though less frequently assessing MHWs scenarios (Britton et al. 2020). For all cases, it has been observed, that, the increase of dissolved CO_2, instead of working as an additional negative pressure, increased the resistance of the organisms to the thermal stress.

Another aspect of growing interest is the effect of artificial light effects combined with the thermal stress. From the beginning of the 20th century, the use of artificial light sources and use of outdoor artificial lighting at night has increased greatly around the globe. Consequently, light pollution has started to affect the natural daily and seasonal existing light cycles (Cinzano et al. 2001). Yet no study has yet addressed this potential local stressor on marine photosynthetic organisms, such as Kelps.

Here, the isolated effect of heatwaves (+3ºC) and heatwaves combined with Artificial Light at Night (ALAN, 24h light-0h dark), were tested on photosynthetic parameters, growth and respiration rates (R) and C/N ratio in the tissues of the kelp species *Laminaria digitata*. The effects of MHW period were tested for a ~14 day simulated event, followed by a recovery period of ~10 days, simulating conditions in short term mesocosm experiments at the Plymouth Marine Laboratory ("PML", UK).

2.9.2 Materials and Methods

2.9.2.1 Sampling and laboratory conditions

Individuals of *Laminaria digitata* were collected from the Plymouth Hoe coastal area (50.3640 N, 4.1459 W), in March 2022. After sampling, they were immediately transferred to PML's mesocosm laboratory, kept at the bottom of the tanks.

Each tank was maintained in a closed recirculating system, with mean salinity value of 35.24± 0.452, control temperature of 13.27± 1.124, and light system consisting of the mesocosm room light (with a 12h photoperiod) and individual LED lights placed at each tank (environmental photoperiod variation) with an intensity of 10,000-14,000 lux (Fig. 78). All organisms were set in these conditions during the acclimation.

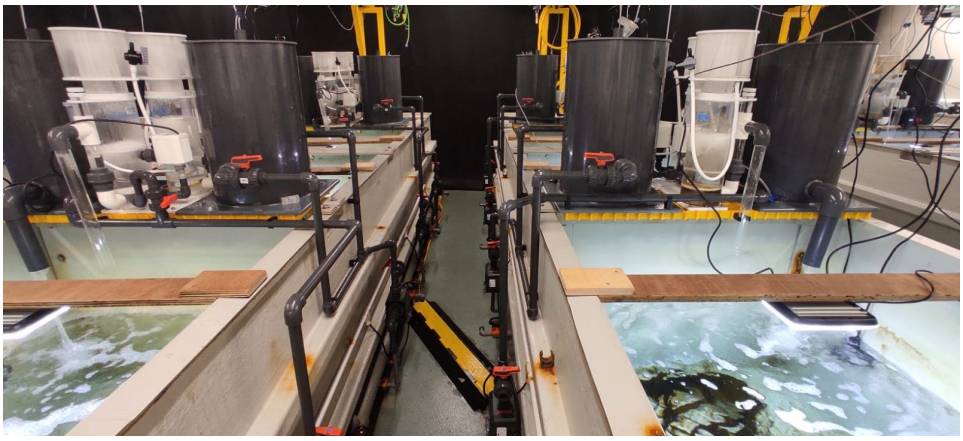

Figure 78 Mesocosm tanks where kelp organisms were maintained during the experiment, with white cold LED lights placed at the top.

2.9.2.2 Experimental setup

The experimental design was defined as a "collapsed factorial design", as mentioned in previous studies to decrease the number of treatments and increase the replicates in multi-factor studies (Boyd et al. 2018), for multiple drivers experiments. *Water Temperature* was defined as the main factor and *Light Availability nested within Water Temperature* as the secondary one. The experiment consisted of an initial acclimation period of 7 days (T1), followed by a simulated 14-day heatwave (T3), and lastly by a 10-day recovery period (end of heatwave) (T4). In total 3 treatments were defined: controls "C" (baseline temperature exposures + ~12hr light-dark photoperiod), Marine Heatwave "MHW" (+3ºC temperature increase + ~12hr light-dark photoperiod) and Marine Heatwave combined with ALAN "MHW+ALAN" (+3ºC temperature increase + 24hr light exposure), where the ALAN exposure was set simultaneously to the heatwave period lasting until the end of the recovery period. For each treatment 4 replicates were used.

2.9.2.3 Response variables measured

Photosynthetic parameters: Photosynthetic variables were measured using the Junior PAM device (WALZ). Measurements were taken at the meristem of the organisms, observing the values of: maximum photochemical quantum yield of PSII (photosystem II) (Fv/Fm), quantum efficiency α, and maximum Electron Transport Rate (ETRm).

Growth rates: Growth rates were measured by the hole-punching method, on the meristem of all organisms at T1, and their migration and perforation area measured during the course of experiments (T3 and T4).

Respiration (R) rates: Incubations for R were performed outside of the mesocosm tanks, in incubation chambers, using an optic oxygen sensor (OxyMini), with the rates being calculated as the difference in the final oxygen concentrations per the initial ones.

Carbon and Nitrogen tissue content: As the last part of the experiment, meristem samples of each organism were collected to measure their Carbon and Nitrogen content and C/N.

2.9.2.4 Statistical analysis

All statistical testes were done using the statistical software R, version 4.0.3. To identify the significance of the independent variables tested (Sea water Temperature and Artificial Light availability), nested Linear Models (LM) and PERMANOVA analyses were performed. When significant effects of the tested factors were observed (p-value < 0.05), Tukey's Honestly Significant Different (THSD) post hoc tests were performed to identify any significant groupings within the tested treatment levels (C, MHW, MHW+ALAN).

2.9.3 Results

For Fv/Fm, after the heatwave (T3), the MHW had the highest values compared to controls and MHW+ALAN, while for α the lowest value corresponded to the MHW+ALAN treatment. No significant differences were found for either parameter after recovery (Fig. 79). For the growth rate measures, both in area increase rates and perforation migration rates, MHW had the lowest values and MHW+ALAN the highest (Fig 80), a pattern also found for the Carbon/Nitrogen ratio, at recovery (Fig 81). Regarding respiration rates, there was a high degree of variability and no significant differences were statistically found, nevertheless, during recovery, in the MHW treatment higher O_2 consumption values were still observed (Fig. 82).

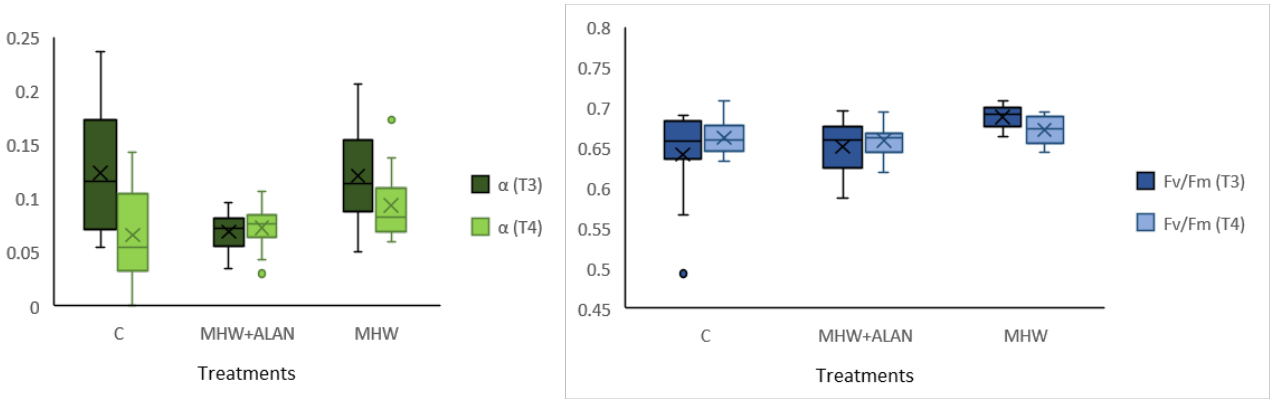

Figure 79 Quantum efficiency (right) and maximum quantum yield (left) values after heatwave period (T3) and recovery (T4).

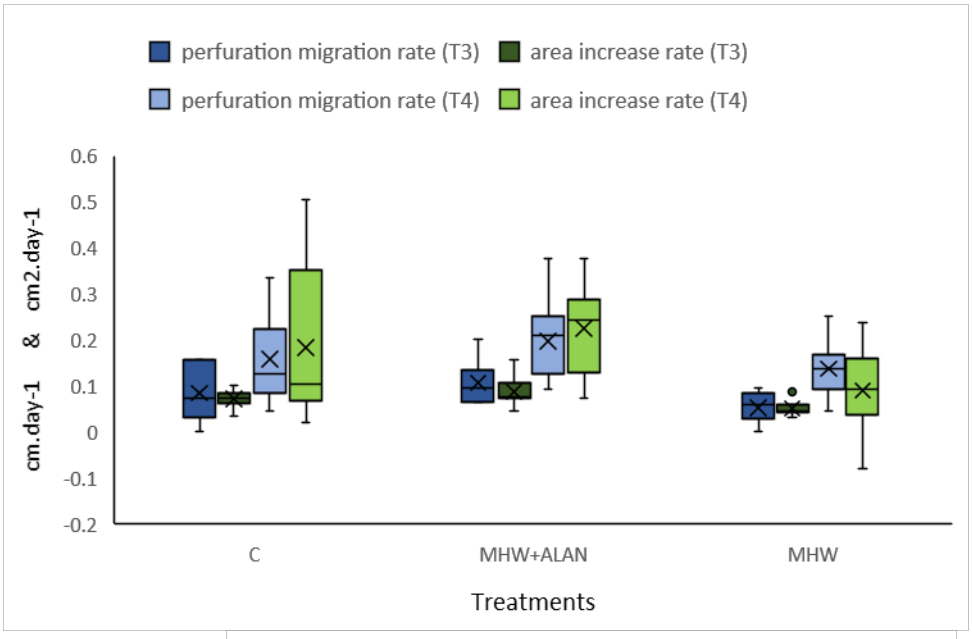

Figure 80 Perforation migration and area increase rates after heatwave period (T3) and recovery (T4).

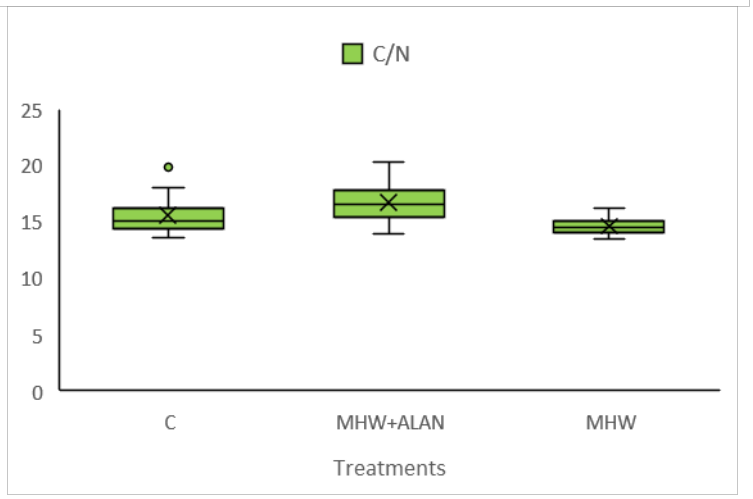

Figure 81 Carbon/Nitrogen meristem tissue ratios after recovery period (T4).

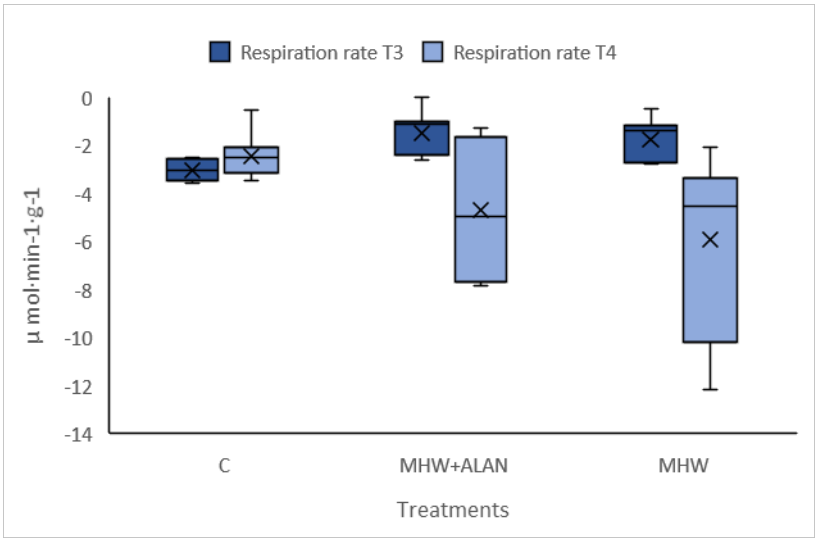

Figure 82 Respiration rates after heatwave period (T3) and recovery (T4).

2.9.4 Discussion

This study tests, for the first time, the combined effect of MHWs and ALAN on the physiology of the species L. digitata. It was found that increased light availability helped organisms to better respond to the MHW, when compared to those exposed to MHW alone. The combined effect of MHW and ALAN resulted in generally positive responses, in comparison to the other tested conditions, with the ALAN effect compensating the negative effects caused by increased temperature.

After the MHW, two different patterns were observed for the photosynthetic and growth rate parameters. By being exposed to increased light conditions, a down regulation of the light used by the organisms was observed, resulting in a decrease in their quantum efficiency. On the other hand, an increase in the maximum quantum yield was found when exposing organisms to MHW alone, being hypothesised that the thermal stress implied may not have negatively affected the PSII of the studied species, that was seen to present higher photoprotection mechanisms in previous studies (Burdett et al. 2019). For growth rate and C/N ratio, both the MHW and MHW+ALAN treatments were found as significantly different from control groups, presenting the lowest and highest's values, respectively. This might result from an energetic trade off, where energy normally directed to photosynthesis is in turn used in thermal protection mechanisms (Hurd et al. 2014, Britton et al. 2020). The increased light exposure of the Kelp showed general positive effects on growth and C/N, counteracting the effects caused by high temperature. By being exposed to extra available light, the organisms increased their photosynthetic metabolic rates, and hence, their carbohydrates production (carbon fixation). Resulting this way in higher growth and producing the increased amount of energy necessary to address the temperature stress and/or increase their thermal optimum (Koch et al. 2013).

Regarding the respiration rates, contrary to our hypothesis, no significant effects of either factor were observed, although these results should be carefully considered. While during the heatwave no visible differences were seen among the obtained values of respiration, the treatment groups presented a considerable variation among them during recovery. Lower respiration, that is less oxygen consumption values, were observed in the control groups and slightly higher in the MHW compared to the MHW+ALAN, though no significant different groups were found. It should be noted, however, that since net primary production (NPP) rates (i.e. oxygen production in the light) were not measured in this study due to experimental difficulties, the analysis of the complete oxygen dynamic cycle was not possible.

2.9.5 Conclusion

By exposing kelp organisms to ALAN, the additional source of light energy may contribute to their greater resilience to heatwave events by increasing their photosynthetic activity and carbon fixation, and thus producing the amount of energy needed to withstand the thermal pressure. Such discovery can be of great importance, in the context of Kelp ecosystems management and restoration programs, as well as for the Kelp farming industry. Even so, being, to date, the first study performed on the topic, for a full understanding of the effects of ALAN on kelp organisms more studies should be performed, testing its effects on other parameters and different simulations.

3. General summary

The work presented here provides diverse experimental evidence for the sensitivity and functioning of different benthic species and communities on Mediterranean and northeast Atlantic coasts. Here, we summarize the main, general, findings from this extensive and diverse work done in many regions with very different environmental settings.

The functioning of alternative states of Mediterranean shallow reef macroalgal communities

Healthy shallow-water reefs around the Mediterranean are considered highly productive and ecologically diverse, and the presence of marine forests of Fucales brown algae, mainly of the genius *Cystoseira* sensu lato, are considered as a clear sign of a healthy reef state (Sala et al. 2012, Bevilacqua et al. 2020, Bevilacqua et al. 2021). But, in many parts of the Mediterranean, shallow reefs are rapidly altering due to varied local and global stressors with both similar and different main drivers in the eastern and western basins, and Fucales forests in many places are becoming rare. Instead of typical canopy forests, other community dominates and many different ecological states are now present on the reefs, and it is assumed that their ecological contribution and functioning are inferior to that of the Fucales forests. This assumption, however, has rarely been tested. Here, using very similar methods (incubation domes) testing the habitat and metabolic functioning of macroalgal-dominated communities on Mediterranean shallow reefs we have shown the existence of different reef macrophyte functional states. Our results provide evidence that some of those alternate reef states may not be that functionally inferior to the pristine Fucales forests and thus provide some hope for relatively persistence ecosystem services into the future, even with the rise of novel ecosystems; however, where possible, restoration of *Cystoseira* forests should be attempted, as it evidently can work and restore functions as well where conditions allow – i.e., where it was present in the past and where local stressors are removed (Fig. 83):

1) On **southeastern shallow reefs** most of the reefs today are mainly characterized by low-laying, overgrazed (by the invasive rabbitfish), turf barrens that are biologically poor and with low productivity. Fucales forests on the other hand are rare (Sala et al. 2011, Rilov et al. 2018) and they also have a very short growth season (Mulas et al. 2022). But, our work showed that meadows of alien bushy or leafy macroalgae that are becoming widespread in the region, are just as biologically diverse, productive and are found year-round, and their thermal performance indicate that they can handle better resent and future coastal warming. This provides hope that some of the ecosystem functioning may be maintained in the system. Some indication of higher cover of macroalgal meadows inside a well-functioning MPA (Rilov et al. 2018) suggests that protection might aid in the maintenance of higher primary productivity of the reef thus sustaining a more intact food web.
2) On **Northern Tyrrhenian Sea reefs** that are coastal and urbanized, Fucales are also rare, and reefs are now dominated by bushy and “turf” algae (mainly *Janía*). But these alternate communities again were found to be as diverse and productive as healthy *Cystoseira* forests on more pristine reefs in Capraia Island, giving hope that, if restoration is not possible, those novel communities are good replacements, at least in terms of ecological functioning (habitat provisioning and carbon sinks).
3) On the **Balearic Islands reefs** where the *Cystoseira* forest have been destroyed in many areas, our work showed that long-term restoration efforts can indeed be successful. Ten years after a forest restoration was initiated, our work showed that the area is almost equally diverse and productive as a healthy forest, and is much more

functional than a nearby still-degraded reef. This suggests that if the driver of the forest destruction has been removed, there is a good chance for restoration, given that ocean warming will not affect the algae.

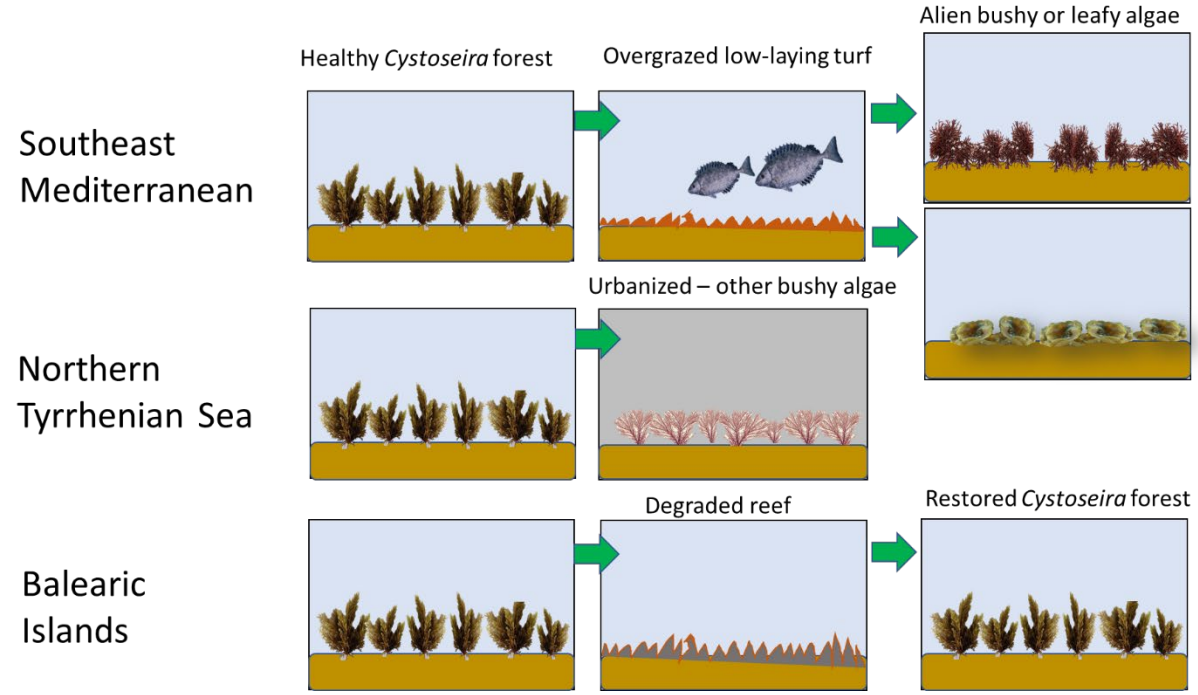

Figure 83 Different shifts in community state of macroalgal communities in shallow water reefs in the Mediterranean Sea in the different study regions.

Alternative states were also tested using incubations in healthy and degraded (epiphytised) kelp communities in Norway but results are not finalized.

Threats to Northeast Atlantic rockweed and kelp forests

The lab and outdoor mesocosm work from Portugal, Norway and the UK showed the potential for additive and antagonistic effects of different combinations of drivers to macroalgae forest functioning and community structure (Fig. 84).

In Portugal, the experiments have shown complicated interactions between warming and nutrient levels (both influenced by changes in upwelling regime expected due to climate change) on two species of kelp as well as turf. In particular, for *Laminaria ochroleuca*, the reduction of growth, productivity and photosynthetic functioning indicated a lower fitness when both stressors (high temperature/low nutrients – simulating a reduction in upwelling) were interacting. These results are consistent with previous studies, which have suggested a decrease in eco-physiological performance with decreasing nutrient concentration and increasing temperature in *Laminaria* species and other canopy forming seaweeds.

In Norway, similarly, there were both additive and contradicting impacts of darkening and nutrient additions at both the species and community levels. Specifically, the rockweed species *Fucus vesiculosus* and *F. serratus*, are both sensitive to coastal darkening and increased nutrient supply. Furthermore, the stressors reduce faunal abundance and species diversity of the community associated with *F. serratus*, through synergistic negative impact. The results indicate complex, not always non-intuitive ecosystem responses that cannot be understood without doing experimental studies in complex ecosystems, and made possible by the large scale mesocosm facilities used in this project. Preliminary results from the incubation study

indicate a negative impact of filamentous algae on the kelp community production rate. Hence, an increasing trend of coastal darkening and nutrient enrichment will further promote the presence of filamentous algae as demonstrated in the mesocosm experiments, and thereby contribute to regime shifts towards a dominance of filamentous algae or fouled rockweed and kelps.

In the UK experiments, we have shown complex interactions between the impacts of artificial light at night (ALAN) and the exposure to a marine heatwave, with some evidence that ALAN can counteract the negative impact of heatwaves on growth and metabolic functioning of the kelp.

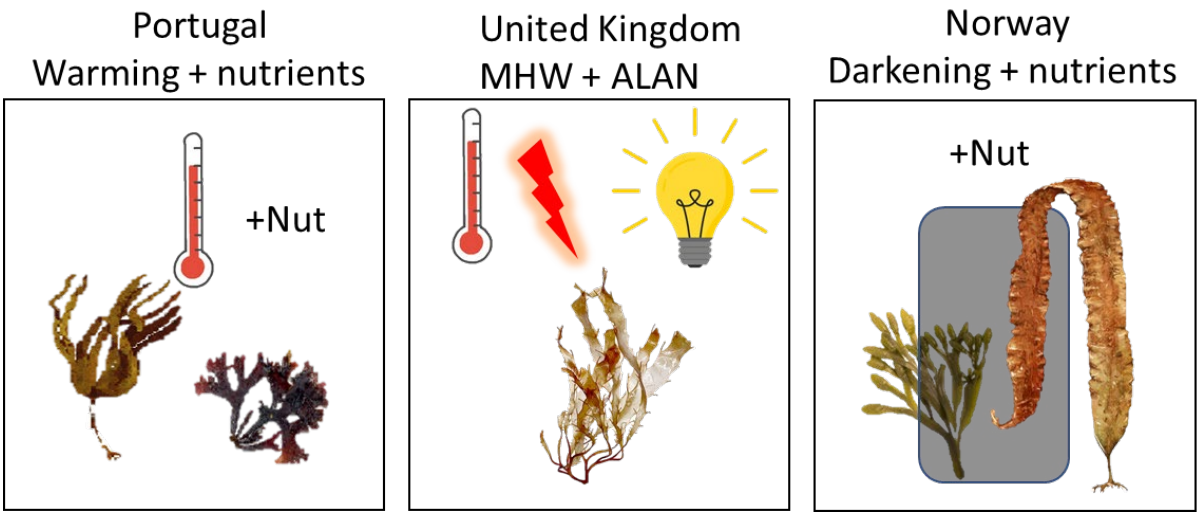

Figure 84 The different multiple stressor experiments tested on Kelp in different locations and scenarios.

In Italy, a lab experiment has also shown that seagrass has the capacity to mitigate the impacts of ocean acidification on sea urchin larvae demonstrating the interactive effect of biotic and abiotic factors, as was also shown with the ameliorating impact of epiphytes on calcareous algae exposed to ocean acidification (Guy-Haim et al. 2020). Specifically, *Posidonia oceanica*, by altering seawater chemistry through their photosynthetic activity, mitigated the negative impacts of ocean acidification on the larval development and total body length of the sea urchin, *Paracentrotus lividus,* thus providing future biotic OA refugia for the most sensitive stage in the life of the urchin.

Finally, **in the Netherlands**, pioneering work on intertidal oyster reef metabolic functioning testing if they are a sink or a source of carbon, have showed some interesting results but, as some data still needs to be further processed, the question cannot yet be answered if oyster reefs are a sink or source and will facilitate carbon sequestration. The percentage of organic matter increased with depth suggesting burial of organic matter, However, an effect of the reef was not observed as there was no clear change with distance from the reef. Fundamental understanding of the physiological constraints of climate-driven warming (TPCs) were developed for sensitive larval stages to better understand the effects of CC on the survival and recruitment mechanisms maintaining reefs in the wild.

In conclusion: Our field results provide, on the one hand, hope that, if local conditions are right, successful restoration of canopy-forming Fucales forests is possible and can provide functions similar to those of a healthy forest. On the other hand, the results from Italy and Israel indicate

that some alternative/altered (non-Fucales dominated) benthic communities can also provide similar functions as the original Fucales forests, but fully degraded turf-barren communities indeed offer very poor habitat for associated species and reduced metabolic functions. From managerial perspectives, altered but highly functional communities can be viewed as "alternative NBS" if restoration is not possible. Our lab experiments demonstrate the great value of multiple-stressor experiments because they show the complex interactions among tested local and global stressors, which are essential when developing predictive models (e.g. in WP4) required for projecting the impacts of CC on coastal habitat-forming species and for planning successful restoration (NBS1) and/or conservation (NBS2) interventions.

4. Indexes

Index of Figures

Index of Tables

5. References

Adamantopoulou, S., K. Anagnostopoulou, and et_al. 2000. Special Environmental Study of N. Karpathos – Saria.

Aksnesa, D. L., and M. D. Ohman. 2009. Multi-decadal shoaling of the euphotic zone in the southern sector of the California Current System. Limnology and Oceanography **54**:1272-1281.

Albano, P. G., J. Steger, M. Bošnjak, B. Dunne, Z. Guifarro, E. Turapova, Q. Hua, D. S. Kaufman, G. Rilov, and M. Zuschin. 2021. Native biodiversity collapse in the eastern Mediterranean. Proceedings of the Royal Society B **288**:20202469.

Allakhverdiev, S. I., V. D. Kreslavski, V. V. Klimov, D. A. Los, R. Carpentier, and P. Mohanty. 2008. Heat stress: an overview of molecular responses in photosynthesis. Photosynthesis Research **98**:541-550.

Alter, K., S.J. Andrewartha, T.D. Clark, N.G. Elliott. 2017. Thermal preference increases during larval development of pure and hybrid abalone. Journal of Shellfish Research **36**: 141-149.

Alter, K., C.J.M. Philippart, S. Teng, H. Boiler, P. Drenth, M. Dubbeldam. 2023. Consequences of thermal history for growth, development and survival during metamorphosis and settlement for the European flat oyster. Aquaculture **566**: 739174.

Amsalem, E., and G. Rilov. 2021. High thermal plasticity, and vulnerability, in extreme environments at the warm distributional edge: The case of a tidepool shrimp. Journal of Experimental Marine Biology and Ecology **545**:151641.

Apostolaki, E. T., S. Vizzini, V. Santinelli, H. Kaberi, C. Andolina, and E. Papathanassiou. 2019. Exotic Halophila stipulacea is an introduced carbon sink for the Eastern Mediterranean Sea. Scientific reports **9**.

Bakun, A. 1990. Global climate change and intensification of coastal ocean upwelling. Science **247**:198-201.

Ballesteros, E. 1990. Structure and dynamics of the community of *Cystoseira zosteroides* (Turner) C. Agardh (Fucales, Phaeophyceae) in the Northwestern Mediterranean. Scientia Marina **54**:217-299.

Barbier, E. B., S. D. Hacker, C. Kennedy, E. W. Koch, A. C. Stier, and B. R. Silliman. 2011. The value of estuarine and coastal ecosystem services. Ecological Monographs **81**:169-193.

Bartsch, I., C. Wiencke, K. Bischof, C. M. Buchholz, B. H. Buck, A. Eggert, P. Feuerpfeil, D. Hanelt, S. Jacobsen, R. Karez, U. Karsten, M. Molis, M. Y. Roleda, H. Schubert, R. Schumann, K. Valentin, F. Weinberger, and J. Wiese. 2008. The genus Laminaria sensu lato : recent insights and developments. European Journal of Phycology **43**:1-86.

Beardall, J., S. Stojkovic, and K. Gao. 2014. Interactive effects of nutrient supply and other environmental factors on the sensitivity of marine primary producers to ultraviolet radiation: implications for the impacts of global change. Aquatic Biology **22**:5-23.

Beaugrand, G., E. Goberville, C. Luczak, and R. R. Kirby. 2014. Marine biological shifts and climate. Proceedings of the Royal Society B: Biological Sciences **281**:20133350.

Beaumont, N. J., M. C. Austen, S. C. Mangi, and M. Townsend. 2008. Economic valuation for the conservation of marine biodiversity. Marine Pollution Bulletin **56**:386-396.

Beiras, R., A.P. Camacho, M. Albentosa. 1995. Short-term and long-term alterations in the energy budget of young oyster *Ostrea edulis* L. in response to temperature change. Journal of Experimental Marine Biology and Ecology **186**: 221–236.

Benazzouz, A., S. Mordane, A. Orbi, M. Chagdali, K. Hilmi, A. Atillah, J. Lluís Pelegrí, and D. Hervé. 2014. An improved coastal upwelling index from sea surface temperature using satellite-based approach – The case of the Canary Current upwelling system. Continental Shelf Research **81**:38-54.

Benedetti-Cecchi, L., F. Bulleri, and F. Cinelli. 1998. Density dependent foraging of sea urchins in shallow subtidal reefs on the west coast of Italy (western Mediterranean). Marine Ecology-Progress Series **163**:203-211.

Benedetti-Cecchi, L., F. Pannacciulli, F. Bulleri, P. S. Moschella, L. Airoldi, G. Relini, and F. Cinelli. 2001. Predicting the consequences of anthropogenic disturbance: large-scale effects of loss of canopy algae on rocky shores. Marine Ecology-Progress Series **214**:137-150.

Bertocci, I., R. Araújo, P. Oliveira, and I. Sousa-Pinto. 2015. Potential effects of kelp species on local fisheries. Journal of Applied Ecology **52**:1216-1226.

Bevilacqua, S., L. Airoldi, E. Ballesteros, L. Benedetti-Cecchi, F. Boero, F. Bulleri, E. Cebrian, C. Cerrano, J. Claudet, F. Colloca, M. Coppari, A. Di Franco, G. Guarnieri, C. Guerranti, P. Guidetti, B. S. Halpern, S. Katsanevakis, M. C. Mangano, F. Micheli, M. Milazzo, A. Pusceddu, M. Renzi, G. Rilov, G. Sarà, and A. Terlizzi. 2021. Mediterranean rocky reefs in the Anthropocene: Present status and future concerns. Advances in Marine Biology **89**:53-78.

Bevilacqua, S., S. Katsanevakis, F. Micheli, E. Sala, G. Rilov, G. Sarà, D. A. Malak, A. Abdulla, V. Gerovasileiou, and E. Gissi. 2020. The status of coastal benthic ecosystems in the Mediterranean Sea: evidence from ecological indicators. Frontiers in Marine Science **7**:475.

Biscéré, T., M. Zampighi, A. Lorrain, S. Jurriaans, A. Foggo, F. Houlbrèque, and R. Rodolfo-Metalpa. 2019. High p CO2 promotes coral primary production. Biology Letters **15**:20180777.

Biskup, S., I. Bertocci, F. Arenas, and F. Tuya. 2014. Functional responses of juvenile kelps, Laminaria ochroleuca and Saccorhiza polyschides, to increasing temperatures. Aquatic Botany **113**:117-122.

Bokn, T. L., C. M. Duarte, M. F. Pedersen, N. Marba, F. E. Moy, C. Barrón, B. Bjerkeng, J. Borum, H. Christie, and S. Engelbert. 2003. The response of experimental rocky shore communities to nutrient additions. Ecosystems **6**:577-594.

Boutahar, L., F. Espinosa, and H. Bazairi. 2022. Reconstruction of Cymodocea nodosa's dynamics as a tool to examine the conservation status of a Mediterranean declared marine protected area. Mediterranean marine science **23**:754-765.

Brito, M. C., D. Martin, and J. Núñez. 2005. Polychaetes associated to a Cymodocea nodosa meadow in the Canary Islands: assemblage structure, temporal variability and vertical distribution compared to other Mediterranean seagrass meadows. Marine Biology **146**:467-481.

Brix, H. 1997. Do macrophytes play a role in constructed treatment wetlands? Water Science and Technology **35**:11-17.

Bulleri, F., L. Benedetti-Cecchi, S. Acunto, F. Cinelli, and S. J. Hawkins. 2002. The influence of canopy algae on vertical patterns of distribution of low-shore assemblages on rocky coasts in the northwest Mediterranean. Journal of Experimental Marine Biology and Ecology **267**:89-106.

Bulleri, F., A. Cucco, M. Dal Bello, E. Maggi, C. Ravaglioli, and L. Benedetti-Cecchi. 2018a. The role of wave-exposure and human impacts in regulating the distribution of alternative habitats on NW Mediterranean rocky reefs. Estuarine, Coastal and Shelf Science **201**:114-122.

Bulleri, F., B. K. Eriksson, A. Queirós, L. Airoldi, F. Arenas, C. Arvanitidis, T. J. Bouma, T. P. Crowe, D. Davoult, and K. Guizien. 2018b. Harnessing positive species interactions as a tool against climate-driven loss of coastal biodiversity. PLoS Biology **16**:e2006852-e2006852.

Byrne, M., S. A. Foo, P. M. Ross, and H. M. Putnam. 2020. Limitations of cross-and multigenerational plasticity for marine invertebrates faced with global climate change. Global Change Biology **26**:80-102.

Byrne, M., and J. C. Hernández. 2020. Sea urchins in a high CO2 world: impacts of climate warming and ocean acidification across life history stages. Pages 281-297. Elsevier.

Byrne, M., M. Lamare, D. Winter, S. A. Dworjanyn, and S. Uthicke. 2013. The stunting effect of a high CO2 ocean on calcification and development in sea urchin larvae, a synthesis from the tropics to the poles. Philosophical Transactions of the Royal Society B: Biological Sciences **368**:20120439-20120439.

Camp, E. F., D. J. Smith, C. Evenhuis, I. Enochs, D. Manzello, S. Woodcock, and D. J. Suggett. 2016. Acclimatization to high-variance habitats does not enhance physiological tolerance of two key Caribbean corals to future temperature and pH. Proceedings of the Royal Society B: Biological Sciences **283**:20160442-20160442.

Casado-Amezúa, P., R. Araújo, I. Bárbara, R. Bermejo, Á. Borja, I. Díez, C. Fernández, J. M. Gorostiaga, X. Guinda, I. Hernández, J. A. Juanes, V. Peña, C. Peteiro, A. Puente, I. Quintana, F. Tuya, R. M.

Viejo, M. Altamirano, T. Gallardo, and B. Martínez. 2019. Distributional shifts of canopy-forming seaweeds from the Atlantic coast of Southern Europe. Biodiversity and Conservation **28**:1151-1172.

Chan, D., E. C. Kent, D. I. Berry, and P. Huybers. 2019. Correcting datasets leads to more homogeneous early-twentieth-century sea surface warming. Nature **571**:393-397.

Chatzigeorgiou, G., T. Dailianis, S. Faulwetter, M. Pettas, and C. Arvanitidis. 2013. MANOSS-a manually operated suction sampler for hard bottom benthos. Transitional Waters Bulletin **6**:42-49.

Chefaoui, R. M., C. M. Duarte, and E. A. Serrão. 2018. Dramatic loss of seagrass habitat under projected climate change in the Mediterranean Sea. Global Change Biology **24**:4919-4928.

Cheminée, A., E. Sala, J. Pastor, P. Bodilis, P. Thiriet, L. Mangialajo, J.-M. Cottalorda, and P. Francour. 2013. Nursery value of Cystoseira forests for Mediterranean rocky reef fishes. Journal of Experimental Marine Biology and Ecology **442**:70-79.

Christie, H., G. S. Andersen, T. Bekkby, C. W. Fagerli, J. K. Gitmark, H. Gundersen, and E. Rinde. 2019. Shifts between sugar kelp and turf algae in Norway: regime shifts or fluctuations between different opportunistic seaweed species? Frontiers in Marine Science **6**:72.

Christie, H., P. Kraufvelin, L. Kraufvelin, N. Niemi, and E. Rinde. 2020. Disappearing blue mussels–can mesopredators be blamed? Frontiers in Marine Science **7**:550.

Clark, H. R., and C. J. Gobler. 2016. Diurnal fluctuations in CO2 and dissolved oxygen concentrations do not provide a refuge from hypoxia and acidification for early-life-stage bivalves. Marine Ecology Progress Series **558**:1-14.

Cloern, J. E., and A. D. Jassby. 2012. Drivers of change in estuarine-coastal ecosystems: Discoveries from four decades of study in San Francisco Bay. Reviews of Geophysics **50**.

Coleman, M. A., and T. Wernberg. 2017. Forgotten underwater forests: The key role of fucoids on Australian temperate reefs. Ecology and evolution **7**:8406-8418.

Colvard, N., and B. Helmuth. 2017. Nutrients influence the thermal ecophysiology of an intertidal macroalga: multiple stressors or multiple drivers? Ecological Applications **27**:669-681.

Connell, S., M. Foster, and L. Airoldi. 2014. What are algal turfs? Towards a better description of turfs. Marine Ecology Progress Series **495**:299-307.

Connell, S. D., Z. A. Doubleday, S. B. Hamlyn, N. R. Foster, C. D. Harley, B. Helmuth, B. P. Kelaher, I. Nagelkerken, G. Sarà, and B. D. Russell. 2017. How ocean acidification can benefit calcifiers. Current Biology **27**:R95-R96.

Connell, S. D., and B. D. Russell. 2010. The direct effects of increasing CO2 and temperature on non-calcifying organisms: increasing the potential for phase shifts in kelp forests. Proceedings of the Royal Society B: Biological Sciences **277**:1409-1415.

Cornwall, C. E., C. D. Hepburn, C. M. McGraw, K. I. Currie, C. A. Pilditch, K. A. Hunter, P. W. Boyd, and C. L. Hurd. 2013. Diurnal fluctuations in seawater pH influence the response of a calcifying macroalga to ocean acidification. Proceedings of the Royal Society B: Biological Sciences **280**:20132201-20132201.

Corsini-Foka, M., A. Zenetos, F. Crocetta, M. E. Çinar, F. Koçak, D. Golani, S. Katsanevakis, K. Tsiamis, E. Cook, C. Froglia, M. Triandaphyllou, S. Lakkis, G. Kondylatos, E. Tricarico, A. Zuljevic, M. Almeida, F. Cardigos, S. Çağlar, F. Durucan, A. M. D. Fernandes, J. Ferrario, I. Haberle, P. Louizidou, J. Makris, M. Marić, D. Micu, C. Mifsud, C. Nall, E. Kytinou, D. Poursanidis, D. Spigoli, G. Stasolla, S. Yapici, and H. E. Roy. 2015. Inventory of alien and cryptogenic species of the dodecanese (Aegean sea, Greece): Collaboration through COST action training school. Management of Biological Invasions **6**:351-366.

Costanza, R., R. d'Arge, R. De Groot, S. Farber, M. Grasso, B. Hannon, K. Limburg, S. Naeem, R. V. O'neill, and J. Paruelo. 1997. The value of the world's ecosystem services and natural capital. Nature **387**:253-260.

Davies, T. W., S. R. Jenkins, R. Kingham, J. Kenworthy, S. J. Hawkins, and J. G. Hiddink. 2011. Dominance, biomass and extinction resistance determine the consequences of biodiversity loss for multiple coastal ecosystem processes. PLoS One **6**:e28362.

Davison, I. R. 1991. Environmental effects on algal photosynthesis: Temperature. Journal of Phycology **27**:2-8.

Dayton, P. K. 1975. Experimental studies of algal canopy interactions in a sea otter dominated kelp community at Amchitka-Island, Alaska. Fishery Bulletin **73**:230-237.

Dickson, A. G., C. L. Sabine, and J. R. Christian. 2007. Guide to best practices for ocean CO2 measurements. North Pacific Marine Science Organization.

Diedrich, S., G. Nehls, J.E.E. van Beusekom, K. Reise. 2005. Introduced Pacific oyster (Crassostrea gigas) in the northern Wadden Sea: invasion accelerated by warm summers? Helgoland Marine Research **95**, 97-106.

Díez, I., N. Muguerza, A. Santolaria, U. Ganzedo, and J. M. Gorostiaga. 2012. Seaweed assemblage changes in the eastern Cantabrian Sea and their potential relationship to climate change. Estuarine, Coastal and Shelf Science **99**:108-120.

Doney, S. C., V. J. Fabry, R. A. Feely, and J. A. Kleypas. 2009. Ocean Acidification: The Other CO2 Problem. Annual Review of Marine Science **1**:169-192.

Duarte, B., I. Martins, R. Rosa, A. R. Matos, M. Y. Roleda, T. B. Reusch, A. H. Engelen, E. A. Serrão, G. A. Pearson, and J. C. Marques. 2018. Climate change impacts on seagrass meadows and macroalgal forests: an integrative perspective on acclimation and adaptation potential. Frontiers in Marine Science **5**:190.

Duarte, C. M., J.-P. Gattuso, K. Hancke, H. Gundersen, K. Filbee-Dexter, M. F. Pedersen, J. J. Middelburg, Michael T. Burrows, K. A. Krumhansl, T. Wernberg, P. Moore, A. Pessarrodona, S. B. Ørberg, I. S. Pinto, J. Assis, Ana M. Queirós, D. A. Smale, T. Bekkby, Ester A. Serrão, and D. Krause-Jensen. 2022. Global estimates of the extent and production of macroalgal forests. Global Ecology and Biogeography **31**:1422-1439.

Duarte, L., R. M. Viejo, B. Martínez, M. deCastro, M. Gómez-Gesteira, and T. Gallardo. 2013. Recent and historical range shifts of two canopy-forming seaweeds in North Spain and the link with trends in sea surface temperature. Acta Oecologica **51**:1-10.

Dupont, N., and D. L. Aksnes. 2013. Centennial changes in water clarity of the Baltic Sea and the North Sea. Estuarine, Coastal and Shelf Science **131**:282-289.

Dworjanyn, S. A., and M. Byrne. 2018. Impacts of ocean acidification on sea urchin growth across the juvenile to mature adult life-stage transition is mitigated by warming. Proceedings of the Royal Society B: Biological Sciences **285**:20172684-20172684.

Edelist, D., G. Rilov, D. Golani, J. Carlton, and E. Spanier. 2013. Restructuring the Sea: profound shifts in the world's most invaded marine ecosystem. Diversity and Distributions **19**:69-77.

Edwards, M., and A. J. Richardson. 2004. Impact of climate change on marine pelagic phenology and trophic mismatch. Nature **430**:881-884.

Eger, A. M., E. M. Marzinelli, R. Beas-Luna, C. O. Blain, L. K. Blamey, J. E. K. Byrnes, P. E. Carnell, C. G. Choi, M. Hessing-Lewis, K. Y. Kim, N. H. Kumagai, J. Lorda, P. Moore, Y. Nakamura, A. Pérez-Matus, O. Pontier, D. Smale, P. D. Steinberg, and A. Vergés. 2023. The value of ecosystem services in global marine kelp forests. Nature communications **14**:1894.

Elsherbini, J., C. Corzett, C. Ravaglioli, L. Tamburello, M. Polz, and F. Bulleri. 2023. Epilithic Bacterial Assemblages on Subtidal Rocky Reefs: Variation Among Alternative Habitats at Ambient and Enhanced Nutrient Levels. Microbial Ecology:1-13.

Ershov, D., M.S. Phan, J.M. Pylvänäinen, S.U. Rigaud, L. Le blanc, A. Charles-Orszag, J.R.W. Conway, R.F. Laine, N.H. Roy, D. Donazzi, G. Duménil, G. Jacquemet, J.Y. Tinevez. 2021. Bringing TrackMate in the era of machine-learning and deep-learning. bioRxiv.

Eymann, C., S. Götze, C. Bock, H, Guderley, A.H. Knoll, G. Lannig, I.M. Sokolova, M. Aberhan, H.O. Pörtner. 2020. Thermal performance of the European flat oyster, *Ostrea edulis* (Linnaeus, 1758) – explaining ecological findings under climate change. Marine Biology **167**: 17.

Falace, A., and G. Bressan. 2006. Seasonal variations of Cystoseira barbata (Stackhouse) C. Agardh frond architecture. Hydrobiologia **555**:193-206.

Falace, A., S. Kaleb, G. De La Fuente, V. Asnaghi, and M. Chiantore. 2018. Ex situ cultivation protocol for Cystoseira amentacea var. stricta (Fucales, Phaeophyceae) from a restoration perspective. PLoS One **13**:e0193011-e0193011.

Falkenberg, L. J., E. Scanes, J. Ducker, and P. M. Ross. 2021. Biotic habitats as refugia under ocean acidification. Conservation Physiology **9**:coab077-coab077.

Fernández, C. 2016. Current status and multidecadal biogeographical changes in rocky intertidal algal assemblages: The northern Spanish coast. Estuarine, Coastal and Shelf Science **171**:35-40.

Figueroa, F. L., and N. Korbee. 2010. Interactive Effects of UV Radiation and Nutrients on Ecophysiology: Vulnerability and Adaptation to Climate Change. Pages 157-183 *in* E. R. Israel A, Sckbach J (eds), editor. Seaweeds and their role in globally changing environments. Springer.

Filbee-Dexter, K., and T. Wernberg. 2018. Rise of turfs: A new battlefront for globally declining kelp forests. Bioscience **68**:64-76.

Filbee-Dexter, K., and T. Wernberg. 2020. Substantial blue carbon in overlooked Australian kelp forests. Scientific reports **10**:1-6.

Flukes, E. B., C. R. Johnson, and J. T. Wright. 2014. Thinning of kelp canopy modifies understory assemblages: the importance of canopy density. Marine Ecology Progress Series **514**:57-70.

Franco, J. N., F. Tuya, I. Bertocci, L. Rodríguez, B. Martínez, I. Sousa-Pinto, and F. Arenas. 2018. The 'golden kelp' Laminaria ochroleuca under global change: Integrating multiple eco-physiological responses with species distribution models. Journal of Ecology **106**:47-58.

Frieder, C. A., J. P. Gonzalez, E. E. Bockmon, M. O. Navarro, and L. A. Levin. 2014. Can variable pH and low oxygen moderate ocean acidification outcomes for mussel larvae? Global Change Biology **20**:754-764.

Frigstad, H., G. S. Andersen, H. C. Trannum, M. McGovern, L.-J. Naustvoll, Ø. Kaste, A. Deininger, and D. Ø. Hjermann. 2023. Three decades of change in the Skagerrak coastal ecosystem, shaped by eutrophication and coastal darkening. Estuarine, Coastal and Shelf Science:108193.

Gagic, V., I. Bartomeus, T. Jonsson, A. Taylor, C. Winqvist, C. Fischer, E. M. Slade, I. Steffan-Dewenter, M. Emmerson, S. G. Potts, T. Tscharntke, W. Weisser, and R. Bommarco. 2015. Functional identity and diversity of animals predict ecosystem functioning better than species-based indices. Proceedings of the Royal Society B: Biological Sciences **282**:20142620.

Gagnon, K., H. Christie, K. Didderen, C. W. Fagerli, L. L. Govers, M. L. E. Gräfnings, J. H. T. Heusinkveld, K. Kaljurand, W. Lengkeek, and G. Martin. 2021. Incorporating facilitative interactions into small-scale eelgrass restoration—challenges and opportunities. Restoration Ecology **29**:e13398.

Galobart, C., E. Ballesteros, R. Golo, and E. Cebrian. 2023. Addressing marine restoration success: evidence of species and functional diversity recovery in a ten-year restored macroalgal forest. Frontiers in Marine Science **10**.

Gao, K., and K. R. McKinley. 1994. Use of macroalgae for marine biomass production and CO2 remediation: a review. Journal of Applied Phycology **6**:45-60.

Gao, X., H. Endo, K. Taniguchi, and Y. Agatsuma. 2013. Combined effects of seawater temperature and nutrient condition on growth and survival of juvenile sporophytes of the kelp Undaria pinnatifida (Laminariales; Phaeophyta) cultivated in northern Honshu, Japan. Journal of Applied Phycology **25**:269-275.

García-Reyes, M., W. J. Sydeman, D. S. Schoeman, R. R. Rykaczewski, B. A. Black, A. J. Smit, and S. J. Bograd. 2015. Under Pressure: Climate Change, Upwelling, and Eastern Boundary Upwelling Ecosystems. Frontiers in Marine Science **2**.

Garnier, E., J. Cortez, G. Billès, M.-L. Navas, C. Roumet, M. Debussche, G. Laurent, A. Blanchard, D. Aubry, A. Bellmann, C. Neill, and J.-P. Toussaint. 2004. Plant functional markers capture ecosystem properties during secondary succession. Ecology **85**:2630-2637.

Garval, T. 2015. Population dynamics and ecological impacts of the alien macroalgae Galaxaura rugosa (J. Ellis & Solander) J.V. Lamouroux on the Israeli shore. University of Haifa, Haifa, Israel.

Gattuso, J. P., and e. al. 2023. The carb function of the R package seacarb v3.3.2.

Gazeau, F., L. Urbini, T. Cox, S. Alliouane, and J.-P. Gattuso. 2015. Comparison of the alkalinity and calcium anomaly techniques to estimate rates of net calcification. Marine Ecology Progress Series **527**:1-12.

Gerard, V. A. 1997. The Role of Nitrogen Nutrition in High-Temperature Tolerance of the Kelp, Laminaria Saccharina (Chromophyta) 1. Journal of Phycology **33**:800-810.

Gilman, S. E., M. C. Urban, J. Tewksbury, G. W. Gilchrist, and R. D. Holt. 2010. A framework for community interactions under climate change. Trends in Ecology & Evolution **25**:325-331.

Gonzalez, A., R. M. Germain, D. S. Srivastava, E. Filotas, L. E. Dee, D. Gravel, P. L. Thompson, F. Isbell, S. Wang, and S. Kéfi. 2020. Scaling-up biodiversity-ecosystem functioning research. Ecology Letters **23**:757-776.

Gorman, D., B. D. Russell, and S. D. Connell. 2009. Land-to-sea connectivity: linking human-derived terrestrial subsidies to subtidal habitat change on open rocky coasts. Ecological Applications **19**:1114-1126.

Gravel, D., F. Guichard, M. Loreau, and N. Mouquet. 2010. Source and sink dynamics in meta-ecosystems. Ecology **91**:2172-2184.

Guy-Haim, T., J. Silverman, M. Wahl, J. Aguirre, F. Noisette, and G. Rilov. 2020. Epiphytes provide micro-scale refuge from ocean acidification. Marine Environmental Research:105093.

Guy-Haim, T., J. Silverman, S. Raddatz, M. Wahl, A. Israel, and G. Rilov. 2016. The carbon turnover response to thermal stress of a dominant coralline alga on the fast warming Levant coast. Limnology and Oceanography **61**:1120-1133.

Hall-Spencer, J. M., R. Rodolfo-Metalpa, S. Martin, E. Ransome, M. Fine, S. M. Turner, S. J. Rowley, D. Tedesco, and M.-C. Buia. 2008. Volcanic carbon dioxide vents show ecosystem effects of ocean acidification. Nature **454**:96-99.

Harley, C. D. G., K. M. Anderson, K. W. Demes, J. P. Jorve, R. L. Kordas, T. A. Coyle, and M. H. Graham. 2012. Effects of Climate Change on Global Seaweed Communities. Journal of Phycology **48**:1064-1078.

Heller, N. E., and E. S. Zavaleta. 2009. Biodiversity management in the face of climate change: a review of 22 years of recommendations. Biological Conservation **142**:14-32.

Helm, M.M., N. Bourne, A. Lovatelli. 2004. Hatchery culture of bivalves: a practical manual. In: FAO Fisheries Technical Paper 471: 1–203. Food and Agriculture Organization of the United Nations, Rome, Italy

Hendriks, I. E., Y. S. Olsen, L. Ramajo, L. Basso, A. Steckbauer, T. S. Moore, J. Howard, and C. M. Duarte. 2014. Photosynthetic activity buffers ocean acidification in seagrass meadows. Biogeosciences **11**:333-346.

Hernes, P. J., and R. Benner. 2002. Transport and diagenesis of dissolved and particulate terrigenous organic matter in the North Pacific Ocean. Deep Sea Research Part I: Oceanographic Research Papers **49**:2119-2132.

Ho, M., J. McBroom, E. Bergstrom, and G. Diaz-Pulido. 2021. Physiological responses to temperature and ocean acidification in tropical fleshy macroalgae with varying affinities for inorganic carbon. ICES Journal of Marine Science **78**:89-100.

Hoffman, R., A. Israel, Y. Lipkin, Z. Dubinsky, and D. Iluz. 2008. First record of two seaweeds from the Israeli Mediterranean: Galaxaura rugosa (J. Ellis and Solander) JV Lamouroux (Rhodophyta) and Codium adhaerens C. Agardh (Chlorophyta). Israel Journal of Plant Sciences **56**:123-126.

Holm-Hansen, O., C. J. Lorenzen, R. W. Holmes, and J. D. Strickland. 1965. Fluorometric determination of chlorophyll. Journal du Conseil **30**:3-15.

Hooper, D. U., F. S. Chapin, J. J. Ewel, A. Hector, P. Inchausti, S. Lavorel, J. H. Lawton, D. M. Lodge, M. Loreau, S. Naeem, B. Schmid, H. Setala, A. J. Symstad, J. Vandermeer, and D. A. Wardle. 2005. Effects of biodiversity on ecosystem functioning: A consensus of current knowledge. Ecological Monographs **75**:3-35.

Huang, B., P. W. Thorne, V. F. Banzon , T. Boyer, G. Chepurin, J. H. Lawrimore, M. J. Menne, T. M. Smith, R. S. Vose, and H.-M. Zhang. 2017. NOAA Extended Reconstructed Sea Surface Temperature (ERSST), Version 5. *.in* N. N. C. f. E. Information, editor.

Human, L. R., G. C. Snow, J. B. Adams, G. C. Bate, and S.-C. Yang. 2015. The role of submerged macrophytes and macroalgae in nutrient cycling: A budget approach. Estuarine, Coastal and Shelf Science **154**:169-178.

Illa-López, L., À. Aubach-Masip, T. Alcoverro, G. Ceccherelli, L. Piazzi, P. Kleitou, J. Santamaría, J. Verdura, N. Sanmartí, and E. Mayol. 2023a. Nutrient conditions determine the strength of herbivore-mediated stabilizing feedbacks in barrens. Ecology and evolution **13**:e9929-e9929.

Illa-López, L., À. Aubach-Masip, T. Alcoverro, G. Ceccherelli, L. Piazzi, P. Kleitou, J. Santamaría, J. Verdura, N. Sanmartí, E. Mayol, X. Buñuel, M. Minguito-Frutos, F. Bulleri, and J. Boada. 2023b.

Nutrient conditions determine the strength of herbivore-mediated stabilizing feedbacks in barrens. Ecology and evolution **13**:e9929.

IPCC. 2019. Summary for Policymakers. In: IPCC Special Report on the Ocean and Cryosphere in a Changing Climate.

Israel, A., and R. Einav. 2017. Alien seaweeds from the Levant basin (Eastern Mediterranean Sea), with emphasis to the Israeli shores. Israel Journal of Plant Sciences **64**:99-110.

Izquierdo, J., I. M. Pérez-Ruzafa, and T. Gallardo. 2002. Effect of temperature and photon fluence rate on gametophytes and young sporophytes of Laminaria ochroleuca Pylaie. Helgoland marine research **55**:285-292.

Jacobs, P., Y. Greeve, M. Sikkema, M. Dubbeldam, C.J.M. Philippart. 2020. Successful rearing of *Ostrea edulis* from parents originating from the Wadden Sea, the Netherlands. Aquaculture Reports **18**: 100537.

Jones, H. P., and O. J. Schmitz. 2009. Rapid recovery of damaged ecosystems. PLoS One **4**:e5653.

Kapsenberg, L., and T. Cyronak. 2019. Ocean acidification refugia in variable environments. Global Change Biology **25**:3201-3214.

Kapsenberg, L., A. Miglioli, M. C. Bitter, E. Tambutté, R. Dumollard, and J. P. Gattuso. 2018. Ocean pH fluctuations affect mussel larvae at key developmental transitions. Proceedings of the Royal Society B **285**:20182381-20182381.

Karelitz, S., M. Lamare, F. Patel, N. Gemmell, and S. Uthicke. 2020. Parental acclimation to future ocean conditions increases development rates but decreases survival in sea urchin larvae. Marine Biology **167**:1-16.

Koch, M., G. Bowes, C. Ross, and X.-H. Zhang. 2013. Climate change and ocean acidification effects on seagrasses and marine macroalgae. Global Change Biology **19**:103-132.

Kolker, D., R. Bookman, B. Herut, N. David, and J. Silverman. 2021. An initial assessment of the contribution of fresh submarine ground water discharge to the alkalinity budget of the Mediterranean Sea. Journal of Geophysical Research: Oceans **126**:e2020JC017085.

Korringa, P. 1946. The decline of natural oyster beds. Basteria **10**: 36–41

Kraufvelin, P., H. Christie, and J. K. Gitmark. 2020. Top-down release of mesopredatory fish is a weaker structuring driver of temperate rocky shore communities than bottom-up nutrient enrichment. Marine Biology **167**:1-20.

Kraufvelin, P., F. E. Moy, H. Christie, and T. L. Bokn. 2006a. Nutrient addition to experimental rocky shore communities revisited: delayed responses, rapid recovery. Ecosystems **9**:1076-1093.

Kraufvelin, P., S. Salovius, H. Christie, F. E. Moy, R. Karez, and M. F. Pedersen. 2006b. Eutrophication-induced changes in benthic algae affect the behaviour and fitness of the marine amphipod Gammarus locusta. Aquatic Botany **84**:199-209.

Krause-Jensen, D., and C. M. Duarte. 2016. Substantial role of macroalgae in marine carbon sequestration. Nature Geoscience **9**:737.

Krause-Jensen, D., N. Marbà, M. Sanz-Martin, I. E. Hendriks, J. Thyrring, J. Carstensen, M. K. Sejr, and C. M. Duarte. 2016. Long photoperiods sustain high pH in Arctic kelp forests. Science Advances **2**:e1501938-e1501938.

Kroeker, K. J., R. L. Kordas, R. Crim, I. E. Hendriks, L. Ramajo, G. S. Singh, C. M. Duarte, and J.-P. Gattuso. 2013. Impacts of ocean acidification on marine organisms: quantifying sensitivities and interaction with warming. Global Change Biology **19**:1884-1896.

Kroeker, K. J., R. L. Kordas, R. N. Crim, and G. G. Singh. 2010. Meta-analysis reveals negative yet variable effects of ocean acidification on marine organisms. Ecology Letters **13**:1419-1434.

Kroeker, K. J., R. L. Kordas, and C. D. G. Harley. 2017. Embracing interactions in ocean acidification research: confronting multiple stressor scenarios and context dependence. Biology Letters **13**:20160802-20160802.

Kroeker, K. J., F. Micheli, M. C. Gambi, and T. R. Martz. 2011. Divergent ecosystem responses within a benthic marine community to ocean acidification. Proceedings of the National Academy of Sciences **108**:14515-14520.

Krom, M., N. Kress, S. Brenner, and L. Gordon. 1991. Phosphorus limitation of primary productivity in the eastern Mediterranean Sea. Limnology and Oceanography **36**:424-432.

Krumhansl, K. A., D. K. Okamoto, A. Rassweiler, M. Novak, J. J. Bolton, K. C. Cavanaugh, S. D. Connell, C. R. Johnson, B. Konar, and S. D. Ling. 2016. Global patterns of kelp forest change over the past half-century. Proceedings of the National Academy of Sciences **113**:13785-13790.

Kübler, J. E., and I. R. Davison. 1995. Thermal acclimation of light-use characteristics of Chondrus crispus (Rhodophyta). European Journal of Phycology **30**:189-195.

Lamare, M. D., M. Liddy, and S. Uthicke. 2016. In situ developmental responses of tropical sea urchin larvae to ocean acidification conditions at naturally elevated p CO2 vent sites. Proceedings of the Royal Society B: Biological Sciences **283**:20161506-20161506.

Larkum, A. W. D., S. E. Douglas, and J. E. Raven. 2003. Photosynthesis in Algae. Springer Dordrecht.

Leray, M., J. Y. Yang, C. P. Meyer, S. C. Mills, N. Agudelo, V. Ranwez, J. T. Boehm, and R. J. Machida. 2013. A new versatile primer set targeting a short fragment of the mitochondrial COI region for metabarcoding metazoan diversity: application for characterizing coral reef fish gut contents. Frontiers in zoology **10**:1-14.

Lima, F. P., P. A. Ribeiro, N. Queiroz, S. J. Hawkins, and A. M. Santos. 2007. Do distributional shifts of northern and southern species of algae match the warming pattern? Global Change Biology **13**:2592-2604.

Littler, M. M. 1980. Morphological form and photosynthetic performances of marine macroalgae: tests of a functional/form hypothesis. Botanica Marina **61**:521-535.

Loreau, M., N. Mouquet, and R. D. Holt. 2003. Meta-ecosystems: a theoretical framework for a spatial ecosystem ecology. Ecology Letters **6**:673-679.

Loreau, M., S. Naeem, P. Inchausti, J. Bengtsson, J. P. Grime, A. Hector, D. U. Hooper, M. A. Huston, D. Raffaelli, B. Schmid, D. Tilman, and D. A. Wardle. 2001. Biodiversity and ecosystem functioning: Current knowledge and future challenges. Science **294**:804-808.

Lowe, S., M. Browne, S. Boudjelas, and M. De Poorter. 2000. 100 of the World's Worst Invasive Alien Species A selection from the Global Invasive Species Database. The Invasive Species Specialist Group (ISSG).

Lueker, T. J., A. G. Dickson, and C. D. Keeling. 2000. Ocean pCO2 calculated from dissolved inorganic carbon, alkalinity, and equations for K1 and K2: validation based on laboratory measurements of CO2 in gas and seawater at equilibrium. Marine Chemistry **70**:105-119.

Mackas, D. L., P. Strub, A. Thomas, and V. Montecino. 2006. Eastern ocean boundaries pan-regional overview. The Sea:21-59.

Macreadie, P. I., M. D. Costa, T. B. Atwood, D. A. Friess, J. J. Kelleway, H. Kennedy, C. E. Lovelock, O. Serrano, and C. M. Duarte. 2021. Blue carbon as a natural climate solution. Nature Reviews Earth & Environment **2**:826-839.

Mann, K. H. 1973. Seaweeds: Their Productivity and Strategy for Growth. Science **182**:975-981.

Marsh Jr, J. A. 1970. Primary productivity of reef-building calcareous red algae. Ecology **51**:255-263.

Marx, L., S. Flecha, M. Wesselmann, C. Morell, and I. E. Hendriks. 2021. Marine Macrophytes as Carbon Sinks: Comparison Between Seagrasses and the Non-native Alga Halimeda incrassata in the Western Mediterranean (Mallorca). Frontiers in Marine Science **8**.

Maxwell, K., and G. N. Johnson. 2000. Chlorophyll fluorescence—a practical guide. Journal of Experimental Botany **51**:659-668.

McMahon, K., E. A. Sinclair, C. D. H. Sherman, K.-J. van Dijk, U. E. Hernawan, J. Verduin, and M. Waycott. 2018. Genetic Connectivity in Tropical and Temperate Australian Seagrass Species. Pages 155-194 *in* A. W. D. Larkum, G. A. Kendrick, and P. J. Ralph, editors. Seagrasses of Australia: Structure, Ecology and Conservation. Springer International Publishing, Cham.

Meijering, E., O. Dzyubachyk, I. Smal. 2012. Chapter nine – Methods for cell and particle tracking. Methods in Enzymology **504**: 183–200.

Mooney, H., A. Larigauderie, M. Cesario, T. Elmquist, O. Hoegh-Guldberg, S. Lavorel, G. M. Mace, M. Palmer, R. Scholes, and T. Yahara. 2009. Biodiversity, climate change, and ecosystem services. Current opinion in environmental sustainability **1**:46-54.

Mouillot, D., S. Villéger, M. Scherer-Lorenzen, and N. W. Mason. 2011. Functional structure of biological communities predicts ecosystem multifunctionality. PLoS One **6**:e17476.

Mulas, M., J. Neiva, S. S. Sadogurska, E. Ballesteros, E. A. Serrão, G. Rilov, and Á. Israel. 2020. Genetic affinities and biogeography of putative Levantine-endemic seaweed Treptacantha rayssiae (Ramon) M. Mulas, J. Neiva & Á. Israel, comb. nov.(Phaeophyceae). Cryptogamie, Algologie **41**:91-103.

Mulas, M., J. Silverman, T. Guy-Haim, S. Noé, and G. Rilov. 2022. High climate vulnerably of the Levantine endemic and endangered habitat-forming macroalga, Gongolaria rayssiae: implications for reef carbon budget. Frontiers in Marine Science:1447.

Naeem, S. 2012. Ecological consequences of declining biodiversity: a biodiversity-ecosystem function (BEF) framework for marine systems. Pages 34-51 *in* M. Solan, R. Aspden, and D. Paterson, editors. Marine Biodiversity and Ecosystem Functioning. Oxford University Press, Oxford, UK.

Naeem, S., D. E. Bunker, A. Hector, M. Loreau, and C. Perrings. 2009. Biodiversity, ecosystem functioning, and human wellbeing: An ecological and economic perspective. Oxford University Press.

Ngan, Y., and I. R. Price. 1980. Seasonal growth and reproduction of intertidal algae in the Townsville region (Queensland, Australia). Aquatic Botany **9**:117-134.

Nixon, S. W. 1988. Physical energy inputs and the comparative ecology of lake and marine ecosystems. Limnology and Oceanography **33**:1005-1025.

Odum, W. E., and E. J. Heald. 1975. The detritus-based food web of an. Estuar. Res. Chem. Biol. Estuar. Syst **1**:265.

Oksanen, J., F. G. Blanchet, M. Friendly, R. Kindt, P. Legendre, D. McGlinn, P. R. Minchin, R. B. O'Hara, G. L. Simpson, and P. Solymos. 2022. vegan: Community Ecology Package. R package version 2.5-7. 2020.

Olabarria, C., F. Arenas, R. M. Viejo, I. Gestoso, F. Vaz-Pinto, M. Incera, M. Rubal, E. Cacabelos, P. Veiga, and C. Sobrino. 2013. Response of macroalgal assemblages from rockpools to climate change: effects of persistent increase in temperature and CO2. Oikos **122**:1065-1079.

Opsahl, S., and R. Benner. 1997. Distribution and cycling of terrigenous dissolved organic matter in the ocean. Nature **386**:480-482.

Ozer, T., I. Gertman, H. Gildor, and B. Herut. 2022. Thermohaline Temporal Variability of the SE Mediterranean Coastal Waters (Israel)–Long-Term Trends, Seasonality, and Connectivity. Frontiers in Marine Science **8**:799457.

Ozer, T., I. Gertman, N. Kress, J. Silverman, and B. Herut. 2016. Interannual thermohaline (1979–2014) and nutrient (2002–2014) dynamics in the Levantine surface and intermediate water masses, SE Mediterranean Sea. Global and Planetary Change **151**:60-67.

Pacella, S. R., C. A. Brown, G. G. Waldbusser, R. G. Labiosa, and B. Hales. 2018. Seagrass habitat metabolism increases short-term extremes and long-term offset of CO2 under future ocean acidification. Proceedings of the National Academy of Sciences **115**:3870-3875.

Padfield, D., H. O'Sullivan, and S. Pawar. 2021. rTPC and nls. multstart: a new pipeline to fit thermal performance curves in R. Methods in Ecology and Evolution **12**:1138-1143.

Parmesan, C. 2006. Ecological and evolutionary responses to recent climate change. Annual Review of Ecology Evolution and Systematics **37**:637-669.

Pechenik, J.A. 2006. Larval experience and latent effects—metamorphosis is not a new beginning. Integrative Comparative Biology **46**: 323–333.

Peleg, O., T. Guy-Haim, E. Yeruham, J. Silverman, and G. Rilov. 2020. Tropicalisation may invert trophic state and carbon budget of shallow temperate rocky reefs. Journal of Ecology **108**:884-854.

Pereira, T. R., A. H. Engelen, G. A. Pearson, M. Valero, and E. A. Serrão. 2015. Response of kelps from different latitudes to consecutive heat shock. Journal of Experimental Marine Biology and Ecology **463**:57-62.

Perry, A. L., P. J. Low, J. R. Ellis, and J. D. Reynolds. 2005. Climate change and distribution shifts in marine fishes. Science **308**:1912-1915.

Pessarrodona, A., J. Assis, K. Filbee-Dexter, M. T. Burrows, J.-P. Gattuso, C. M. Duarte, D. Krause-Jensen, P. J. Moore, D. A. Smale, and T. Wernberg. 2022. Global seaweed productivity. Science Advances **8**:eabn2465.

Pfister, C. A., M. A. Altabet, and B. L. Weigel. 2019. Kelp beds and their local effects on seawater chemistry, productivity, and microbial communities. Ecology **100**:e02798-e02798.

Pineiro-Corbeira, C., R. Barreiro, and J. Cremades. 2016. Decadal changes in the distribution of common intertidal seaweeds in Galicia (NW Iberia). Marine Environmental Research **113**:106-115.

Pineiro-Corbeira, C., R. Barreiro, J. N. Franco, J. Cremades, J. Cunha, and F. Arenas. 2019. Unexpected nutrient influence on the thermal ecophysiology of seaweeds that recently followed opposite abundance shifts. Marine Environmental Research:104747.

Pressey, R. L., M. Cabeza, M. E. Watts, R. M. Cowling, and K. A. Wilson. 2007. Conservation planning in a changing world. Trends in Ecology & Evolution **22**:583-592.

Price, I. 1989. Seaweed phenology in a tropical Australian locality (Townsville, North Queensland). Botanica Marina **32**:399-406.

Queirós, A. M., K. Tait, J. R. Clark, M. Bedington, C. Pascoe, R. Torres, P. J. Somerfield, and D. A. Smale. 2023. Identifying and protecting macroalgae detritus sinks toward climate change mitigation. Ecological Applications **33**:e2798.

Rahav, E., O. Raveh, O. Hazan, N. Gordon, N. Kress, J. Silverman, and B. Herut. 2018. Impact of nutrient enrichment on productivity of coastal water along the SE Mediterranean shore of Israel-A bioassay approach. Marine Pollution Bulletin **127**:559-567.

Rahav, E., O. Raveh, K. Yanuka-Golub, N. Belkin, P. Astrahan, M. Maayani, N. Tsumi, Y. Kiro, B. Herut, and J. Silverman. 2020. Nitrate-Enrichment Structures Phytoplankton Communities in the Shallow Eastern Mediterranean Coastal Waters. Frontiers in Marine Science **7**:611497.

Ravaglioli, C., J. Langeneck, A. Capocchi, A. Castelli, D. Fontanini, P. E. Gribben, and F. Bulleri. 2021a. Positive cascading effects of epiphytes enhance the persistence of a habitat-forming macroalga and the biodiversity of the associated invertebrate community under increasing stress. Journal of Ecology **109**:1078-1093.

Ravaglioli, C., J. Langeneck, A. Capocchi, A. Castelli, D. Fontanini, P. E. Gribben, and F. Bulleri. 2021b. Positive cascading effects of epiphytes enhance the persistence of a habitat-forming macroalga and the biodiversity of the associated invertebrate community under increasing stress. Journal of Ecology **109**:1078-1093.

Ricart, A. M., M. Ward, T. M. Hill, E. Sanford, K. J. Kroeker, Y. Takeshita, S. Merolla, P. Shukla, A. T. Ninokawa, K. Elsmore, and B. Gaylord. 2021. Coast-wide evidence of low pH amelioration by seagrass ecosystems. Global Change Biology **27**:2580-2591.

Rico-Villa, B., P. Woerther, C. Mingant, D. Lepiver, S. Pouvreau, M. Hamon, R. Robert. 2008. A flow-through rearing system for ecophysiological studies of Pacific oyster *Crassostrea gigas* larvae. Aquaculture **282**: 54–60.

Riebesell, U., A. Körtzinger, and A. Oschlies. 2009. Sensitivities of marine carbon fluxes to ocean change. Proceedings of the National Academy of Sciences **106**:20602-20609.

Rilov, G. 2016. Multi-species collapses at the warm edge of a warming sea. Scientific reports **6, 36897**.

Rilov, G., N. David, T. Guy-Haim, R. Arav, and S. Filin. 2021. Sea level rise can severely reduce biodiversity and community net production on rocky shores Science of the Total Environment **in press**.

Rilov, G., S. Fraschetti, E. Gissi, C. Pipitone, F. Badalamenti, L. Tamburello, E. Menini, P. Goriup, D. A. Mazaris, J. Garrabou, L. Benedetti-Cecchi, R. Danovaro, C. Loiseau, J. Claudet, and S. Katsanevakis. 2020a. A fast-moving target: achieving marine conservation goals under shifting climate and policies. Ecological Applications **30**:e02009.

Rilov, G., and B. Galil. 2009. Marine bioinvasions in the Mediterranean Sea - history, distribution and ecology. Pages 549-575 *in* G. Rilov and J. A. Crooks, editors. Biological invasions in marine ecosystems: Ecological, management, and geographic perspectives. Springer-Verlag, Heidelberg, Germany.

Rilov, G., L. Klein, D. Iluz, Z. Dubinsky, and T. Guy-Haim. 2022. Last snail standing? superior thermal resilience of an alien tropical intertidal gastropod over natives in an ocean-warming hotspot. Biological Invasions:1-17.

Rilov, G., A. D. Mazaris, V. Stelzenmüller, B. Helmuth, M. Wahl, T. Guy-Haim, N. Mieszkowska, J.-B. Ledoux, and S. Katsanevakis. 2019. Adaptive marine conservation planning in the face of

climate change: What can we learn from physiological, ecological and genetic studies? Global Ecology and Conservation **17**:e00566.

Rilov, G., O. Peleg, T. Guy-Haim, and E. Yeruham. 2020b. Community dynamics and ecological shifts on Mediterranean vermetid reefs. Marine Environmental Research **160**.

Rilov, G., O. Peleg, E. Yeruham, T. Garval, A. Vichik, and O. Raveh. 2018. Alien turf: overfishing, overgrazing and invader domination in southeastern Levant reef ecosystems. Aquatic Conservation: Marine and Freshwater Ecosystems **28**:351-369.

Rinde, E., J. K. Gitmark, D. Ø. Hjermann, C. W. Fagerli, M. R. Kile, and H. Christie. 2017. Utvikling av metodikk for overvåking av fremmede marine arter. Rapport, Norsk institutt for vannforskning.

Riquet, F., C.-A. De Kuyper, C. Fauvelot, L. Airoldi, S. Planes, S. Fraschetti, V. Mačić, N. Milchakova, L. Mangialajo, and L. Bottin. 2021. Highly restricted dispersal in habitat-forming seaweed may impede natural recovery of disturbed populations. Scientific reports **11**:16792-16792.

Robert, R., J. Vignier, B. Petton. 2017. Influence of feeding regime and temperature on development and settlement of oyster *Ostrea edulis* (Linnaeus, 1758) larvae. Aquaculture Research **48**: 4756–4773.

Rocha, J., J. Yletyinen, R. Biggs, T. Blenckner, and G. Peterson. 2015. Marine regime shifts: drivers and impacts on ecosystems services. Philosophical Transactions of the Royal Society B: Biological Sciences **370**:20130273.

Rodriguez, J.L., F.J. Sedano, L.O. Garcia-Martin, A. Perez-Camacho, J.L. Sanchez. 1990. Energy metabolism of newly settled *Ostrea edulis* spat during metamorphosis. Marine Biology **106**: 109–111.

Root, T. L., and S. H. Schneider. 2006. Conservation and climate change: the challenges ahead. Conservation Biology **20**:706-708.

Roth, F., C. Wild, S. Carvalho, N. Rädecker, C. R. Voolstra, B. Kürten, H. Anlauf, Y. C. El-Khaled, R. Carolan, and B. H. Jones. 2019. An in situ approach for measuring biogeochemical fluxes in structurally complex benthic communities. Methods in Ecology and Evolution **10**:712-725.

Sala, E., E. Ballesteros, P. Dendrinos, A. Di Franco, F. Ferretti, D. Foley, S. Fraschetti, A. Friedlander, J. Garrabou, H. Guclusoy, P. Guidetti, B. S. Halpern, B. Hereu, A. A. Karamanlidis, Z. Kizilkaya, E. Macpherson, L. Mangialajo, S. Mariani, F. Micheli, A. Pais, K. Riser, A. A. Rosenberg, M. Sales, K. A. Selkoe, R. Starr, F. Tomas, and M. Zabala. 2012. The structure of Mediterranean rocky reef ecosystems across environmental and human gradients, and conservation implications. PLoS One **7**.

Sala, E., Z. Kizilkaya, D. Yildirim, and E. Ballesteros. 2011. Alien marine fishes deplete algal biomass in the eastern Mediterranean. PLoS One **6**.

Santos, C. F., T. Agardy, F. Andrade, H. Calado, L. B. Crowder, C. N. Ehler, S. García-Morales, E. Gissi, B. S. Halpern, and M. K. Orbach. 2020. Integrating climate change in ocean planning. Nature Sustainability:1-12.

Sass, E., and S. Ben-Yaakov. 1977. The carbonate system in hypersaline solutions: Dead Sea brines. Marine Chemistry **5**:183-199.

Schiel, D. R., and M. S. Foster. 2006. The Population Biology of Large Brown Seaweeds: Ecological Consequences of Multiphase Life Histories in Dynamic Coastal Environments. Annual Review of Ecology, Evolution, and Systematics **37**:343-372.

Schumacher, J., and C. Roscher. 2009. Differential effects of functional traits on aboveground biomass in semi-natural grasslands. Oikos **118**:1659-1668.

Seabra, R., R. Varela, A. M. Santos, M. Gómez-Gesteira, C. Meneghesso, D. S. Wethey, and F. P. Lima. 2019. Reduced nearshore warming associated with eastern boundary upwelling systems. Frontiers in Marine Science **6**:104.

Short, F. T., T. J. R. Carruthers, M. Waycott, G. A. Kendrick, J. W. Fourqurean, A. Callabine, W. J. Kenworthy, and W. C. Dennison. 2010. Cymodocea nodosa - IUCN Red List of Threatened Species.

Silverman, J., B. Lazar, L. Cao, K. Caldeira, and J. Erez. 2009. Coral reefs may start dissolving when atmospheric CO2 doubles. Geophysical Research Letters **36**.

Silverman, J., B. Lazar, and J. Erez. 2007. Effect of aragonite saturation, temperature, and nutrients on the community calcification rate of a coral reef. Journal of Geophysical Research: Oceans **112**.

Smale, D. A. 2020. Impacts of ocean warming on kelp forest ecosystems. New Phytologist **225**:1447-1454.

Smale, D. A., M. T. Burrows, P. Moore, N. O'Connor, and S. J. Hawkins. 2013. Threats and knowledge gaps for ecosystem services provided by kelp forests: a northeast A tlantic perspective. Ecology and evolution **3**:4016-4038.

Smale, D. A., and T. Wernberg. 2013. Extreme climatic event drives range contraction of a habitat-forming species. Proceedings of the Royal Society B: Biological Sciences **280**:20122829.

Smale, D. A., T. Wernberg, A. L. Yunnie, and T. Vance. 2015. The rise of Laminaria ochroleuca in the Western English Channel (UK) and comparisons with its competitor and assemblage dominant Laminaria hyperborea. Marine Ecology **36**:1033-1044.

Smith, S., and G. Key. 1975. Carbon dioxide and metabolism in marine environments 1. Limnology and Oceanography **20**:493-495.

Solan, M., R. J. Aspden, and D. M. Paterson, editors. 2012. Marine biodiversity and ecosystem functioning: frameworks, methodologies, and integration. Oxford university press, Oxford.

Sousa, M. C., A. Ribeiro, M. Des, M. Gomez-Gesteira, M. deCastro, and J. M. Dias. 2020. NW Iberian Peninsula coastal upwelling future weakening: Competition between wind intensification and surface heating. Science of the Total Environment **703**:134808.

Steneck, R. S., M. H. Graham, B. J. Bourque, D. Corbett, J. M. Erlandson, J. A. Estes, and M. J. Tegner. 2002. Kelp forest ecosystems: biodiversity, stability, resilience and future. Environmental Conservation **29**:436-459.

Steven ADL, Bustamante RL, Silliman BR (2020) Bright spots in coastal marine ecosystems restoration. Current Biology **30**: PR1500-R1510

Strain, E. M. A., R. J. Thomson, F. Micheli, F. P. Mancuso, and L. Airoldi. 2014. Identifying the interacting roles of stressors in driving the global loss of canopy-forming to mat-forming algae in marine ecosystems. Global Change Biology **20**:3300-3312.

Stratmann, T., L. Mevenkamp, A. K. Sweetman, A. Vanreusel, and D. Van Oevelen. 2018. Has phytodetritus processing by an abyssal soft-sediment community recovered 26 years after an experimental disturbance? Frontiers in Marine Science **5**:59.

Suding, K., E. Higgs, M. Palmer, J. B. Callicott, C. B. Anderson, M. Baker, J. J. Gutrich, K. L. Hondula, M. C. LaFevor, B. M. H. Larson, A. Randall, J. B. Ruhl, and K. Z. S. Schwartz. 2015. Committing to ecological restoration. Science **348**:638-640.

Sunday, J. M., K. E. Fabricius, K. J. Kroeker, K. M. Anderson, N. E. Brown, J. P. Barry, S. D. Connell, S. Dupont, B. Gaylord, and J. M. Hall-Spencer. 2017. Ocean acidification can mediate biodiversity shifts by changing biogenic habitat. Nature Climate Change **7**:81-85.

Susini, M., L. Mangialajo, T. Thibaut, and A. Meinesz. 2007. Development of a transplantation technique of Cystoseira amentacea var. stricta and Cystoseira compressa. Hydrobiologia **580**:241-244.

Sydeman, W., M. García-Reyes, D. Schoeman, R. Rykaczewski, S. Thompson, B. Black, and S. Bograd. 2014. Climate change and wind intensification in coastal upwelling ecosystems. Science **345**:77-80.

Tait, L. W., I. Hawes, and D. R. Schiel. 2017. Integration of chlorophyll a fluorescence and photorespirometry techniques to understand production dynamics in macroaglal communities. Journal of Phycology **53**:476-485.

Tait, L. W., and D. R. Schiel. 2013. Impacts of temperature on primary productivity and respiration in naturally structured macroalgal assemblages. PLoS One **8**:e74413.

Takahashi, S., and N. Murata. 2008. How do environmental stresses accelerate photoinhibition? Trends in Plant Science **13**:178-182.

Talmage, S. C., and C. J. Gobler. 2011. Effects of elevated temperature and carbon dioxide on the growth and survival of larvae and juveniles of three species of northwest Atlantic bivalves. PLoS One **6**:e26941.

Tamburello, L., L. Benedetti-Cecchi, G. Ghedini, T. Alestra, and F. Bulleri. 2012. Variation in the structure of subtidal landscapes in the NW Mediterranean Sea. Marine Ecology Progress Series **457**:29-41.

Teagle, H., S. J. Hawkins, P. J. Moore, and D. A. Smale. 2017. The role of kelp species as biogenic habitat formers in coastal marine ecosystems. Journal of Experimental Marine Biology and Ecology **492**:81-98.

Topping, J. 1972. Errors of observation and their treatment. London: Chapman and Hall.

Tuya, F., E. Cacabelos, P. Duarte, D. Jacinto, J. J. Castro, T. Silva, I. Bertocci, J. N. Franco, F. Arenas, J. Coca, and T. Wernberg. 2012. Patterns of landscape and assemblage structure along a latitudinal gradient in ocean climate. Marine Ecology Progress Series **466**:9-19.

Uthicke, S., T. Ebert, M. Liddy, C. Johansson, K. E. Fabricius, and M. Lamare. 2016. Echinometra sea urchins acclimatized to elevated pCO 2 at volcanic vents outperform those under present-day pCO 2 conditions. Global Change Biology **22**:2451-2461.

Utting, S.D., Spencer, B.E., 1991. The Hatchery Culture of Bivalve Mollusc Larvae and Juveniles, vol. 68. Ministry of Agriculture, Fisheries and Food, Diectorate of Fisheries Research, p. 32.

Vasseur DA, DeLong JP, Gilbert B, Greig HS, Harley CDG, McCann KS, Van Savage, Tunney TD, O'Connor MI (2014) Increased temperature variation poses a greater risk to species than climate warming. Proceedings of the Royal Society B: Biological Sciences **281**: 20132612.

Vázquez-Domínguez, E., D. Vaque, and J. M. Gasol. 2007. Ocean warming enhances respiration and carbon demand of coastal microbial plankton. Global Change Biology **13**:1327-1334.

Verdiell-Cubedo, D., F. J. Oliva-Paterna, and M. Torralva-Forero. 2007. Fish assemblages associated with Cymodocea nodosa and Caulerpa prolifera meadows in the shallow areas of the Mar Menor coastal lagoon. Limnetica **26**:341-350.

Verdura, J., M. Sales, E. Ballesteros, M. E. Cefalì, and E. Cebrian. 2018. Restoration of a canopy-forming alga based on recruitment enhancement: methods and long-term success assessment. Frontiers in plant science **9**:1832.

Vergés, A., C. Doropoulos, H. A. Malcolm, M. Skye, M. Garcia-Pizá, E. M. Marzinelli, A. H. Campbell, E. Ballesteros, A. S. Hoey, and A. Vila-Concejo. 2016. Long-term empirical evidence of ocean warming leading to tropicalization of fish communities, increased herbivory, and loss of kelp. Proceedings of the National Academy of Sciences **113**:13791–13796.

Vergés, A., E. McCosker, M. Mayer-Pinto, M. A. Coleman, T. Wernberg, T. Ainsworth, and P. D. Steinberg. 2019. Tropicalisation of temperate reefs: Implications for ecosystem functions and management actions. Functional Ecology **33**:1000-1013.

Vergés, A., P. D. Steinberg, M. E. Hay, A. G. Poore, A. H. Campbell, E. Ballesteros, K. L. Heck, D. J. Booth, M. A. Coleman, and D. A. Feary. 2014a. The tropicalization of temperate marine ecosystems: climate-mediated changes in herbivory and community phase shifts. Proceedings of the Royal Society B: Biological Sciences **281**.

Vergés, A., F. Tomas, E. Cebrian, E. Ballesteros, Z. Kizilkaya, P. Dendrinos, A. A. Karamanlidis, D. Spiegel, and E. Sala. 2014b. Tropical rabbitfish and the deforestation of a warming temperate sea. Journal of Ecology **102**:1518-1527.

Videla, J.A., Chaparro, O.R., Thompson, R.J., Concha, I.I., 1998. Role of biochemical energy reserves in the metamorphosis and early juvenile development of the oyster *Ostrea chilensis*. Marine Biology **132:** 635–640.

Vieira, C., A. Aharonov, G. Paz, A. H. Engelen, K. Tsiamis, R. Einav, and O. De Clerck. 2019. Diversity and origin of the genus Lobophora in the Mediterranean Sea including the description of two new species. Phycologia **58**:163-168.

Viejo, R. M., B. Martinez, J. Arrontes, C. Astudillo, and L. Hernandez. 2011. Reproductive patterns in central and marginal populations of a large brown seaweed: drastic changes at the southern range limit. Ecography **34**:75-84.

Vile, D., B. Shipley, and E. Garnier. 2006. Ecosystem productivity can be predicted from potential relative growth rate and species abundance. Ecology Letters **9**:1061-1067.

Wahl, M., B. Buchholz, V. Winde, D. Golomb, T. Guy Haim, J. Müller, G. Rilov, M. Scotti, and M. Boettcher. 2015. A mesocosm concept for the simulation of near-natural shallow underwater

climates: The Kiel Outdoor Benthocosms (KOB). Limnology and Oceanography: Methods ***13***:651-663.

Wahl, M., S. Schneider Covachã, V. Saderne, C. Hiebenthal, J. Müller, C. Pansch, and Y. Sawall. 2018a. Macroalgae may mitigate ocean acidification effects on mussel calcification by increasing pH and its fluctuations. Limnology and Oceanography **63**:3-21.

Wahl, M., S. Schneider Covachã, V. Saderne, C. Hiebenthal, J. D. Müller, C. Pansch, and Y. Sawall. 2018b. Macroalgae may mitigate ocean acidification effects on mussel calcification by increasing pH and its fluctuations. Limnology and Oceanography **63**:3-21.

Walles, B., K. Troost, D. van den Ende, S. Nieuwhof, A. C. Smaal, and T. Ysebaert. 2016. From artificial structures to self-sustaining oyster reefs. Journal of Sea Research **108**:1-9.

Wanninkhof, R. 2014. Relationship between wind speed and gas exchange over the ocean revisited. Limnology and Oceanography: Methods **12**:351-362.

Wernberg, T., and K. Filbee-dexter. 2019. Missing the marine forest for the trees. Marine Ecology Progress Series **612**.

Wernberg, T., D. A. Smale, and M. S. Thomsen. 2012. A decade of climate change experiments on marine organisms: procedures, patterns and problems. Global Change Biology **18**:1491-1498.

Wernberg, T., D. A. Smale, F. Tuya, M. S. Thomsen, T. J. Langlois, T. de Bettignies, S. Bennett, and C. S. Rousseaux. 2013. An extreme climatic event alters marine ecosystem structure in a global biodiversity hotspot. Nature Clim. Change **3**:78-82.

Wesselmann, M., A. Anton, C. M. Duarte, I. E. Hendriks, S. Agustí, I. Savva, E. T. Apostolaki, and N. Marbà. 2020. Tropical seagrass Halophila stipulacea shifts thermal tolerance during Mediterranean invasion. Proceedings of the Royal Society B **287**:20193001.

Whyte, J.N.C., Bourne, N., Ginther, N.G., Hodgson, C.A., 1992. Compositional changes in the larva to juvenile development of the scallop *Crassadoma gigantea* (gray). Journal of Experimental Marine Biology and Ecology **163**: 13–29.

Wiencke, C., and K. Bischof. 2012. Seaweed biology. Springer, New York.

Wiggins, P.R., P.B. Frappell. 2000 The influence of haemoglobin on behavioural thermoregulation and oxygen consumption in *Daphnia carinata*. Physiological and Biochemical Zoology **73**: 153–160.

Winters, G., S. Beer, D. A. Willette, I. G. Viana, K. L. Chiquillo, P. Beca-Carretero, B. Villamayor, T. Azcárate-García, R. Shem-Tov, B. Mwabvu, L. Migliore, A. Rotini, M. A. Oscar, J. Belmaker, I. Gamliel, A. Alexandre, A. H. Engelen, G. Procaccini, and G. Rilov. 2020. The tropical seagrass halophila stipulacea: Reviewing what we know from its native and invasive habitats, alongside identifying knowledge gaps. Pages 1-28 Frontiers in Marine Science. Frontiers Media S.A.

Worm, B., E. B. Barbier, N. Beaumont, J. E. Duffy, C. Folke, B. S. Halpern, J. B. C. Jackson, H. K. Lotze, F. Micheli, S. R. Palumbi, E. Sala, K. A. Selkoe, J. J. Stachowicz, and R. Watson. 2006. Impacts of biodiversity loss on ocean ecosystem services. Science **314**:787-790.

Xing, K., A.A. Hoffmann, C.S. Ma. 2014. Does thermal variability experienced at the egg stage influence life history traits across life cycle stages in a small invertebrate? PLoS ONE **9**: e99500.

Yates, K. K., and R. B. Halley. 2006. Diurnal variation in rates of calcification and carbonate sediment dissolution in Florida Bay. Estuaries and Coasts **29**:24-39.

Yeruham, E., G. Rilov, M. Shpigel, and A. Abelson. 2015. Collapse of the echinoid *Paracentrotus lividus* populations in the Eastern Mediterranean - result of climate change? Scientific reports **5**:13479.

Yeruham, E., M. Shpigel, A. Abelson, and G. Rilov. 2020. Ocean warming and tropical invaders erode the performance of a key herbivore. Ecology **101**:e02925.

Young, C. S., L. H. Sylvers, S. J. Tomasetti, A. Lundstrom, C. Schenone, M. H. Doall, and C. J. Gobler. 2022. Kelp (Saccharina latissima) Mitigates Coastal Ocean Acidification and Increases the Growth of North Atlantic Bivalves in Lab Experiments and on an Oyster Farm. Frontiers in Marine Science:513-513.

Zirler, R., L. A. Leck, T. F. Farkash, M. Holzknecht, A. Kroh, V. Gerovasileiou, M. Fatih Huseyinoglu, C. Jimenez, V. Resaikos, B. Yokes, and O. Bronstein. 2023. Gaining a (tube) foothold-trends and status following two decades of the long-spined echinoid Diadema setosum (Leske, 1778) invasion to the Mediterranean Sea. Frontiers in Marine Science **10**:970.